



**HAL**  
open science

# Transforming alum sludge into value-added products for various reuse

Baiming Ren

## ► To cite this version:

Baiming Ren. Transforming alum sludge into value-added products for various reuse. Chemical and Process Engineering. Ecole des Mines d'Albi-Carmaux; University College Dublin, 2019. English. NNT : 2019EMAC0002 . tel-03091970

**HAL Id: tel-03091970**

**<https://theses.hal.science/tel-03091970>**

Submitted on 1 Jan 2021

**HAL** is a multi-disciplinary open access archive for the deposit and dissemination of scientific research documents, whether they are published or not. The documents may come from teaching and research institutions in France or abroad, or from public or private research centers.

L'archive ouverte pluridisciplinaire **HAL**, est destinée au dépôt et à la diffusion de documents scientifiques de niveau recherche, publiés ou non, émanant des établissements d'enseignement et de recherche français ou étrangers, des laboratoires publics ou privés.

Université Fédérale



Toulouse Midi-Pyrénées

# THÈSE

en vue de l'obtention du

## DOCTORAT DE L'UNIVERSITÉ DE TOULOUSE

*délivré par*

*IMT - École Nationale Supérieure des Mines d'Albi-Carmaux*

*Cotutelle Internationale avec University College Dublin, Ireland*

---

**Présentée et soutenue par**

**Baiming REN**

**Le 11 Juillet 2019**

## Transforming Alum Sludge into Value-Added Products for Various Reuse

---

**École doctorale et discipline ou spécialité :**

MEGEP : Génie des procédés et de l'Environnement

**Unité de recherche :**

Centre RAPSODEE, UMR CNRS 5302, IMT Mines Albi

**Directeur(s) de Thèse :**

Ange NZIHOU, Professeur, IMT Mines Albi

Yaqian ZHAO, Professeur, University College Dublin

**Membres du jury :**

Hélène CARRERE, Directeur de recherche, LBE Narbonne (*Présidente*)

Diane THOMAS, Professeur, Université de Mons - Belgique (*Rapporteur*)

Zoubeir LAFHAJ, Professeur, Ecole Centrale de Lille (*Rapporteur*)

Nathalie LYCZKO, Ingénieur de Recherche, IMT Mines Albi (*Encadrante*)



## **Acknowledgements**

To my late father Hongcheng Ren, because I owe it all to you.

Heartfelt thanks go to my mother Yajuan Zhang, who have provided me through moral and emotional support in my life.

A very special gratitude goes out to my life coach, supervisor Prof. Yaqian Zhao, for making every beautiful thing happens, for his patience, motivation, enthusiasm, and immense knowledge.

My research would have been impossible without the aid and support of my co-supervisors Prof. Ange Nzihou and Dr. Nathalie Lyczko, thanks a million for offering me the opportunities and leading me working on diverse exciting projects.

I am profoundly grateful to my fiancée Qianyi Yang, four years' time and eight thousand kilometers can't cut off your understanding and caring to me.

I would also like to acknowledge China Scholarship Council sincerely, for helping and providing the funding for me to study abroad.

I am also grateful to all the staff in RAPSODEE (IMT Mines-Albi): with a special mention to Mickaël Ribeiro, Pierre Bertorelle, Jean-Marie Sabathier, Céline Boachon, Denis Marty, Christine Rolland, Sylvie Del Confetto, Séverine Patry, Philippe Accart, Chrystel Auriol Alvarez, Valérie Vèrès, for their unfailing support and assistance.

And finally, last but by no means least, also to everyone in CWRR (UCD) and RAPSODEE (IMT Mines Albi), it was great with all of you during the last four years.



## Abstract

The production of drinking water always accompanied by the generation of water treatment residues (WTRs). Alum sludge is one of the WTRs, it is an easily, locally and largely available by-product worldwide. This work focuses on the identification of different ways to valorize the alum sludge for environmentally friendly reuse. Two alum sludges collected from France and Ireland have been reused in various fields as a function of their characteristics.

Firstly, alum sludge was used as a partial replacement for clay in brick making, by incorporating different percentages of alum sludge and calcined at different temperatures (range from 800 to 1200 °C). The resultant bricks were tested for compression, Loss on Ignition, water absorption, appearance, etc. Results show that alum sludge-clay bricks have met the “European and Irish Standards” and demonstrated the huge industrial application potential for alum sludge in Irish clay brick manufacturing. Glyphosate is an active ingredient in pesticide which is massive employed in agriculture. Alum sludge and Irish peat were compared for glyphosate removal in pot tests, results show that alum sludge present significant glyphosate removal capacity (>99 %) and could reduce the level of Chemical Oxygen Demand (COD). It provided a scientific clue for sorbents selection when considering the agricultural wastewater treatment in Ireland and to maximize their value in practice. The co-conditioning and dewatering of sewerage sludge with liquid alum sludge was also investigated in Jar-test based on the case analysis of a water industry in France. Results show that the optimal sludge mix ratio is 1:1, the use of the alum sludge has been shown to beneficially enhance the dewaterability of the resultant mixed sludge, and highlighting a huge polymer saving (14 times less than the current technologies) and provided a sustainable and technical sludge disposal route for the local water industry. The use of alum sludge as a sorbent for gas purification was studied by H<sub>2</sub>S adsorption experiments in a fixed-bed reactor with various operating parameters. The experimental breakthrough data were modeled with empirical models based on adsorption kinetics. Results show that alum sludge is an efficient sorbent for H<sub>2</sub>S removal (capacity of 374.2 mg/g) and the mechanisms including dissociative adsorption and oxidation were proposed. Moreover, the overall mass transfer coefficients were calculated which could be used for the process scaling up. Finally, alum sludge cakes were reused in the novel aerated alum sludge constructed wetland (CW), which were designed for simultaneous H<sub>2</sub>S purification and wastewater treatment. Results show that H<sub>2</sub>S was completely removed in the six months’ trials, while the high removal efficiencies of COD, total nitrogen (TN), total phosphates (TP) were achieved. Thus, a novel eco-friendly CW for simultaneous H<sub>2</sub>S purification and wastewater treatment was developed. In the different approaches and process considered, in particular it was put in investigating and describing the mechanisms involved.

Overall, this work demonstrated alum sludge could be a promising by-product for various novel beneficial reuse rather than landfilling and provided a “Circular Economy” approach for WTRs management.

**Keywords:** Wastewater treatment, Alum sludge, Gas purification, Process adsorption mechanisms, Brick manufacturing, Valorization, Circular economy

## Résumé

### Transformation de boues issues du traitement d'eau potable en produit à haute valeur ajoutée

La forte augmentation de la population mondiale entraîne une demande croissante en eau potable. La production d'eau potable est accompagnée par la génération de résidus du traitement de l'eau dont la boue d'aluminium qui est donc largement disponible mondialement. Ce travail se concentre sur l'identification des différentes voies de valorisation des boues d'aluminium afin de les réutiliser dans le domaine de l'environnement. Deux sources de boues d'aluminium, collectées en France et en Irlande, ont été étudiées dans divers domaines d'application en fonction de leurs caractéristiques.

Tout d'abord, les boues d'aluminium ont été utilisées en remplacement d'une partie de l'argile dans la fabrication des briques, en incorporant différents pourcentages de boues d'aluminium et à différentes températures. Les briques résultantes ont été caractérisées et les résultats ont montré que les briques composées de boues d'aluminium et d'argile sont conformes aux « normes européennes et irlandaises » et démontrent ainsi le potentiel pour une application industrielle des boues d'aluminium dans la fabrication de briques en terre cuite irlandaises.

Dans un second temps, les boues d'aluminium ont été utilisées comme adsorbant des polluants présents dans l'agriculture. Le glyphosate est un ingrédient actif dans les pesticides utilisés massivement dans l'agriculture irlandaise et représente une problématique environnementale. La boue d'aluminium et la tourbe irlandaise ont été comparées pour l'élimination du glyphosate lors de tests en pot à l'échelle laboratoire. Les résultats ont montré que la boue d'aluminium permet d'éliminer le glyphosate à plus de 99% et réduire les niveaux de DCO. Cet aspect scientifique a permis d'être dans la sélection des adsorbants possibles pour le traitement des eaux usées agricoles en Irlande.

Le co-conditionnement et la déshydratation des boues de station d'épuration avec des boues d'aluminium liquides ont également été étudiés. Pour cela, le Jar test a été effectué sur des boues issues d'une station de traitement des eaux française. Les résultats ont montré que le rapport optimal de mélange des boues est de 1:1 (boues d'épuration : boues d'aluminium). Ainsi, la quantité de polymère utilisée peut être diminuée de 14 fois par rapport aux technologies actuelles. Cette approche a permis de montrer la possible valorisation des boues d'aluminium comme un moyen durable et technique permettant ainsi l'élimination des boues localement pour une même station de traitement des eaux.

Une autre voie de valorisation des boues d'aluminium comme adsorbant pour la purification des gaz a été étudiée lors d'expériences d'adsorption de  $H_2S$  dans un réacteur à lit fixe dans différentes conditions expérimentales. Les données expérimentales d'adsorption du  $H_2S$  ont été modélisées à l'aide de modèles empiriques basés sur la cinétique des processus d'adsorption. Les résultats ont montré que les boues d'aluminium sont un adsorbant efficace pour l'élimination du  $H_2S$  (capacité de 374,2 mg  $H_2S$  / g solide) et que des mécanismes mis en jeu sont l'adsorption dissociative et l'oxydation. Les coefficients de transfert de masse globaux ont également été calculés et pouvant ainsi être utilisés pour la prédiction.

Enfin, les gâteaux de boues d'aluminium ont été réutilisés pour la purification simultanée d' $H_2S$  et le traitement des eaux usées. Les résultats ont montré la capacité de cet adsorbant pour éliminer tout le  $H_2S$  présent avec une grande efficacité d'élimination de la DCO, TN et TP. Ainsi, il a été démontré la valorisation des boues d'aluminium en tant qu'adsorbant pour une purification du  $H_2S$  simultanée avec le traitement des eaux usées.

**Mots clés :** Traitement des eaux usées, Boue d'aluminium, Purification de gaz, Mécanismes d'adsorption, Matériaux de construction, Valorisation, Économie circulaire

## Résumé Long en français

### Introduction

L'essor démographique et l'urbanisation entraînent une demande mondiale croissante en eau potable. Les stations de traitement des eaux potables utilisent des processus de coagulation, floculation, sédimentation, filtration et désinfection qui génèrent une grande quantité de résidus. Lorsque le sulfate d'aluminium est utilisé dans les processus de floculation et de coagulation, la boue d'aluminium qui en résulte est un de ces résidus disponible dans les villes et métropoles du monde entier.

La production des résidus provenant du traitement de l'eau potable représente de 1 à 3% en volume de l'eau brute traitée. Une station de traitement produit environ 100 kg / an de boues. A titre d'exemple, la Corée est le pays produisant la plus grande quantité annuelle de résidus / personnes avec 8,5 kg / personne/an. Le Danemark et l'Allemagne eux sont les pays produisant la plus faible quantité avec environ 1,6 kg/personne/an. La France est parmi les pays qui produisent le plus résidus avec une production d'environ 7,9 kg/personne/an.

La production de ces résidus reste une préoccupation majeure en ce qui concerne leur élimination, leur coût et leur impact environnemental. Dans ce contexte, différentes voies d'élimination sont actuellement utilisées comme : le rejet dans l'environnement naturel, dans les égouts, dans les lagunes ou une mise en décharge. Ces différentes voies sont moins coûteuses, mais doivent être maîtrisées dans le cycle de l'eau. Ces rejets sont donc aujourd'hui de plus en plus souvent interdits par la réglementation en raison des impacts environnementaux négatifs. La mise en décharge a été la méthode la plus largement utilisée dans la plupart des pays du monde entraînant ainsi une possible contamination des nappes phréatique par les produits chimiques utilisés lors du traitement. Néanmoins, les coûts croissants des sites d'enfouissement et la réduction de l'espace disponible incitent les industries à explorer d'autres méthodes d'élimination de ces résidus. Par conséquent, il est essentiel de définir des options de gestion viables pour ces résidus afin de les valoriser efficacement de manière durable et écologiquement acceptable.

À ce jour, il existe quatre grandes catégories de réutilisation des boues d'aluminium comme le montre la Figure 0.3 (« The beneficial reusing ways af alum sludge »). La valorisation des boues d'aluminium dans les processus de traitement des eaux usées, comme matériau de construction ou pour des applications au niveau du sol sont les principales voies étudiées. Bien que de nombreuses études de recherche aient été menées au cours des dernières décennies, il reste encore un énorme défi à relever pour examiner les options potentielles de recyclage et de réutilisation des boues d'aluminium, tout en quantifiant les économies potentielles et les avantages environnementaux pouvant en découler.

Ce travail de thèse se concentre sur l'identification de différentes voies de valorisation des boues d'aluminium (collectées en France et en Irlande) dans différents domaines d'application comme par exemple la purification du gaz

La structure générale de ce manuscrit présentée sur la Figure 0.4 (« Structure of the thesis ») est composée de 7 chapitres. Les chapitres de 3 à 7 ont été rédigés sous forme d'articles

---

scientifiques qui ont déjà été publiés ou en cours de soumission dans des journaux scientifiques internationaux. Cette thèse de doctorat a été effectuée en cotutelle entre l'University College Dublin, Irlande et IMT Mines Albi, France.

## **Chapitre 1 : Contexte et revue bibliographique**

L'objectif de ce premier chapitre est de présenter le contexte de l'origine des boues d'aluminium utilisées, ainsi qu'un état de l'art sur les voies de valorisation possibles. Un état de l'art des technologies actuelles du contrôle des odeurs est également présenté avec une attention plus particulière sur l'élimination de l'H<sub>2</sub>S.

Dans un premier temps, la section 1.1 décrit les différents procédés de traitement des eaux utilisés classiquement comme schématisé sur la Figure 1.1 (« Conventional water treatment processes »). Lors de ces traitements des résidus solides sont produits dont les boues d'aluminium qui doivent ensuite être traitées et stockées et leur valorisation est à ce jour devenue un enjeu environnemental majeur. La réduction, le recyclage et la réutilisation de ces boues d'aluminium doivent constituer une solution durable aux problèmes de gestion de ces boues dans le cadre des lois environnementales qui sont de plus en plus strictes.

Ainsi, la section 1.2 décrit les différentes voies de valorisation durables des boues d'aluminium dans différents domaines d'application. La première voie décrite est l'utilisation des boues d'aluminium dans les matériaux de construction comme substituts de l'argile dans la production de briques d'argile. Ces boues ont également été utilisées pour améliorer les performances des procédés de traitement des eaux usées sous différents aspects soit comme coagulant soit comme adsorbant pour les contaminants et métaux lourds. Le co-conditionnement et la déshydratation des boues d'aluminium mélangées avec des boues de traitement des eaux usées sont également décrits afin d'être utilisés comme substrat dans les zones humides aménagées. Une quatrième voie étudiée est la réutilisation de ces boues d'aluminium comme matériau bénéfique pour la récupération de coagulant lors des traitements des eaux. La dernière voie explorée correspond aux applications terrestres des boues d'aluminium sous trois aspects : l'amortissement du sol, l'amélioration de la structure du sol et l'immobilisation des éléments nutritifs du sol.

La section 1.3 présente un état de l'art des technologies utilisées pour le contrôle des odeurs dans les stations de traitement d'eau potable avec une attention plus particulière pour le traitement de l'H<sub>2</sub>S qui est le polluant étudié lors de cette étude. Les traitements physico-chimiques (systèmes d'adsorption, mécanismes mis en jeu, modèles de transfert de masse) ainsi que les traitements biologiques existants sont détaillés.

## **Chapitre 2 : Matériels et méthodes expérimentales**

Ce chapitre décrit les matériaux et les méthodes de caractérisation utilisés ainsi que les méthodes expérimentales mises au point lors de cette étude.

La section 2.1 décrit les deux sources de boues d'aluminium étudiées et provenant de deux stations de traitement d'eau potable, une située à Dublin (Irlande) et une à Carmaux (France).

Les méthodes de caractérisation utilisées pour déterminer les propriétés de ces deux boues sont présentées dans la section 2.2. Elles ont permis de déterminer les propriétés physico-chimiques (surface spécifique, porosité, granulométrie, ...) et thermiques (thermogravimétrie) de ces deux

boues afin de comprendre ensuite leur comportement lors de leur utilisation lors des différentes expérimentations mises en place.

Afin d'étudier les différentes voies de valorisation de ces deux boues, différents dispositifs expérimentaux ont été mis en place comme décrit dans la section 2.3.

Lors de la première approche concernant les matériaux de construction, les boues d'aluminium ont été introduites dans des briques d'argile avec différentes quantités. Ces formulations ont ensuite subi une étape de séchage, mise en forme (cylindre) et cuisson à différentes températures. Les briques ainsi obtenues ont ensuite été testées à la résistance à la compression, à la perte au feu, des tests de compression après immersion dans l'eau pendant 24 h et d'adsorption d'eau ont également été mis en œuvre.

Lors de l'étude portant sur l'adsorption du glyphosate, les tourbes utilisées ont été extraites de deux tourbières situées en Irlande. Les expériences ont été menées avec quatre conteneurs en plastique identiques. La base des pots était remplie de gravier lavé et la tourbe a été introduite dans le premier pot. Les jeunes roseaux coupés ont ensuite été plantés sur le dessus de chaque pot pour suivre leur évolution.

Les essais de conditionnement ont été réalisés à l'aide d'un appareil d'agitation de pots standard à quatre palettes, le Jar test. La déshydratation des boues avant et après le co-conditionnement a été évaluée à l'aide de la mesure à la résistance spécifique à la filtration et du temps d'aspiration capillaire.

L'utilisation de boues comme adsorbant pour la purification de l' $H_2S$  a été démontrée lors d'expériences menées dans un réacteur à lit fixe contenant la boue d'aluminium préalablement séchée dans lequel un gaz synthétique contenant de l' $H_2S$  est injecté. L'adsorption de l' $H_2S$  a été suivie au cours du temps dans le gaz. Une caractérisation des boues après leur utilisation a également été effectuée. Cette étude expérimentale a été suivie par une modélisation cinétique et par la détermination des coefficients de transfert de masse régissant les processus mis en évidence.

Afin d'évaluer l'adsorption simultanée de l' $H_2S$  et la purification d'une eau usée, un montage expérimental a été mis au point. Celui-ci est constitué de trois colonnes en plexiglas d'un diamètre de 15 cm et d'une hauteur de 100 cm. Les diffuseurs d'aération se situent dans le bas de deux des colonnes pour assurer une distribution homogène de l'air.

### **Chapitre 3 : Boues d'aluminium incorporées dans la fabrication de briques d'argile**

Ce chapitre présente une étude expérimentale sur l'incorporation des boues d'aluminium en remplacement partiel de l'argile dans la fabrication de briques.

Dans le monde, les boues d'aluminium sont déshydratées et les gâteaux qui en résultent sont mis en décharge. Ce chapitre a pour objectif de présenter une voie de valorisation dans les matériaux de construction afin d'éviter cela.

Les gâteaux de boue d'aluminium et l'argile ont été séchés, broyés et tamisés séparément en vue de la fabrication des éprouvettes. Des briques d'argile cylindriques ont été fabriquées à différentes températures (800, 1000, 1100, 1200 °C), en incorporant différents pourcentages (0, 5, 10, 15, 20, 30, 40, 40% en poids sec) de boue d'aluminium. Les briques ont ensuite été

soumises à un test de résistance à la compression et à une immersion dans l'eau. Les pertes au feu, l'absorption d'eau et la réduction de poids ont été calculés pour les différentes formulations mises en œuvre. Il a été montré que les briques contenant jusqu'à 20% de boues et cuites à 1200°C ou à 5% de boues d'aluminium et cuites à 1100°C respectaient les normes européennes. La valeur optimale de l'incorporation des boues d'aluminium permettant d'assurer une résistance à la compression adéquate avant et après absorption d'eau est de 5%. Même après l'absorption d'eau, la brique possède toujours une résistance à la compression considérable de 37,5 N / mm<sup>2</sup>.

Ainsi, il a été montré la possible utilisation des gâteaux de boues d'aluminium déshydratés dans la fabrication de briques. D'un aspect commercial, cette valorisation des boues permet de diminuer les problèmes de coût.

#### **Chapitre 4 : Boues d'eau potable comme adsorbants pour le traitement des eaux usées agricoles (élimination du glyphosate)**

Cette étude compare l'efficacité de l'élimination du glyphosate des boues d'aluminium à la tourbe irlandaise qui est actuellement utilisée.

Le phosphonate organique contenu dans une solution aqueuse de glyphosate a été éliminé lors des essais en pots remplis séparément de boue de tourbe et boue d'aluminium. Les échantillons d'effluents ont été prélevés dans chaque pot pour analyser l'évolution de la concentration en phosphore (P) et en DCO (demande chimique en oxygène). Des caractérisations physiques et chimiques des deux milieux avant et après utilisation ont ensuite été effectuées.

Les essais en pot ont duré 10 semaines et ont montré que la capacité d'enlèvement de la tourbe était inférieure à 10%, tandis que les boues d'aluminium présentaient une élimination moyenne du glyphosate de 99,8%.

Les résultats ont montré que la capacité d'élimination de P par des boues d'aluminium était significative (> 99%), tandis que la capacité d'élimination de la tourbe était inférieure à 10% après 10 semaines de traitement. Les deux matériaux ont considérablement réduit les niveaux de DCO, mais il a été noté que la tourbe avait une capacité initiale d'élimination du P légèrement supérieure (68 ± 22%) et donnait de meilleurs résultats que les boues d'aluminium (57 ± 12%).

Cette étude a permis de montrer la possibilité d'utiliser les boues d'aluminium comme adsorbant pour l'élimination des polluants tels que le glyphosate contenu dans les eaux usées.

#### **Chapitre 5 : Co-conditionnement de boues activées avec des boues d'aluminium**

Ce chapitre est consacré au co-conditionnement et à la déshydratation des boues d'aluminium avec des boues activées provenant d'une usine de traitement des eaux usées en France.

L'expansion rapide des zones urbaines et le développement industriel sont souvent associés à une demande en eau importante qui nécessite un traitement intensif de l'eau potable et des eaux usées. Une grande quantité de boues en tant que sous-produit sont produites et doivent subir un traitement. Ainsi, la déshydratation des boues en tant qu'étape essentielle pour réduire le volume des boues est un processus coûteux. En conséquence, un conditionnement efficace des



boues avant la déshydratation mécanique est nécessaire.

Cette étude vise à examiner la faisabilité du co-conditionnement de boues d'épuration avec des boues d'aluminium liquides de la station de traitement des eaux de la ville de Graulhet, en France.

Des expériences en JAR-Test ont été effectuées avec différents rapports volumiques boues activées : boues d'aluminium variant de 1 : 1 à 1 : 4 et 2 : 1. La mesure de la résistance spécifique à la filtration et le temps d'aspiration capillaire ont été effectuées après chaque test. Ainsi, il a été montré que le rapport de mélange optimal pour les deux boues est de 1 : 1 (boues activées / boues d'aluminium ; v / v). La présence de boue d'aluminium améliore la déshydratation des boues mélangées résultantes, en diminuant à la fois la résistance spécifique à la filtration d'un facteur 5 et le temps d'aspiration capillaire d'un facteur 1,5.

Des essais ont été effectués avec différents dosages de polymère (Sueprfloc-492HMW) pour les boues mélangées (rapport optimal de mélange 1 : 1) allant de 10 à 400 mg/L. Ainsi, il a été montré que la quantité optimale de polymère à utiliser était de 0,2 g / l, alors que le dosage actuel pour les boues activées dans la station d'épuration de Graulhet est de 2,8 g / l. Cette diminution de polymère met en évidence une économie considérable (14 fois).

Une évaluation intégrée rentable des capacités de traitement, du transport des boues, de l'élimination accrue des gâteaux, de l'administration supplémentaire, etc. a montré que la stratégie de co-conditionnement et de déshydratation était réalisable. Un investissement initial pourrait être rentabilisé au bout de 11 ans.

## **Chapitre 6 : Les boues d'aluminium comme adsorbant pour l'élimination du sulfure d'hydrogène**

Ce chapitre présente une étude expérimentale sur l'adsorption du H<sub>2</sub>S par des boues d'aluminium ainsi que les mécanismes d'adsorption mis en jeu lors des réactions.

La population est généralement préoccupée et intolérante à l'égard des odeurs et autres contaminants atmosphériques provenant des installations de traitement des eaux usées. La gestion des émissions d'air / odeurs est devenue une priorité afin de répondre à la réglementation et au confort des habitants. Le sulfure d'hydrogène (H<sub>2</sub>S) a toujours été une préoccupation majeure c'est un gaz toxique, inflammable et incolore avec une odeur caractéristique d'œuf pourri. Le seuil moyen d'odeur de H<sub>2</sub>S est de 7 à 9 parties par milliard (ppb).

L'étude expérimentale de l'adsorption de l'H<sub>2</sub>S pour les boues d'aluminium a été effectuée dans un lit fixe dans lequel est introduit un gaz synthétique contenant du sulfure d'hydrogène (200 ppmv) à température ambiante. Ce gaz pollué passe au travers du lit de particules de boues d'aluminium avant de ressortir par le haut de la colonne. La concentration en H<sub>2</sub>S à la sortie de la colonne est suivie au cours du temps. L'effet du débit de gaz (0,34 et 5 L/h) et de la masse du lit de particules (0,5 et 1 g) sur l'efficacité de l'adsorption ont été étudiés. Ainsi, il a été montré que la capacité d'adsorption des boues d'aluminium était de 374,2 mg de H<sub>2</sub>S / g de boues d'aluminium. Cette quantité a légèrement diminué avec l'augmentation du débit et considérablement augmenté avec l'augmentation de la masse du lit (165,8 mg de H<sub>2</sub>S / g de boues d'aluminium avec 0,5g d'adsorbant et 374,2 mg de H<sub>2</sub>S / g de boues d'aluminium avec 1g d'adsorbant).

Dans un second temps, trois modèles cinétiques, Thomas, Bed Depth Service Time et Yoon-

Nelson ont été utilisés pour modéliser les cinétiques d'adsorption obtenues expérimentalement. Ces modèles permettent de déterminer les facteurs prédominants lors du processus d'adsorption. L'utilisation de ces modèles a montré une bonne corrélation entre les valeurs expérimentales et simulées avec une déviation comprise entre 2 et 30%. L'utilisation de ces modèles a permis de montrer qu'ils permettaient de prédire avec succès les courbes du comportement dynamique de l'adsorption dans un lit fixe et pouvant ainsi servir comme modèle prédictif en fonction des conditions opératoires (hauteur du lit de particules, débit de gaz) et être utilisés pour la reproduction à plus grande échelle.

Les mécanismes d'adsorption de H<sub>2</sub>S sur les boues d'aluminium ainsi que le phénomène de transfert de masse ont été étudiés en détail. Les mécanismes d'adsorption de H<sub>2</sub>S sur les boues d'aluminium ont été examinés au moyen de différentes caractérisations physico-chimiques des boues d'aluminium avant et après utilisation. De plus, plusieurs coefficients de transfert de masse (externes, globaux, etc.) ont été déterminés à partir de la description mathématique des courbes d'adsorption.

La structure microporeuse, le pH alcalin, les espèces métalliques inhérentes aux boues d'aluminium favorisent la formation d'espèces de sulfures métalliques et de sulfates métalliques comme cela est présenté sur la Figure 6.9 (« Mechanisms of H<sub>2</sub>S adsorption onto alum sludge »). Les propriétés importantes des boues d'aluminium pour l'élimination de H<sub>2</sub>S sont les suivantes : surface spécifique et volume microporeux élevés, pH de surface alcalin, présence d'espèces métalliques (notamment Ca, Al, Fe), groupes contenant de l'oxygène. L'étude des mécanismes a mis en évidence la grande variété de composés soufrés produits lors des essais d'élimination de H<sub>2</sub>S par un mécanisme réactionnel complexe. Les mécanismes mis en jeu sont l'adsorption dissociative et l'oxydation comme cela est présenté sur la Figure 6.9 (« Mechanisms of H<sub>2</sub>S adsorption onto alum sludge »).

Enfin, les coefficients de transfert de masse globaux ont été déterminés en tenant compte de la résistance du film et de la résistance au pore ce qui a permis d'évaluer la diffusivité superficielle de H<sub>2</sub>S sur la surface intérieure des boues d'aluminium. Comme les boues d'aluminium ont une structure microporeuse, il a été conclu que la diffusion de Knudsen était le principal mécanisme de diffusion. De plus, la diffusivité de Knudsen, la diffusivité moléculaire, la diffusion dans les pores restent constantes pour les différentes conditions opératoires testées (masse d'adsorbant, débit de gaz).

Cette étude a permis de montrer que les boues d'aluminium, disponibles en grande quantité peuvent être valorisées comme adsorbant pour la purification des gaz à température ambiante. Cela ouvre donc de nouvelles perspectives de valorisation des boues d'aluminium ainsi qu'une solution économique pour l'épuration des gaz résiduels.

## **Chapitre 7 : Système d'aération innovant à partir de boues d'aluminium pour l'élimination d'H<sub>2</sub>S et la purification des eaux usées**

Ce chapitre décrit une voie de valorisation des boues d'aluminium comme système de biofiltration pour des zones humides construites à base de ces boues. Grâce à un système innovant à écoulement vertical aéré et piloté par les « gaz résiduels », il est possible d'obtenir simultanément une élimination des polluants dans les eaux usées et une purification des gaz résiduels.



Il a été mis en place à l'échelle de laboratoire trois colonnes à flux vertical aérées en parallèle contenant des boues d'aluminium. La colonne 1 a été aérée de façon intermittente avec du H<sub>2</sub>S (basé sur l'air), la colonne 2 est aérée par intermittence avec de l'air et la colonne 3 n'est pas aérée et sert de témoin. Des eaux usées synthétiques ont été utilisées et chaque zone humide a été exploitée selon un modèle de traitement par lots et aérée par intermittence 4 heures par jour. Des analyses au cours du temps de l'eau usée (phosphore total, azote total, ammoniac, demande chimique en oxygène) et du H<sub>2</sub>S contenu dans le gaz épuré sont effectuées au niveau de la colonne 1 au cours du temps. Les essais se sont déroulés sur une durée de six mois et les colonnes en parallèle ont été ventilées par intermittence avec 200 ppm de H<sub>2</sub>S (colonne 1), d'air (colonne 2) et non dilué (colonne 3 à blanc).

Les résultats montrent que les trois colonnes présentent une efficacité d'élimination élevée (> 98%) du phosphore total (Figure 6). Les gaz pollués (H<sub>2</sub>S) et l'air pourraient augmenter de manière significative l'efficacité d'élimination de la DCO de  $94,3 \pm 3,0$ ,  $94,8 \pm 1,9\%$  et le TN de  $86,2 \pm 14,2$ ,  $91,6 \pm 5,4\%$ . En effet, aucune différence significative n'a été observée en ce qui concerne les performances d'élimination de DCO et de TN sans aération.

Le suivi de la concentration en H<sub>2</sub>S en sortie de la colonne 1 a montré que l'H<sub>2</sub>S restait en totalité dans la colonne 1 lors des étapes d'aération. La boue d'aluminium joue ainsi un rôle de biofiltre.

Pour la première fois, les gâteaux de boues d'aluminium étaient utilisés simultanément comme moyen de réduction du H<sub>2</sub>S et du traitement des eaux usées. En effet, il a été largement admis que les biofiltres devraient avoir une grande surface spécifique, une faible perte de charge, une excellente rétention de l'humidité et une durabilité élevée. Le support devrait également fournir des nutriments et un environnement propice à une couche biologique active communauté de microbes

Cette étude a montré que les gâteaux de boues d'aluminium pouvaient être utilisées comme adsorbant pour le traitement simultané de l'H<sub>2</sub>S et l'épuration des eaux usées.

## Conclusions

L'eau potable est une ressource vitale et l'élimination des résidus provenant des stations de traitement des eaux potables est un problème sociétal et environnemental car leur mise en décharge et leur rejet direct dans la nature constitue un danger pour l'environnement et la santé publique. Dans ce contexte, la valorisation de ces boues d'aluminium est devenue primordiale. Cette valorisation doit tenir compte de deux aspects, la durabilité économique mais aussi environnementale. Cette thèse a permis d'étudier et de montrer cinq options de réutilisation des boues d'aluminium tout en tenant compte de la gestion des déchets et du développement durable répondant à des normes environnementales strictes.

Ces travaux ont confirmé que les propriétés des boues d'aluminium étaient «spécifiques au site» (elles varient selon la période et le lieu). Par exemple, en ce qui concerne les deux sources de boues d'aluminium considérées dans ce travail, les boues d'aluminium de Carmaux présentaient un caractère alcalin (pH = 10), une taille de particule plus petite (d<sub>50</sub> = 16,5 µm), une structure poreuse microporeuse, une phase plus cristalline et une grande quantité de composition des éléments (53419 mg / kg), etc. Ceci est dû aux importantes variabilités des propriétés, qui sont principalement influencées par la qualité de l'eau de source, la nature des produits chimiques utilisés et le type de processus de purification de l'eau brute impliqués. Les

résultats des différentes caractérisations ont également indiqué que ces propriétés sont importantes pour le choix de la possible valorisation. Par conséquent, une connaissance préalable des propriétés physiques et chimiques des boues d'aluminium est nécessaire afin de les réutiliser et les recycler de façon sûre et durable.

Tout d'abord, les boues d'aluminium ont été utilisées en remplacement d'une partie de l'argile dans la fabrication des briques, en incorporant différents pourcentages de boues d'aluminium. Les résultats ont montré que les briques composées de boues d'aluminium et d'argile sont conformes aux « normes européennes et irlandaises » et démontrent ainsi le potentiel pour une application industrielle des boues d'aluminium dans la fabrication de briques en terre cuite.

Dans un second temps, les boues d'aluminium ont été utilisées comme adsorbant des polluants présents dans l'agriculture. Le glyphosate est un ingrédient actif dans les pesticides utilisés massivement dans l'agriculture et représente une problématique environnementale majeure. La boue d'aluminium et la tourbe irlandaise ont été comparées pour l'élimination du glyphosate lors de tests en pot à l'échelle laboratoire. Les résultats ont mis en évidence la possibilité d'utiliser les boues d'eau potable comme adsorbants pour le traitement des eaux usées agricoles.

Le co-conditionnement et la déshydratation des boues de station d'épuration avec des boues d'aluminium ont également été étudiés et validés. Cette approche a permis de montrer la possible valorisation des boues d'aluminium des stations de traitement des eaux avec une approche durable.

Une autre voie de valorisation des boues d'aluminium comme adsorbant pour la purification des gaz a été étudiée lors d'expériences d'adsorption de  $H_2S$  dans un réacteur à lit fixe dans différentes conditions expérimentales. Les données expérimentales d'adsorption de  $H_2S$  ont été modélisées à l'aide d'équations empiriques basées sur la cinétique d'adsorption. Les résultats ont montré que les boues d'aluminium sont un adsorbant efficace pour l'élimination de  $H_2S$  (capacité de 374,2 mg  $H_2S$ /g solide) et que des mécanismes mis en jeu sont l'adsorption dissociative et l'oxydation. Les coefficients de transfert de masse globaux ont également été déterminés et peuvent servir pour le changement d'échelle. Dans les différentes approches abordées, une attention particulière a été portée sur la compréhension des processus et mécanismes mis en œuvre.

Enfin, les gâteaux de filtration des boues d'aluminium ont été réutilisés pour la purification simultanée de  $H_2S$  et le traitement des eaux usées. Les résultats ont montré la capacité de cet adsorbant pour éliminer l' $H_2S$  présent avec une grande efficacité d'élimination de la Demande Chimique en Oxygène, l'azote total, le phosphore total.

Ainsi, ce travail a permis de démontrer le potentiel de valorisation de boues d'eau potable dans différents domaines avec un réel intérêt environnemental de même que pour déterminer les mécanismes réactionnels mis en œuvre dans les différents processus ont également été étudiés et mis en évidence.

## Perspectives

L'élimination des boues de traitement d'eau potable est un sujet de préoccupation croissante, et leur possible valorisation dans différents domaines est donc nécessaire. Afin de compléter ce travail, des travaux complémentaires portant sur la compréhension des mécanismes, la validation à l'échelle pilote seraient nécessaires.

Deux origines des boues d'aluminium ont été considérées dans ce travail (Dublin, Carmaux). Une cartographie plus élargie à différentes régions, pays seraient intéressante afin de déterminer leur pertinence pour des utilisations bénéfiques. La nature physicochimique des boues d'aluminium produites au cours des différentes opérations de traitement est différente, ainsi la caractérisation de ces résidus est essentielle pour un recyclage plus approprié en fonction des caractéristiques de ces boues.

L'utilisation des boues dans la fabrication de briques en terre cuite constitue un moyen économique et écologique comme cela a été montré pour les boues en Irlande. Cette étude a montré que les briques commerciales devaient être cuites à 1200 °C, une incorporation de boue de 10% à 20% massique donne des caractéristiques de résistance et d'absorption d'eau satisfaisantes pour les briques à usage commercial. Cette proportion de boue lorsqu'elle est cuite à 1100 °C a l'apparence la plus proche des briques en terre cuite traditionnelles. À ce jour, aucun projet pilote n'a été mis en place pour étudier l'utilisation des boues de traitement des eaux dans la fabrication de briques en terre cuite à l'échelle industrielle en Irlande et en France. Une étude à l'échelle pilote devrait être faite afin de confirmer les résultats obtenus à l'échelle laboratoire. La réutilisation dans le domaine du génie civil est aussi à envisager afin d'utiliser les briques en argile-boue d'aluminium pour les chaussées et parkings ou comme matériaux de construction tout en respectant la réglementation en vigueur.

L'efficacité significative d'élimination du glyphosate par les boues d'aluminium a dépassé les attentes basées sur la littérature. Des recherches plus poussées pourraient être menées sur une période plus longue (supérieure à 10 semaines) et en passant à l'échelle pilote afin de mieux comprendre la capacité des boues d'aluminium en tant qu'adsorbant à faible coût. Il serait également nécessaire d'effectuer des expériences au cours desquelles l'effet du pH et de la concentration initiale du glyphosate serait étudiée afin d'avoir une meilleure compréhension et analyse de la capacité d'élimination. En outre, les futures études sur la tourbe doivent inclure un examen complet des méthodes de prétraitement de la tourbe et de leurs effets sur la performance d'élimination des polluants.

La stratégie de co-conditionnement et de déshydratation a été identifiée comme une situation «gagnant-gagnant» du point de vue technique. D'autre part, pour diverses applications complètes sur site de boues d'aluminium dans le processus de co-conditionnement, une analyse rentable «spécifique au site» locale de l'efficacité du processus, du transport des boues, d'une administration supplémentaire et d'autres paramètres de processus devrait être considérés en dernière analyse.

D'après les expériences d'élimination de l'H<sub>2</sub>S, la capacité d'adsorption des boues d'aluminium s'est révélée élevée par rapport à la majorité des adsorbants utilisés classiquement. De manière significative, les boues d'aluminium pourraient être directement réutilisées en tant que «média prêt à l'emploi» sans aucun traitement supplémentaire. Cette étude a démontré que l'utilisation de boues d'aluminium pour le contrôle de l'H<sub>2</sub>S pourrait constituer un bon matériau / adsorbant pour les systèmes d'adsorption. Leur utilisation ouvre une nouvelle voie pour la désulfuration,

mais aussi pour la réduction des odeurs et la gestion des boues. Afin de confirmer les résultats obtenus lors de cette étude, des expériences montrant la répétabilité, des essais plus longs en laboratoire pour déterminer le temps de saturation du solide sont nécessaires. Le passage à l'échelle pilote est également nécessaire afin de confirmer les résultats obtenus à l'échelle du laboratoire. Les boues d'aluminium présentant des caractéristiques différentes selon les sites, elles doivent être testées ultérieurement afin de comprendre quelles sont les principales propriétés qui contrôlent l'adsorption de H<sub>2</sub>S par les boues d'aluminium. Un autre aspect devra également être abordé, la régénération de l'absorbant.

Les boues d'aluminium se sont d'abord révélées être un adsorbant efficace pour l'élimination de l'H<sub>2</sub>S contenu dans l'atmosphère mais également dans des milieux humides construits aérés. Les différentes substances odorantes telles que l'ammoniac (NH<sub>3</sub>), les COV et les mélanges de polluants doivent être prises en compte dans les études futures. Les problèmes d'élimination finale ou de la régénération des absorbants, après leur utilisation doivent être étudiés en détails. Il est nécessaire de rappeler que la caractérisation des boues d'aluminium est une étape essentielle pour sélectionner l'adsorbant avant les essais d'adsorption. Par exemple, il a été montré que les boues d'aluminium de Dublin et de Carmaux présentent une différence significative en ce qui concerne l'efficacité d'élimination de l'H<sub>2</sub>S.

## Contents

Acknowledgements .....	i
Abstract .....	ii
Résumé .....	iii
Résumé Long en français .....	iv
Nomenclature .....	xvii
Symbols .....	xvii
Abbreviations .....	xviii
General Introduction .....	1
Bibliography .....	5
Chapter 1 .....	7
Background and Literature Review .....	7
Introduction .....	7
1.1 Overview of conventional water treatment processes .....	7
1.2 Beneficial reuse of water treatment plant residues .....	9
1.2.1 Alum sludge incorporation in brick manufacturing .....	10
1.2.2 Alum sludge reuse in wastewater treatment .....	11
1.2.3 Recovery and reuse of coagulants from alum sludge .....	17
1.2.4 Alum sludge application in land-based uses .....	18
1.3 Current states of odor control technologies in WWTPs .....	20
1.3.1 Physical/chemical technologies .....	20
1.3.2 Biotechnological treatment .....	27
1.3.3 Summary of different odor control technologies .....	38
1.3.4 Challenges and perspectives of odor abatement technologies in WWTPs .....	39
1.4 Motivation and objectives of the study .....	40
Bibliography .....	40
Chapter 2 .....	51
Materials and Methods .....	51
Introduction .....	51
2.1 Materials .....	51
2.2 Characterization of alum sludge .....	53
2.2.1 Characterization methods .....	53
2.2.2 Results .....	56
2.3 Experimental Methods .....	66
2.3.1 Alum sludge incorporated in clay brick manufacturing .....	66
2.3.2 Alum sludge and Irish peat for glyphosate removal .....	67
2.3.3 Co-conditioning of waste-activated sludge with alum sludge .....	69
2.3.4 Alum sludge as an efficient sorbent for hydrogen sulfide removal .....	70
2.3.5 Simultaneous hydrogen sulfide purification and wastewater treatment in a novel aerated alum sludge based constructed wetland .....	74
2.4 Summary .....	76
Bibliography .....	76
Chapter 3 .....	78
Alum sludge incorporated in clay brick manufacturing .....	78
3.1 Introduction .....	78
3.2 Materials and methods .....	79
3.2.1 Alum sludge and clay .....	79
3.2.2 Production of the sample bricks .....	79
3.3 Testing the sample bricks .....	81

---

3.3.1 Compression strength testing .....	81
3.3.2 Loss on ignition testing .....	82
3.3.3 Water absorption testing.....	82
3.3.4 Compression testing after being submerged in water for 24 h.....	83
3.3.5 General appearance & texture .....	83
3.4 Results and discussion .....	83
3.4.1 Compressive strength results .....	83
3.4.2 Loss on ignition.....	84
3.4.3 Water absorption testing.....	84
3.4.4 Compressive Strength after Submersion in Water for 24 h.....	87
3.4.5 General appearance and texture .....	87
3.5 Prospects.....	89
3.6 Conclusions .....	90
Bibliography.....	90
Chapter 4 .....	92
Alum Sludge and Irish Peat for Glyphosate Removal .....	92
4.1 Introduction .....	92
4.2 Materials and methods .....	94
4.2.1 Materials.....	94
4.2.2 Pot setup .....	94
4.2.3 Dosing and sampling.....	95
4.2.4 Analysis .....	96
4.3 Results and discussion.....	96
4.4 Conclusions .....	100
Bibliography.....	100
Chapter 5 .....	103
Co-conditioning of Waste-activated Sludge with Alum Sludge .....	103
5.1 Introduction .....	103
5.2 Materials and Methods .....	105
5.2.1 Materials.....	105
5.2.2 Co-conditioning procedure.....	106
5.2.3 Characterization and analyses .....	107
5.3 Results and discussion.....	107
5.3.1 Characterization of the two kinds of sludges .....	107
5.3.2 Optimal mixing ratio of the sludges .....	109
5.3.3 Polymer conditioning of the mixed sludge .....	111
5.3.4 Case analysis .....	112
5.4 Conclusion.....	114
Bibliography.....	114
Chapter 6 .....	117
Alum Sludge as An Efficient Sorbent for Hydrogen Sulfide Removal .....	117
6.1 Introduction .....	117
6.2 Materials and Methods .....	119
6.2.1 Sorbent and Characterization .....	119
6.2.2 Sorption Test.....	120
6.2.3 Modeling .....	122
6.2.4 Determination of mass transfer coefficient .....	123
6.3 Results and Discussion.....	124
6.3.1 Sorbent characterization.....	124
6.3.2 Sorption trials .....	126

---

6.3.3 Breakthrough through curves modeling.....	128
6.3.4 Adsorption Mechanisms of H <sub>2</sub> S onto alum sludge .....	133
6.3.5 Determination of the mass transfer coefficient .....	140
6.4 Perspectives.....	143
6.5 Conclusions .....	143
Bibliography.....	144
Chapter 7 .....	148
Simultaneous Hydrogen Sulfide Purification and Wastewater Treatment in a Novel Aerated Alum Sludge- Based Constructed Wetland.....	148
7.1 Introduction .....	148
7.2 Material and methods .....	150
7.2.1 Alum sludge based VFCW configuration .....	150
7.2.2 Analysis .....	153
7.2.3 Data interpretation.....	154
7.3. Results and discussion.....	154
7.3.1 Pollutants removal performance of the three columns.....	154
7.3.2 The overall removal efficiency of pollutants in three columns.....	158
7.3.3 H <sub>2</sub> S removal efficiency .....	160
7.3.4 Alum sludge as a media for H <sub>2</sub> S abatement .....	162
7.4 Conclusions .....	162
Bibliography.....	163
Conclusions and Prospects .....	166
Conclusions .....	166
Prospects .....	170
Appendix I.....	172
List of Figures .....	172
Appendix II .....	175
List of Tables.....	175
Appendix III .....	176
Scientific Contributions.....	176

# Nomenclature

## Symbols

$A$ ( $m^2$ )	Area
$a_{ads}$ ( $m^2$ )	Surface area for external transfer
$L$ ( $m$ )	Length
$R^2$	Coefficient of determination
$Q$ ( $L/min$ )	Inlet flow rate
$M$ ( $g/mol$ )	The molecular weight of $H_2S$
$C_t$ ( $mg/kg$ )	Effluent concentration
$C_0$ ( $mg/kg$ )	Inlet concentration
$C_b$ ( $mg/kg$ )	Breakthrough $H_2S$ concentration
$C_e$ ( $mol/m^3$ )	Concentration at the surface of the sorbent
$d_p$ ( $m$ )	Mean particle diameter
$d_{pore}$ ( $m$ )	Mean pore diameter
$D$ ( $mm$ )	Internal diameter
$D_e$ ( $m^2/s$ )	Effective diffusivity
$D_k$ ( $m^2/s$ )	Knudsen diffusivity
$D_m$ ( $m^2/s$ )	Molecular diffusivity
$D_p$ ( $m^2/s$ )	Pore diffusion coefficient
$D_s$ ( $m^2/s$ )	Surface diffusivity
$J$ ( $mol/m^2 \cdot s$ )	The transferred flux
$h$ ( $cm$ )	Bed depth
$K_{ext}$ ( $m/s$ )	External mass transfer coefficient
$K_{Th}$ ( $m^3/mg \cdot min$ )	Thomas rate constant (Thomas model)
$K_a$ ( $s^{-1}$ )	Overall effective mass transfer coefficient
$K_e$	Equilibrium constant
$q_0$ ( $kg/L$ )	The maximum adsorption capacity (Thomas model)
$K$ ( $L/mg \cdot min$ )	Adsorption rate constant (BDST model)
$N_0$ ( $kg/L$ )	Adsorption capacity (BDST model)
$u$ ( $cm/min$ )	Linear flow rate (BDST model)
$K_{YN}$ ( $min^{-1}$ )	YN rate constant (YN model)
$\tau$ ( $min$ )	The time required for 50 % adsorbate breakthrough
$M$ ( $g/mol$ )	Molecular weight
$m$ ( $kg$ )	Mass of sorbent
$T$ ( $K$ )	Absolute temperature
$t$ ( $min$ )	Adsorption time
$t_b$ ( $min$ )	Breakthrough time
$P$ ( $atm$ )	Pressure of gas
$R$ ( $J/mol \cdot K$ )	Ideal gas constant
$V_{gas}$	Diffusion volume of gas
$V$ ( $m^3$ )	Volume of the adsorption bed
$v$	Specific filtrate volume
$r_m$	Resistance
$\alpha_m$	Specific resistance



---

$\phi_0$	Bulk or initial porosity
$\rho_s$	Density
$\varepsilon$	Bed void fraction
$\varepsilon_p$	Porosity
$q$ (mol/kg)	The amount adsorbed
$\mu$	Gas viscosity
$f_{tor}$	Tortuosity factor
$\eta_L$	Liquid viscosity

### Abbreviations

AC	Activated carbon
Alum	Aluminium sulfate
Al-VFCW	Alum sludge based vertical flow constructed wetlands
ASD	Activated sludge diffusion
BDST	Bed service time
BET	Brunauer, Emmett and Teller
BF	Biofilter
BOD	Biochemical oxygen demand
BPEO	Best practicable environmental option
BS	Bioscrubbers
BTC	Breakthrough curve
BTF	Biotrickling filters
COD	Chemical oxygen demand
CS	Chemical scrubbers
CST	Capillary suction time
CWs	Constructed wetlands
DO	Dissolved oxygen
DSC	Differential scanning calorimetry
DTG	Derivative thermogravimetric
EBCT	Empty bed contact time
EBRT	Empty bed residence time
EDS	Energy-dispersive spectrometry
EDTA	Ethylenediaminetetraacetic acid
EPS	Extracellular polymeric substances
FTIR	Fourier transformed infrared
GAC	Granular activated carbon
HRT	Hydraulic retention time
ICP	Inductively-coupled plasma discharge
Lab.	Laboratory
LOI	Loss on ignition
MC	Moisture content
MOF	Metal-organic frameworks
MSWI	Municipal solid waste incineration
MTZ	Mass transfer zone
MWCNT	Multi-wall carbon nanotubes
NH <sub>4</sub> -N	Ammonia-nitrogen
NLDFT	Non-local Density Functional Theory
NOM	Natural organic matter
NSC	National Science Council

---

PAC	Powdered activated carbon
PACl	Polyaluminium chloride
PMS	Peroxymonosulfate
RE	Removal efficiency
RHA	Rice husk ash
SS	Suspended solids
SEM	Scanning electron microscope
SRF	Specific resistance to filtration
TCD	Thermal conductivity detector
TDRP	Tire-derived rubber particles
TEM	Transmission electron microscopy
TGA	Thermogravimetric analysis
TN	Total nitrogen
TOC	Total organic carbon
TP	Total phosphates
TSS	Total suspended solids
UASB	Up-flow anaerobic sludge blanket
UV	Ultraviolet
VFCW	Vertical flow constructed wetlands
VF	Volatile Matter
VOCs	Volatile organic compounds
WTP	Water treatment plant
WWTP	Wastewater treatment plant
WTRs	Water treatment residues
XRD	X-ray diffraction
YN	Yoon-Nelson



## General Introduction

Booming of population and urbanization brought worldwide potable water demand. However, from a technical point of view the production of reliable and safe drinking water process always accompanied by the generation of water treatment residues (WTRs) [1]. Since the conventional water treatment plants (WTPs) involve the process of coagulation, flocculation, sedimentation, filtration and disinfection, large quantity of residues as inevitable by-product was generated during the “flocculation/ coagulation” processes known as WTRs [2]. Alum sludge is one of the WTRs when aluminum sulphate was used as the main agent in flocculation and coagulation process. It is a locally, easily and largely available by-product in towns, cities and metropolis worldwide.

WTRs production from drinking water treatment is generally estimated to represent 1–3 % in volume of the raw water used during the treatment process [3]. A typical WTP produces about 100,000 tons/year of sludge whereas, on a global scale, available literature estimates that at present the daily production of sludge exceeds 10,000 tons [4]. Surprisingly, specific data on global- or regional-level WTRs generation are seldom available because the local authorities usually publish the waste statistics in a broad category instead of specifying each waste type. Within the EU members, the WTRs is included in the Code 19 in the List of Waste [5]; thus, it is difficult to retrieve the exact WTRs generation of a country or region. Figure 0.1 presents the WTRs annual generation of several countries [1,4,6]. The WTRs generation in China is the largest of 2.3 million tons per year, however the largest quantity of annual WTRs generation per person was Korea. By contrast, Denmark has the least WTRs generation of 9000 tons/year as well as the quantity of annual WTRs generation per person among the thirteen countries. The sludge disposal cost in Netherlands stand at a huge sum of £30-40 million per year, and \$6.2 million per year in Australia, it was also estimated that the alum sludge disposal cost in Ireland will be doubled by the end of the next decade from the present assessment of 15,000-18,000 tons/year of the dried solids [7].

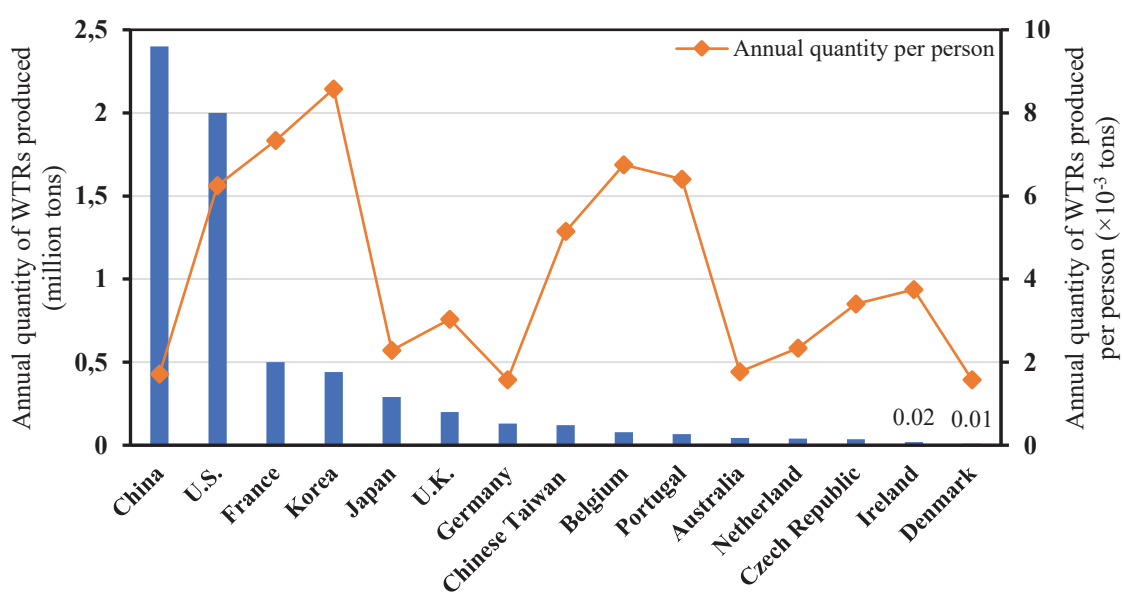
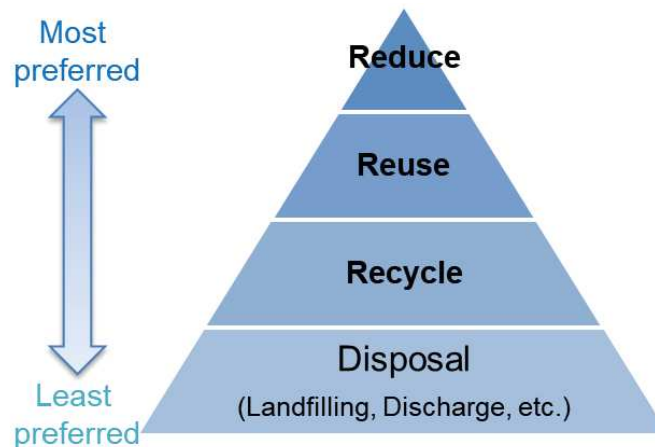


Figure 0.1 Annual WTRs generation by countries (2015) [1,4,6,7]

Although the WTRs generation may not dramatically increase, its disposal, as well as the associated cost and environmental impacts, is still a worldwide issue. There are a number of popular disposal routes for WTRs [1]:

- discharge to a natural water body;
- discharge to sewer;
- discharge to lagoons;
- waste landfill;
- engineering fill.

Historically, there are several popular disposal routes for WTRs, such as discharge to a nearby natural water body, to sewer, and to lagoons. These disposal routes are favorable and less costly, but ultimately meet the water source on downstream side of intake [8]. However, regulations implemented in many countries such as Australia, New Zealand, U.K., and USA have made these routes forbidden or less attractive due to the adverse environmental impacts [3]. Recently, landfilling has been the most widely applied method in most countries over the world (i.e. China, Ireland, France, etc.) and still with the possibility of contamination of water bodies and soil from the chemical products used in the treatment. Notwithstanding, the escalating landfill costs and the reduction in available space push the industries to explore alternative disposal methods. The waste hierarchy, which is a vital approach of “Circular Economy”, as defined by European Directive [5] is regulating which waste technologies should be applied preferentially. As illustrated in Figure 0.2, the hierarchy starts as the “3R principle”: reduce, reuse, and recycle. Disposal (such as landfill) is ranking in the last. Therefore, it is crucial to identify viable management options for WTRs, particularly where WTRs can be effectively utilized in an environmentally acceptable and sustainable manner.



**Figure 0.2** Diagram of waste hierarchy as regulated European Directive [5]

To date, there are four broad categories of alum sludge beneficial reuse, as illustrated in Figure 0.3 [9-12]. These efforts include the use in wastewater treatment process, use as building/construction materials, and land-based application [4]. Although numerous research studies can be found in the last decades, there is still a huge challenge to examine potential options for recycling and reusing of alum sludge, while quantifying any potential savings and environmental benefits may arise.

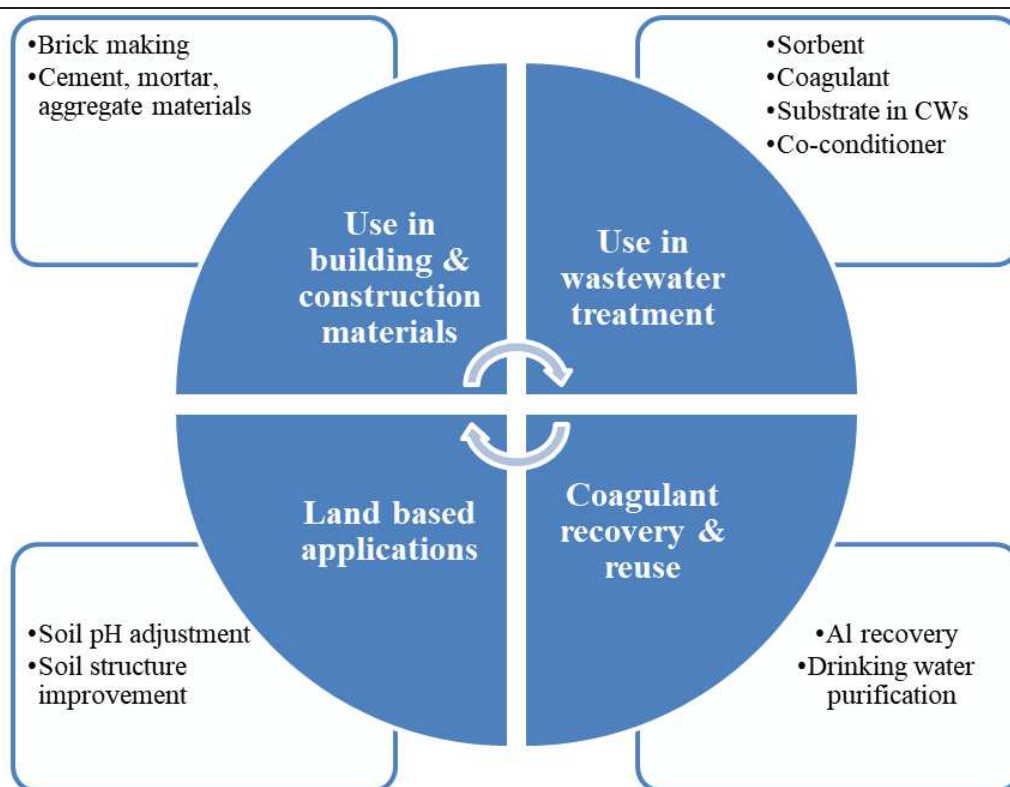


**Figure 0.3** The beneficial reusing ways of alum sludge [9-12]

Thus, the main aim of this work was to identify and explore the novel beneficial reusing routes of alum sludge which could contribute to the state of the art of alum sludge beneficial reuse, taking into account the geographical difference in alum sludge characteristics is also considered.

The structure of this thesis is shown in Figure 0.4. The PhD study was developed according to an international cooperation between University College Dublin, Ireland and IMT Mines Albi, France.

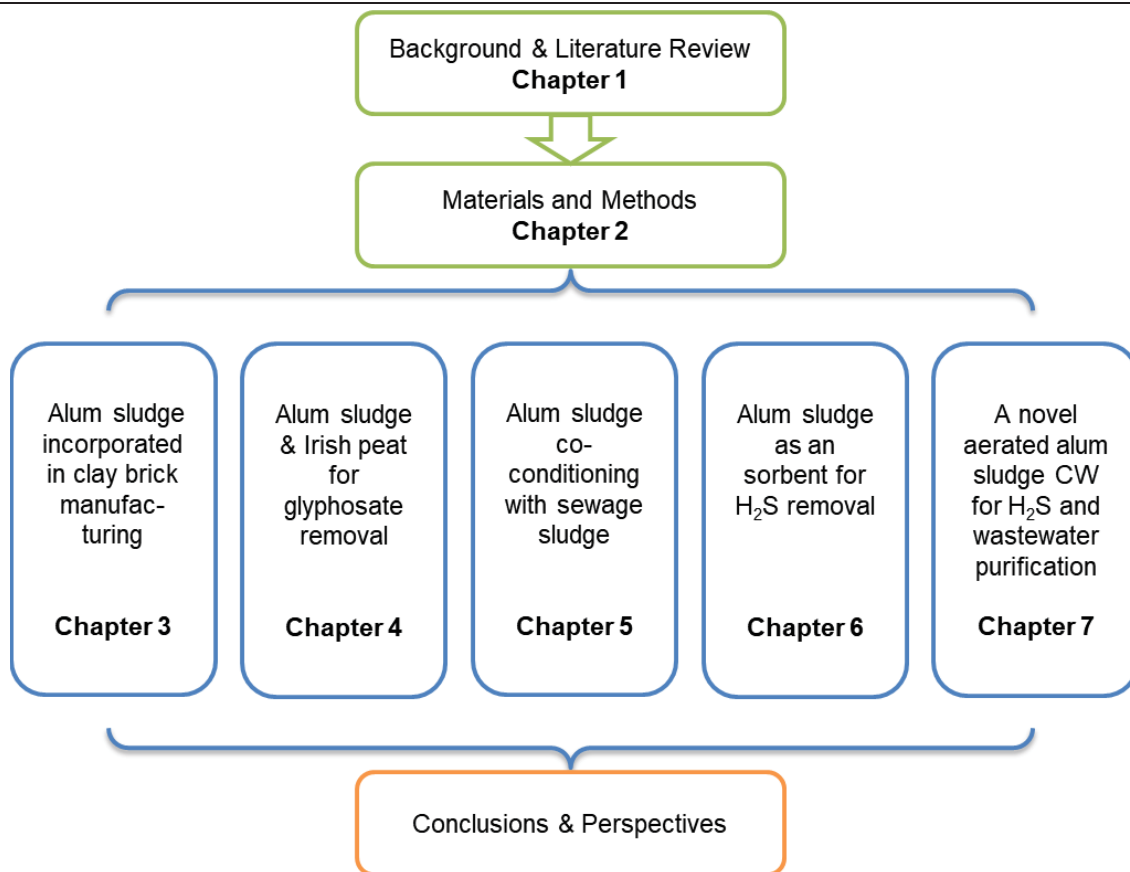


Figure 0.4 Structure of the thesis

**Chapter 1** provides the background information on the origin of alum sludge, i.e. the various water treatment processes. Afterwards, the state of the art of alum sludge beneficial reuse in different fields was presented. The third section is focused on the current states of odor control technologies in WWTPs, which were comprehensively reviewed and allowed to identify a novel alum sludge reuse route as an sorbent for waste gas purification.

**Chapter 2** describes the two sources of alum sludge which are collected from Dublin, Ireland and Carmaux, France, respectively. Afterwards, physiochemical and thermal characterization of the two alum sludges was presented, and the various experimental methods and models used were summarized.

**Chapter 3** conducts an experimental study to investigate the possible incorporation of alum sludge as a partial replacement for clay in brick manufacturing. It is the first study of this kind of problem in Ireland. Clay bricks were made at different temperatures, incorporating different percentages of alum sludge, and then subjected to various tests (compression, LoI, water absorption, appearance, etc.). It was found that the final alum sludge clay bricks have met the European and Irish Standards and demonstrated the promising potential and prospects for Irish dewatered alum sludge cakes in clay-sludge brick making.

**Chapter 4** compares the glyphosate (an active ingredient in pesticide which is massive employed in Irish agriculture) removal efficiency of alum sludge and Irish peat in aqueous solution. Organic phosphonate of glyphosate was removed in pot tests separately filled with two kinds of media, i.e. alum sludge and peat, while effluent samples were taken for the concentration of phosphorus and COD (chemical oxygen demand) analyzing; The results show that the P removal capacity of alum sludge was significant (>99 %), while the removal capacity

of peat was considerably less than 10 % after ten weeks. This Chapter provides a scientific clue for sorbents selection when considering alum sludge and peat to maximize their value in practice.

**Chapter 5** focuses on alum sludge co-conditioning and dewatering with waste-activated sludge from a wastewater treatment plant in France. Jar-test experiment has demonstrated that the optimal mix ratio for the two sludges is 1:1 (waste-activated sludge/alum sludge; v/v). The use of the alum sludge has been shown to beneficially enhance the dewaterability of the resultant mixed sludge, highlighting a huge savings in polymer addition (14 times less than the current technologies). Significantly, it provided an “win-win” solution for sludge disposal of Graulhet water industry.

**Chapter 6** presents the first experimental, mechanisms and modeling studies of using alum sludge for H<sub>2</sub>S adsorption at room temperature. The effect of flow rate and bed depth (mass) was investigated and three kinetics models namely, Thomas, Bed Depth Service Time and Yoon-Nelson were used for breakthrough curves modeling. The mechanisms of H<sub>2</sub>S adsorption onto alum sludge as well as the mass transfer phenomenon were studied in detail, i.e. the various mass transfer coefficient. Results show that alum sludge is an efficient sorbent for H<sub>2</sub>S removal (capacity of 374.2 mg/g) and the mechanisms including dissociative adsorption and oxidation were proposed. Moreover, the overall mass transfer coefficients were calculated which could be used for the scaling up of the process.

**Chapter 7** deals with the integration of alum sludge based constructed wetlands (CWs) with biofiltration system. By using the “waste gas” driven aerated vertical flow CWs, the improved pollutant removal in wastewater and the waste gas purification can be simultaneously achieved. Three lab-scale parallel alum sludge-based aerated vertical flow CWs were set up, column 1 was intermittently aerated with H<sub>2</sub>S (based on air); Column 2 was intermittently aerated with air, while Column 3 was unaerated and served as a control. Synthetic wastewater was used and each wetland was operated by batch model and intermittently aerated for four hours per day. The long-term pollutant removal performance as well as the H<sub>2</sub>S removal efficiency were examined and compared. Results show that H<sub>2</sub>S was completely removed during the six-month’s trials, while the high removal efficiency of COD, TN, TP were achieved. It demonstrated a novel eco-friendly alum sludge based CW for H<sub>2</sub>S purification and simultaneous wastewater treatment.

Finally, the general conclusions derived from the present work are summarized, and prospects are proposed for future research studies to expend the current investigations.

## Bibliography

1. Zhao, Y., Liu, R., Awe, O.W., Yang, Y., Shen, C.: Acceptability of land application of alum-based water treatment residuals – An explicit and comprehensive review. *Chemical Engineering Journal* **353**, 717-726 (2018). doi:<https://doi.org/10.1016/j.cej.2018.07.143>
2. Ahmad, T., Ahmad, K., Alam, M.: Sustainable management of water treatment sludge through 3‘R’ concept. *J. Clean Prod.* **124**(Supplement C), 1-13 (2016). doi:<https://doi.org/10.1016/j.jclepro.2016.02.073>
3. Hidalgo, A.M., Murcia, M.D., Gomez, M., Gomez, E., Garcia-Izquierdo, C., Solano, C.: Possible Uses for Sludge from Drinking Water Treatment Plants. *Journal of Environmental Engineering* **143**(3), 7 (2017). doi:10.1061/(asce)ee.1943-7870.0001176
4. Babatunde, A.O., Zhao, Y.Q.: Constructive Approaches Toward Water Treatment Works



- Sludge Management: An International Review of Beneficial Reuses. *Critical Reviews in Environmental Science and Technology* **37**(2), 129-164 (2007). doi:10.1080/10643380600776239
5. Communities, C.o.E.: Directive 2008/98/EC of the European Parliament and of the Council of 19 November 2008 on waste and repealing certain Directives. <https://eur-lex.europa.eu/eli/dir/2008/98/oj> (2008). Accessed Feb. 2019
  6. Ahmad, T., Ahmad, K., Alam, M.: Sustainable management of water treatment sludge through 3'R' concept. *J. Clean Prod.* **124**, 1-13 (2016). doi:10.1016/j.jclepro.2016.02.073
  7. Dassanayake, K.B., Jayasinghe, G.Y., Surapaneni, A., Hetherington, C.: A review on alum sludge reuse with special reference to agricultural applications and future challenges. *Waste Management* **38**, 321-335 (2015). doi:<https://doi.org/10.1016/j.wasman.2014.11.025>
  8. Ackah, L.A., Guru, R., Peiravi, M., Mohanty, M., Ma, X.M., Kumar, S., Liu, J.: Characterization of Southern Illinois Water Treatment Residues for Sustainable Applications. *Sustainability* **10**(5), 14 (2018). doi:10.3390/su10051374
  9. Aghapour, A.A., Khorsandi, H., Dehghani, A., Karimzade, S.: Preparation and characterization and application of activated alumina (AA) from alum sludge for the adsorption of fluoride from aqueous solutions: new approach to alum sludge recycling. *Water Sci. Technol.-Water Supply* **18**(5), 1825-1831 (2018). doi:10.2166/ws.2018.006
  10. Ahmad, T., Ahmad, K., Alam, M.: Investigating calcined filter backwash solids as supplementary cementitious material for recycling in construction practices. *Construction and Building Materials* **175**, 664-671 (2018). doi:10.1016/j.conbuildmat.2018.04.227
  11. Dube, S., Muchaonyerwa, P., Mapanda, F., Hughes, J.: Effects of sludge water from a water treatment works on soil properties and the yield and elemental uptake of *Brachiaria decumbens* and lucerne (*Medicago sativa*). *Agric. Water Manage.* **208**, 335-343 (2018). doi:10.1016/j.agwat.2018.06.015
  12. Foroughi, M., Chavoshi, S., Bagheri, M., Yetilmezsoy, K., Samadi, M.T.: Alum-based sludge (AbS) recycling for turbidity removal in drinking water treatment: an insight into statistical, technical, and health-related standpoints. *Journal of Material Cycles and Waste Management* **20**(4), 1999-2017 (2018). doi:10.1007/s10163-018-0746-1

## Chapter 1

# Background and Literature Review

In this Chapter, section 1.3 has been published as: **Baiming Ren**, Yaqian Zhao, Nathalie Lyczko, Ange Nzihou. *Current Status and Outlook of Odor Removal Technologies in Wastewater Treatment Plant*. (2019) **Waste and Biomass Valorization**. 10(6) 1443-1458. doi:10.1007/s12649-018-0384-9.

### Introduction

The aim of this Chapter is to provide the background information and the literature review. Firstly, the conventional water treatment process, i.e. the coagulation-flocculation processes, was introduced to provide a general background and origin of alum sludge. Afterwards, the state of the art of alum sludge beneficial reusing in different fields was presented. The main aspects of their reuse are construction materials, wastewater treatment and land-based applications. The third section is focused on the current state of odor control technologies in WWTPs. The current state of waste gas purification technologies including physiochemical and biological treatment process were comprehensively reviewed and allowed to identify a novel alum sludge reuse route as a sorbent for waste gas purification. From the developed literature review, the motivations and objectives of this study were summarized.

### 1.1 Overview of conventional water treatment processes

Raw water from reservoirs, rivers, aquifers and the like may contain a wide variety of contaminants, including micro-organisms, inorganic and organic chemicals, and radionuclides. These impurities may be present as dissolved species, as suspended solid particles, or as species bound to such particles. The term “conventional water treatment processes” refers to the treatment of water from a surface/underground water source by a series of processes and aiming at achieving the following objectives:

- Removal of suspended and colloidal matter to an acceptable level by means of coagulation-flocculation, sedimentation and filtration;
- Disinfection to produce drinkable water;
- Chemical stabilization of the water to prevent corrosion of pipelines, attack on concrete pipes and structures or the formation of chemical scale in distribution systems and fixtures.

The conventional drinking water treatment process is well-established, and robust. Figure 1.1 presents the conventional water treatment processes. The methods for removal of suspended and colloidal material from water include chemical coagulation of small colloidal particles, flocculation of the small particles to form larger flocs or aggregates, followed by sedimentation and filtration. When the water contains a large amount of suspended material, larger suspended particles such as sand particles can be removed by means of settling without coagulation and flocculation.

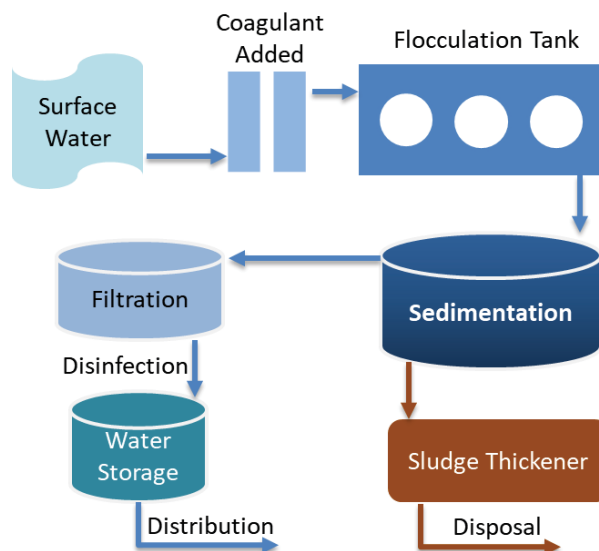


Figure 1.1 Conventional water treatment processes

**Coagulation-Flocculation** is the process by means of which the colloidal particles in water are destabilized (i.e. the nature of the colloidal particles is changed) by adding chemicals (called coagulants), so that they form flocs through the process of flocculation that can be readily separated from the water.

Different chemicals can be used as coagulants. The most common coagulants are:

- ✧ Aluminum sulphate:  $\text{Al}_2(\text{SO}_4)_3 \cdot 16\text{H}_2\text{O}$  is dissolved in water and the aluminum ions  $\text{Al}^{3+}$ , have a high capacity to neutralize the negative charges which are carried by the colloidal particles and which contribute to their stability. Typically, the feedwater is adjusted to a pH range of 5.5 to 7.0 [1]. The aluminum ions hydrolyze and in the process form aluminum hydroxide,  $\text{Al}(\text{OH})_3$  which precipitates as a solid. During flocculation when the water is slowly stirred the aluminum hydroxide flocs enmesh the small colloidal particles. The flocs settle readily and most of them can be removed in a sedimentation tank.
- ✧ Ferric chloride:  $\text{FeCl}_3$  is also commonly used as coagulant. When added to water, the iron precipitates as ferric hydroxide,  $\text{Fe}(\text{OH})_3$  and the hydroxide flocs enmesh the colloidal particles in the same way as the aluminum hydroxide flocs do. The optimum pH for precipitation of iron is not as critical as with aluminum and pH values of between 5 and 8 give good precipitation.
- ✧ Lime: Lime is also used as coagulant, but its action is different to that of alum and ferric chloride. When lime is added to water the pH increases to 10-10.5 [2]. This results in the formation of carbonate ions from the natural alkalinity in the water. The increase in carbonate concentration together with calcium added in the lime results in the precipitation of calcium carbonate,  $\text{CaCO}_3$ . The calcium carbonate crystals also enmesh colloidal particles and facilitate their removal.

**Sedimentation** is the process in which the aggregates that have been formed during coagulation and flocculation are allowed to settle from the water. The flocs collect as sludge at the bottom of the sedimentation tank from where it must be removed on a regular basis. The flocs settle to the bottom of the tank and the clean water leaves the sedimentation tank through collection troughs located at the top of the tank.

**Filtration** normally follows sedimentation or flotation as the final 'polishing' step in conventional water treatment. For instance, Sand filtration is a process in which the water is allowed to filter through a layer of sand in a specially constructed container. In the filtration process the small remaining floc particles are removed by the sand grains and are retained in the bed of sand, while clean water flows out from the bottom of the sand bed.

**Disinfection.** A large fraction of bacteria and larger micro-organisms are removed during clarification processes, especially by sand filtration. However, many bacteria and viruses remain in clarified water even at low turbidity levels. Therefore, essential to disinfect water to prevent the diseases are spread by pathogens (disease-causing micro-organisms) in water. Disinfection of water entails the addition of the required amount of a chemical agent (disinfectant) to the water and allowing contact between the water and disinfectant for a pre-determined period of time (under specified conditions of pH and temperature). Physical methods of disinfection of water include irradiation with ultra-violet light and boiling. The most commonly used disinfectant is chlorine gas  $\text{Cl}_2$ .

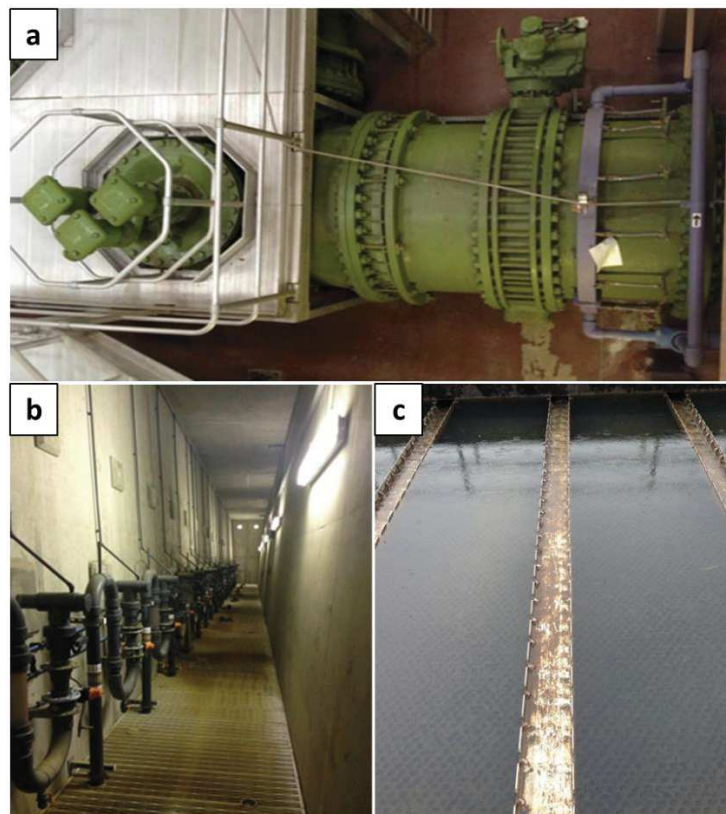


**Figure 1.2** Dublin (Ireland) Ballymore Eustace Water Treatment Plant. (a). the 1600mm intake pipes (green) and the coagulant dosing system (purple pipework); (b). desludging pipes & drain of clarifier; (c). Clarifier

## 1.2 Beneficial reuse of water treatment plant residues

As mentioned above, drinking water treatment plant produce a hygienically safe drinking water for consumption through a variety of treatment processes. However, they also produce waste by-products (water treatment residues or WTRs) including organic and inorganic compounds in liquid and solid phases. Thus, WTRs is defined as “the accumulated solids or precipitate removed from a sedimentation basin, settling tank, or clarifier in a water treatment plant”.

WTRs typically comprise [2]:

- naturally-occurring colloidal and other particulate matter (e.g. silt, clay, algae);
- dissolved natural organic matter (NOM) (e.g. humic acids, fulvic acids);
- precipitated water treatment chemicals;
- oxide precipitates of inorganic species dissolved in the raw water (e.g. iron, manganese);
- filter media flushed out during backwashing.

Indeed, aluminum sulphate which is the main agent in flocculation and coagulation for pre-treatment process has been applied in most of the water treatment plants worldwide [3]. It has been utilized in this regard over the years, due to its availability, effectiveness, easy to use and cheap cost supply. As a result, the largely and inevitable alum sludge was generated from water treatment plant when aluminum sulphate was used for portable water purification and it's the core by-product of "coagulation and flocculation" processes. Generally, alum sludge from most of the water treatment plants are being discharged into nearby drains, which ultimately meet the water source on down-stream side of intake. Otherwise, clarifiers are cleaned once in a year and the sludge is disposed on nearby open lands [4]. The simple method of final disposal, although a less expensive, is not a proper solution due to the possibility of contamination of water bodies and soil from the chemical products used in the treatment.

Therefore, the alum sludge is of environmental concern and requires careful consideration if it is managed in an environmentally acceptable and sustainable manner. The reduce, recycling and reuse, may provide a sustainable solution to the alum sludge management problems under stringent environmental laws [4,5]. In the last decades, various methods have been reported in peer-reviewed journals, conference proceedings, published reports and other documents, environmentally friendly and sustainable alum sludge management has been done to solve this issue. Hence, some of the prominent reuse options identified across the world have been comprehensively reviewed as followed in in the following sections.

### **1.2.1 Alum sludge incorporation in brick manufacturing**

Clay has been used in the past to produce building brick and constant demand of clay for production of brick has made this material expensive and source of clay is depreciating with time. In this context, alum sludge has been utilized in different procedures as fully or partially as substitute to clay in production of clay bricks.

For instances, Elangovan and Subramanian [6] investigated the use of alum sludge in the manufacturing of clay bricks. Sludge was added in different percentage (from 0 to 50 %, in 5 % increments) of dry weight and resulted in 11 varieties of brick which were fired from 700 to 950°C in 50°C increments. The resultant bricks were employed in the loss on ignition (LOI), compressive strength, water absorption and efflorescence tests. It was concluded that using alum-sludge in the clay brick manufacturing process was a worthwhile endeavor. The resulting light-weight bricks from the incorporation of 20 % sludge would result in less dead-weight (0.20 N/mm<sup>2</sup>) of a masonry structure and due to the increased pores in the fired bricks, better insulation properties would be present, this percentage of sludge incorporated into a clay brick fired at 850°C would be the most suitable for load-bearing masonry walls. Additionally, Faris and Aiban [7] replaced ball clay with alum sludge blended with silica fume and zeolite to control deformation and cracking during firing, results have shown that the optimum ratio obtained to produce bricks was 70, 26, 2, 2 % of alum sludge, ball clay, silica fume and zeolite respectively. Usage of 70 % of alum sludge can essentially become a vital step towards sustainable development.



Meanwhile, Hegazy et al. [8] investigated the effects of the use of alum sludge mixed with Rice Husk Ash (RHA) on two mechanical properties of brick: water absorption and compressive strength. Three different series of sludge to rice husk ash (RHA) proportions were studied, which exclusively involved the addition of sludge with ratios 25, 50, and 75 % of the total weight of sludge-RHA mixture. Each brick series was fired at 900, 1000, 1100, and 1200 °C. It concluded that 75 % was the optimum sludge addition to produce brick from sludge-RHA mixture, according to Egyptian Standard Specifications and compared to control brick made entirely from clay. It demonstrated that alum sludge can be a successful partial substitute for brick clay incorporated with agricultural waste materials. Moreover, the addition of some agricultural waste materials, such as rice husk ash can enhance the physical properties of sludge brick, i.e. the compressive strength rising from 28.78 to 79.96 kg/cm<sup>2</sup>. Chiang et al. [9] also reports that lightweight bricks were produced by incorporating alum sludge with an agricultural waste, using heating method that gave a total organic matter burnout and the result indicates that, materials containing 15 wt% rice husk that were sintered at 1100 °C produced low bulk density (less than 1.8 g/cm<sup>3</sup>) and relatively high strength (100 kg/cm<sup>2</sup>) materials that were compliant with relevant standards for use as lightweight bricks. It indicated that alum sludge with agricultural waste would be beneficial to the environment and a good substitute to clay in clay brick production.

Additionally, Huang et al. [10] discussed that, 15 % addition of alum sludge can be utilized in brick production to achieve a first grade brick that can be compared to the commercial brick, which is specified by the Chinese National Science Council (NSC). Moreover, Yadav et al. [11] incorporated sludge in brick manufacturing and discussed that the method of conventional clay brick manufacturing is the same with sludge bricks procedure and no additional requirement is needed in terms of production of alum sludge brick and the findings was encouraging. On the other hand, Cornwell [12] stated that, the chemical and physical properties (such as the lightweight element, aluminum in the sludge, the pores caused when volatile organic matter burnout) of alum sludge are similar to clay used in brick manufacturing and a potential replacement to clay in manufacturing of brick for sustainable building.

In addition, Dassanayake et al. and Babatunde et al. [13,14] reviewed that, the utilization of alum sludge in high content (above 50 %) when producing brick for building purpose would result in decrease in strength (98 %) and other properties such as the texture shrinking observed from the appearance and appearance color turn from red to dark. and recommended that more studies need to be done to establish the suitable alum sludge content in brick production.

Different studies have proven the benefit of reuse of the by-product in manufacturing of brick and the rapid growing market for building in most developing countries whereby employing alum sludge in brick making will be a better sustainable disposal option. However, despite the obvious advantages and increasing researches into the incorporation of alum sludge in building and construction materials, they are yet to be fully accepted in the industry [15]. Of particular concern is the variability in the final product made from alum sludge, due to the variability in their chemical composition and water and organic content, even when such products wholly conform to industry standards. In other words, for sludge products to become fully integrated into the industry, they must be seen to be reliable, with a high degree of compositional stability to make them cost effective and justify their use.

### **1.2.2 Alum sludge reuse in wastewater treatment**

Alum sludge have been used to enhance treatment performance in wastewater treatment

processes from various aspects:

### **a) Alum sludge as coagulant in wastewater treatment plants**

Guan et al. [16] reported that large portion of insoluble aluminum hydroxides present in the alum sludge can be reused as a coagulant to achieve enhanced suspended solids (SS) and chemical oxygen demand (COD) removal in primary sewage treatment. The study reported the improved removal efficiencies of SS as well as COD by 20 % and 15 % respectively at a sludge dose of 18-20 mg Al/L. It has also been noticed that alum sludge improves the thickening and dewatering properties of the combined sludge. Contemporarily, post-treatment of the effluent from an Up-flow Anaerobic Sludge Blanket (UASB) reactor has been investigated by Nair and Ahammed [17] through the coagulation-flocculation process using alum sludge in combination with fresh polyaluminum chloride (PACl) as coagulant. It has been reported that at the optimum conditions of alum sludge dose was 15 g/L, pH 9 and PACl dose of 4.2 mg Al/L, 74 % removal of COD and 89 % removal of turbidity from the UASB effluent could be achieved. The removal of phosphate, suspended solids, biochemical oxygen demand (BOD), and total coliforms was also found to be 79 %, 84 %, 78 % and 99.7 % respectively in addition to high removal of COD and turbidity at the optimum conditions. In addition, Jangkorn et al. [18] found that alum sludge alone could significantly remove turbidity, COD and anionic surfactants present in the wastewater discharged from the industry producing detergents, soaps and other consumer products. However, total suspended solids (TSS) level has increased, but can be removed by adding fresh alum.

Overall, excellent removal efficiencies are reported with combination of alum sludge and fresh alum, which could not have been possible to achieve with fresh alum alone [1]. Sweep-floc mechanism was found to be predominant as compared to physical adsorption and charge neutralization in most of the cases using alum sludge for the removal of contaminants [19]. Alum sludge has the potential of utilization in industrial as well as municipal wastewater treatment processes and thus, can be implemented for enhancing the treatment plant efficiency.

### **b) Alum sludge as a sorbent for contaminants and heavy metal removal from wastewater**

Currently, the development of cost-effective sorbents from by-products is gaining considerable attention, as a possible alternative to commonly used sorbents. Alum sludge is no exception, and so far it has been widely studied as a potential sorbent for the removal of various pollutants and metals in wastewater.

Table 1.1 presents various studies regarding the pollutants and heavy metals adsorbed by alum sludge. It shows that a wide range of contaminants such as phosphorus, boron, fluorides, perchlorate, glyphosate, mercury, arsenate, lead and selenium from the wastewater could be removed through adsorption technique by using alum sludge as low-cost sorbent. The amorphous aluminum is abundantly found in the alum sludge which has greater affinity for anions, making them potential sorbent for removing phosphorus from wastewater. The pH of the adsorption capacity is different for each element. Moreover, among the different phosphate species (organic phosphate, polyphosphate and orthophosphate), orthophosphate sorption on the alum sludge is maximum and follow the order of orthophosphate > polyphosphate > organic phosphate. The difference in adsorption capacities suggests that different mechanisms are responsible for the removal of inorganic and organic phosphates [20]. Apart from that, the phosphate structure and the structure of the complexes formed between phosphate and the sludge can explain the difference between the adsorption capacity. Orthophosphate occupies

the sorbent surface more rapidly since it has a greater diffusion rate due to its smaller molecular weight (94.97 g/mol) than polyphosphate (> 200 g/mol) and organic phosphate (about 400 g/mol) [21].



**Table 1.1** Various pollutants and heavy metals adsorbed by alum sludge

Adsorbate	Adsorption capacity (mg/g)	pH	Concentration (mg/l)	Contact time	Model	Reference
Arsenic (As)	0.34	7.92	83 µg/L	/	Langmuir	[22]
Arsenic As (III)	0.25 mmol/g	9	1mmol	360mins	Langmuir-Freundlich	[23]
Arsenic As (V)	0.28 mmol/g	6				
Boron (B)	0.98	8.3	200	2d	Langmuir	[24]
Cadmium (Cd)	9.2	2-10	10-100	24h	Langmuir	[25]
Cationic Dye	0.45	/	100	10-60mins	pseudo-second order I	[26]
Chromium Cr (III)	0.37					
Chromium Cr (vi)	0.21	6	1 mmol	2h	Langmuir	[27]
Fluorine (F)	5	3.5-8.8	5-35	2-240mins	Langmuir	[28]
Glyphosate	113.6	4.3-9	10-500	24	Langmuir	[29]
Lead Pb (II)	0.3 mmol/g	2-9	0.4-8 mmol	2h	Langmuir	[27]
Mercury (Hg)	79	3-8	10-80 ppm	96h	Langmuir	[30]
Mercury Hg (II)	0.43	6.0	0.2 mmol	10mins	Freundlich	[31]
Molybdate (Mo)	94.65 mmol/kg	6.7	0.1-4 mmol	2h	Langmuir-Freundlich	[32]
P organic phosphate	4.8	4-11				
P orthophosphate	10.2	4-9	5-3500	24h	/	[20]
P polyphosphate	7.4	4-10				
Perchlorate	0.25	/	10-200	1-96h	/	[33]

Phosphate	1.11	6.04	1.5	12d	Langmuir	[34]
	1.59	6.8	4.2			
Selenium (Se)	1.8	5--9	60	24h	/	[35]
Selenium Se (IV)	0.14 mmol/g	5	1mmol	360 mins	Langmuir-Freundlich	[23]
Selenium Se (VI)	0.28 mmol/g	4				
Vanadate (V)	268.13 mmol/kg	6.7	0.1-4	2h	Langmuir-Freundlich	[32]

It was proposed that phosphate adsorption onto the alum sludge is through a kind of inner-sphere complex reaction, which occurs when phosphate replaces the functional groups on the surface of alum sludge and becomes bound to the surface. As a result, phosphate is adsorbed via a precipitation reaction with the aluminum ions, as explained by Eq. (1.1), indicating that ligand exchange is the dominating adsorption mechanism [14].



The electrostatic interactions were identified as main mechanisms for dye removal [22]. Three mechanisms for arsenic (arsenate + arsenite) removal from water through coagulation with alum coagulants were identified: precipitation, coprecipitation, or adsorption. When pre-formed aluminum hydroxide solids were added to a solution containing arsenate, adsorption was the only arsenate removal method [32].

The mechanism of metal ion sorption and nature of adsorption process can be interpreted using equilibrium, kinetics and thermodynamics studies [27]. It was observed that inorganic and organic mineral phase present in sludge plays an important role in sorption of metal ions on sorbent surface. Further, the surface functional group also play a major role in adsorption on alum sludge [25]. The adsorption mechanism of Cd onto alum sludge was proposed by ion exchange, electrostatic attraction and complexation mechanisms [36]. Similarly, Zhou et al. [27] reported that the ion exchange with  $Ca^{2+}$ ,  $Mg^{2+}$ ,  $K^+$  and  $Na^+$  and complexation and precipitation with surface functional groups (carboxyl, hydroxyl) was the main mechanism for Pb(II) removal by sludge. Other researchers also reported that the ion exchange, precipitation and interaction with surface functional groups are the main mechanisms for the removal of metal ions [32,37,38].

### c) Alum sludge co-conditioning and dewatering with sewerage sludge

Although attempts at co-discharging waterworks sludge and sewage sludge are not entirely new, the use of waterworks sludge in co-conditioning and enhancing sewage sludge treatability remains an attractive option in research and practice. However, only few studies have been report in the last decades.

For example, Lai and Liu [39] investigated the co-conditioning and dewatering behaviors of two different sludges (alum sludge and waste activated sludge), which were mixed at various ratios (2:1; 1:1; 1:2; 1:4). It indicates that alum sludge may act as a skeleton builder in the mixed sludge, and renders the mixed sludge more incompressible which is beneficial for sludge dewatering. Afterwards, Yang et al. [40] examines the role of alum sludge in improving the dewaterability of anaerobic digested activated sludge from the municipal WWTP located in northeast Dublin, Ireland [41]. It was found that anaerobic digested sludge mixed with alum sludge in the optimal ratio of 2:1 on volume basis can cause about 99 % reduction in phosphorus loading in the reject water along with the improvement in dewaterability of the resultant sludge. At this mix ratio, the optimal polymer (Superfloc C2260) dose required to improve dewaterability is also reduced to 15 mg/L from 120 mg/L, thus providing a huge saving in polymer addition. However, the haul distance (50 km) between water treatment plant and WWTPs, benefits of sludge transport and related economics became the deciding factor in large scale application.

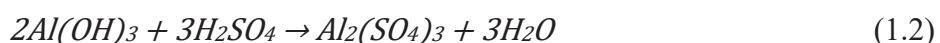
#### d) Alum sludge as substrate in constructed wetlands

Constructed wetlands (CWs) are engineered systems that have been designed and constructed to enhance the natural processes for wastewater treatment, which have been well recognized as low-cost, sustainable, robust, and efficient systems [42]. Alum sludge has been successfully reused as main substrate for the removal of phosphorous, nitrogen and organic matter, with the removal efficiency of  $71.8 \pm 10.2$ ,  $22.8$ ,  $97.6 \pm 1.9$  % of COD, total nitrogen (TN) and phosphate (P), respectively [43]. Significantly, a pilot field-scale alum sludge-based CW system has been setup to achieve the enhanced removal of phosphorus and organic matter from animal farm wastewater, the mean monthly removal efficiencies obtained were determined that ranged 57-84, 36-84, 11-78, 49-93, 75-94, 73-97 and 46-83 % for BOD<sub>5</sub>, COD, TN, NH<sub>4</sub>-N, TP, P (inorganic phosphorus) and SS, respectively [44].

Although, alum sludge based CWs demonstrated the excellent capability to remove organic matter, ammoniacal nitrogen and phosphorus, Zhao et al. [43] found that the overall TN removal has been observed to be still below the desired level (the average TN removal efficiency was 22.8 %). Moreover, Hu et al. [45] reported step-feeding strategy for four-stage alum sludge-based tidal flow constructed wetlands to get better aeration for nitrification and stepwise introduction of the influent to the nitrified liquid that would more efficiently use the influent carbon source for denitrification, enhanced total nitrogen removal of 83 % is achieved under high nitrogen loading rate of 19.1 g N/m<sup>2</sup> d. Further Hu et al. [46] constructed a single-stage alum sludge CW with intermittent aeration to treat high strength wastewater having influent COD in the range of 3000-6000 mg/L and TN ranged between 250 and 700 mg/L. The study found that, effective TN removal up to 97 % was achieved after sufficient oxygen supplied in the system showing substantial increment in treatment efficiency and nitrogen loading rate.

### 1.2.3 Recovery and reuse of coagulants from alum sludge

Aluminum content in the alum sludge after coagulation of drinking water treatment process is 39 % by weight, and this unique properties make it possible to reuse them as a beneficial material for coagulant recovery [47]. Moreover, successful attempts have been made to recover the coagulants and reused for the removal of turbidity, COD, suspended solids and phosphate from the wastewater [48]. Different techniques have been adopted to recover the aluminum salts from the precipitate viz. acid treatment (H<sub>2</sub>SO<sub>4</sub> & HCL digestion), alkaline treatment (using Caustic soda), ion exchanging (through liquid, resins and membranes) and pressure driven membranes such as ultrafiltration and electro dialysis processes [4]. For instance, the application of recovered coagulant in wastewater treatment process is being used at the Only waterworks in France, where coagulant recovered from alum sludge through acidification is recycled with fresh coagulant [14]. To recover alum, sulfuric acid is dosed to the alum sludge and the aluminum is dissolved according to the following Eq.:



Although 70-90 % of aluminum recovery can be achieved by using acidification techniques (pH between 1.0 and 3.0) [13,14], it is known that to dissolve 1 g Al<sup>3+</sup> in the form of aluminum hydroxide, 5.4 g of H<sub>2</sub>SO<sub>4</sub> is needed, the recovery process is expensive and laborious. Afterwards, Keeley et al. [48] reported that Donnan dialysis membrane process has been found to have greater potential in selective recovery over 70 % of alum, free of particulate matter, organic matter, and other trace metals, and the economic assessment was carried out of selective coagulant recovery through different membrane technologies. They have reported the

economic feasibility of coagulant recovery as a function of external prices, performance criteria and process practices, but the overall operational cost becomes halved if acid recovery is integrated with any coagulant recovery system. Therefore, the effectiveness of the involved technique, quality of the recovered coagulants and related economics varies, and still remains subject of discussion [49].

Additionally, the AquaCritox unit [13] which can convert this environmental and costly issue into a sustainable and economically comprehensive solution. This technology is evident to recover the pure aluminum which can be reconstituted to generate new coagulant for reuse in water treatment process. The process is a supercritical water oxidation process in which sludge is heated to between 374 °C and 500 °C at 221 bar pressure in the presence of oxygen. Organic matter content in the alum sludge is completely oxidized in an exothermic reaction creating water, carbon dioxide and aluminum hydroxide as a water insoluble precipitate.

Although, the coagulant recovery process may be little difficult, the lab and plant scale tests showed the practical feasibility and provided some economic benefits [50]. Recovery and reuse of coagulants from alum sludge could significantly reduce the fresh coagulant dose and hence related cost [51].

#### **1.2.4 Alum sludge application in land-based uses**

The controlled spreading of the alum sludge onto or incorporation into the surface layer of soil to stabilize, degrade, and immobilize the sludge constituents is the main objective of land-based applications [14]. It is viewed as a low-cost alternative for sustainable disposal of sludge and at the same time enhancing certain soil qualities or using as part of growing medium in agricultural fields. Indeed, the land application has been widely regarded throughout the EU as the Best Practicable Environmental Option (BPEO) and supported by local authorities, however land application of WTRs is not a widely accepted practice in most part of the world due to in part the inconsistent plant response [5]. Concerns remains for land application of WTRs due to limited guidance and universal acceptance [52].

Generally, there are three aspects of land-based applications of alum sludge: soil buffer, soil structure improvement and soil nutrients immobilization [53]. The first land-application study was carried out by Russell [54] in 1975. The sludge is pumped to lagoons to concentrate and store the solids produced from the softening operation, results of tests carried out with the use of a dry spreader for application of the dewatered sludge to farmlands. Afterwards numerous investigations have been carried out to appraise the impact of alum sludge on soil and eco systems, for instance Kim et al [55] reported an acid soil was treated with alum sludge at 0 to 18 % rate, Indian mustard was grown on the treated soil in a greenhouse for 5 weeks, and irrigated with pH 4 water during growth. Results shows that the sludge treatment increased the buffer capacity to acidity, hydraulic conductivity, water-holding capacity, and phosphate adsorption of the soil and decreased the bulk density and mobility of small particles. Application of alum sludge to an acid soil was found to be safe and beneficial to plant growth. However, there are also some negative effects regarding the alum sludge land-based applications, for example, Dayton and Basta [56] evaluated the alum sludge as potential source of topsoil for land reclamation and on tomato cultivation, it conclude that the available P and crop yield were reduced at higher alum sludge rates, due to a strong affinity of alum sludge with P. Moreover, the leachability of Al from alum sludge, increase the potential for Al phytotoxicity has been a concern in several studies [13].

Overall, previous studies presented both positive and negative effects on the alum sludge reuse in land application [14,36,57]. The promoting factors can be classified into soil improvement, nutrients supply, toxicity mitigation [3]. However, it has been indicated that the success of alum sludge application in agriculture will not be limited by  $Al^{3+}$  toxicity so long as pH is higher than 5.0 [53]. Another risk of the P immobilization by alum sludge can also be mitigated by adopting surface applied scheme or supplementing fertilizers [14] and surface application or incorporation is also one of the key recommendations to alum sludge land application. By adopting surface applied scheme and controlling the coverage depth, the adverse effect of the alum sludge to reduce the plants available P could be minimized [4].

Land application of alum sludge is far beyond the situation of just identifying a sustainable solution to WTRs management. Since there is limited specific legislation for the WTRs application in agriculture. Regulations are enacted and adopted based on the scientific knowledge, and data from full scale efforts is limited. It should be highlighted again that the land application of alum sludge is analyzed and discussed with the current assumption that alum sludge is a general waste rather than a hazardous waste [58].

In summary, the utilization of alum sludge has been proven feasible in a wide variety of environmental applications (brick manufacturing, wastewater treatment etc.), from small-scale laboratory to field-scale settings. According to the above sections focused on the beneficial reuse of alum sludge, four categories of reuse (summarized in Figure 0.3) were identified, and the reuse of the alum sludge should have a “multipronged” approach, offering both economic and environmental sustainability. From the preceding sections, the following conclusions can be made:

- ◆ The physical and chemical composition of alum sludge varies from the water purification processes as well as the various treatment plants worldwide, so there is always a need to establish its physical and chemical properties, such as elemental composition, pore structure, surface functional groups, etc. before it is applied or reused in any of the reuse option.
- ◆ The use of alum sludge in manufacturing of brick has been explored. Alum sludge are highly varied in elemental composition and concentration, even when from a single source, thus the engineering properties of the end product should be rigorously studied to understand its durability and long-time effect when they are used to produce this green building materials and research is still needed in this area.
- ◆ Different applications of alum sludge in wastewater treatment would provide some significant chemical savings and environmental benefits; enhance the treatment efficiency and reduce the sludge volume. However, it is unlikely that the WWTP would be cited close to a WTP.
- ◆ While land application is one of the economical advantageous options, regulatory clarifications are essential. Moreover, the phytotoxicity of  $Al^{3+}$  is unlikely to occur under the circumstance where the soil pH is higher than 5.

However, by reviewing the various beneficial reusing ways thoroughly, we realized that alum sludge has never been used as the sorbent even the media in waste gas purification (such as the odor control of wastewater treatment plant). Thus, it is necessary to review wastewater treatment plant odor abatement technologies to enhance the alum sludge reuse potential in this

field.

### 1.3 Current states of odor control technologies in WWTPs

Among the gas components that generated odors,  $\text{NH}_3$ ,  $\text{H}_2\text{S}$  and VOCs are the most abundant. In this section,  $\text{H}_2\text{S}$  is widely covered while  $\text{NH}_3$  is less and VOCs almost not. For technological reasons, WWTPs always occupy a large surface area, ranging from several to more than a dozen hectares and, as a result, are often considered responsible for odor emissions [59]. They not only have a negative impact on the local population but also represent a significant contribution to photochemical smog formation and particulate secondary contaminant emission [60-62]. Odorous compounds in sewage mainly originate from two processes: anaerobic decomposition of biodegradable materials in the wastewater or direct emission of specific chemicals with wastewater discharges [63,64]. Furthermore, odors emanating from WWTPs are composed of a mixture of various chemical compounds including ammonia ( $\text{NH}_3$ ), hydrogen sulfide ( $\text{H}_2\text{S}$ ) and butanone etc., seventy-eight kinds of main odor-producing compounds relating to wastewater collection and treatment facilities have been reported [65-68], such as various volatile organic compounds (VOCs), indoles, skatoles, mercaptans etc. Among the gas components that generated odors,  $\text{NH}_3$ ,  $\text{H}_2\text{S}$  and VOCs are the most abundant. Significantly,  $\text{H}_2\text{S}$  is considered the most important cause for both odor emission and corrosion in wastewater collection and treatment facilities [69].  $\text{H}_2\text{S}$  is a toxic, flammable, and colorless gas with an unpleasant smell, similar to that of rotten eggs. It can be smelled at low concentrations (about 0.5 ppb) [70]. Based on the European, American, and Chinese standards, the maximum permissible  $\text{H}_2\text{S}$  emission through a chimney is 5-10 ppm [65].

Consequently, a careful management of WWTP odor is required to avoid the annoyance and to meet the strict regulations. Until now, odour treatment technologies can be classified into physical/chemical and biological methods. Adsorption and chemical scrubbers are among the physical/chemical methods, while biofilters, biotrickling filters, bioscrubbers, and activated sludge diffusion reactors etc. are biological approaches for odour control. Physical/chemical technologies have been broadly implemented since their rapid start-up, low empty bed residence time (EBRT) and extensive experience in design and operation [71-75]. These techniques are often based on the transfer of odorants from the gas emission to either a solid (adsorption) or liquid (absorption) phase. These pollutants can be further transformed into by-products according to their reactivity with the chemicals used. However, in the last decades biological systems have been increasingly implemented due to their ability to efficiently treat malodorous emissions at lower operating costs. The main merits of biotechnologies compared to their physical/chemical counterparts derive from their low generation of secondary wastes and low demand of resources, such as chemicals or sorbent media. On the other hand, biological processes often require larger EBRT (2-120s vs. 1-5s) and associated footprint than physical/chemical alternatives at similar odor removal efficiencies [76-79]. The state of art of the relevant technologies have been discussed in the following subsections:

#### 1.3.1 Physical/chemical technologies

Physical/chemical technologies consist of two types of reactors, namely adsorption systems and chemical scrubbing, as illustrated in Figure 1.3. Either of them is commonly used in practice for odor removal in WWTPs because of their low EBRT, extensive experience in design and operation, and rapid start-up, etc. [60].



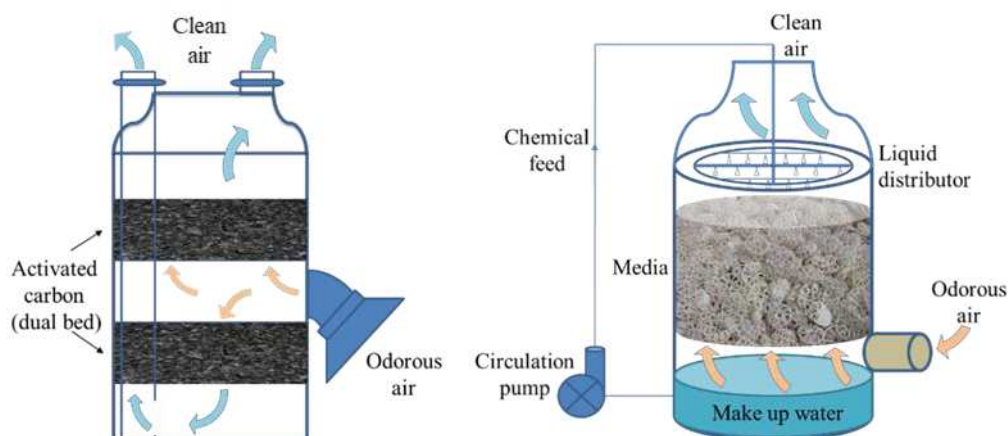


**Figure 1.3** Physical/chemical abatement technologies: adsorption system (left), chemical scrubber (right)

### ➤ Adsorption systems

Adsorption systems generally consist of static beds of granular materials in vertical cylindrical columns (Figure 1.3). Accordingly, the odorous air stream enters the column, process in the direction of air flow, and continues until odor “breakthrough” at the exit end. Its efficiency is severely limited by the high moisture content prevailing in WWTPs malodors emissions. Moreover, capacity, temperature etc. are the vital characteristics of a robustness adsorption system [80]. Several sorbents have been studied, including fly ash, carbon, activated carbon, polymers, carbon-coated polymers, ceramics, micro- and mesoporous materials, metal organic frameworks, natural zeolites, and synthetic zeolites [81]. It’s worth noting that specific surface area, pore structure together with surface chemical functional groups are three crucial factors of sorbents, which would directly determine their performance on odorants adsorption [82]. However, it is difficult to find a sorbent with all the features of an excellent sorbent, some of the sorbent properties must be compromised, such as removal capacity, regeneration, or cost impact [83].

Activated carbon (AC) is widely used as sorbent for odor control in WWTPs [65]. In the initial stage, AC was impregnated with caustics (NaOH or KOH) for H<sub>2</sub>S control [66]. Both NaOH and KOH reacted with atmospheric CO<sub>2</sub> to form the corresponding carbonates, thus facilitating H<sub>2</sub>S removal. Other impregnated sorbents for H<sub>2</sub>S removal are carbons impregnated with heavy metal salts such as copper sulphate or lead acetate [84]. These media are usually classified as hazardous materials because of their content of heavy metals. Among non-carbonaceous sorbents, activated alumina impregnated with potassium permanganate has also been used for oxidative removal of H<sub>2</sub>S [69]. However, it has been demonstrated by Bandosz et al. [85] that unmodified carbon can provide enough capacity (295 mg/g) to efficiency removal of H<sub>2</sub>S from effluent gas, it was carried out at room temperature, 3000 ppm H<sub>2</sub>S based on wet air was adopted onto various AC. It is worth noting that AC adsorption presented the highest operating costs (0.45 € per 1000 m<sup>3</sup> treated) among the odor abatement technologies [60]. This is because the AC filtration presented the highest annual packed-bed-material requirements and the 6 months replacement short life span as well as the needs for specific management procedures (regeneration or disposal as hazardous waste). Thus, although lots of efforts have been made in terms of the development of different sorbents in WWTPs odor treatment, the high cost of operation continues to be their major drawbacks for wide engineering application of the AC system. As such, generation of high-performance sewage sludge-based ACs is continuously studied world-wide, while Yang et al. [86] reported a new generated sewage sludge-based ACs, which possesses excellent adsorption capacity (259.9 mg/g) of methyl

mercaptan ( $\text{CH}_3\text{SH}$ ) in a fixed-bed column dynamic adsorption trials, breakthrough time reach 90 min and saturation end-time up to 140 min. Additionally, Aziz and Kim [83] investigated the removal of VOCs (benzene, toluene, ethylbenzene, and p-xylene) by Na-ZSM-5 and H-ZSM-5 (a synthesized material have a high ratios of  $\text{SiO}_2 / \text{Al}_2\text{O}_3$ ) in a Tedlar bag reactor with a volume of 3-5 L at atmospheric pressure and room temperature. NaZSM-5 rapidly removed 75 % of toluene and ethylbenzene and 50 % of Benzene, but xylene was not efficiently removed. On the other hand, HZSM-5 could remove all of the VOCs. Furthermore, Sempere et al. [87] reported that a AC adsorption combined with biotechnologies to form the hybrid technology becomes a popular odor control approach, the removal of a 1:1 by weight mixture of ethanol and ethyl acetate was reported in a gas phase biotrickling filter running under conditions that simulated industrial emissions from the flexographic sector, i.e. discontinuous loading and oscillating concentration of the inlet stream. Results indicated that the use of the AC prefilter with a volume 25 times lower than that of the bioreactor was shown to reach an average outlet emission concentration lower than  $50 \text{ mg/m}^3$  operating the biotrickling filter at an empty-bed residence time of 40 s, with a maximum removal efficiency of 92 %. Overall, adsorption-based systems provide an excellent performance in the treatment of highly hydrophobic odorants (90-99 %) [81,88].

**i). Adsorption mechanisms:** Several mechanisms have been proposed for the adsorption reactions. However, it is not yet fully understood. Generally, the mechanism of odor adsorption consists of seven steps as follows: (i) transport of the gas from the bulk of a mixture to a solid particle, (ii) transport of the reactants in the pores of the sorbent particles to an active site, (iii) adsorption of the reactants to the active site via Van der Waals forces, (iv) reaction of reactants to form an adsorbed product, (v) desorption of the product from the active site, (vi) transport of the products in the pores of the catalytic particle out of the particle, (vii) and transport of the products from the particle to the bulk of the mixture [89,90]. In particular, regarding the  $\text{H}_2\text{S}$  adsorption mechanisms, in the presence of oxygen and humidity, the interactions between  $\text{H}_2\text{S}$  and the complex surface properties of the materials (such as O-containing groups, mineral species, pH) lead to several retention mechanisms including dissociative adsorption and oxidation [91,92,160].

**ii). Mass transfer models:** The kinetic models are important not only for estimation of transport coefficients from kinetic curves but also as basic constituents of fixed-bed adsorber models. In general, there are three steps of the molecules bind to the surface of a solid [93]:

**a).** Film diffusion (external diffusion) comprises the transport of the adsorbate from the bulk gas/liquid to the external surface of the sorbent particle. the concentration at the external sorbent surface is always lower than in the bulk liquid due to the continuing adsorption process. Thus, a concentration gradient results that extends over a boundary layer of thickness  $\delta$ . The difference between the concentration in the bulk phase,  $c$ , and the concentration at the external surface,  $c_s$ , acts as a driving force for the mass transfer through the boundary layer. Figure 1.4 shows the typical concentration profile for the limiting case where the adsorption rate is determined only by film diffusion and the diffusion within the particle is very fast.

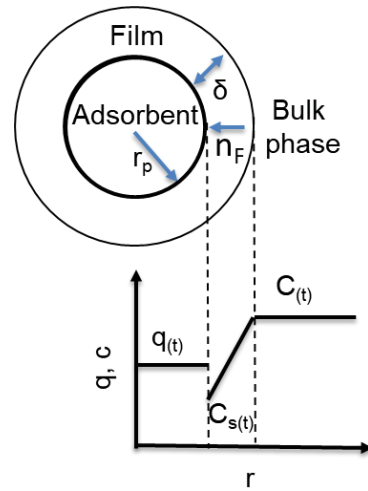


**Figure 1.4** Concentration profiles in the case of rate-limiting film diffusion

The film mass transfer equation is as follows:

$$-\frac{dC_t}{dt} = K_f \left( \frac{a_{ads}}{V} \right) (C_t - C_e) \quad (1.3)$$

Where:

$C_t$ : the concentration of the compound in the bulk phase ( $\text{mol}/\text{m}^3$ );

$C_e$ : the concentration of the compound at the surface of the sorbent ( $\text{mol}/\text{m}^3$ );

$K_f$ : the external mass transfer coefficient ( $\text{m}/\text{s}$ );

$a_{ads}$ : the surface area for external transfer ( $\text{m}^2$ );

$V$ : Volume of the adsorption bed ( $\text{m}^3$ ).

**b).** Internal diffusion presents that the adsorbate transport within the sorbent particles can also take place in the pore. The concentration profiles for pore diffusion is given in Figure 1.5. Where  $n_p$  is the mass transfer rate per unit of surface area,  $r$  is the radial coordinate,  $c_p$  is the adsorbate concentration in the pore fluid,  $q$  is the sorbent loading.

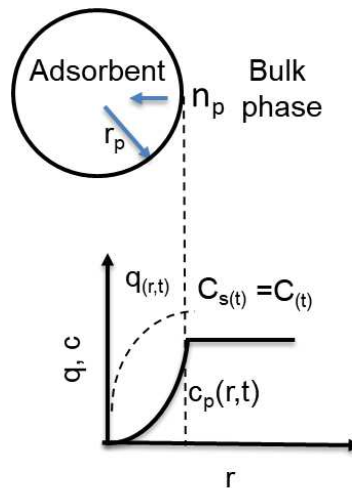


**Figure 1.5** Concentration profiles in the case of pore diffusion

The internal diffusion is often expressed by the following Eq.:

$$J = -D_p \frac{\varepsilon_p}{\tau} \frac{\partial c_p}{\partial r} \quad (1.4)$$

Where:

- J: the transferred flux ( $\text{mol}\cdot\text{m}^{-2}\cdot\text{s}^{-1}$ );
- $D_p$ : the pore diffusion coefficient ( $\text{m}^2/\text{s}$ );
- $\epsilon_p$ : the porosity;
- $\tau$ : the tortuosity.

c). Surface diffusion, the gradient of the solid-phase concentration within the particle acts as driving force for the transport. The concentration profiles for Surface diffusion is shown in Figure 1.6,  $n_s$  is the mass transfer rate per unit of surface area,  $q_s$  is the sorbent loading at the outer surface,  $C_s$  is the concentration at the outer surface.

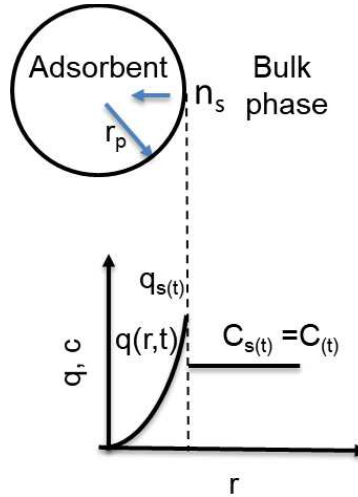


Figure 1.6 Concentration profiles in the case of surface diffusion

The surface diffusion is defined by Eq. 1.5:

$$J = -D_s \frac{\epsilon_p}{\tau} \frac{\partial q}{\partial r} \quad (1.5)$$

Where:

- $D_s$  is the surface diffusivity ( $\text{m}^2/\text{s}$ );
- $q$  is the amount adsorbed ( $\text{mol}/\text{kg}$ ).

### iii). Adsorption dynamics in fixed-bed columns

Adsorption in a fixed-bed column is a time- and distance-dependent process. The equilibration takes place in a more or less broad zone of the sorbent bed, referred to as the mass transfer zone (MTZ) [94]. The concentration versus time curve, which is measurable at the column outlet, is referred to as the breakthrough curve (BTC). The BTC is a mirror of the MTZ and is therefore affected by the same factors, in particular adsorption rate and shape of the equilibrium curve. The position of the BTC on the time axis depends on the traveling velocity of the MTZ, which in turn depends on the flow velocity and on the strength of adsorption. For a given flow velocity holds that the better adsorbable the solute is, the later the breakthrough occurs. The relation between the traveling of the MTZ and the development of the BTC is schematically shown in Figure 1.7. Regarding the various adsorption kinetic models in order to simulate the BTC will be presented in Chapter 2.

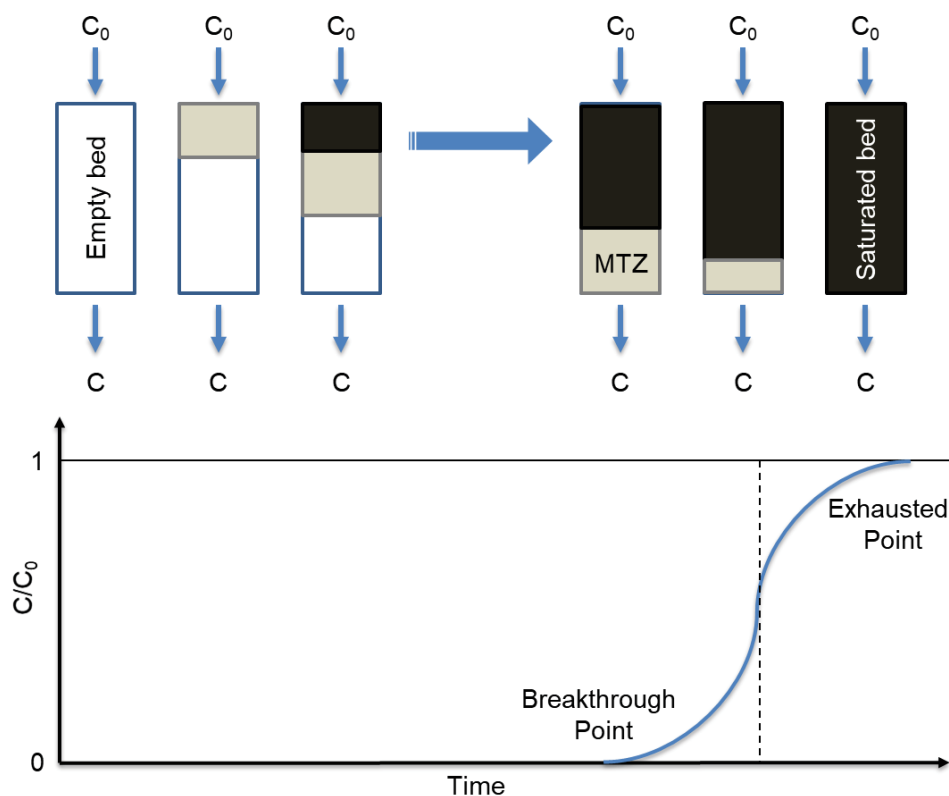
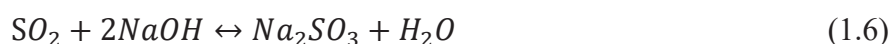


**Figure 1.7** Traveling of the mass transfer zone (MTZ) through the column and development of the breakthrough curve (BTC)

### ➤ Chemical Odor Scrubbing

Chemical scrubbers (CS) are among the most commonly employed abatement techniques in WWTPs due to the extensive experience and high robustness as well as the short gas retention time (as low as 1–2.5s) [95]. Various types of CS include the counter-current scrubber, cross-flow scrubber, and venture scrubber have been reported [65]. The most common configuration (Figure 1.3) is a vertical shell with gas flow going up through packing and the liquid solution (depending on the target compounds) going down. Liquid solution is usually circulated over the packing by pumping from a collection sump in the bottom of the tower, while chemicals are added either in the sump or in the recirculation piping.

For best performance, a multi-stage scrubber is often used. Yang and Chen [96] investigated the oxidation of 150 ppm nitric oxide with a two-stage chemical scrubber using the dc corona as an alternative for one of the scrubbing chemicals, the dc corona was able to convert NO to NO<sub>2</sub> effectively while sodium sulfite was found effective for NO<sub>2</sub> absorption. Bandyopadhyay and Biswas [97] studied the scrubbing of sulfur dioxide in a two-stage hybrid scrubber using water and dilute sodium alkali, the overall mechanisms is as follows:



Results shows that near 100 % removal efficiency of SO<sub>2</sub> was achieved in all the sections in alkali scrubbing using dilute NaOH solutions.

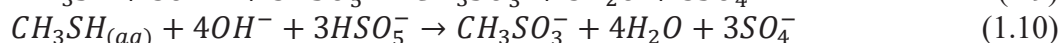
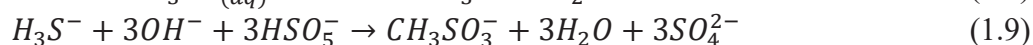
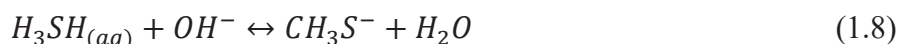
Chen et al. [98] reported a novel two-stage wet scrubbing for composting gases treatment, which consisted of acidic chlorination followed by alkaline sulfurization, it concluded that

chlorine and thiosulfate were more effective oxidizing and reducing agents, respectively. The mechanisms are that odor-containing compounds were firstly reacted by oxidation, whereas the excess chlorines and those non-oxidized odorous chemicals and VOCs, were effectively removed by reduction with sodium thiosulfate. The reaction between chlorine and sodium thiosulfate can be explained as follows:



Moreover, a water/oil emulsion for VOCs removal has recently been developed by Harizet al. [99], it is an alternative that reduces the number of towers and thus reduces the investment and operation costs. Significantly, thermal regeneration of the VOC-saturated oil was reported in the first time to reduce the solvent consumption and to reduce the impact on the environment.

Generally, since a portion of solution is continually wasted to remove the accumulated contaminants, CS required the large annual amounts of chemical reagents and higher quality (preferably softened) potable water. The purchase of chemicals accounts for the highest contribution (69 %) to the CS operating cost and followed by the energy consumption (22 %) as a result of the high liquid recycling rates [100]. Moreover, NaClO as the commonly used oxidant in CS is likely to form chlorinated by-products which are harmful for human health and to produce another pungent odor, hypochloric acid [101,102]. Alfonsín et al. [78] also pointed out that CS presented the highest impacts in freshwater eutrophication, photochemical oxidant formation, human toxicity and ecotoxicity due to the use of large amounts of chemicals. H<sub>2</sub>O<sub>2</sub> is a promising oxidant except for its instability in basic aqueous solution and the low efficiency of CH<sub>3</sub>SH removal [103,104]. The emerging oxidants of CS like peroxymonosulfate (PMS) has a similar structure with H<sub>2</sub>O<sub>2</sub> but the oxidation–reduction potential is stronger than H<sub>2</sub>O<sub>2</sub> was reported by Yang et al. [105]. The possible mechanism of CH<sub>3</sub>SH oxidation by PMS was proposed by the following reactions:



In addition, Talaiekhosani et al. [65] pointed out that Venturi scrubbers can be a highly cost-efficient candidate for many industries, due to their simplicity of construction and usage, the ability to purify large volume of air in a short time and to simultaneously remove particles and gases. Significantly, Venturi scrubbers can even be distinguished from biological methods, such as biofilters, since it can quickly reach the maximum efficiency comparison with biofilters, while the alkaline substances, such as limewater, can convert sulfur into calcium sulfide and inhibit the reproduction of hydrogen sulfide etc. On the other hand, CS showed the lowest geographic dependence worldwide, because chemicals, which constitute the main cost in these systems, were considered to be part of a global market and their prices did not depend on the geographical location [106]. Overall, despite the high removal efficiencies (> 99 %) achieved for H<sub>2</sub>S [105,107], CS presents serious limitations in the elimination of hydrophobic VOCs (high Henry Law constants) as they are finally based on odorant transfer to an aqueous solution of oxidant. In addition, the hazardous nature of the chemical reagents employed and by-products generated represent a serious challenge to its supremacy in a world increasingly devoted to sustainable development.



### 1.3.2 Biotechnological treatment

Biotechnologies, particularly hybrid technologies (physical/chemical+ biotechnologies) become the main approach in the last decades for odor control, since their low-cost and environmentally friendly nature. To date, four types of reactors are commonly used in WWTPs [108]: biofilters (BF), biotrickling filters (BTF), bioscrubbers (BS) and activated sludge diffusion reactors (ASD), as illustrated in Figure 1.8.

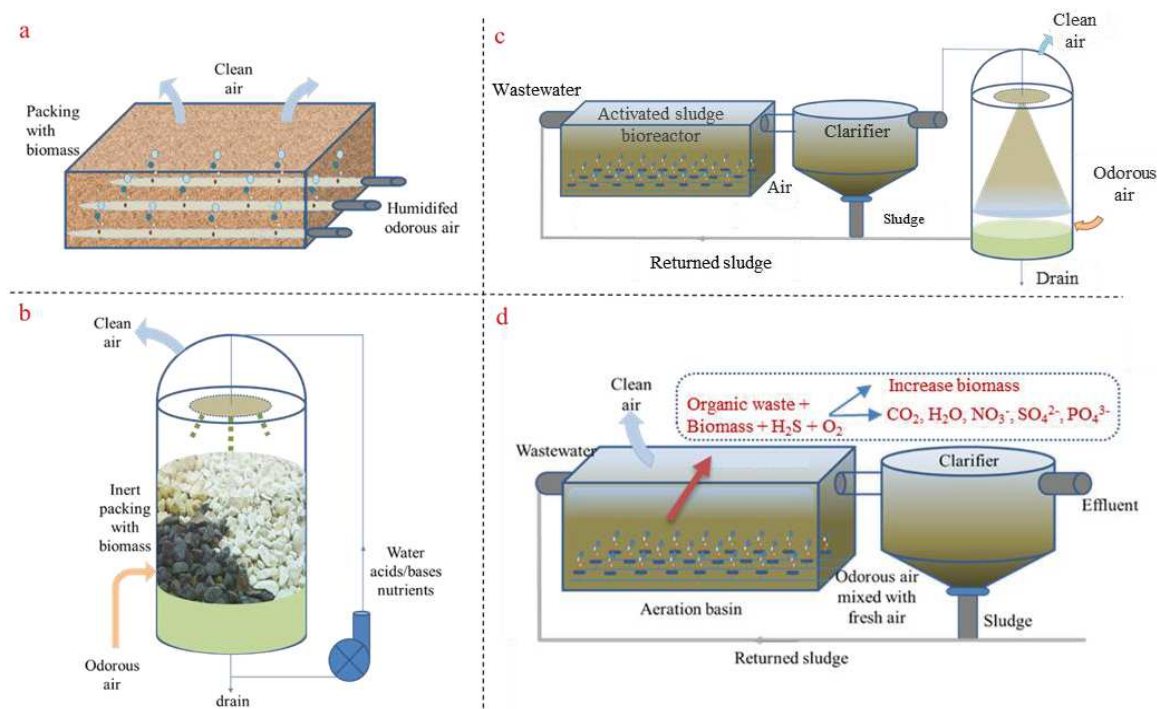


**Figure 1.8** Biotechnological treatment: (a) open biofilter; (b) biotrickling filter; (c) bioscrubber; (d) activated sludge diffusion.

#### ➤ Biofiltration

BF is the oldest biological method for the removal of undesired gaseous compounds from air and indisputably the most commonly employed biotechnology for odor treatment in WWTPs [84]. From the late 1970's most of the development work on biological off-gas treatment has been carried out in Germany and The Netherlands, In the 1980's intensive progress has started in Western Europe, Japan and the United States and since then research on biofiltration is being focused on industrial applications, using different filter designs and different microorganisms [109].

In a biofilter system (Figure 1.8a), the humidified odorant is forced through a packed bed (compost, peat, bark or a mixture of these) on which the microorganisms are attached as a biofilm [110-115]. The pollutants are sorbed by the filter material and degraded by the biofilm. However, to control the key parameters such as pH and moisture content within the packed bed, and to avoid the accumulation of inhibitory by-products are still the technical difficulties and limitations [87,116,117].

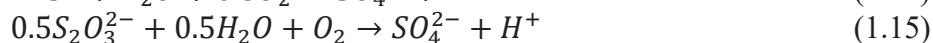
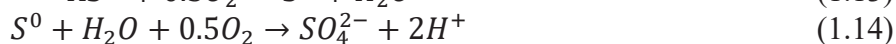
Performance data of a series of lab-scale BF and engineering applications are summarized in Table 1.2. An important advantage of biological treatment methods over physical and chemical technologies is that the biological processes can be conducted at moderate



temperatures (10–40 °C) and atmospheric pressure. The first step of the biofiltration process is the transfer of pollutants from the gas to the moist bed material, or to the liquid phase, and further into the biofilm; The second step is biodegradation. The biofilm, i.e. the mass of microorganisms that grow on the surface of the bed material (packing) and carry out the metabolic activities converting the pollutant to harmless compounds, is the key biofilter component involved in destroying the pollutants [118]. Moreover, microbial degradation processes are generally oxidative in nature and produce compounds such as carbon dioxide, water, sulfate and nitrate that are ecologically safe [110]. The microorganisms are the engine of the biotreatment process. Biofilms contain a mixture of bacteria, fungi, yeasts, ciliated protozoa, amoebae, nematodes and algae. Bacteria and fungi are the two dominant microorganisms groups in biofilters, however as bacteria populations (primary degraders) grow they can sustain yeasts and other fungi, algae and higher organisms such as protozoa, rotifers, nematodes, etc., the optimum pH for microorganisms is 7 [108]. In the case of H<sub>2</sub>S or ammonia removal, the primary degraders are autotrophs; usually, the pollutant is a source of energy, and atmospheric carbon dioxide is used as a source of carbon for growth [119]. For instance, during biocatalytic reactions, sulfide is oxidized to elemental sulfur by *Cholorobium limicola*, which requires only light, CO<sub>2</sub>, and inorganic nutrients for growth under strictly anaerobic conditions [120]. The decomposition of H<sub>2</sub>S into elemental sulfur is shown in Eq. (1.11).



Additionally, use of oxygen as an electron acceptor for oxidation of H<sub>2</sub>S is a well-known process of colorless sulfur-oxidizing bacteria [121]. As these bacteria can maintain high growth rates without light, they are preferred over green or purple sulfur-oxidizing bacteria [122]. Oxidation of sulfide can be induced in *Thiobacillus* species via the sulfite-oxidase pathway as following:



Microorganisms oxidize sulfides as well as other reduced sulfur compounds (e.g., thiosulfate) to sulfate, releasing the dominant fraction of energy  $\Delta G = -145.5$  kcal/mol (Eq. 1.12) [120]. The sulfide oxidation pathway often involves elemental sulfur as an intermediate (Eq. 1.13 and 1.14). Oxidation of sulfides only produces elemental sulfur, yielding less energy than the conversion to sulfate under oxygen-limited conditions, possibly due to the higher energy barriers of Equations 1.14 and 1.15 [121]. Generated sulfur is deposited both inside and outside cell membranes. This type of oxidation also produces energy from other reduced S species, such as thiosulfate (Eq. 1.15) [122].

By providing support for microbial growth, BF media are very often regarded as the key issue to determine removal efficiencies and BF lifespan [123]. From Table 1.2, the common bed media of biofilters are soils, peats, composts and wood chips. These materials satisfy most of the process-specific requirements and are widely available at low cost. Some media provide micro-nutrients to the microorganisms and may also provide a surface chemistry that promotes their growth [124]. The ratio of surface area to bed volume (specific surface area) for biofilter media ranges from 100 to 1100 m<sup>2</sup>/m<sup>3</sup>, with wood chips having a ratio of 160 m<sup>2</sup>/m<sup>3</sup>, while a mixture of heather and peat had an area to volume ratio of 1100 m<sup>2</sup>/m<sup>3</sup> [125]. It can be concluded that nontoxic organic or inorganic supports with high specific surface areas and

porosities, good water retention capacities, high buffer capacities, and high nutrients content have provided the best odor removal performances. Organic media provide an extra C source necessary to maintain microbial activity, likely challenged by the extremely low C concentrations present at the biofilm-water/air interface [126,127,121]. On the other hand, inorganic materials such as ceramic, plastics, lava rock, and activated carbon provide an extra structural stability, which increases BF lifespan [128,129].

Moisture content of the packing is the most critical parameter to control in BF. Indeed, many references listed in Table 1.2 mentioned system upsets causing excessive drying of the packed bed and declining performance. Although the relative humidity of the air undergoing treatment is often over 80 % at WWTPs, the waste air is frequently humidified in packed towers before entering the BF [130].

As shown in Table 1.2, BFs at industrial applications are operated at EBRTs from 20 to 290s. Removal of H<sub>2</sub>S is generally between 90 and 100 %, indicating the effectiveness of BF. On the other hand, removal of odorous compounds like dimethyl sulfide, DMDS, and methyl mercaptan is often instable, with reported removal efficiencies ranging from about 20 to 100 % [131-134]. However, Jaber et al. [135] pointed out the accumulation of sulfuric acid, the most abundant product of the biological oxidation of sulfur compounds in the packing material caused the pH decreasing, led to a reduction of the elimination efficiencies of DMDS etc., while the microorganisms involved in H<sub>2</sub>S degradation appeared active in a large pH range, from 3 to 9.

Because of the need to maintain low pressure drops across the packing bed and the high EBRT needed for efficient odor treatment, BF presented the highest land requirements [136]. This footprint was 7 and 25 times higher than that of the BTF and CS, respectively, and can limit the application of this biotechnology during plant upgrading in WWTPs when facing land limitations [137,124].

Table 1.2 Performance of BF in lab and on-site systems

Reference/ Location*	Media	Parameters			Nutrients	Odorant	Concentration (mg/m <sup>3</sup> )	RE (%)
		EBRT (s)	pH	T (°C)				
[129]	Perlite, polyurethane foam, compost, wood chips, straw	/	7- 7.5	20	NaNO <sub>3</sub> , KH <sub>2</sub> PO <sub>4</sub> ,	Acetone, n-butanol, methane, ethylene, ammonia	23.9	100
					Na <sub>2</sub> HPO <sub>4</sub> ,		7.0	100
					MgSO <sub>4</sub> ,		21.7 ppm	0
					CaCl <sub>2</sub> ·2H <sub>2</sub> O, FeSO <sub>4</sub> ·7H <sub>2</sub> O, etc.		20.2 ppm	95
						10-30 ppm	85-98	
[135]	Pine bark, composted wood mulch	70-290	2.7- 8.7	Room temp.	K <sub>2</sub> HPO <sub>4</sub> , (NH <sub>4</sub> ) <sub>2</sub> SO <sub>4</sub> , Na <sub>2</sub> CO <sub>3</sub> ,	H <sub>2</sub> S, DMDS, ethanethiol	3.8-7.6	100
[130]	Compost & woodchip	34	6.1-8.1	Room temp.	None	Ammonia	40 ppm	35-63
[134]	Wood bark	1.6-3.1	/	11.3- 30.8	None	Ammonia,	0.25-75.00 ppm	95.2-97.9
						H <sub>2</sub> S	0.05-8.00 ppm	95.8-100
						Benzene,	0.002-0.003	0-50
						Xylenes,	0.18-0.66	40-75
						Toluene,	0.077-0.23	42-86
						Dichloro- Benzene,	0.024-0.049	43-60
						H <sub>2</sub> S,	10-50	> 99
						Carbon disulfide,	0.02-0.03	32-36
						Methyl mercaptan,	0.30-0.33	91-94
						Dimethyl sulfide,	0.02-0.03	0-21
Carbonyl sulfide	0.05-0.13	30-35						
Los Angeles, U.S.	Compost, perlite, oyster shell	14-69	7-9	/	None			
Ojai Valley, U.S.	Lava rock	18-54	7.9-8.1	/	Nitrogen, Phosphorous, Potassium	MTBE	1.8	20
						Acetone	1.6	80
						Toluene	2.3	60

						Xylenes	1.3	40
						Dichloro- methane	3.5	30
						Chloroform	0.3	15
						H <sub>2</sub> S	0.01-42	> 90
						Benzene	3.0	83-95
						Toluene	4.0	88-97
Carson, U.S.	Compost, wood chips, oyster shell, perlite	45-180	/	/	None	m,p-Xylene	1.1	88-93
						o-Xylene	0.4	88-91
						H <sub>2</sub> S	13.9	> 99
						α- pinene,	675 ppb	100
						β- pinene,	345	100
						Dimethyl sulfide,	0.02	100
Yarmouth, U.S.	Compost, bark mulch, wood chips	45	/	Low temp.	Chemical misting	DMDS,	0.16	100
						D-limonene,	70	97
						Carbon disulfide,	0.01	100
						Methyl mercaptan	0.006	100
Tampa, U.S.	Top soil, peat, mulch	60	/	/	None	H <sub>2</sub> S	7-120	100
						H <sub>2</sub> S	200	100
						Dimethyl sulfide,	8.8	21
Albany, U.S.	/	150	/	/	/	Methyl mercaptan	22	66
						H <sub>2</sub> S,	140	99.5
Hillsborough, U.S.	Pine bark	115	/	/	None	DMDS,	936	97
						Carbon disulfide,	618	82
						Methyl mercaptan	330	100
Boca- Grande, U.S.	Peat, wood chips, top soil	130	/	/	None	H <sub>2</sub> S	140	100
Charlotte,	Wood chips,	111	/	/	/	Dimethyl	625	100

U.S.	compost, perlite, granular fill					sulfide, Carbon disulfide	448	100
						Benzene,	0.01	36-93
						Toluene,	0.1	24-99
						Xylenes,	0.08	96
						Dimethyl sulfide,	0.07	35
Fountain Valley, U.S.	Two units with GAC and yard waste compost	17-70	1-2,7	/	/	Chloroform,	0.06	11
						TCE,	0.01	82
						PCE,	0.37	98
						Total gaseous nonmethane organics, H <sub>2</sub> S	26 ppm	99
							4.3	99
						H <sub>2</sub> S,	0.11	95
						Dimethyl sulfide,	0.03	68
Martinez, U.S.	Wood chips, yard waste, compost, lime	38	/	/	/	DMDS,	0.01	41
						Methyl mercaptan	0.054	90
						Acetone	0.03-0.09	55
						H <sub>2</sub> S	1.5-34	97
						Benzene	0.01-0.25	25
Renton, U.S.	Bark, topsoil, compost, peat, moss, oyster shells	40-60	/	/	/	Mercaptans	0.16-3.8 ppm	62
						Amines	2.5-6 ppm	> 60
						TCE	0.02-0.05	44
						PCE	0.02-0.5	40
						Chloroform	0.10-0.21	43

\*Adapted from [78,138,109]

## ➤ **Biotrickling**

To overcome the disadvantages of BF, such as H<sub>2</sub>S and certain organic compounds are difficult to remove reliably and economically in biofilters, more sophisticated filtration equipment called biotrickling has been developed. In BTF or fixed-film bioscrubber (Figure 1.8b), the odorous gas is forced through a packed bed filled with a chemically inert carrier material which is colonized by microorganism, similar to trickling filters in wastewater treatment. The liquid medium is circulated over the packed bed and the pollutants are first taken up by the biofilm on the carrier material and then degraded by the microorganisms. The liquid medium can be recirculated continuously or discontinuously and in co- or countercurrent to the gas stream. Flow directions will not affect the efficiency of the process. Compare with BF, BTF has the drawbacks of when treating high pollutant concentrations, too high nutrient doses may lead to filter-bed clogging by growing biomass.

Performance data of BTF in lab and WWTPs are given in Table 1.3. Various types of packing materials have been used: inorganic salts, polyurethane foam, activated carbon fibers, multi-surface hollow balls, random-dump plastic, structured plastic are often used as the bed material. Additionally, lava rock, tire-derived rubber particles (TDRP), glass beads, or ceramics as well as organic materials such as wood chips are also in use. The high porosity (100-1100 m<sup>2</sup>/m<sup>3</sup>) of these packings causes less headloss compared to that of BF with organic packings, even though BTF are operated at a higher gas velocity [138]. It is thus noted that BTF footprints are comparable to those of physical/chemical technologies partly as a result of their relative higher media depth. Moreover, a distinctive feature of BTF is the continuous trickling of liquid over the packing, which allows for improved control of nutrient addition, pH, acid product neutralization, end product removal, and (potentially) temperature [139]. The composition of liquid phase can affect the efficiency of BTF process, thus the trickling liquid is continuously enriched with elementary mineral nutrients containing nitrogen, phosphorus, potassium, and trace elements. Usually, BTF is operated in the temperature range between 10 and 40 °C, which is characteristics of the mesophilic microorganisms growth. The efficiency of biotreatment process may be limited by both biological reaction rate and the mass transfer rate. Therefore, it is important to notice that temperature can affect either these limitations [109].

The removal mechanisms of BTF is quite similar with BF. Hydrocarbon vapors are removed by aerobic heterotrophic microorganisms that utilize the vapors as a source of carbon and energy [140,141]. In the case of odorous waste air containing reduced sulfur compounds, production of sulfuric acid with declining pH and/or accumulation of sodium sulfate (after neutralization with caustic soda) is an important design parameter. Performance data for BTF indicate that these reactors are capable of efficient removal of high concentrations of H<sub>2</sub>S at relatively low EBRTs. Thus, BTF appear to be a good option when the gas to be treated contains high concentrations of H<sub>2</sub>S and possibly other reduced sulfur compounds. BTF performance could be limited by mass transfer of oxygen into the biofilm because oxygen solubility in water is low [142,143]. However, there are still some drawbacks of BTF, such as the problem of gas transfer arising from the necessity of dissolving the gaseous pollutants in the aqueous phase, the biofilm development on the carrier surface which progressively reduces the empty volume of the filter bed and may lead to excessive pressure drop even the complete clogging of the bed [109].

**Table 1.3** Performance of BTF in lab and on-site systems

Reference/ Location*	Media	EBRT (s)	Odorant	Concentration (mg/m <sup>3</sup> )	RE (%)
[131]	A special inorganic salt	9.6	Dichloromethane	0.7-3.12	72-99
[87]	Polypropylene rings	25-60	Ethanol & ethyl acetate	50-90	46.6-68.9
[144]	Activated carbon fibers & multi- surface hollow balls	28-56	Chlorobenzene	878.53-1522.48	91.34
[145]	Polyurethane foam cubes	4-84	Methyl mercaptan, toluene, $\alpha$ -pinene, hexane	0.75-4.9	> 90
[136]	Tween-20 & Zn(II)	15-60	Ethylbenzene	64.8-189.0	54-94
[133]	Seashell	19/13	H <sub>2</sub> S	10-18 ppm	> 99
/Penn Valley, California, U.S.		1 <sup>st</sup> /2 <sup>nd</sup> stage	Methyl mercaptan	--	
			Dimethyl sulfide	--	
			H <sub>2</sub> S	10-50	> 99
			Xylenes	0.18-0.66	0-23
Headworks, Los Angeles, U.S.	Structured PVC	24	Toluene	0.077-0.23	0-17
			Methyl mercaptan	0.30-0.33	64-72
			Dichlorobenzene	0.024-0.049	0-6
Headworks, Los Angeles, U.S.	Lava rock	14	H <sub>2</sub> S	14-100	99
			Benzene	0-0.11	19-29
			H <sub>2</sub> S	1.8-16	87-99
			Xylenes	0.08-0.42	6-57
			Toluene	0.10-0.74	50-74
			1,1,1,-Trichloro- ethane	0.08-0.64	0-38
Primary clarifier; Fountain Valley, U.S.	Continuous synthetic type	11-20	Carbon tetrachloride	0.003-0.012	2-15
			Chloroform		
			Dichloromethane	0.05-0.17	0-25
			TCE	0.07-0.57	0-61
			PCE	0.01-0.04	0-24
			Vinylchloride	0.36-4.8	0-8
				0.003-0.02	0-13



Industrial wastewater treatment; San Diego, U.S.	Random inorganic	36	Benzene	0.03	59
			H <sub>2</sub> S	0-2	> 99
			Xylenes	3.5	92
			Toluene	0.7	85
			MTBE	0.09	60
			Chloroform	0.01	3
			Dichloromethane	1.2	11

\*Adapted from [78,138,109]

## ➤ Bioscrubbers

BS or suspended growth BS could be a solution of the limited suitability of BTF for handling high pollutant concentrations and large gas flows. In the early 1980's, the first BS units were applied to the treatment of waste gases [109]. In the literature, BS has been applied for amines, phenol, formaldehyde, ammonia, alcohols, glycols, ketons, glycol ether, aromatic compounds, resins, hydrochloric acid, nitric acid, hydrofluoric acid and SO<sub>2</sub> removal [146], it also can be used for degradation of such pollutants as solvent vapors discharged from coating facilities, carboxyl acids and their esters, heterocyclical sulfur and nitrogen components, mercaptans, chlorophenols and H<sub>2</sub>S [78].

In BS (Figure 1.8c), the pollutant is adsorbed in an aqueous phase in an absorption tower then converted by the active microorganisms into CO<sub>2</sub>, H<sub>2</sub>O, and biomass in a separate activated sludge unit, the effluent is circulated over the absorption tower in a co-or countercurrent way to the gas stream. Bubble size is an important factor in supplying air to the BS, and Bowker [147] has proofed that the reduction of H<sub>2</sub>S and odors in fine-bubble diffusers can be higher (above 99.5 %) than in coarse-bubble diffusers (95 % for odors and 92 % for H<sub>2</sub>S).

Most existing BSs are designed for the removal of a single pollutant. For example, Nisola et al. [148] developed a single BS for ammonia removal, the reactor was consisted of a bubble column (gas absorption) and a packed bed (nitrification) which contained poly-urethane foams with immobilized nitrifying activated sludge, the entering gas and scrubbing liquid were contacted counter currently, results shows that the bubble column has over 99 % ammonia gas removal efficiency dominated by ammonia oxidation; Potivichayanon et al. [149] investigated a fixed-film BS for hydrogen sulfide removal, the dominant strains of microorganisms found in the BS systems were *Acinetobacter* sp. and *A. faecalis*. The system exhibited more than 91 % of hydrogen sulfide removal efficiency, the mixture of two strains increased the removal efficiency to 98 %. Contrarily, various design modifications have been reported to handling pollutant mixtures, such as sorptive-slurry BS, anoxic BS, two-liquid phase BS, airlift BS, spray column or two-stage BS [125]. Friedrich et al. [150] investigated a 3-stage system (two identical BS from lava rock media + dry chemical scrubber) for the abatement of odors from sludge thickeners. Over 90 % abatement efficiency was observed from the first BS and the removal efficiency exceeded 99 % when applied two series-connected BS; Liu et al. [151] reported a two-series connected field-scale BS for simultaneous removal of NH<sub>3</sub> and CH<sub>4</sub> from the exhaust air of three intensive pig houses in northern Germany. Average NH<sub>3</sub> removal efficiencies of 86, 80, and 77 % were observed for the three BSs, respectively. The dominant NH<sub>3</sub> oxidizing and methanotrophic bacteria in the BS were *Nitrosomonas* sp. and Type I methanotrophs, respectively. After inoculating isolated methanotrophic bacteria into BS, the average CH<sub>4</sub> removal was enhanced to 35 %, offering a great option for a two-series connected BS application to intensify the removal of CH<sub>4</sub> and NH<sub>3</sub>, which are the greenhouse gases.

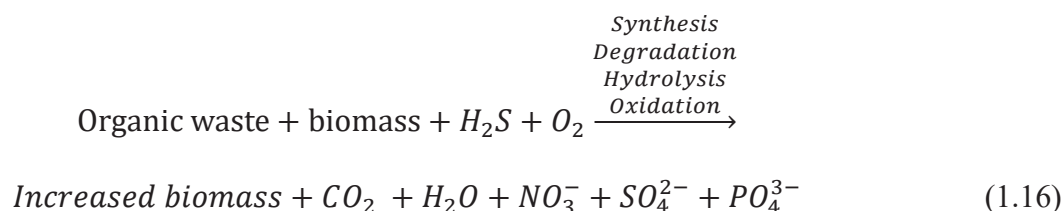
Furthermore, BS offers operational stability and effective control of operating parameters such as pH and nutrients dosage, relatively low gas pressure drop and small space requirement. For example, Hansen and Rindel [146] pointed out the pH values of 8.5-9.0 as the optimal range that facilitates maintaining a high biological activity and at the same time, ensuring effective absorption of H<sub>2</sub>S. Compared to BTF, the risk of clogging of the packing material by growing biomass is avoided, large gas flow rates and high pollutant concentrations can be handled, moreover, as reaction products are removed by washing, concentrations of toxic byproducts generated in the reactor can be maintained at low levels. However, the separate treatment system of the liquid phase increases the initial costs of establishing such kind systems. BS also possess

low capacity for treatment in the removal of poorly soluble contaminants, such as hydrogen sulfide [139], thus, adding chemical compounds such as sodium hydroxide or lime water to the circulating liquid provides higher removal rates for such kind of compounds. Alternatively, the choice of microorganisms could be considered, since immobilized cells of *Chlorobium limicola* have been identified to transform H<sub>2</sub>S into elemental sulfur in an autotrophic reaction, and heterotrophic Xanthomonas species are also known to remove H<sub>2</sub>S from gas streams [152]. Efficient degradation of sulfur-containing compounds by certain strains of *Thiobacillus* and *Hyphomicrobium* has also been reported by Toth et al. [153].

The mechanisms of odorous compounds removal in BS involves mainly the physical and biochemical processes, which has been discussed in BF section, such as absorption, biodegradation or biotransformation, significantly, biodegradation is the main process for the removal of the pollutants [109].

### ➤ Activated sludge diffusion

The economical and practical odor abatement choice is simply moving them from the gaseous phase to the liquid phase [109]. A variety of systems can be employed for this purpose, for WWTPs, ASD offers a low-cost alternative. As shown in Figure 1.8d, by collection of the odorous gas and its diversion into an activated sludge aeration basin, odours can be eliminated using relatively technology. Complete mixing ensures an adequate food supply for the microbial cells and maximizes the oxygen gradient to optimize mass transfer and disperse the products of metabolism from inside the flocs, wastewater entry displaces mixed liquor into a clarifier, where the flocculated biomass separates into sludge and clarified effluent. Contaminant removal mechanisms in ASD of waste gas include absorption (the solution of gases into the mixed liquor; limited by bubble size and gas residence time), adsorption (adsorb onto flocs), or condensation (volatile organic compounds in warm air condense on contact with the cooler mixed liquor), followed by biodegradation, which could be expressed by the following Eqs.:



Lebrero et al. [95] compared BF with ASD for the synthetic odor (H<sub>2</sub>S, butanone and toluene at 23.6-43.3, 4.3-6.3 and 0.4-0.6 mg/m<sup>3</sup>) removal. The removal efficiency for butanone and toluene remained higher than 95 % in both bioreactors. The continuous supply of wastewater in the ASD unit did not affect removal and appeared to be a requirement for efficient pollutant abatement. Despite the narrow carbon source spectrum treated, the ASD system maintained a large bacterial diversity over time and confirmed ASD being a robust and efficient technology. Recently, Rodríguez et al. [154] investigated the microbial community and bioreactor function relationships at different EBRTs in an ASD, when treating a synthetic malodorous (H<sub>2</sub>S, toluene, butanone and alpha-pinene). A stable and efficient abatement performance of H<sub>2</sub>S, butanone and toluene was observed, regard less of the EBRT and fluctuations applied, while no clear positive or negative relationship between community characteristics and bioreactor functions was confirmed. The most abundant groups namely Actinobacteria, Proteobacteria and Fungi (Hypocreales, Chaetothyriales) play a putative key role in the degradation of butanone and toluene.

On the other hand, Barbosa et al. [155] reported the effects of H<sub>2</sub>S diffusion into ASD on odor and VOC concentrations in off gas, it was found that the VOC concentrations generally decreased when H<sub>2</sub>S was introduced to the AS compared with the control, indicating a negative effect of H<sub>2</sub>S on VOC removal and ASD provides effective H<sub>2</sub>S removal with minimal effect on odor emissions. Moreover, Barbosa and Stuetz [156] investigated the effects of continuous H<sub>2</sub>S diffusion at 25 ppmv, with weekly peaks of approximately 100 ppmv, on H<sub>2</sub>S removal efficiency and wastewater treatment performance was evaluated over a 2-month period using an ASD pilot plant. It concludes that H<sub>2</sub>S removal averaged 100 % during diffusion at 25 ppmv, and 98.9 % during the 100 ppmv peak periods. A significant increase in mixed liquor volatile suspended solids concentration was observed during H<sub>2</sub>S diffusion, which due to an increase in H<sub>2</sub>S-degrading microorganisms, identified hydrogen sulfide can act as an energy source for microorganisms, while the carbon sources can be provided by compounds such as glucose, methanol or untreated domestic sewage. It also indicated that no adverse effect of H<sub>2</sub>S on nitrification throughout the ASD trials. Ammonia (NH<sub>3</sub>) removal was slightly better in the test receiving H<sub>2</sub>S diffusion (87.6 %) than in the control (85.4 %). As the solubility of hydrogen sulfide in water with pH of 7 and temperature of 19 °C is 4 g/l [65], ASD are recommended in treatment of this contaminant [157]. Additionally, Blonda et al. [158] reported that the removal of odours from WTPs through ASD from a bench scale experimental campaign which lasted more than 200 days, results showed an average sulphide removal of 94 % in the reactor supplied with Na<sub>2</sub>S. Moreover, microbial composition did not show relevant variations after the addition of sulphide, and the good features of activated sludge flocs were maintained also in terms of sludge settleability. Nitrification and denitrification efficiencies were always above 75, 95, and 50 % respectively, and comparable across the two reactors, indicated that there is no significant effects of sulphide on COD removal efficiencies as well as nitrification and denitrification in ASD. Contaminant removal mechanisms in ASD include absorption, adsorption (high molecular mass compounds with low solubility adsorb onto flocs) or condensation (VOCs in warm air condense on contact with the cooler mixed liquor), followed by biodegradation [66].

Overall, ASD is used as an alternative to more established bioreactors for waste gas treatment, such as BF, BS, BTF. Despite ASD systems have been used for over 30 years with high H<sub>2</sub>S removal efficiencies, their widespread implementation is still limited by the lack of reliable data concerning its performance during the treatment of odorous volatile organic compounds (VOCs).

### 1.3.3 Summary of different odor control technologies

The benefits and disadvantages of various odor treatment technologies in WWTPs are presented in Table 1.4. It should be noted that none of the six main odor abatement technologies could be “one-size-fits-all”. In the last decades, lot of efforts have been done in the selection of various odor control technologies.

**Table 1.4** Summary of different odor control technologies in WWTPs

<b>Technology</b>	<b>Benefits</b>	<b>Disadvantages</b>
Adsorption System	- High odor removal efficiency - Simplicity of mechanism	- Short life span - Air humidity and small molecule size - High reduction costs - Efficient only in small concentrations of contaminant
Chemical scrubbing	- Simple, effective, efficient, reliable & proper utilization;	- High costs than biotechnologies - Secondary treatment of leftover sludge

---

	- Low maintenance costs	
Biofilter system	- Low investment & operating costs - Absence of secondary waste streams - Low pressure drop & suitability for treating large volume of low concentration odorous gases	- Low efficiency of the treatment of high concentration pollutants - Difficult control of moisture and pH - Filter bed replacement every 2-5 years & Risk of bed clogging by particulate matter
Biotrickling	- Simple and low-cost technology - Medium capital, low operating costs - Effective removal of pollutants including acid-producing ones - Low pressure drop	- When treating high pollutant concentrations, too high nutrient doses may lead to filter-bed clogging by growing biomass
Bioscrubber	- Stability of operation - Proper biological parameters control, including pH, temperature, nutrients - High pressure drop - Harmful environmental compounds are easily eliminated - Avoids inhibitory effects	- Low efficiency in case of poorly soluble substances - Treatment efficiency is reduced by special contact area of gas/liquid - High pressure drop
Activated sludge diffusion	- Utilization of available equipment (lower costs) & easy operation - Higher management capability for larger loadings - Simultaneous treatment of air and wastewater	- Complex steering by experts - Tower efficiency due to the limits of gas/liquid transference - Possibility of corrosion in equipment

---

The range of thirty-seven kinds of odorant removal performance in AC adsorption, BF and BTF are reviewed and summarized in the above sections. Generally, the performance data of odorant removal in AC adsorption were less reported than the relevant biotechnologies, nineteen kinds of odorants were investigated by AC adsorption in the lab and/or field tests, H<sub>2</sub>S and methyl mercaptan are well removed by AC, however, dimethyl disulfide was poorly removed since its generation from the breakdown of methyl mercaptan on AC systems [159]. Moreover, the removal of benzene, xylene, toluene, TCE and PCE reduced with the active lifetime decreased of the AC systems. Although AC has a longer history than BTF, in-depth studies on the performance of field units generally rely on one or two samples to justify removal. It's worth to note that there is little data available on the long-term performance of these units, particularly with respect to removal efficiency other than H<sub>2</sub>S. The majority odorants could be removed by BF and nearly thirty-five kinds of different odorants were reported. BF is good at removing H<sub>2</sub>S (RE range from 90-100 %), Toluene (20-100 %) while dimethyl disulfide and carbonyl sulfide exhibit poor removal efficiency, higher retention times might facilitate dimethyl disulfide and carbonyl sulfide removal. Twenty-one kinds of odorants were removed by BTF in the past. BTF was able to remove H<sub>2</sub>S at lower EBRT than in BF due to the high solubility of the pollutant. They were widely used in the higher load of H<sub>2</sub>S. However, VOC removal is poorer in BTF than BF which could be due to the low solubility of many VOCs and the continuous trickling water layer acting as a barrier to VOC bioreaction in BTF.

### 1.3.4 Challenges and perspectives of odor abatement technologies in WWTPs

Based on the last 30 years' research and development, hybrid technologies (physical/chemical with biological technologies) have become the robustness system [106]. Although it presents a highly reliable removal efficiency for various odorants, a large amount

of media replacement cost in hybrid technologies, significantly, the replacement of AC in adsorption system still the major concerns. Consequently, development of low-cost and environmentally friendly sorbents/media for odor adsorption system/biotechnologies is urgently needed in the future study [160]. As it has been discussed in section 1.2, alum sludge has been intensively studied and reused in four broad categories. However, to the best of our knowledge, none of the studies ever chose alum sludge as the low-cost sorbent even the media in odor control of WWTPs, even it has been intensively studied and demonstrated to be a good material for wastewater treatment.

#### 1.4 Motivation and objectives of the study

The literature review has demonstrated the current states and outlook in two fields, which are alum sludge beneficial reusing and the odor control technologies in WWTPs. Nevertheless, previous studies have provided good insights into different topics, further investigations are still required to fulfill the novel routes of research and development as well as facilitating the industrial application. Therefore, the objectives of this study are five fold, together with the detailed motivation of each aspect presented as follows:

- ◆ **To determine the physicochemical, thermal characteristics of the two alum sludges collected from Dublin, Ireland and Carmaux, France, respectively (Chapter 2);**
- ◆ **To demonstrate the potential and prospects for alum sludge in clay brick manufacturing (Chapter 3);**
- ◆ **To provide scientific clues for alum sludge onsite applications in wastewater treatment (Chapter 4) and sewerage sludge dewatering (Chapter 5);**
- ◆ **To develop the novel alum sludge based effective waste gas purification systems (Chapter 6 and 7).**

#### Bibliography

1. Mazari, L., Abdessemed, D., Szymczyk, A.: Evaluating Reuse of Alum Sludge as Coagulant for Tertiary Wastewater Treatment. *Journal of Environmental Engineering* **144**(12) (2018). doi:10.1061/(asce)ee.1943-7870.0001462
2. Ahmad, T., Ahmad, K., Alam, M.: Characterization and constructive utilization of sludge produced in clari-flocculation unit of water treatment plant. *Materials Research Express* **5**(3), 035511 (2018). doi:10.1088/2053-1591/aab23a
3. Odimegwu, T.C., Zakaria, I., Abood, M.M., Nketsiah, C.B.K., Ahmad, M.: Review on Different Beneficial Ways of Applying Alum Sludge in a Sustainable Disposal Manner. *Civ. Eng, J.-Tehran* **4**(9), 2230-2241 (2018). doi:10.28991/cej-03091153
4. Ahmad, T., Ahmad, K., Alam, M.: Sustainable management of water treatment sludge through 3'R' concept. *J. Clean Prod.* **124**(Supplement C), 1-13 (2016). doi:<https://doi.org/10.1016/j.jclepro.2016.02.073>
5. Zhao, Y., Liu, R., Awe, O.W., Yang, Y., Shen, C.: Acceptability of land application of alum-based water treatment residuals – An explicit and comprehensive review. *Chemical Engineering Journal* **353**, 717-726 (2018). doi:<https://doi.org/10.1016/j.cej.2018.07.143>
6. Elangovan, C., Subramanian, K.: Reuse of alum sludge in clay brick manufacturing. *Water Supply* **11**(3), 333-341 (2011). doi:10.2166/ws.2011.055
7. Faris, F., Abdulhakim Saeed, A.: A New Approach to Reuse Alum Sludge in Brick Manufacturing Using Ball clay, Silica Fume and Zeolite. (2014)
8. Hegazy, B.E.-D., Hegazy, E., Fouad, H., Hassanain, A.: Brick Manufacturing From Water Treatment Sludge And Rice Husk Ash, vol. 6. (2012)



9. Chiang, K.-Y., Chou, P.-H., Hua, C.-R., Chien, K.-L., Cheeseman, C.: Lightweight bricks manufactured from water treatment sludge and rice husks. *Journal of Hazardous Materials* **171**(1), 76-82 (2009). doi:<https://doi.org/10.1016/j.jhazmat.2009.05.144>
10. Huang, C.-P., Ruhsing Pan, J., Liu, Y.: *Mixing Water Treatment Residual with Excavation Waste Soil in Brick and Artificial Aggregate Making*, vol. 131. (2005)
11. Yadav, S., Agnihotri, S., Gupta, S., Tripathi, R.K.: *Incorporation of STP Sludge and Fly ash in Brick Manufacturing: An attempt to save the Environment*, vol. 3. (2014)
12. Cornwell, D.A., Foundation, A.R.: *Water Treatment Residuals Engineering*. AWWA Research Foundation and American Water Works Association, (2006)
13. Dassanayake, K.B., Jayasinghe, G.Y., Surapaneni, A., Hetherington, C.: A review on alum sludge reuse with special reference to agricultural applications and future challenges. *Waste Management* **38**, 321-335 (2015). doi:<https://doi.org/10.1016/j.wasman.2014.11.025>
14. Babatunde, A.O., Zhao, Y.Q.: Constructive Approaches Toward Water Treatment Works Sludge Management: An International Review of Beneficial Reuses. *Critical Reviews in Environmental Science and Technology* **37**(2), 129-164 (2007). doi:10.1080/10643380600776239
15. Wang, L., Zou, F.L., Fang, X.L., Tsang, D.C.W., Poon, C.S., Leng, Z., Baek, K.: A novel type of controlled low strength material derived from alum sludge and green materials. *Construction and Building Materials* **165**, 792-800 (2018). doi:10.1016/j.conbuildmat.2018.01.078
16. Guan, X.H., Chen, G.H., Shang, C.: Re-use of water treatment works sludge to enhance particulate pollutant removal from sewage. *Water Res* **39**(15), 3433-3440 (2005). doi:10.1016/j.watres.2004.07.033
17. Nair, A.T., Ahammed, M.M.: The reuse of water treatment sludge as a coagulant for post-treatment of UASB reactor treating urban wastewater. *J. Clean Prod.* **96**, 272-281 (2015). doi:<https://doi.org/10.1016/j.jclepro.2013.12.037>
18. Jangkorn, S., Kuhakaew, S., Theantanoo, S., Klinla-or, H., Sriwiriyarat, T.: Evaluation of reusing alum sludge for the coagulation of industrial wastewater containing mixed anionic surfactants. *Journal of Environmental Sciences* **23**(4), 587-594 (2011). doi:[https://doi.org/10.1016/S1001-0742\(10\)60451-2](https://doi.org/10.1016/S1001-0742(10)60451-2)
19. Mazari, L., Abdessemed, D., Szymczyk, A., Trari, M.: Assessment of coagulation-ultrafiltration performance for the treatment of primary wastewater using alum sludge. *Water Environ. J.* **32**(4), 621-629 (2018). doi:10.1111/wej.12359
20. Razali, M., Zhao, Y.Q., Bruen, M.: Effectiveness of a drinking-water treatment sludge in removing different phosphorus species from aqueous solution. *Separation and Purification Technology* **55**(3), 300-306 (2007). doi:<https://doi.org/10.1016/j.seppur.2006.12.004>
21. Hou, Q.J., Meng, P.P., Pei, H.Y., Hu, W.R., Chen, Y.: Phosphorus adsorption characteristics of alum sludge: Adsorption capacity and the forms of phosphorus retained in alum sludge. *Materials Letters* **229**, 31-35 (2018). doi:10.1016/j.matlet.2018.06.102
22. Devi, P., Saroha, A.K.: Utilization of sludge based sorbents for the removal of various pollutants: A review. *Science of The Total Environment* **578**, 16-33 (2017). doi:<https://doi.org/10.1016/j.scitotenv.2016.10.220>
23. Zhou, Y.-F., Haynes, R.J.: A Comparison of Water Treatment Sludge and Red Mud as Sorbents of As and Se in Aqueous Solution and Their Capacity for Desorption and Regeneration. *Water, Air, & Soil Pollution* **223**(9), 5563-5573 (2012). doi:10.1007/s11270-012-1296-0
24. Irawan, C., Liu, J.C., Wu, C.-C.: Removal of boron using aluminum-based water treatment residuals (Al-WTRs). *Desalination* **276**(1), 322-327 (2011).



- doi:<https://doi.org/10.1016/j.desal.2011.03.070>
25. Siswoyo, E., Mihara, Y., Tanaka, S.: Determination of key components and adsorption capacity of a low cost sorbent based on sludge of drinking water treatment plant to adsorb cadmium ion in water, vol. 97-98. (2014)
  26. Md Nor, M.A., Ong, K.K., Mohamad, S., Ahmad Nasaruddin, N.A., Jamari, N.L.A., Wan Yunus, W.M.Z.: Kinetic study of a cationic dye adsorption by dewatered alum sludge. *Materials Research Innovations* **18**(sup6), S6-140-S146-143 (2014). doi:10.1179/1432891714Z.000000000945
  27. Zhou, Y.-F., Haynes, R.J.: Removal of Pb(II), Cr(III) and Cr(VI) from Aqueous Solutions Using Alum-Derived Water Treatment Sludge. *Water, Air, & Soil Pollution* **215**(1), 631-643 (2011). doi:10.1007/s11270-010-0505-y
  28. Sujana, M.G., Thakur, R.S., Rao, S.B.: Removal of Fluoride from Aqueous Solution by Using Alum Sludge. *Journal of Colloid and Interface Science* **206**(1), 94-101 (1998). doi:<https://doi.org/10.1006/jcis.1998.5611>
  29. Hu, Y.S., Zhao, Y.Q., Sorohan, B.: Removal of glyphosate from aqueous environment by adsorption using water industrial residual. *Desalination* **271**(1), 150-156 (2011). doi:<https://doi.org/10.1016/j.desal.2010.12.014>
  30. Hovsepyan, A., Bonzongo, J.-C.J.: Aluminum drinking water treatment residuals (Al-WTRs) as sorbent for mercury: Implications for soil remediation. *Journal of Hazardous Materials* **164**(1), 73-80 (2009). doi:<https://doi.org/10.1016/j.jhazmat.2008.07.121>
  31. Wu, C.-H., Lin, C.-F., Chen, W.-R.: Regeneration and Reuse of Water Treatment Plant Sludge: Sorbent for Cations. *Journal of Environmental Science and Health, Part A* **39**(3), 717-728 (2004). doi:10.1081/ESE-120027737
  32. Hua, T., Haynes, R.J., Zhou, Y.F.: Competitive adsorption and desorption of arsenate, vanadate, and molybdate onto the low-cost sorbent materials alum water treatment sludge and bauxite. *Environ. Sci. Pollut. Res.* **25**(34), 34053-34062 (2018). doi:10.1007/s11356-018-3301-7
  33. Makris, K.C., Sarkar, D., Datta, R.: Aluminum-based drinking-water treatment residuals: A novel sorbent for perchlorate removal. *Environmental Pollution* **140**(1), 9-12 (2006). doi:<https://doi.org/10.1016/j.envpol.2005.08.075>
  34. Gibbons, M.K., Mortula, M.M., Gagnon, G.A.: Phosphorus adsorption on water treatment residual solids. *Journal of Water Supply: Research and Technology-Aqua* **58**(1), 1-10 (2009). doi:10.2166/aqua.2009.017
  35. Ippolito, J.A., Scheckel, K.G., Barbarick, K.A.: Selenium adsorption to aluminum-based water treatment residuals. *Journal of Colloid and Interface Science* **338**(1), 48-55 (2009). doi:<https://doi.org/10.1016/j.jcis.2009.06.023>
  36. Tay, D.Y.Y., Fujinuma, R., Wendling, L.A.: Drinking water treatment residual use in urban soils: Balancing metal immobilization and phosphorus availability. *Geoderma* **305**, 113-121 (2017). doi:10.1016/j.geoderma.2017.05.047
  37. Li, X.Q., Cui, J., Pei, Y.S.: Granulation of drinking water treatment residuals as applicable media for phosphorus removal. *J. Environ. Manage.* **213**, 36-46 (2018). doi:10.1016/j.jenvman.2018.02.056
  38. Geng, Y.N., Zhang, J., Zhou, J.H., Lei, J.: Study on adsorption of methylene blue by a novel composite material of TiO<sub>2</sub> and alum sludge. *RSC Adv.* **8**(57), 32799-32807 (2018). doi:10.1039/c8ra05946b
  39. Lai, J.Y., Liu, J.C.: Co-conditioning and dewatering of alum sludge and waste activated sludge. *Water Science and Technology* **50**(9), 41-48 (2004).
  40. Yang, Y., Zhao, Y.Q., Babatunde, A.O., Kearney, P.: Co-conditioning of the anaerobic digested sludge of a municipal wastewater treatment plant with alum sludge: Benefit of phosphorus reduction in reject water. *Water Environment Research* **79**(13), 2468-2476

- (2007). doi:10.2175/106143007x184753
41. Yang, Y., Zhao, Y.Q., Babatunde, A.O., Kearney, P.: Two strategies for phosphorus removal from reject water of municipal wastewater treatment plant using alum sludge. *Water Science and Technology* **60**(12), 3181-3188 (2009). doi:10.2166/wst.2009.609
  42. Yang, Y., Zhao, Y., Liu, R., Morgan, D.: Global development of various emerged substrates utilized in constructed wetlands. *Bioresource Technology* **261**, 441-452 (2018). doi:<https://doi.org/10.1016/j.biortech.2018.03.085>
  43. Zhao, X.H., Zhao, Y.Q., Wang, W.K., Yang, Y.Z., Babatunde, A., Hu, Y.S., Kumar, L.: Key issues to consider when using alum sludge as substrate in constructed wetland. *Water Science and Technology* **71**(12), 1775-1782 (2015). doi:10.2166/wst.2015.138
  44. Zhao, Y.Q., Babatunde, A.O., Zhao, X.H., Li, W.C.: Development of alum sludge-based constructed wetland: An innovative and cost effective system for wastewater treatment. *J. Environ. Sci. Health Part A-Toxic/Hazard. Subst. Environ. Eng.* **44**(8), 827-832 (2009). doi:10.1080/10934520902928685
  45. Hu, Y.S., Zhao, Y.Q., Zhao, X.H., Kumar, J.L.G.: Comprehensive analysis of step-feeding strategy to enhance biological nitrogen removal in alum sludge-based tidal flow constructed wetlands. *Bioresource Technology* **111**, 27-35 (2012). doi:<https://doi.org/10.1016/j.biortech.2012.01.165>
  46. Hu, Y., Zhao, Y., Zhao, X., Kumar, J.L.G.: High Rate Nitrogen Removal in an Alum Sludge-Based Intermittent Aeration Constructed Wetland. *Environmental Science & Technology* **46**(8), 4583-4590 (2012). doi:10.1021/es204105h
  47. Khattab, R.M., Badr, H.A., Abo-Almaged, H.H., Sadek, H.E.H.: Recycling of alum sludge for alpha Al<sub>2</sub>O<sub>3</sub> production using different chemical treatments. *Desalination and Water Treatment* **113**, 148-159 (2018). doi:10.5004/dwt.2018.22240
  48. Keeley, J., Jarvis, P., Judd, S.J.: Coagulant Recovery from Water Treatment Residuals: A Review of Applicable Technologies. *Critical Reviews in Environmental Science and Technology* **44**(24), 2675-2719 (2014). doi:10.1080/10643389.2013.829766
  49. Skoronski, E., Ohrt, A.C., Cordella, R.D., Trevisan, V., Fernandes, M., Miguel, T.F., Menegaro, D.A., Dominghini, L., Martins, P.R.: Using Acid Mine Drainage to Recover a Coagulant from Water Treatment Residuals. *Mine Water Environ.* **36**(4), 495-501 (2017). doi:10.1007/s10230-016-0423-3
  50. Nair, A.T., Ahammed, M.M.: Influence of sludge characteristics on coagulant recovery from water treatment sludge: a preliminary study. *Journal of Material Cycles and Waste Management* **19**(3), 1228-1234 (2017). doi:10.1007/s10163-016-0513-0
  51. Jung, K.W., Hwang, M.J., Park, D.S., Ahn, K.H.: Comprehensive reuse of drinking water treatment residuals in coagulation and adsorption processes. *J. Environ. Manage.* **181**, 425-434 (2016). doi:10.1016/j.jenvman.2016.06.041
  52. Dube, S., Muchaonyerwa, P., Mapanda, F., Hughes, J.: Effects of sludge water from a water treatment works on soil properties and the yield and elemental uptake of *Brachiaria decumbens* and lucerne (*Medicago sativa*). *Agric. Water Manage.* **208**, 335-343 (2018). doi:10.1016/j.agwat.2018.06.015
  53. Ippolito, J.A., Barbarick, K.A., Elliott, H.A.: Drinking Water Treatment Residuals: A Review of Recent Uses. *Journal of Environmental Quality* **40**(1), 1-12 (2011). doi:10.2134/jeq2010.0242
  54. Russell, G.A.: From Lagooning to Farmland Application: The Next Step in Lime Sludge Disposal. *Journal - American Water Works Association* **67**(10), 585-588 (1975). doi:10.1002/j.1551-8833.1975.tb02300.x
  55. Kim, J.G., Lee, S.S., Moon, H.-S., Kang, I.M.: Land application of alum sludge from water purification plant to acid mineral soil treated with acidic water. *Soil Science and Plant Nutrition* **48**(1), 15-22 (2002). doi:10.1080/00380768.2002.10409166

56. Dayton, E.A., Basta, N.T.: Characterization of Drinking Water Treatment Residuals for Use as a Soil Substitute. *Water Environment Research* **73**(1), 52-57 (2001). doi:10.2175/106143001x138688
57. Kluczka, J., Zolotajkin, M., Ciba, J., Staron, M.: Assessment of aluminum bioavailability in alum sludge for agricultural utilization. *Environ. Monit. Assess.* **189**(8), 8 (2017). doi:10.1007/s10661-017-6133-x
58. Zhao, Y.Q., Liu, R.B., Awe, O.W., Yang, Y., Shen, C.: Acceptability of land application of alum-based water treatment residuals - An explicit and comprehensive review. *Chemical Engineering Journal* **353**, 717-726 (2018). doi:10.1016/j.cej.2018.07.143
59. Stellacci, P., Liberti, L., Notarnicola, M., Haas, C.N.: Hygienic sustainability of site location of wastewater treatment plants: A case study. II. Estimating airborne biological hazard. *Desalination* **253**(1), 106-111 (2010). doi:<https://doi.org/10.1016/j.desal.2009.11.024>
60. Estrada, J.M., Kraakman, N.J.R.B., Muñoz, R., Lebrero, R.: A Comparative Analysis of Odour Treatment Technologies in Wastewater Treatment Plants. *Environmental Science & Technology* **45**(3), 1100-1106 (2011). doi:10.1021/es103478j
61. Latos, M., Karageorgos, P., Kalogerakis, N., Lazaridis, M.: Dispersion of Odorous Gaseous Compounds Emitted from Wastewater Treatment Plants. *Water, Air, & Soil Pollution* **215**(1), 667-677 (2011). doi:10.1007/s11270-010-0508-8
62. Hayes, J.E., Stevenson, R.J., Stuetz, R.M.: The impact of malodour on communities: A review of assessment techniques. *Science of The Total Environment* **500-501**, 395-407 (2014). doi:<https://doi.org/10.1016/j.scitotenv.2014.09.003>
63. Easter, C., Quigley, C., Burrowes, P., Witherspoon, J., Apgar, D.: Odor and air emissions control using biotechnology for both collection and wastewater treatment systems. *Chemical Engineering Journal* **113**(2), 93-104 (2005). doi:<https://doi.org/10.1016/j.cej.2005.04.007>
64. Jiang, G., Melder, D., Keller, J., Yuan, Z.: Odor emissions from domestic wastewater: A review. *Critical Reviews in Environmental Science and Technology* **47**(17), 1581-1611 (2017). doi:10.1080/10643389.2017.1386952
65. Talaiekhosani, A., Bagheri, M., Goli, A., Talaie Khoozani, M.R.: An overview of principles of odor production, emission, and control methods in wastewater collection and treatment systems. *J. Environ. Manage.* **170**, 186-206 (2016). doi:<https://doi.org/10.1016/j.jenvman.2016.01.021>
66. Burgess, J.E., Parsons, S.A., Stuetz, R.M.: Developments in odour control and waste gas treatment biotechnology: a review. *Biotechnology Advances* **19**(1), 35-63 (2001). doi:[https://doi.org/10.1016/S0734-9750\(00\)00058-6](https://doi.org/10.1016/S0734-9750(00)00058-6)
67. Suffet, I.H., Rosenfeld, P.: The anatomy of odour wheels for odours of drinking water, wastewater, compost and the urban environment. *Water Science and Technology* **55**(5), 335-344 (2007). doi:10.2166/wst.2007.196
68. Shaw, A.R., Koh, S.-H.: Gaseous Emissions from Wastewater Facilities. *Water Environment Research* **84**(10), 1325-1331 (2012). doi:10.2175/106143007X1340727513
69. Stuetz, R.M., Frechen, F.-B.: *Odours in wastewater treatment*. IWA publishing, (2001)
70. Omri, I., Aouidi, F., Bouallagui, H., Godon, J.-J., Hamdi, M.: Performance study of biofilter developed to treat H<sub>2</sub>S from wastewater odour. *Saudi Journal of Biological Sciences* **20**(2), 169-176 (2013). doi:<https://doi.org/10.1016/j.sjbs.2013.01.005>
71. Lagoudianaki, E., Manios, T., Geniatakis, M., Frantzeskaki, N., Manios, V.: Odor Control in Evaporation Ponds Treating Olive Mill Wastewater Through the Use of Ca(OH)<sub>2</sub>. *Journal of Environmental Science and Health, Part A* **38**(11), 2537-2547 (2003). doi:10.1081/ESE-120024445
72. Zhang, L., De Schryver, P., De Gussemé, B., De Muynck, W., Boon, N., Verstraete, W.: Chemical and biological technologies for hydrogen sulfide emission control in sewer

- systems: A review. *Water Research* **42**(1), 1-12 (2008). doi:<https://doi.org/10.1016/j.watres.2007.07.013>
73. Anfruns, A., Canals-Batlle, C., Ros, A., Lillo-Ródenas, M.A., Linares-Solano, A., Fuente, E., Montes-Morán, M.A., Martín, M.J.: Removal of odour-causing compounds using carbonaceous sorbents/catalysts prepared from sewage sludge. *Water Science and Technology* **59**(7), 1371-1376 (2009). doi:10.2166/wst.2009.126
74. Karageorgos, P., Latos, M., Kotsifaki, C., Lazaridis, M., Kalogerakis, N.: Treatment of unpleasant odors in municipal wastewater treatment plants. *Water Science and Technology* **61**(10), 2635-2644 (2010). doi:10.2166/wst.2010.211
75. Rajbansi, B., Sarkar, U., Hobbs, S.E.: Hazardous odor markers from sewage wastewater: A step towards simultaneous assessment, dearomatization and removal. *Journal of the Taiwan Institute of Chemical Engineers* **45**(4), 1549-1557 (2014). doi:<https://doi.org/10.1016/j.jtice.2013.10.004>
76. Kim, J.R., Dec, J., Bruns, M.A., Logan, B.E.: Removal of Odors from Swine Wastewater by Using Microbial Fuel Cells. *Applied and Environmental Microbiology* **74**(8), 2540 (2008). doi:10.1128/AEM.02268-07
77. Xie, B., Liang, S.B., Tang, Y., Mi, W.X., Xu, Y.: Petrochemical wastewater odor treatment by biofiltration. *Bioresource Technology* **100**(7), 2204-2209 (2009). doi:<https://doi.org/10.1016/j.biortech.2008.10.035>
78. Alfonsín, C., Lebrero, R., Estrada, J.M., Muñoz, R., Kraakman, N.J.R., Feijoo, G., Moreira, M.T.: Selection of odour removal technologies in wastewater treatment plants: A guideline based on Life Cycle Assessment. *J. Environ. Manage.* **149**, 77-84 (2015). doi:<https://doi.org/10.1016/j.jenvman.2014.10.011>
79. Lebrero, R., Rodríguez, E., Martín, M., García-Encina, P.A., Muñoz, R.: H<sub>2</sub>S and VOCs abatement robustness in biofilters and air diffusion bioreactors: A comparative study. *Water Research* **44**(13), 3905-3914 (2010). doi:<https://doi.org/10.1016/j.watres.2010.05.008>
80. Zarra, T., Giuliani, S., Naddeo, V., Belgiorno, V.: Control of odour emission in wastewater treatment plants by direct and undirected measurement of odour emission capacity. *Water Science and Technology* **66**(8), 1627-1633 (2012). doi:10.2166/wst.2012.362
81. Gil, R.R., Ruiz, B., Lozano, M.S., Martín, M.J., Fuente, E.: VOCs removal by adsorption onto activated carbons from biocollagenic wastes of vegetable tanning. *Chemical Engineering Journal* **245**, 80-88 (2014). doi:<https://doi.org/10.1016/j.cej.2014.02.012>
82. Zhang, X., Gao, B., Creamer, A.E., Cao, C., Li, Y.: Adsorption of VOCs onto engineered carbon materials: A review. *Journal of Hazardous Materials* **338**, 102-123 (2017). doi:<https://doi.org/10.1016/j.jhazmat.2017.05.013>
83. Aziz, A., Kim, K.S.: Adsorptive Volatile Organic Removal from Air onto NaZSM-5 and HZSM-5: Kinetic and Equilibrium Studies. *Water, Air, & Soil Pollution* **228**(9), 319 (2017). doi:10.1007/s11270-017-3497-z
84. Lebrero, R., Bouchy, L., Stuetz, R., Muñoz, R.: Odor Assessment and Management in Wastewater Treatment Plants: A Review. *Critical Reviews in Environmental Science and Technology* **41**(10), 915-950 (2011). doi:10.1080/10643380903300000
85. Badosz, T.J., Bagreev, A., Adib, F., Turk, A.: Unmodified versus Caustics-Impregnated Carbons for Control of Hydrogen Sulfide Emissions from Sewage Treatment Plants. *Environmental Science & Technology* **34**(6), 1069-1074 (2000). doi:10.1021/es9813212
86. Yang, J., Xu, W., He, C., Huang, Y., Zhang, Z., Wang, Y., Hu, L., Xia, D., Shu, D.: One-step synthesis of silicon carbide foams supported hierarchical porous sludge-derived activated carbon as efficient odor gas sorbent. *Journal of Hazardous Materials* **344**, 33-41 (2018). doi:<https://doi.org/10.1016/j.jhazmat.2017.09.056>



87. Sempere, F., Gabaldón, C., Martínez-Soria, V., Peña-roja, J.M., Álvarez-Hornos, F.J.: Evaluation of a combined activated carbon prefilter and biotrickling filter system treating variable ethanol and ethyl acetate gaseous emissions. *Engineering in Life Sciences* **9**(4), 317-323 (2009). doi:[doi:10.1002/elsc.200900011](https://doi.org/10.1002/elsc.200900011)
88. Anfruns, A., Martin, M.J., Montes-Morán, M.A.: Removal of odorous VOCs using sludge-based sorbents. *Chemical Engineering Journal* **166**(3), 1022-1031 (2011). doi:<https://doi.org/10.1016/j.cej.2010.11.095>
89. Bamdad, H., Hawboldt, K., MacQuarrie, S.: A review on common sorbents for acid gases removal: Focus on biochar. *Renewable and Sustainable Energy Reviews* **81**, 1705-1720 (2018). doi:<https://doi.org/10.1016/j.rser.2017.05.261>
90. Papurello, D., Santarelli, M., Fiorilli, S.: Physical Activation of Waste-Derived Materials for Biogas Cleaning. *Energies* **11**(9), 12 (2018). doi:10.3390/en11092338
91. Shang, G.F., Li, Q.W., Liu, L., Chen, P., Huang, X.M.: Adsorption of hydrogen sulfide by biochars derived from pyrolysis of different agricultural/forestry wastes. *Journal of the Air & Waste Management Association* **66**(1), 8-16 (2016). doi:10.1080/10962247.2015.1094429
92. Hervy, M., Pham Minh, D., Gérente, C., Weiss-Hortala, E., Nzihou, A., Villot, A., Le Coq, L.: H<sub>2</sub>S removal from syngas using wastes pyrolysis chars. *Chemical Engineering Journal* **334**, 2179-2189 (2018). doi:<https://doi.org/10.1016/j.cej.2017.11.162>
93. Patel, H.: Fixed-bed column adsorption study: a comprehensive review. *Applied Water Science* **9**(3), 45 (2019). doi:10.1007/s13201-019-0927-7
94. Liu, L., Liu, J., Pei, J.: Towards a better understanding of adsorption of indoor air pollutants in porous media—From mechanistic model to molecular simulation. *Building Simulation* **11**(5), 997-1010 (2018). doi:10.1007/s12273-018-0445-9
95. Lebrero, R., Rodríguez, E., García-Encina, P.A., Muñoz, R.: A comparative assessment of biofiltration and activated sludge diffusion for odour abatement. *Journal of Hazardous Materials* **190**(1), 622-630 (2011). doi:<https://doi.org/10.1016/j.jhazmat.2011.03.090>
96. Yang, C.-L., Chen, L.: Oxidation of nitric oxide in a two-stage chemical scrubber using dc corona discharge. *Journal of Hazardous Materials* **80**(1), 135-146 (2000). doi:[https://doi.org/10.1016/S0304-3894\(00\)00291-0](https://doi.org/10.1016/S0304-3894(00)00291-0)
97. Bandyopadhyaya, A., Biswasa, M.N.: Prediction of the Removal Efficiency of a Novel Two-Stage Hybrid Scrubber for Flue Gas Desulfurization. *Chemical Engineering & Technology* **29**(1), 130-145 (2006). doi:[doi:10.1002/ceat.200500160](https://doi.org/10.1002/ceat.200500160)
98. Wei-Hsiang, C., Yuan-Chung, L., Jun-Hong, L., Po-Ming, Y., Syu-Ruei, J.: Treating Odorous and Nitrogenous Compounds from Waste Composting by Acidic Chlorination Followed by Alkaline Sulfurization. *Environmental Engineering Science* **31**(11), 583-592 (2014). doi:10.1089/ees.2013.0272
99. Hariz, R., del Rio Sanz, J.I., Mercier, C., Valentin, R., Dietrich, N., Mouloungui, Z., Hébrard, G.: Absorption of toluene by vegetable oil–water emulsion in scrubbing tower: Experiments and modeling. *Chemical Engineering Science* **157**, 264-271 (2017). doi:<https://doi.org/10.1016/j.ces.2016.06.008>
100. Bindra, N., Dubey, B., Dutta, A.: Technological and life cycle assessment of organics processing odour control technologies. *Science of The Total Environment* **527-528**, 401-412 (2015). doi:<https://doi.org/10.1016/j.scitotenv.2015.05.023>
101. Yang, S., Li, Y., Wang, L., Feng, L.: Use of peroxymonosulfate in wet scrubbing process for efficient odor control. *Separation and Purification Technology* **158**, 80-86 (2016). doi:<https://doi.org/10.1016/j.seppur.2015.12.010>
102. Wu, C.-Y., Chou, M.-S., Lin, J.-H.: Oxidative scrubbing of DMS-containing waste gases by hypochlorite solution. *Journal of the Taiwan Institute of Chemical Engineers* **45**(2), 596-602 (2014). doi:<https://doi.org/10.1016/j.jtice.2013.06.017>

103. Ding, L., Liu, T.-X., Li, X.-Z.: Removal of CH<sub>3</sub>SH with in-situ generated ferrate(VI) in a wet-scrubbing reactor. *Journal of Chemical Technology & Biotechnology* **89**(3), 455-461 (2014). doi:[doi:10.1002/jctb.4139](https://doi.org/10.1002/jctb.4139)
104. Charron, I., Féliers, C., Couvert, A., Laplanche, A., Patria, L., Requieme, B.: Use of hydrogen peroxide in scrubbing towers for odor removal in wastewater treatment plants. *Water Science and Technology* **50**(4), 267-274 (2004). doi:[10.2166/wst.2004.0281](https://doi.org/10.2166/wst.2004.0281)
105. Couvert, A., Charron, I., Laplanche, A., Renner, C., Patria, L., Requieme, B.: Treatment of odorous sulphur compounds by chemical scrubbing with hydrogen peroxide—Application to a laboratory plant. *Chemical Engineering Science* **61**(22), 7240-7248 (2006). doi:<https://doi.org/10.1016/j.ces.2006.07.030>
106. Estrada, J.M., Kraakman, N.J.R., Lebrero, R., Muñoz, R.: A sensitivity analysis of process design parameters, commodity prices and robustness on the economics of odour abatement technologies. *Biotechnology Advances* **30**(6), 1354-1363 (2012). doi:<https://doi.org/10.1016/j.biotechadv.2012.02.010>
107. Biard, P.-F., Couvert, A., Renner, C., Lévassieur, J.-P.: Wet scrubbing intensification applied to hydrogen sulphide removal in waste water treatment plant. *The Canadian Journal of Chemical Engineering* **88**(4), 682-687 (2010). doi:[doi:10.1002/cjce.20310](https://doi.org/10.1002/cjce.20310)
108. Shareefdeen, Z., Herner, B., Singh, A.: *Biotechnology for Air Pollution Control — an Overview*. In: Shareefdeen, Z., Singh, A. (eds.) *Biotechnology for Odor and Air Pollution Control*. pp. 3-15. Springer Berlin Heidelberg, Berlin, Heidelberg (2005)
109. Barbusinski, K., Kalemba, K., Kasperczyk, D., Urbaniec, K., Kozik, V.: Biological methods for odor treatment – A review. *J. Clean Prod.* **152**, 223-241 (2017). doi:<https://doi.org/10.1016/j.jclepro.2017.03.093>
110. Elias, A., Barona, A., Arreguy, A., Rios, J., Aranguiz, I., Peñas, J.: Evaluation of a packing material for the biodegradation of H<sub>2</sub>S and product analysis. *Process Biochemistry* **37**(8), 813-820 (2002). doi:[https://doi.org/10.1016/S0032-9592\(01\)00287-4](https://doi.org/10.1016/S0032-9592(01)00287-4)
111. Sakuma, T., Hattori, T., Deshusses, M.A.: Comparison of Different Packing Materials for the Biofiltration of Air Toxics. *Journal of the Air & Waste Management Association* **56**(11), 1567-1575 (2006). doi:[10.1080/10473289.2006.10464564](https://doi.org/10.1080/10473289.2006.10464564)
112. Dumont, E., Andrès, Y., Le Cloirec, P., Gaudin, F.: Evaluation of a new packing material for H<sub>2</sub>S removed by biofiltration. *Biochemical Engineering Journal* **42**(2), 120-127 (2008). doi:<https://doi.org/10.1016/j.bej.2008.06.012>
113. Bhaskaran, K., Nadaraja, A.V., Balakrishnan, M.V., Haridas, A.: Dynamics of sustainable grazing fauna and effect on performance of gas biofilter. *Journal of Bioscience and Bioengineering* **105**(3), 192-197 (2008). doi:<https://doi.org/10.1263/jbb.105.192>
114. Park, J., Evans, E.A., Ellis, T.G.: Development of a Biofilter with Tire-Derived Rubber Particle Media for Hydrogen Sulfide Odor Removal. *Water, Air, & Soil Pollution* **215**(1), 145-153 (2011). doi:[10.1007/s11270-010-0466-1](https://doi.org/10.1007/s11270-010-0466-1)
115. Dumont, E., Cabral, F.D.S., Le Cloirec, P., Andrès, Y.: Biofiltration using peat and a nutritional synthetic packing material: influence of the packing configuration on H<sub>2</sub>S removal. *Environmental Technology* **34**(9), 1123-1129 (2013). doi:[10.1080/09593330.2012.736691](https://doi.org/10.1080/09593330.2012.736691)
116. Premkumar, R., Krishnamohan, N.: Effect of secondary parameters on biofilter treating industrial effluent. *Pharm. Tech* **4**, 1279-1287 (2012).
117. Zehraoui, A., Hassan, A.A., Sorial, G.A.: Biological treatment of n-hexane and methanol in trickle bed air biofilters under acidic conditions. *Biochemical Engineering Journal* **77**, 129-135 (2013). doi:<https://doi.org/10.1016/j.bej.2013.06.001>
118. Das, J., Rene, E.R., Dupont, C., Dufourny, A., Blin, J., van Hullebusch, E.D.: Performance of a compost and biochar packed biofilter for gas-phase hydrogen sulfide removal. *Bioresource Technology* **273**, 581-591 (2019).

- doi:<https://doi.org/10.1016/j.biortech.2018.11.052>
119. Yuan, J., Du, L.L., Li, S.Y., Yang, F., Zhang, Z.Y., Li, G.X., Wang, G.Y.: Use of mature compost as filter media and the effect of packing depth on hydrogen sulfide removal from composting exhaust gases by biofiltration. *Environ. Sci. Pollut. Res.* **26**(4), 3762-3770 (2019). doi:[10.1007/s11356-018-3795-z](https://doi.org/10.1007/s11356-018-3795-z)
  120. Vikrant, K., Kailasa, S.K., Tsang, D.C.W., Lee, S.S., Kumar, P., Giri, B.S., Singh, R.S., Kim, K.-H.: Biofiltration of hydrogen sulfide: Trends and challenges. *J. Clean Prod.* **187**, 131-147 (2018). doi:<https://doi.org/10.1016/j.jclepro.2018.03.188>
  121. Rakia, C., Wahida, D., Faten, S., Ben, R.M., Denis, L.P., Abdelghani, S.: Microbial Analysis and Efficiency of Biofiltration Packing Systems for Hydrogen Sulfide Removal from Wastewater Off Gas. *Environmental Engineering Science* **32**(2), 121-128 (2015). doi:[10.1089/ees.2014.0290](https://doi.org/10.1089/ees.2014.0290)
  122. Allievi, M.J., Silveira, D.D., Cantão, M.E., Filho, P.B.: Bacterial community diversity in a full scale biofilter treating wastewater odor. *Water Science and Technology* **77**(8), 2014-2022 (2018). doi:[10.2166/wst.2018.114](https://doi.org/10.2166/wst.2018.114)
  123. Oyarzún, P., Arancibia, F., Canales, C., Aroca, G.E.: Biofiltration of high concentration of hydrogen sulphide using *Thiobacillus thioparus*. *Process Biochemistry* **39**(2), 165-170 (2003). doi:[https://doi.org/10.1016/S0032-9592\(03\)00050-5](https://doi.org/10.1016/S0032-9592(03)00050-5)
  124. Cheng, Y., He, H., Yang, C., Zeng, G., Li, X., Chen, H., Yu, G.: Challenges and solutions for biofiltration of hydrophobic volatile organic compounds. *Biotechnology Advances* **34**(6), 1091-1102 (2016). doi:<https://doi.org/10.1016/j.biotechadv.2016.06.007>
  125. Mudliar, S., Giri, B., Padoley, K., Satpute, D., Dixit, R., Bhatt, P., Pandey, R., Juwarkar, A., Vaidya, A.: Bioreactors for treatment of VOCs and odours – A review. *J. Environ. Manage.* **91**(5), 1039-1054 (2010). doi:<https://doi.org/10.1016/j.jenvman.2010.01.006>
  126. Rattanapan, C., Boonsawang, P., Kantachote, D.: Removal of H<sub>2</sub>S in down-flow GAC biofiltration using sulfide oxidizing bacteria from concentrated latex wastewater. *Bioresource Technology* **100**(1), 125-130 (2009). doi:<https://doi.org/10.1016/j.biortech.2008.05.049>
  127. Chung, Y.-C., Cheng, C.-Y., Chen, T.-Y., Hsu, J.-S., Kui, C.-C.: Structure of the bacterial community in a biofilter during dimethyl sulfide (DMS) removal processes. *Bioresource Technology* **101**(18), 7165-7168 (2010). doi:<https://doi.org/10.1016/j.biortech.2010.03.131>
  128. Liu, Q., Li, M., Chen, R., Li, Z., Qian, G., An, T., Fu, J., Sheng, G.: Biofiltration treatment of odors from municipal solid waste treatment plants. *Waste Management* **29**(7), 2051-2058 (2009). doi:<https://doi.org/10.1016/j.wasman.2009.02.002>
  129. Lee, S.-h., Li, C., Heber, A.J., Ni, J., Huang, H.: Biofiltration of a mixture of ethylene, ammonia, n-butanol, and acetone gases. *Bioresource Technology* **127**, 366-377 (2013). doi:<https://doi.org/10.1016/j.biortech.2012.09.110>
  130. Yang, L., Kent, A.D., Wang, X., Funk, T.L., Gates, R.S., Zhang, Y.: Moisture effects on gas-phase biofilter ammonia removal efficiency, nitrous oxide generation, and microbial communities. *Journal of Hazardous Materials* **271**, 292-301 (2014). doi:<https://doi.org/10.1016/j.jhazmat.2014.01.058>
  131. Yu, J.-m., Chen, J.-m., Wang, J.-d.: Removal of dichloromethane from waste gases by a biotrickling filter. *Journal of Environmental Sciences* **18**(6), 1073-1076 (2006). doi:[https://doi.org/10.1016/S1001-0742\(06\)60041-7](https://doi.org/10.1016/S1001-0742(06)60041-7)
  132. Zhang, Y., Liss, S.N., Allen, D.G.: Enhancing and modeling the biofiltration of dimethyl sulfide under dynamic methanol addition. *Chemical Engineering Science* **62**(9), 2474-2481 (2007). doi:<https://doi.org/10.1016/j.ces.2007.01.035>
  133. Abraham, S., Joslyn, S., Suffet, I.H.: Treatment of odor by a seashell biofilter at a wastewater treatment plant. *Journal of the Air & Waste Management Association* **65**(10),



- 1217-1228 (2015). doi:10.1080/10962247.2015.1075918
134. Kafle, G.K., Chen, L., Neibling, H., Brian He, B.: Field evaluation of wood bark-based down-flow biofilters for mitigation of odor, ammonia, and hydrogen sulfide emissions from confined swine nursery barns. *J. Environ. Manage.* **147**, 164-174 (2015). doi:<https://doi.org/10.1016/j.jenvman.2014.09.004>
135. Jaber, M.B., Anet, B., Amrane, A., Couriol, C., Lendormi, T., Cloirec, P.L., Cogny, G., Fillières, R.: Impact of nutrients supply and pH changes on the elimination of hydrogen sulfide, dimethyl disulfide and ethanethiol by biofiltration. *Chemical Engineering Journal* **258**, 420-426 (2014). doi:<https://doi.org/10.1016/j.cej.2014.07.085>
136. Wang, L., Yang, C., Cheng, Y., Huang, J., Yang, H., Zeng, G., Lu, L., He, S.: Enhanced removal of ethylbenzene from gas streams in biotrickling filters by Tween-20 and Zn(II). *Journal of Environmental Sciences* **26**(12), 2500-2507 (2014). doi:<https://doi.org/10.1016/j.jes.2014.04.011>
137. Alfonsín, C., Hernández, J., Omil, F., Prado, Ó.J., Gabriel, D., Feijoo, G., Moreira, M.T.: Environmental assessment of different biofilters for the treatment of gaseous streams. *J. Environ. Manage.* **129**, 463-470 (2013). doi:<https://doi.org/10.1016/j.jenvman.2013.08.009>
138. Iranpour, R., Cox, H.H.J., Deshusses, M.A., Schroeder, E.D.: Literature review of air pollution control biofilters and biotrickling filters for odor and volatile organic compound removal. *Environmental Progress* **24**(3), 254-267 (2005). doi:10.1002/ep.10077
139. Talaiekhosani, A., Ali Fulazzaky, M., Ponraj, M., Abd Majid, M.Z.: Removal of formaldehyde from polluted air in a biotrickling filter reactor. *Desalination and Water Treatment* **52**(19-21), 3663-3671 (2014). doi:10.1080/19443994.2013.854002
140. Vikromvarasiri, N., Juntranapaporn, J., Pisutpaisal, N.: Performance of *Paracoccus pantotrophus* for H<sub>2</sub>S removal in biotrickling filter. *International Journal of Hydrogen Energy* **42**(45), 27820-27825 (2017). doi:<https://doi.org/10.1016/j.ijhydene.2017.05.232>
141. Wu, H., Guo, C., Yin, Z., Quan, Y., Yin, C.: Performance and bacterial diversity of biotrickling filters filled with conductive packing material for the treatment of toluene. *Bioresource Technology* **257**, 201-209 (2018). doi:<https://doi.org/10.1016/j.biortech.2018.02.108>
142. Salamanca, D., Dobslaw, D., Engesser, K.-H.: Removal of cyclohexane gaseous emissions using a biotrickling filter system. *Chemosphere* **176**, 97-107 (2017). doi:<https://doi.org/10.1016/j.chemosphere.2017.02.078>
143. Aguirre, A., Bernal, P., Maureira, D., Ramos, N., Vásquez, J., Urrutia, H., Gentina, J.C., Aroca, G.: Biofiltration of trimethylamine in biotrickling filter inoculated with *Aminobacter aminovorans*. *Electronic Journal of Biotechnology* **33**, 63-67 (2018). doi:<https://doi.org/10.1016/j.ejbt.2018.04.004>
144. Yang, B., Niu, X., Ding, C., Xu, X., Liu, D.: Performance of Biotrickling Filter Inoculated with Activated Sludge for Chlorobenzene Removal. *Procedia Environmental Sciences* **18**, 391-396 (2013). doi:<https://doi.org/10.1016/j.proenv.2013.04.052>
145. Lebrero, R., Gondim, A.C., Pérez, R., García-Encina, P.A., Muñoz, R.: Comparative assessment of a biofilter, a biotrickling filter and a hollow fiber membrane bioreactor for odor treatment in wastewater treatment plants. *Water Research* **49**, 339-350 (2014). doi:<https://doi.org/10.1016/j.watres.2013.09.055>
146. Hansen, N.G., Rindel, K.: Bioscrubbing, an effective and economic solution to odour control at wastewater treatment plants. *Water Science and Technology* **41**(6), 155-164 (2000). doi:10.2166/wst.2000.0105
147. Bowker, R.P.: Biological odour control by diffusion into activated sludge basins. *Water*

- Science and Technology **41**(6), 127-132 (2000). doi:10.2166/wst.2000.0101
148. Nisola, G.M., Cho, E., Orata, J.D., Redillas, M.C.F.R., Farnazo, D.M.C., Tuuguu, E., Chung, W.J.: NH<sub>3</sub> gas absorption and bio-oxidation in a single bioscrubber system. *Process Biochemistry* **44**(2), 161-167 (2009). doi:<https://doi.org/10.1016/j.procbio.2008.10.004>
149. Potivichayanon, S., Pokethitiyook, P., Kruatrachue, M.: Hydrogen sulfide removal by a novel fixed-film bioscrubber system. *Process Biochemistry* **41**(3), 708-715 (2006). doi:<https://doi.org/10.1016/j.procbio.2005.09.006>
150. Friedrich, M., Kośmider, J., Terebecki, P., Mizerna-Nowotna, P.: Odour abatement of waste gases from sludge thickeners in wastewater treatment plant using bioscrubber. *Chemical Engineering Transactions* **40**, 205-210 (2014).
151. Liu, F., Fiencke, C., Guo, J., Rieth, R., Dong, R., Pfeiffer, E.-M.: Performance evaluation and optimization of field-scale bioscrubbers for intensive pig house exhaust air treatment in northern Germany. *Science of The Total Environment* **579**, 694-701 (2017). doi:<https://doi.org/10.1016/j.scitotenv.2016.11.039>
152. Ball, A.S., Nedwell, D.B., Perkins, R.G.: Oxidation of hydrogen sulphide in sour gas by *Chlorobium limicola*. *Enzyme and Microbial Technology* **41**(6), 702-705 (2007). doi:<https://doi.org/10.1016/j.enzmictec.2007.06.003>
153. Tóth, G., Lövitusz, É., Nemestóthy, N., Bélafi-Bakó, K.: Biocatalytic hydrogen sulphide removal from gaseous streams. *Hungarian Journal of Industry and Chemistry* **40**(2), 87-91 (2012).
154. Rodríguez, E., García-Encina, P.A., Muñoz, R., Lebrero, R.: Microbial community changes during different empty bed residence times and operational fluctuations in an air diffusion reactor for odor abatement. *Science of The Total Environment* **590-591**, 352-360 (2017). doi:<https://doi.org/10.1016/j.scitotenv.2017.01.161>
155. Barbosa, V., Hobbs, P., Sneath, R., Burgess, J., Callan, J., Stuetz, R.: Investigating the Capacity of an Activated Sludge Process to Reduce Volatile Organic Compounds and Odor Emissions. *Water Environment Research* **78**(8), 842-851 (2006). doi:10.2175/106143005X72876
156. Barbosa, V.L., Stuetz, R.M.: Performance of activated sludge diffusion for biological treatment of hydrogen sulphide gas emissions. *Water Science and Technology* **68**(9), 1932-1939 (2013). doi:10.2166/wst.2013.444
157. Moussavi, G., Naddafi, K., Mesdaghinia, A., Deshusses, M.A.: THE REMOVAL OF H<sub>2</sub>S FROM PROCESS AIR BY DIFFUSION INTO ACTIVATED SLUDGE. *Environmental Technology* **28**(9), 987-993 (2007). doi:10.1080/09593332808618856
158. Blonda, M., Di Pinto, A.C., Laera, G., Palumbo, R., Pollice, A.: Activated Sludge Diffusion for Odour Removal - Effects of H<sub>2</sub>S on the Biomass. *Environmental Technology* **27**(8), 875-883 (2006). doi:10.1080/09593332708618697
159. Shammay, A., Sivret, E.C., Le-Minh, N., Lebrero Fernandez, R., Evanson, I., Stuetz, R.M.: Review of odour abatement in sewer networks. *Journal of Environmental Chemical Engineering* **4**(4, Part A), 3866-3881 (2016). doi:<https://doi.org/10.1016/j.jece.2016.08.016>
160. Galera Martínez, M., Pham Minh, D., Nzihou, A., Sharrock, P.: Valorization of calcium carbonate-based solid wastes for the treatment of hydrogen sulfide in a semi-continuous reactor. *Chemical Engineering Journal* **360**, 1167-1176 (2019). doi:[10.1016/j.cej.2018.10.169](https://doi.org/10.1016/j.cej.2018.10.169)

## Chapter 2

### Materials and Methods

#### Introduction

In this Chapter the two alum sludges (section 2.1) used in this work as well as the description of their corresponding WTPs are presented. One alum sludge was collected from Dublin (Ireland) and the other from Carmaux (France). Various characterization methods of alum sludge including physicochemical and thermal analysis were described in section 2.2 and the results obtained are presented. Lastly, the five experimental methods which have been applied in this study were outlined in section 2.3.

#### 2.1 Materials

Two sources of alum sludge sample were studied, one is from Dublin Ballymore Eustace water treatment plant, Ireland and the other is from Carmaux water treatment plant, France. As aforementioned in Chapter 1, the characteristics of alum sludge is largely depending on the raw water sources and purification processes. Thus, the background of two relevant WTPs were presented.

The Dublin Ballymore Eustace water treatment plant is the largest water treatment plant in Ireland, with the treatment capacity of 318,000 m<sup>3</sup> per day. Conventional coagulation-filtration treatment processes were employed. The plant takes the raw water from the shore of Blessington reservoir on the Wicklow/Kildare border and currently supplies an average of 300,000 m<sup>3</sup> per day of treated water to consumers in Great Dublin area including Dublin City, Dun-Laoghaire, south Dublin and part of Kildare. Aluminum sulphide (FO-4140 PWG) (Al<sub>2</sub>(SO<sub>4</sub>)<sub>3</sub>·14H<sub>2</sub>O) is used as a coagulation aid, and hence the waste by-product is termed as alum sludge. Alum sludge tends to be amorphous in nature. For example, as shown in Eq. 2.1, when alum is added to water it reacts with bicarbonate to form amorphous Al(OH)<sub>3(s)</sub>.

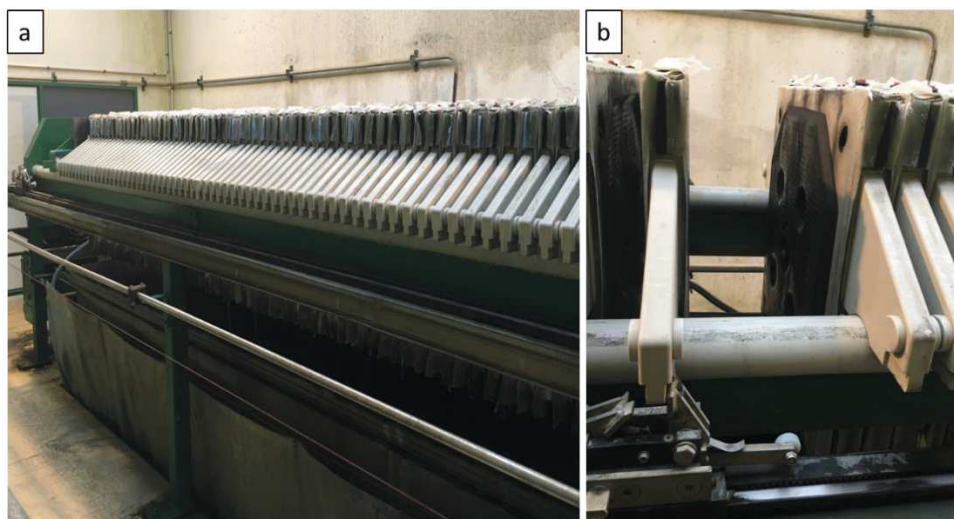


As shown in Figure 2.1, the alum sludge cake was deposited into large containers (Figure 2.1 right) which could hold approximately 30 tons of sludge, and 5 to 6 of these large containers (equates to 165 tons) were filled daily. At a cost of €65 per ton, this plant is spending over €10,000/day on the disposal of alum sludge [1].



**Figure 2.1** Alum sludge being collected for disposal in Dublin Ballymore Eustace WTP

The Carmaux water treatment plant is located in Tarn, France. The plant produces and supplies 3014 m<sup>3</sup>/day drinking water by treating the reservoir water using aluminum chloride hydroxide sulfate (HYDREX 3531 Veolia, France) (Al<sub>2</sub>Cl<sub>2</sub>(OH)<sub>2</sub>SO<sub>4</sub>) as coagulant and the treated water serving for 7,000 consumers. Compare with Dublin Ballymore Eustace WTP (300,000 m<sup>3</sup> per day), the treatment capacity of Carmaux WTP is quite small. but the same main water purification processes were employed, namely coagulation-filtration. The mechanically dewatered alum sludge was disposed by landfilling, Figure 2.2 presents the plate and frame type filter press in Carmaux WTP.



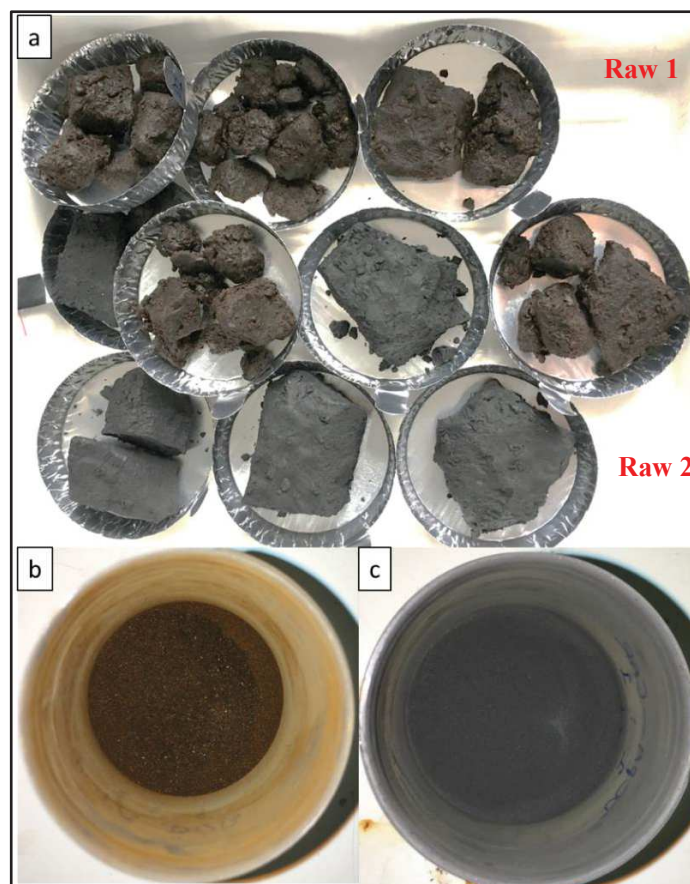
**Figure 2.2** Filter press in Carmaux WTP

Figure 2.3 (a) presents the two sources of raw alum sludge cake which were collected from the holding tank of the sludge dewatering unit of the corresponding WTPs. As shown in Figure 2.3 (a), the two origins of raw alum sludge cake present different colors, the first raw (Raw 1) presents the color of dark brown are from Dublin Ballymore Eustace WTP, while the second raw (Raw 2) presents the color of pitch black are from Carmaux WTP. The different color of raw alum sludge cake could derive from the different raw water sources and treatment processes.

After collection, the raw alum sludge cake was air-dried at a room temperature for two weeks



and crushed mechanically by a blender and sieved by 500  $\mu\text{m}$  mesh for storage and subsequent analysis.



**Figure 2.3** Alum sludge; (a) raw alum sludge cake (b) Dublin alum sludge; (d) Carmaux alum sludge

## 2.2 Characterization of alum sludge

### 2.2.1 Characterization methods

#### ➤ Moisture

Moisture content of two kinds of alum sludge was carried out by drying the raw alum sludge cake in the oven at 105 °C for 24h and measuring the mass differences before and after drying. The moisture content was calculated by:

$$\text{MC (wt\%)} = m_i/m_f \quad (2.2)$$

Where  $m_i$ ,  $m_f$  is the mass of the sample before and after drying respectively.

#### ➤ pH

The pH of the alum sludge was measured by adding 0.5 g of sample to 20mL of distilled water. The suspension was magnetically stirred at room temperature at least 24h before measuring the pH of the suspension with a pH meter.

#### ➤ Volatile Matter

The volatile matter of the alum sludge samples was determined using the EN 15402 protocol. It was determined as the following steps: approximately 1 g of the sample was placed

in a cylindrical crucible with a well-fitting lid to avoid contact with air during devolatilization. The covered crucible and its contents were placed in a furnace at  $900 \pm 10$  °C for about 7 mins. Next, the crucible was removed from the furnace, allowed to cool to room temperature, and then weighed. The volatile matter, VM, expressed as percentage mass fraction of the dried sample, was calculated using the following Eq.:

$$VM = \frac{m_2 - m_3}{m_2 - m_1} \times 100 \quad (2.3)$$

Where  $m_1$  is the mass of the empty crucible and lid;  $m_2$  and  $m_3$  are the mass of the empty crucible and lid plus its contents before and after heating respectively.

➤ **Density**

The true density is the weight per unit volume occupied by the solid fraction. To measure the true density a pycnometer (AccuPyc 1330TC) operating at 20°C and 1.4 bar, was used.

➤ **Particle size distribution**

Particle size distribution was determined by a laser particle sizer MALVERN Laser Mastersizer Hydro 2000 at size interval of 0.01-1000µm. Determining the sample size using the laser particle size is based on the introduction of particles in ethanol as a dispersant. The suspension is subjected to ultrasonic shacking for one minute and the analysis is performed after stopping ultrasound. And then the suspension is introduced into a cell with a circulation pump. Within the cell, a laser beam passes through the suspension before being projected onto the photodiode measurement result of the interaction between the laser and particles. The results are discussed based on the Mie theory assimilating particles to spheres of equivalent volumes. This method allows the identification of the particle mean diameter compared to a mass percentage. For example, the mean diameter  $d_{10}$  corresponding to the particle size whose mass represents 10 % of the total mass of the sample.

➤ **Phase determination (X-ray diffraction)**

X-ray diffraction was used to identify crystalline phase of materials. The device used was a Phillips Panalytical X'pert Pro MPD diffractometer with a  $\theta$ - $\theta$  Bragg-Brentano configuration, a current of 45 kV and an intensity of 40 mA using a Cu  $K\alpha$  radiation source (1.543 Å). The diffraction data were collected between  $2\theta=10$  and  $2\theta=70$  ° (in  $2\theta$ ) with a step size of 0.05°. JCPDS and COD databases are applied to identify the diffraction peaks

➤ **Infrared Analysis (FTIR: Fourier Transformed Infrared)**

Infrared spectroscopy allows to identify functional groups present in the sample. The principle is based on the absorption of molecules of a light beam as energy with a wavelength close to their energy vibration. Measurements were carried out with a FITR-8400S (SHIMADZU) with wave length from 4000 and 400  $\text{cm}^{-1}$ .

➤ **Environmental Scanning Electron Microscope (ESEM-EDX)**

The observation of the morphology of the alum sludge was carried out at a scanning electron microscope (SEM) (Philips XL 30 ESEM FEG). The observations were coupled to EDX chemical microanalysis to analyze the elemental composition of materials.

➤ **Transmission Electron Microscopy (TEM)**

The TEM was carried out at a JEOL JEM-ARM200F transmission electron microscope and elemental mapping of chemical species in the sample was performed using and EDX module in the microscope.

➤ **Elemental analysis**

Mineralization is one of the methods often used in the chemical characterization of material composition. It applies by the dissolution of particles by adding a mixture of hydrogen fluoride (HF), hydrogen peroxide (H<sub>2</sub>O<sub>2</sub>) and nitric acid (HNO<sub>3</sub>) (aqua regia) with a volume ratio of 1:1:1 (2.5ml of each). The dissolution of particles was done on SCP DigiPREP Jr mineralization device by heating samples on heating block (coated graphite Teflon<sup>®</sup>) at temperature of 220°C for 2880 mins.

Inductively Coupled Plasma-Atomic Emission Spectroscopy (ICP-AES) was carried out on HORIBA Jobin Yvon (Ultima 2) for element analysis. This technique is based on the separation and ionization of atoms by ions in a hot flame (injection into argon plasma), the identification and quantification of ionic elements that constitute a sample is done according to their mass.

The analysis of carbon (C), hydrogen (H), nitrogen (N) and sulfur (S) content in alum sludge was performed using a CHNS analyzer (Flash 2000, ThermoFisher Scientific) The method was based on the complete oxidation of the sample in excess air in the presence of a catalyst layer. The combustion products, CO<sub>2</sub>, NO<sub>2</sub>, and SO<sub>2</sub> were then swept into a chromatographic column by the carrier gas (helium) where they were separated and detected quantitatively using a thermal conductivity detector (TCD). Since a few mass of sample was required, the CHNS analysis was repeated at least three times to improve its accuracy.

➤ **Specific surface area and porosity (BET method)**

BET method (Brunauer, Emmett and Teller) is a technique for measuring powders specific surface area (S<sub>s</sub>) by assuming that the adsorption of gases takes place in multimolecular layers. The specific surface area of materials was determined using a device Gemini Vacprep 061 (MICROMETRICS). The general principle of the method involves the adsorption of nitrogen at its liquefaction temperature (-196°C) on the surface of a material to be studied by keeping a cell adsorption. A sample mass of about 300mg was introduced into a tube and degassing is carried out for 6 hours at 105°C under vacuum. The sample is subjected to five different pressures of nitrogen at the temperature of liquid nitrogen. The adsorption isotherm is identified by the nitrogen pressure, which allows deducing the volume of adsorbed gas from the gas pressure P and its saturated vapor pressure P<sub>0</sub> and so deducing the specific surface m<sup>2</sup>/g

The pore structure of alum sludge was determined by nitrogen adsorption at 77K using a Micromeritics 3Flex high-resolution analyzer. Prior to measurements, the samples were degassed in vacuum at 90 °C during 1h and then at 150 °C during 10h. The t-plot model was used to determine the micropore volume of samples, and the Non-local Density Functional Theory (NLDFT) to determine the micropore size distribution. The pore nomenclature according to IUPAC classification is the following: Macropore for size larger than 50 nm, Mesopore for size ranging from 20 to 50 nm; Micropore for size smaller than 20 nm.

➤ **Thermogravimetric analysis (TGA-DSC)**

Thermogravimetric technique allows to determine the mass changes of a material due to transformations during heat treatment. Differential thermal analysis shows the heat released during the transformation of the material.

Thermal analyses were carried out by thermogravimetric analysis (TGA) combined with differential scanning calorimetry (DSC) with a TGA/DSC apparatus, SDT Q600 by TA Instruments. Samples near 20 mg of the solid were heated over the temperature range from



ambient to 1000°C at a heating rate of 20°C/min. in air or nitrogen atmosphere with a 100 mL/min flow rate.

➤ **Mass spectrometer (MS)**

Gas analysis were carried out with a mass spectrometer of Omnistar model of PFEIFFER.

## 2.2.2 Results

### ◆ Physical Characteristics

The moisture, pH, volatile matter and density results were shown in Table 2.1. It can be seen that Dublin alum sludge contents more moisture than Carmaux alum sludge. Dublin alum sludge is neutral while Carmaux alum sludge is alkaline. Moreover the pH of Carmaux alum sludge were higher than typically reported pH ranges of WTRs which are mostly between 5.1 and 8.0 [2]. This can be explained by the addition of CaO during the raw water purification processes of Carmaux WTP. On the other hand, the alkaline pH of Carmaux alum sludge produced a high acid neutralizing potential [3]. Dublin alum sludge contents more VM than Carmaux sludge, this is mostly ascribed to the presence of organic matters, clay minerals and hydroxides in the alum sludge. While the density of Dublin and Carmaux alum sludges was 2.0 and 2.4 g/cm<sup>3</sup>, respectively.

**Table 2.1** Physical characteristics of alum sludge

Characteristics	Dublin	Carmaux
Moisture (%)	75	63
pH	6.9	10.0
Volatile Matter (%)	51.2	30.4
Density (g/cm <sup>3</sup> )	2.0	2.4

### ◆ Particle size distribution

The particle size distribution of the two sources alum sludge was shown in Figure 2.4. It shows that both the alum sludges present a monomodal curve with a mean diameter ( $d_{50}$ ) of 191.5µm for Dublin sludge, and 16.5 µm for Carmaux sludge. The difference is possibly from the materials itself, since the sludges were sieving by exactly the same 500 µm mesh.

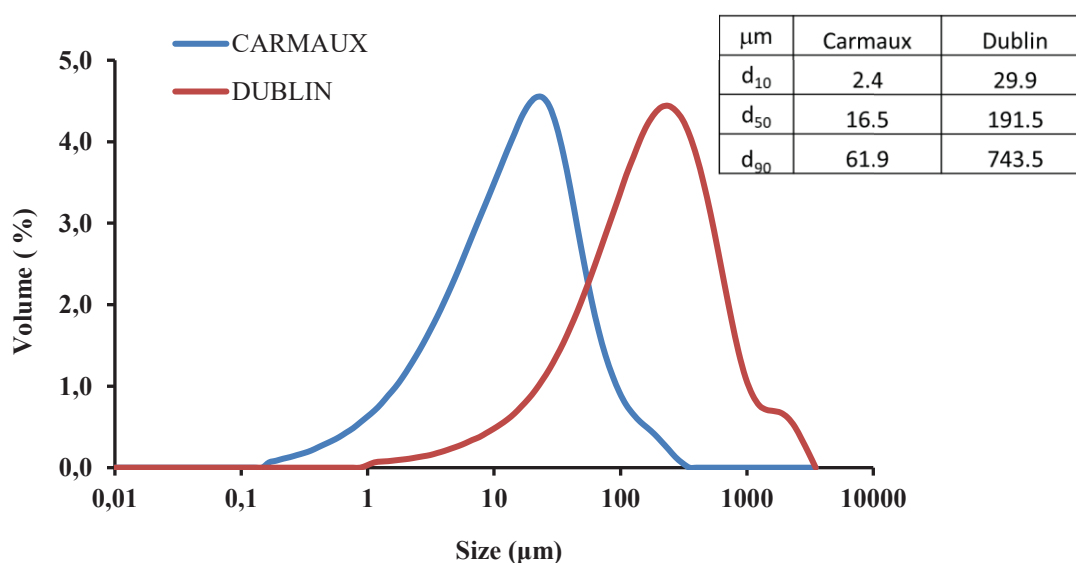


**Figure 2.4** Particle size distribution of alum sludge

### ◆ X-Ray Diffraction

The XRD result of two sources alum sludges is shown in Figure 2.5. The Carmaux alum sludge is composed with crystalline phase while the Dublin alum sludge is mainly composed of amorphous materials. The dominant mineral in the two alum sludges was  $\text{Al}_2\text{CaH}_8\text{O}_{12}\text{Si}_2$ . The Carmaux alum sludge presents more crystalline phase such as calcite ( $\text{CaCO}_3$ ) and quartz ( $\text{SiO}_2$ ) than Dublin alum sludge, which could possibly be resulted from the raw water resources and the lime that was used at the Carmaux WTPs [4].

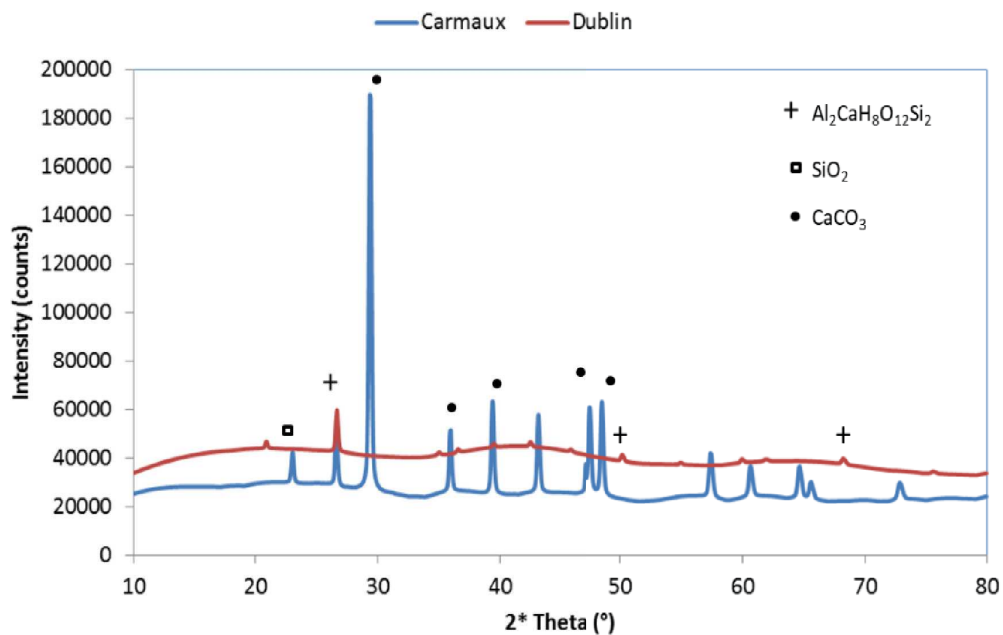


Figure 2.5 X-ray diffraction pattern of two sources alum sludge

### ◆ Fourier Transformed Infrared (FT-IR)

The FT-IR result was shown in Figure 2.6. From the literature, it can be concluded that the wave between  $2300\text{-}2400\text{ cm}^{-1}$  is associated with  $\text{C}\equiv\text{C}$  band [5]; the wave between  $1650\text{-}1600\text{ cm}^{-1}$  of Dublin sludge was H-O-H groups; and the vibrations in  $1420\text{ cm}^{-1}$  is due to stretching vibrations generated by the C-O groups; the band at  $1050\text{ cm}^{-1}$  of Carmaux sludge and a wave at  $1160\text{ cm}^{-1}$  of Dublin sludge correspond to the longitudinal optical modes and the transversal optical modes of the Si-O-Si asymmetric stretching vibrations respectively in silica; the vibration bands at  $780\text{ cm}^{-1}$  of Carmaux sludge corresponding to symmetrical stretching vibrations of Si-O, could be attributed to the quartz mineral [4].

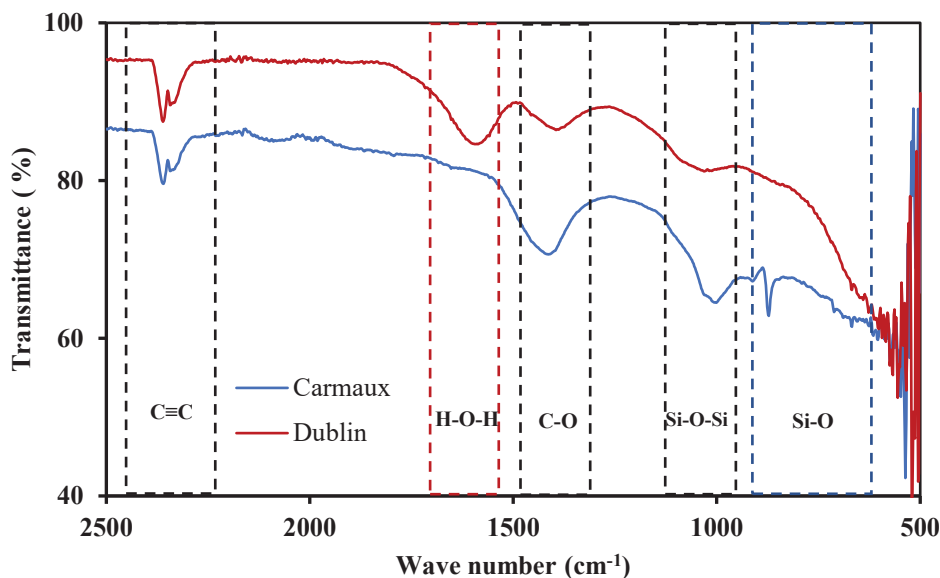
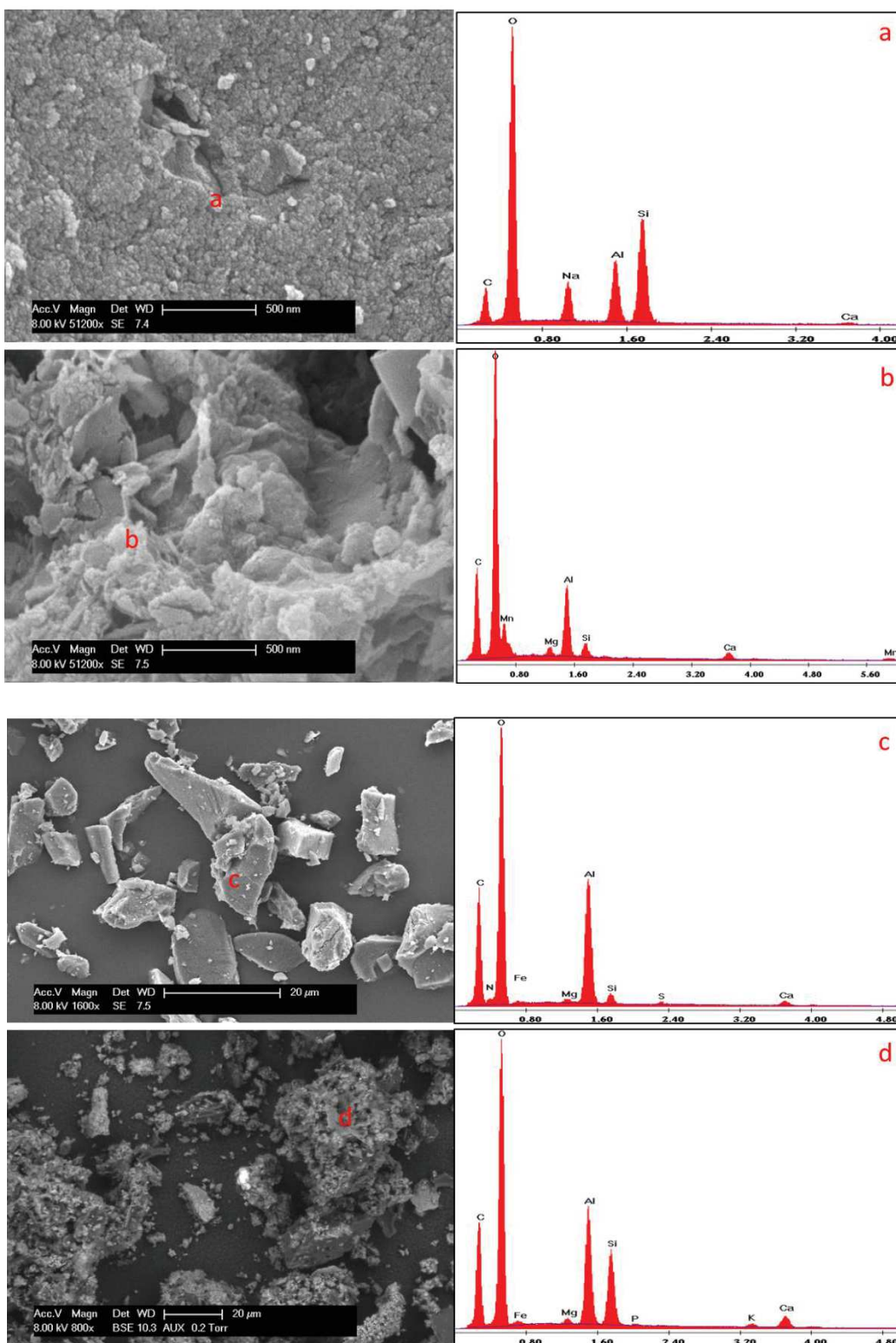


Figure 2.6 FT-IR spectrum of the two sources alum sludge

#### ◆ Environmental Scanning Electron Microscope (ESEM-EDX)

Figure 2.7 presents the morphology and elemental composition on the surface of the two sources alum sludges under various magnitudes (500 nm, 20, 100  $\mu\text{m}$ ). As shown in Figure 2.7 (e & f), irregular silt and clay particles were presented in both raw alum sludge. However, the two kinds of sludge present different surface properties, as illustrated in Figure 2.7 c and d, Dublin sludge has the flat surface compared with the rough surface of Carmaux sludge. Figure 2.7 a and b show small spherical particles aggregated in the surface of Dublin alum sludge while pores are presented at the surface of Carmaux alum sludge. This observation is in agreement with the surface and porosity measurements. Regarding the EDX analysis, various metals (such as Al, Ca, Fe, Mg), C and Si were detected on the surface of both kind of samples, there are no significant difference regarding the elemental composition among the testing points from a to f. This result also agrees with the previous studies [2,6,7].



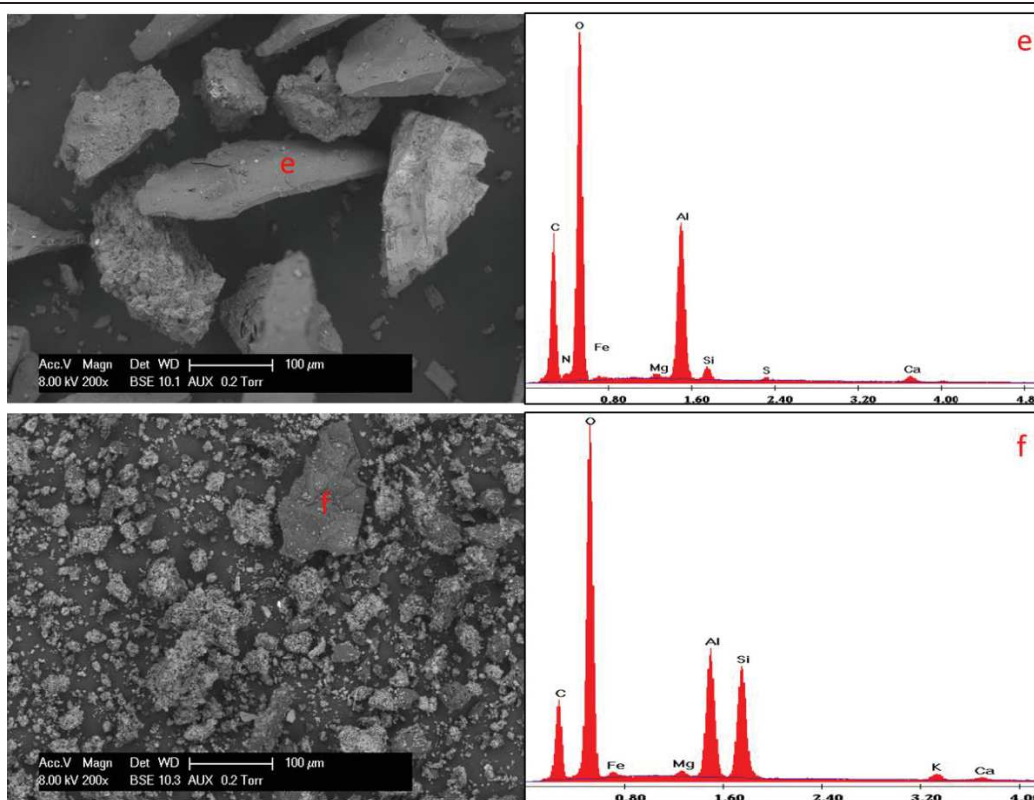


Figure 2.7 SEM-EDX images of two sources of alum sludge, (a, c, e) Dublin sludge; (b, d, f) Carmaux sludge

#### ◆ Transmission Electron Microscopy (TEM)

The TEM-EDX results of Dublin and Carmaux alum sludge were presented in Figure 2.8 and 2.9, respectively. In Figure 2.8, different element distribution map on the surface of Dublin sludge was presented. Generally, the element composition was corresponding to the SEM-EDX and ICP results, with the presence of various metals such as Al, Zn, Fe, Ca, as well as Si, C, O, P being observed. Elements such as Al, Ca, Fe, C, O, P were homogeneously distributed on the surface of Dublin alum sludge besides trace amount of Si was detected.

The element distribution map of Carmaux alum sludge was presented in Figure 2.9. Various metals such as Al, Fe, Ca, Mg, K, as well as Si, C, O were detected. Compared with Dublin sludge, the metal element distribution on the surface of Carmaux sludge is not homogeneous. For example, in the map of Fe and Ca, Fe was intensively distributed in the upper right-side part of the photo while Ca was condensed in the lower middle part of the photo.

The main difference between this two sources alum sludge was that P was detected on the surface of Dublin alum sludge, this is possibly due to the strong affinity of aluminum and phosphate. Indeed, alum sludge is a by-product and highly related with the raw water and purification process. It is common to see elements variability as well as the element distribution variances.



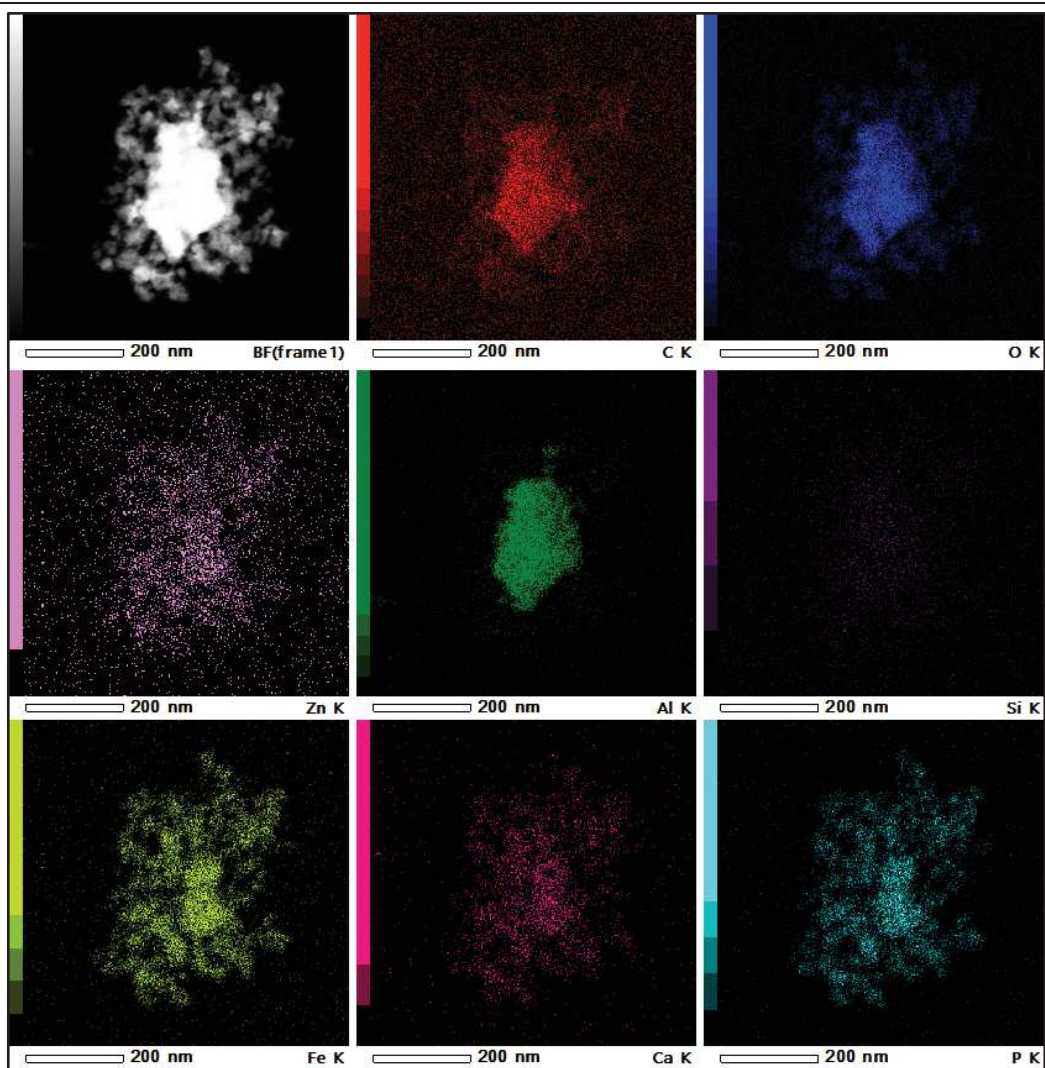


Figure 2.8 TEM-EDX images of Dublin alum sludge

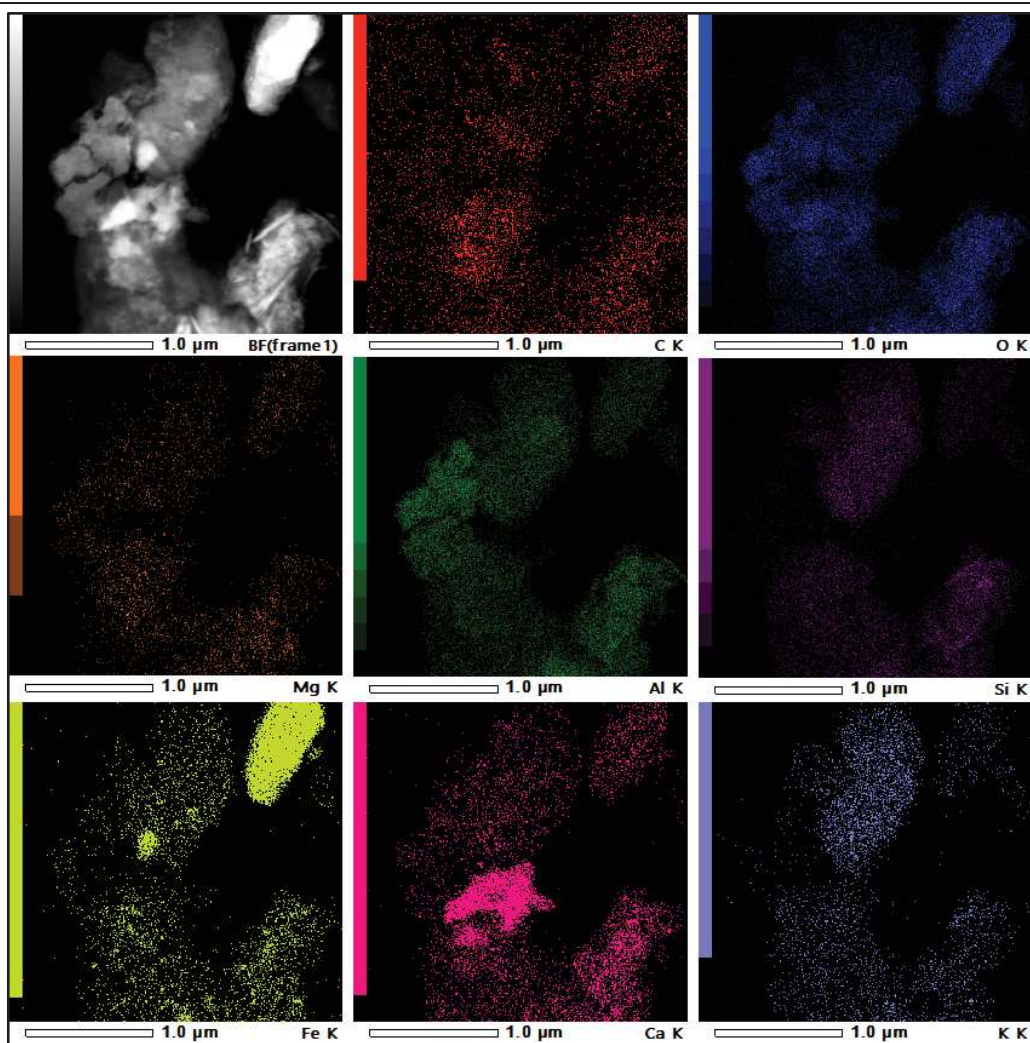


Figure 2.9 TEM-EDX images of Carmaux alum sludge

### ◆ Elemental composition

Elemental composition of the two sources alum sludge is showed in Table 2.2. The two sources of alum sludge were composited of amphoteric, alkaline-earth metal, transition metal, alkali metal, metalloid and nonmetal. There is abundance of Al, Ca, Mg, Fe, other co-occurring metals followed by Si being found in both samples. Although Carmaux sludge is an Al-based sludge, the high quantity of Ca is due to the lime addition in the raw water prior to the treatment processes in Carmaux WTP. Regarding the total amount of elements, Carmaux alum sludge (52240 mg/kg) contains twice more mineral elements than Dublin alum sludge (25556 mg/kg).

For total carbon content, Carmaux alum sludge presents higher amount (30.6 %) than Dublin sludge (22.7 %). This is due to the addition of activated carbon in order to remove odor and taste of the raw water in Carmaux WTP. The total amount of C in Dublin sludge was organic carbon (TOC) and the TOC was 27 % in Carmaux sludge. In addition, the H and N in Carmaux alum sludge of 2, 0.5 % was lower than the H, N in Dublin sludge of 4, 1 % respectively. While the Dublin sludge contains trace amount of S, which is possibly origin from the reservoir and river bank sedimentation. They are mixing with raw water and come into the treatment process.



**Table 2.2** Element composition of two sources alum sludges

Elements	Dublin (mg/kg, dry basis)	Carmaux (mg/kg, dry basis)
Al	17983	17581
Ca	2763	21156
Ba	14	119
Cr	/	4
Mg	98	1331
Mn	220	416
Sn	93	34
Zn	10	5
K	1015	4526
Fe	2919	4892
Mo	256	33
Li	/	1
Na	16	144
As	133	122
V	21	33
Zr	/	6
Si	76	2391
P	106	625
<b>Total</b>	<b>25723</b>	<b>53419</b>
C (%)	22.7 (100 wt% TOC)	30.6 (3.6 wt% IC + 27.0 wt% TOC)
H (%)	4	2
N (%)	1	0.5
S (%)	0.7	0

#### ◆ Specific surface area and porosity

The N<sub>2</sub> adsorption isotherms for the two sludges are illustrated in Figure 2.10. The isotherm obtained for Carmaux sludge is of type II according to the IUPAC classification. It is characteristic of a non macroporous sample and microporosity is presenting. The estimation of the microporous volume by the tracing method gives the volume of the order of 0.076 cm<sup>3</sup>/g which corresponds to approximately 50 % of the surface of the sample. For Dublin sludge, the isotherm obtained is of type IV according to the IUPAC classification, characteristic of a mesoporous sample. Any microporosity is present in Dublin sludge. The estimation of the mesoporous volume is 0.06 cm<sup>3</sup>/g by the application of the BJH law in the adsorption curve with a mean pore diameter of 4.3 nm.

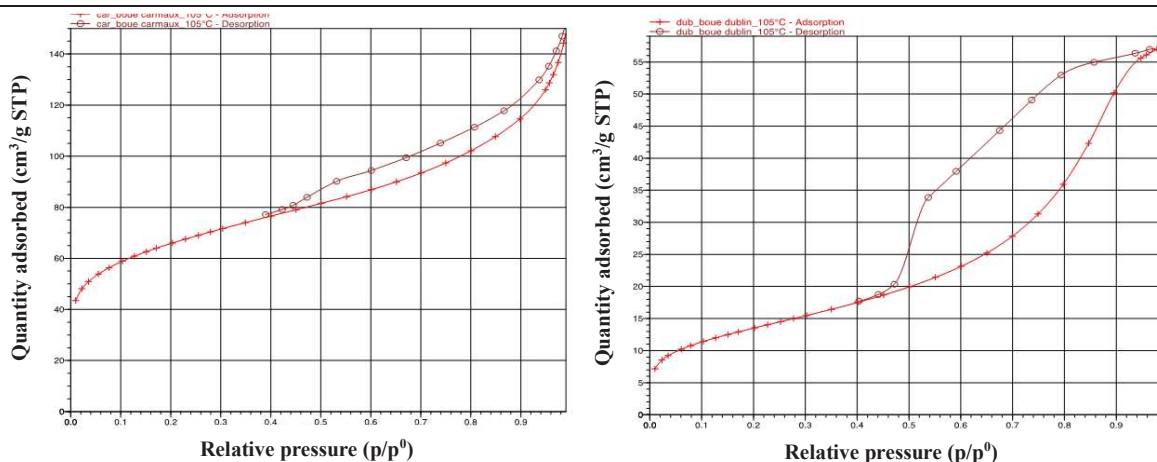


Figure 2.10 N<sub>2</sub> adsorption isotherms for the two sludges; Carmaux sludge (left); Dublin sludge (right)

The pore structure of two sources alum sludge were presented in Table 2.3. It can be seen that the S<sub>p</sub>(BET) of Carmaux sludge is 238 m<sup>2</sup>/g, while the Dublin sludge is 49 m<sup>2</sup>/g. Compared with the data in literature, the specific surface of Carmaux is higher than the average alum sludge in the literature [8]. This is due to the Carmaux WTP employed activated carbon in the pretreatment process in order to remove the odor from the raw water, and thus brings the activated carbon to the alum sludge. Additionally, the Carmaux sludge presents microporous pore structure and the Dublin sludge is mesoporous. Three families of micropores were detected.

Table 2.3 Pore structure of two sources alum sludges

Sludge	S <sub>p</sub> (BET) (m <sup>2</sup> /g)	S <sub>mic</sub> (m <sup>2</sup> /g)	V <sub>mic</sub> (cm <sup>3</sup> /g)	V <sub>mes</sub> (cm <sup>3</sup> /g)	d <sub>pore</sub> (nm)
Carmaux	238	119.56	0.05	/	2.4-3.2-5.0
Dublin	49	2.15	0.00	0.07	3.6-5.5-15

◆ Thermal analysis

The TGA results of Dublin and Carmaux alum sludges were presented in Figure 2.11 and 2.12, respectively. From Figure 2.11, a three stages TGA curve of Dublin sludge under air atmosphere can be observed. The first zone, from 0-290 °C indicated the dehydration process and the corresponding mass loss is 20.1 %. The second zone (from 290-580 °C), an exothermic peak appears under air corresponding to the oxidation of organic compound and the corresponding mass loss is 39.6 %. This oxidation of organic compound was confirmed by analysis under nitrogen atmosphere where the exothermic peak is not presented. The third zone, from 580-1000 °C indicated the carbonization process and the corresponding mass loss is 0.8 %.

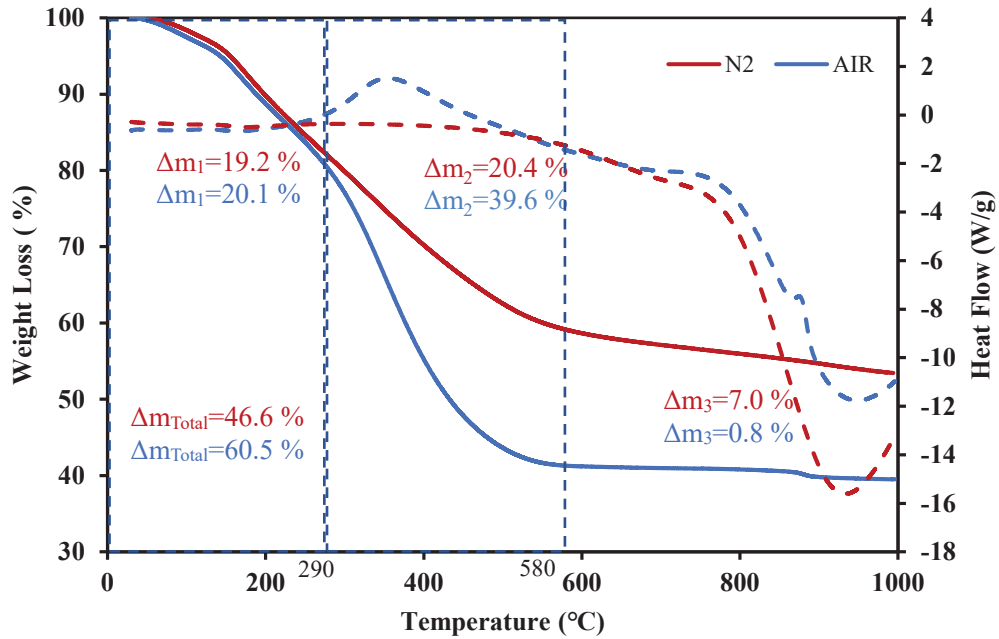


Figure 2.11 TGA-DSC of Dublin alum sludge

Figure 2.12 presents TGA curve of Carmaux sludge. In the first zone, from 0-350 °C indicated the dehydration process and the corresponding mass loss is 13.6 %. The second zone (from 350-650 °C) corresponds to the oxidation of organic compound under air atmosphere and the corresponding mass loss is 28.6 %. This result confirms the results of TOC measurement (Table 2.2); the third zone, i.e. from 650-1000 °C indicated the carbonization process and the mass loss in this stage is 9.3 %.

Compared with the total weight loss of two samples, Dublin sludge loss (60.5 %) more than that of Carmaux sludge (51.5 %) during the TGA analysis, which confirms with the results of volatile matter in Table 2.1.

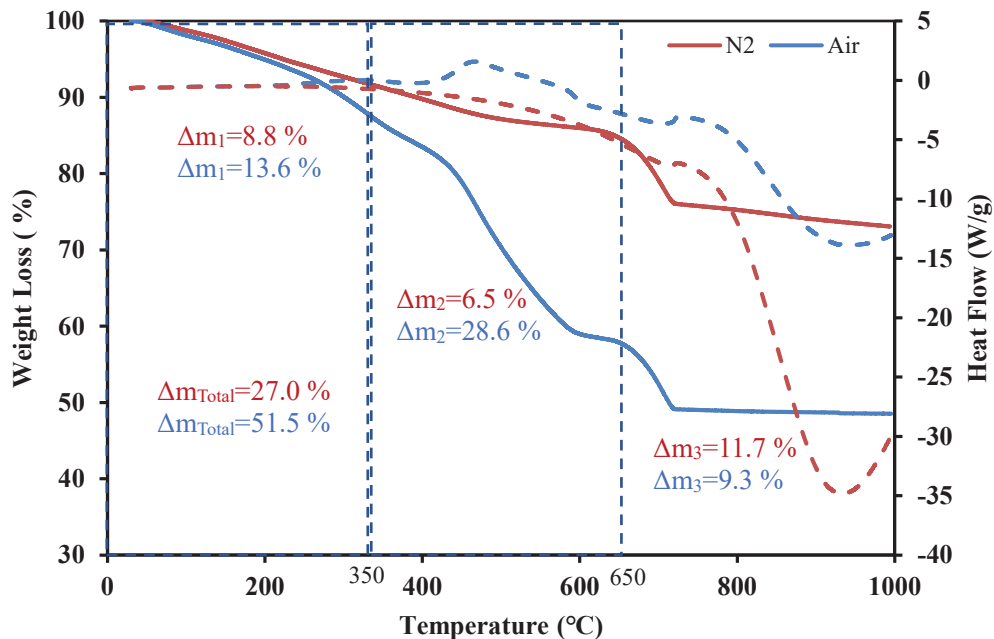


Figure 2.12 TGA-DSC of Carmaux alum sludge

## 2.3 Experimental Methods

### 2.3.1 Alum sludge incorporated in clay brick manufacturing

Generally, there are five phases on alum sludge clay brick manufacturing: materials preparation; mixing the clay with alum sludge under different ratio; forming the bricks; drying; firing and cooling. It was followed by the testing of the resultant bricks using strength and durability testing.

#### a) Materials preparation

The clay used in this experiment was obtained from a delivery of topsoil for use in the landscaping of a residential dwelling. After collection, the sludge and clay were dried separately in a specialist oven at 105 °C for 24h. The particle size was then reduced using a grinding machine to obtain a consistent size, which ensured that the mixing of the materials would be thorough. They were then screened separately using an 850µm sieve.

#### b) Forming the alum sludge clay bricks

The sample bricks were made with ratios ranging from 0 to 40 % sludge by weight, at increments of 10 %. Five pairs of bricks (total of ten bricks) were made in each batch. Four batches were produced. To obtain similar sized brick samples, ten identical moulds were used for the drying of each batch of bricks. The moulds were made of plastic with an internal diameter of 48 mm and a depth of 25 mm. Each mould was cut horizontally in one position to remove the bricks from the mould after drying (as shown in Figure 2.13 (a)). Water was slowly added to 100 g of the dried clay. It was found that 46 ml of water formed a workable but not too moist mixture. This volume of water was not suitable for the mixtures with higher sludge content (they became too moist). This was judged by appearance and physical workability.

Each batch was allowed to dry in a constant temperature room at 20 °C for 24h. Once the drying was complete, the plastic moulds were removed. Each brick was labelled, and the weights were recorded. Each batch of bricks was fired separately in a kiln (Nabertherm, P320, Germany) at varying temperatures of 200-800 °C for Batch 1, 200-1000 °C for Batch 2, and 200-1200 °C for Batch 3, while the temperatures were maintained for a period of 2 h, as shown in Figure 2.13 (b).

To ensure the removal of the maximum amount of water from the bricks, each batch was heated from room temperature to 100 °C. This temperature was maintained for 1 h before the temperature was increased to 200 °C for 1 h. After analyzing the compression strength results from Batches 1-3, the firing criteria for Batch 4 were decided: the temperature of the kiln was increased from 200 to 1100 °C and the temperature was again maintained for a period of 2 h. In all cases, after firing, the kiln door was kept shut until the kiln returned to room temperature, thus allowing the bricks to cool slowly and ensure the vitrification process being complete.

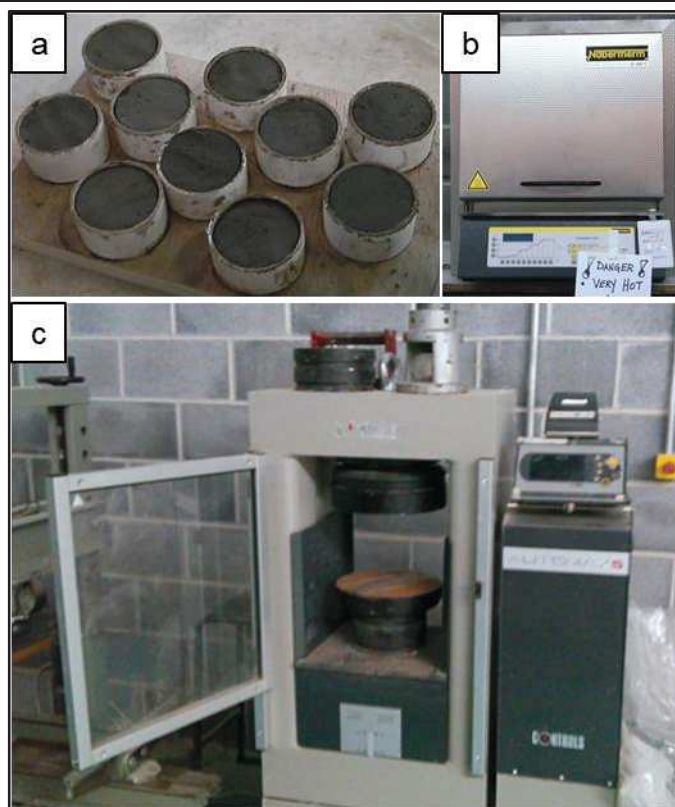


Figure 2.13 (a) the bricks after the drying stage; (b) the kiln; (c) the compression machine

### c) Testing the resultant bricks

Five different testing were carried out including compression strength, loss on ignition, water absorption, compression testing after being submerged in water for 24h and general appearance & texture.

- **Compression strength testing:** As shown in Figure 2.13 (c) the strength testing was carried out using a compression machine (AUTOMAX 5, Control). A brick from each pair was subjected to a compressive force until failure, and the force (kN) at failure was recorded.
- **Loss on ignition testing:** The weights before and after firing of each brick are manipulated to calculate the LoI. The weights that were recorded after firing are used for this comparison.
- **Water absorption testing:** One brick from each pair was submerged immediately in water for 24 h. The bricks each had their weight recorded before this test giving the ‘initial weights’. Each was then weighed after being submerged providing the ‘resultant weights’. The water absorption was then expressed as a percentage of the initial weight.
- **Compression testing after being submerged in water for 24 h:** The purpose of this test is to analyze the difference in strength of the bricks before and after being submerged in water. The bricks were then subjected to the same compression test as described above, and the force at failure recorded.
- **General appearance & texture:** After firing, the bricks are compared within each batch, and also against the entire range of firing temperatures.

### 2.3.2 Alum sludge and Irish peat for glyphosate removal

The peats used in this study were extracted from two ombrotrophic bogs in Co. Mayo, Ireland. After collection, moisture content was determined. Accordingly, the mass of peat used was 2.278 kg for each pot which equals to the mass of alum sludge of 1.498 kg. The P-

containing contaminant used was Roundup™ Bioactive with glyphosate as its active ingredient and a target glyphosate concentration of 50 mg/l in artificial wastewater with the natural pH of 5.2–5.6 was decided. The diluted solution which resulted in 22.2 ml of the stock solution was used to make up the 1600 ml influent solution. The experiments were carried out as the following steps:

### a) Pot setup

As shown in Figure 2.14, four identical plastic containers were sourced and hydraulic valves were attached to each pot at 35 mm from the base of the pot. The pot was 200 mm in diameter and 250 mm in height (see Chapter 4, Figure 4.2). The base of the pots was filled with washed gravel to an approximate height of 50 mm. After calculating the dry weight of both substrate types, the substrate with the large MC (peat) was filled into the first pot until there was only a free board of 50 mm at the top. The mass of the peat added was 2.278 kg. The allowable mass of alum sludge of 1.498 kg, which was equivalent to the dry mass of the peat, was then placed in the corresponding pot to allow the mass of substrates being equal in both corresponding blank and active pots. The trimmed young reeds were then planted on the top of each pot.

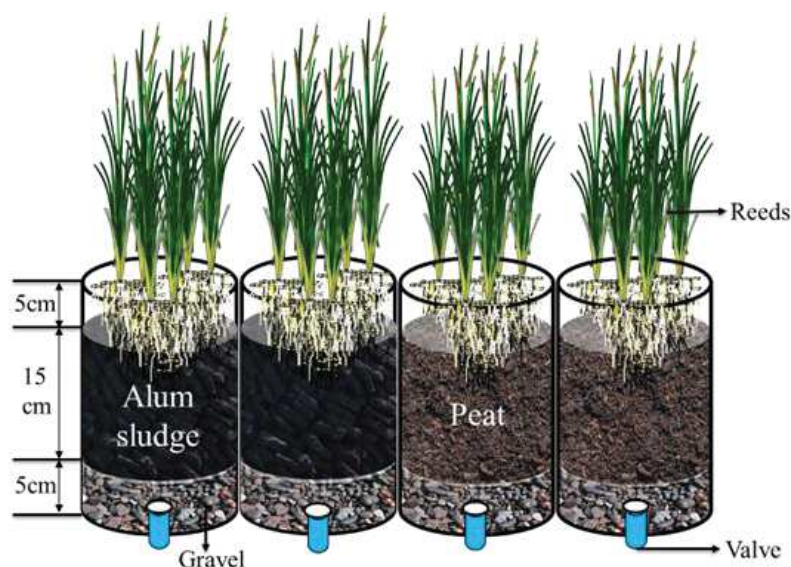


Figure 2.14 Schematic of pot trials

### b) Dosing and sampling

The influent 1600 ml per pot was divided into two doses of 800 ml. One pot of each material was dosed with the selected herbicide solution at room temperature (22 °C), while the remaining two pots were filled with tap water and used as control blanks. The pots were drained via the valve and refilled twice weekly for a 10-week period. Each pot was drained and then individually passed through a vacuum filter using a 0.45 µm pore filter paper. The filtrate was then subjected to water quality monitoring.

### c) Analysis

Monitoring of P and chemical oxygen demand (COD) for filtrate from each pot was conducted via a Unicam Helias-α spectrometer for P and a HACH DR-2400 spectrometer for COD with standard procedure. As the P source was an organic phosphonate the sample had to firstly undergo chemical and thermal treatment by autoclave method. In addition, samples of the alum sludge and peat before and after use in pot testing were naturally dried for physical and chemical properties examination. Their surfaces were observed under a scanning electron microscope (SEM) (LEO 1530 VP Germany) to visualize inner porosity, surface properties and



changes to the surfaces of the four relevant particles from the four pots. The SEM was further combined with energy-dispersive X-ray (EDX) to determine the composition and relative distribution of elements particularly on the surface. The chemical components of four media were examined via Inductively Coupled Plasma Atomic Emission Spectrometry (ICP-AES, Profile DV, America Leeman Labs Inc.).

### 2.3.3 Co-conditioning of waste-activated sludge with alum sludge

The conditioning tests were performed using a four paddles standard jar-stirring apparatus as shown in Figure 2.15, where sludge samples of 600 mL in 1000 mL beakers were used in the experiments. Alum sludge and waste-activated sludge were mixed at different volume ratios of 2:1, 1:1, 1:2, 1:3, 1:4, respectively, for a series of jar tests to optimize the mixing ratio. The optimized mixing ratio (1:1, alum sludge:waste-activated sludge) was determined by the lowest phosphate concentration in the supernatant with the least amount of alum sludge addition.



Figure 2.15 Jar-test apparatus of co-conditioning trials

Thereafter, the precalculated dosage (range from 10-400 mg/l, 10, 50 to 400 mg/l, at increments of 50 mg/l) of polymer Sueprfloc-492HMW was added as chemical conditioner to the optimized mixing ratio sludge to examine and achieve the optimal dosage of polymer. This procedure was also performed using the jar-stirring apparatus, where the sludge and various polymer doses were fast mixing at 200 rpm for 30 seconds, and then slowly mixing at 60 rpm for 300 seconds. In the end, the dewaterability of the resultant sludge was evaluated using capillary suction time (CST) and specific resistance to filtration (SRF).

To examine the elements in the solid phase and supernatant of the sludge, a laboratory-model centrifuge (Sigma 2K15, Germany) was operated at 8000 r/min to separate the sludge. The solids were then washed with distilled water three times. Thereafter, the solid was dried at 105 °C in an oven for 24 hours. The element content was tested by inductively coupled plasma-atomic emission spectroscopy (ICP-AES), and the elemental analyzer of CHNS (Thermoquest NA2100). Scanning electron microscopy (SEM) was associated with a Philips XL30 ESEM apparatus (FEI Company) which was coupled with an energy-dispersive X-ray spectroscopy (EDX analysis) was used to observe the sludge samples before and after dewatering.

The dewaterability of the sludge before and after co-conditioning was evaluated using the



CST apparatus and SRF facility. A Triton CST apparatus (Triton WPRL, Type 130) with a CST paper of size 7×9 cm was used for the CST measurement, while a Buchner funnel with a Whatman No. 1 qualitative filter paper (10 cm diameter) and equipped with a 70 mbar vacuum suction was used for the SRF test and measurement, as illustrated in Figure 2.16.

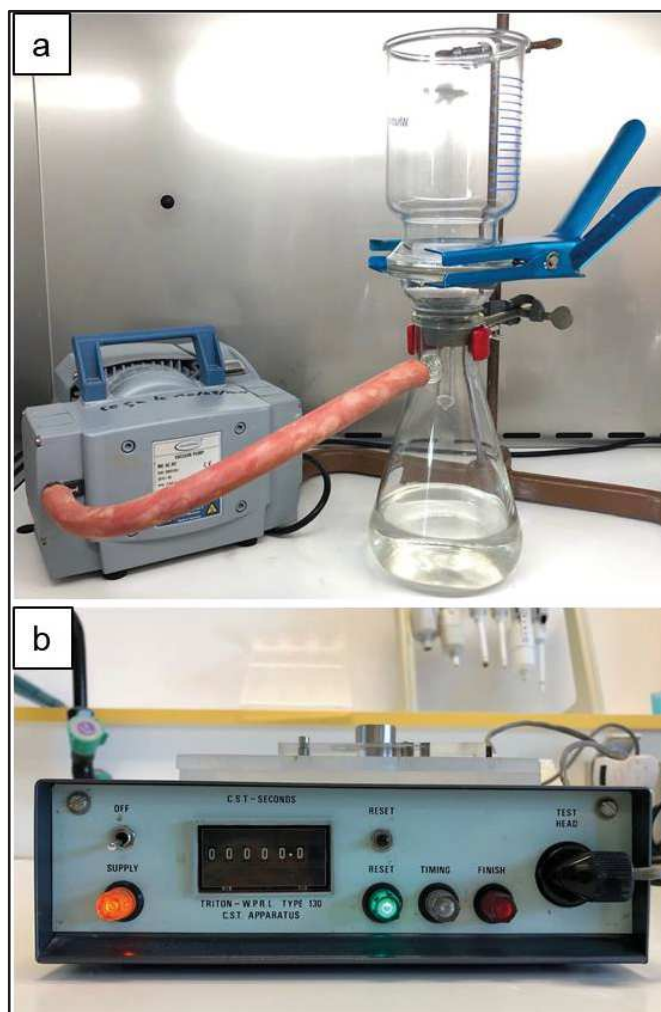


**Figure 2.16** The experiment apparatus of (a) specific resistance to filtration (SRF), (b) capillary suction time (CST).

### 2.3.4 Alum sludge as an efficient sorbent for hydrogen sulfide removal

#### ➤ Experimental setup

The tests of H<sub>2</sub>S removal were carried out at room temperature ( $\pm 20$  °C) and ambient pressure using a glass fixed-bed column. Figure 2.17 presents the experimental apparatus. The column (length 60 mm, internal diameter D=11 mm) was equipped with a porous glass disc at the bottom which could hold the sorbent and allow H<sub>2</sub>S gas passing through. The height of sorbent layer varied from about 0.5 to 1.1 cm, corresponding to the apparent density and the amount of sorbent used for each experiment (0.5 to 1.0 g). A synthetic gas containing 200 ppmv of H<sub>2</sub>S (based on dry air) passed through the sorbent layer with different flow rate of 3, 4, 5 L/h, respectively, was controlled by a flow meter. The output H<sub>2</sub>S concentration was monitored every two minutes using a gas analyzer from BW Technologies (Gas Alert QUATTRO). The effluent gas was treated by CaO solution before it was released to the atmosphere. Sorption experiments were stopped when the sorbent when the H<sub>2</sub>S sorption rate significantly decreased.

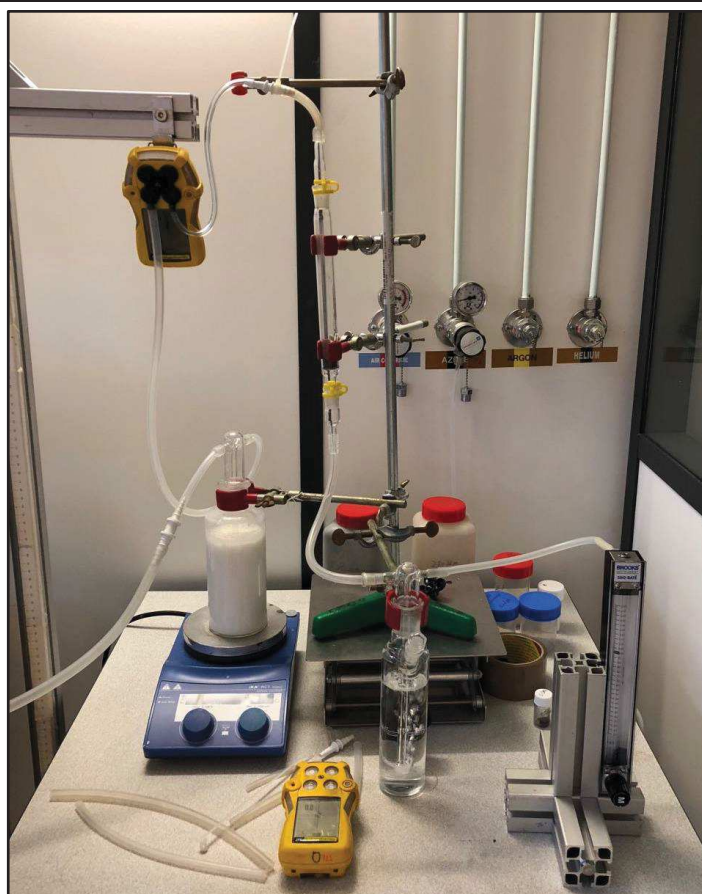


Figure 2.17 The lab-scale experimental apparatus

In this experiment, the following terms are used in order to compare different experimental conditions:

- $H_2S_{input}$  (mg): the total accumulated quantity of  $H_2S$  introduced to the bed at a given reaction time.
- $Accumulated_{sorbent}$  (mg): the total accumulated quantity of  $H_2S$  on the sorbent at a given reaction time.
- $t_{100\%}$  (min): the reaction time wherein the removal of  $H_2S$  was completed. Theoretically  $H_2S_{input}$  is equal to  $Accumulated_{sorbent}$  within  $t_{100\%}$ . The amount of  $H_2S_{input}$  and  $Accumulated_{sorbent}$  was calculated with the Eqs. (2.4) and (2.5), respectively:

$$H_2S_{input} = \frac{PQM}{10^6 RT} C_0 t \quad (2.4)$$

$$Accumulated_{sorbent} = \frac{PQM}{10^6 RT} [C_0 t - \int_0^t C_t dt] \quad (2.5)$$

Where,  $P$  is the pressure of gas (1 atm),  $Q$  is the inlet flow rate ( $L \text{ min}^{-1}$ ),  $M$  is the molecular weight of  $H_2S$  ( $34.06 \text{ g mol}^{-1}$ ),  $W$  is the mass of sorbent used (g),  $C_0$  is the inlet concentration of  $H_2S$  (200 ppmv),  $C_t$  is the outlet concentration of  $H_2S$  (ppmv),  $t$  is the reaction time (min),  $R$  is the ideal gas constant ( $8.31 \text{ J/(mol}\cdot\text{K)}$ ),  $T$  is the absolute temperature (K).

### ➤ Modeling

The most commonly used three empirical models of The Thomas, Bed Depth Service Time, and Yoon-Nelson model were used in this study.

- **The Thomas model** [9] was based on the hypothesis that: (i) the process follows Langmuir isotherms and second-order kinetics of sorption–desorption with no axial dispersion; (ii) the adsorption is not limited by the chemical reaction, but controlled by the mass transfer at the interface. The linearized form of the model is given as:

$$\ln\left(\frac{C_0}{C_t} - 1\right) = \frac{K_{Th}q_0m}{F} - K_{Th}C_0t \quad (2.6)$$

Where,  $K_{Th}$  is the Thomas rate constant ( $L\ mg^{-1}\ min^{-1}$ ),  $q_0$  is the maximum adsorption capacity ( $mg\ g^{-1}$ ),  $m$  is the mass of sorbent in the column ( $g$ ).  $F$  is the Volumetric flow rate ( $L\ min^{-1}$ ).  $C_0$  is the inlet concentration of  $H_2S$ ,  $C_t$  is the outlet concentration of  $H_2S$ . The kinetic coefficient  $K_{Th}$  and the adsorption capacity of the sorbent  $q_0$  can be determined from a plot of  $\ln[(C_0/C_t) - 1]$  against  $t$  at a given flow rate.

- **The Bed Depth Service Time (BDST) model** [10] describes a relation between the service time and the packed-bed depth of the column. This model was derived based on the assumption that the diffusion steps (external and internal) are very fast, and the surface reaction step is rate-controlling. The model has the following form:

$$t = \frac{N_0h}{uC_0} - \frac{1}{KC_0} \ln\left(\frac{C_0}{C_t} - 1\right) \quad (2.7)$$

Where,  $K$  is the adsorption rate constant ( $L\ mg^{-1}\ min^{-1}$ ),  $N_0$  is the adsorption capacity ( $mg\ L^{-1}$ ),  $h$  is the bed depth ( $cm$ ),  $u$  is the linear flow rate ( $cm\ min^{-1}$ ) and  $t$  is the service time to breakthrough ( $min$ ).  $C_0$  is the inlet concentration of  $H_2S$ ,  $C_t$  is the outlet concentration of  $H_2S$ . Experimental data obtained are used to plot BDST curves and estimate the characteristic parameters  $K$  and  $N_0$  from the slope and intercept of the plots.

- **The Yoon–Nelson model** [11] is based on the assumption that the rate of decrease in the probability of adsorption for each adsorbate molecule is proportional to the probability of adsorbate adsorption and the probability of adsorbate breakthrough on the sorbent. The linearized model for a single component system is expressed as:

$$\ln\frac{C_t}{C_0 - C_t} = K_{YN}t - \tau K_{YN} \quad (2.8)$$

Where,  $K_{YN}$  is the rate constant ( $min^{-1}$ ) and  $\tau$  is the time required for 50 % adsorbate breakthrough ( $min$ ).  $C_0$  is the inlet concentration of  $H_2S$ ,  $C_t$  is the outlet concentration of  $H_2S$ . The calculation of theoretical breakthrough curves for a single-component system requires the determination of the parameters  $K_{YN}$  and  $\tau$  for the adsorbate from the plot of  $\ln[C_t/(C_0 - C_t)]$  versus sampling time ( $t$ ).

### ➤ Determination of mass transfer coefficient

In fact, the Thomas model etc. is based on the assumption that the rate of adsorption is controlled by the surface reaction. However, external and internal diffusion limitations are not absent in the overall process. Moreover, adsorption may not be limited by kinetics of chemical reaction, but controlled by external and/or internal mass transfer. Thus, an alternative approach is to consider both inter- and intra-particle mass transfer to control the adsorption process.

The linear-driving-force (LDF) approximation takes this approach in such a way that a lumped overall resistance describes mass transfer, and where the sorbent particle is treated as a

homogeneous phase in which diffusion takes place with a constant effective diffusivity; the reaction kinetics is assumed to be much faster than the mass transport [12]. Thus, the mass transfer rate is represented as proportional to the deviation from equilibrium:

$$\frac{\partial q}{\partial t} = K_a(q_e - q) \quad (2.9)$$

where  $K_a$  is the overall effective mass transfer coefficient,  $q$  is the concentration of  $H_2S$ ,  $q_e$  is the concentration of  $H_2S$  at the equilibrium.

### Analytical solution:

If the equilibrium isotherm is linear ( $q_e = K_e C$ ), an analytic expression can be derived, such as Klinkenberg did [13] using dimensionless equations as follows:

Mass balance in the bed:

$$\frac{\partial \phi}{\partial \xi} + \frac{\partial \varphi}{\partial \tau} = 0 \quad (2.10)$$

Adsorption velocity:

$$\frac{\partial \varphi}{\partial \tau} = \phi - \varphi \quad (2.11)$$

Where:

$$\phi = \frac{C}{C_0}; \quad \varphi = \frac{q}{q_s}; \quad \xi = \frac{K_e K_a Z}{u} \left( \frac{1-\varepsilon}{\varepsilon} \right); \quad \tau = K_a \left( t - \frac{Z}{u} \right)$$

Where  $C$  is the  $H_2S$  concentration in gas phase,  $q_s$  is the saturation value of  $q$ ,  $K_e$  is the equilibrium constant of a linear adsorption isotherm,  $z$  is the distance from the bed entrance,  $u$  is the gas interstitial velocity,  $\varepsilon$  is the bed void fraction,  $t$  is the time.

Thus, using the initial and boundary conditions, the analytical solution is:

$$\frac{C}{C_0} \approx \frac{1}{2} \left[ 1 + \operatorname{erf} \left( \sqrt{\tau} - \sqrt{\xi} + \frac{1}{8\sqrt{\tau}} + \frac{1}{8\sqrt{\xi}} \right) \right] \quad (2.12)$$

where  $\operatorname{erf}(x)$  is the error function of Gauss, defined by Eq. (2.13).

$$\operatorname{erf}(x) = \frac{2}{\sqrt{\pi}} \int_0^x e^{-t^2} dt \quad (2.13)$$

The coefficient of overall mass transfer (which includes both the external and internal mass transfer) was determined as follows:

$$\frac{1}{K_e K_a} = \frac{d_p}{6K_{ext}} + \frac{d_p^2}{60D_e} \quad (2.14)$$

Where  $d_p$  is mean particle diameter,  $D_e$  is the effective diffusivity.

The external mass transfer coefficient ( $K_{ext}$ ) was calculated by the Ranz–Marshall correlation [14]:

$$Sh = 2 + 1.58 Re^{0.4} Sc^{1/3}; \quad 10^{-3} \leq Re \leq 5.8 \quad (2.15)$$

Where:

$$Sh = \frac{K_{ext} d_p}{D_m}; \quad Re = \frac{u \varepsilon d_p \rho}{\mu}; \quad Sc = \frac{\mu}{\rho D_m}$$

$D_m$ ,  $d_p$ ,  $q$  and  $\mu$  are the molecular diffusivity, particle diameter, gas density and gas viscosity,

respectively.  $D_m$  was calculated by the Fuller-Schettler-Gridding correlation [15]:

$$D_m = \frac{10^{-3} T^{1.75} \left( \frac{1}{M_{gas}} + \frac{1}{M_{H_2S}} \right)^{0.5}}{P \left( V_{gas}^{1/3} + V_{H_2S}^{1/3} \right)^2} \quad (2.16)$$

with  $D_m$  in  $\text{cm}^2/\text{s}$ ,  $T$  in K,  $P$  in atm,  $M$  is molecular weight, and  $V$  is the diffusion volume.  $D_e$  is effective diffusivity, which could be calculated by the Bosanquet equation [12]:

$$D_e = \frac{\varepsilon_p}{f_{tor}} \left[ \frac{1}{D_m} + \frac{1}{D_K} \right]^{-1} \quad (2.17)$$

$\varepsilon_p$  is the particle porosity and  $f_{tor}$  is the tortuosity factor. Finally,  $D_K$  is the Knudsen diffusivity, which is calculated by Eq. (2.18).

$$D_K = 4850 d_{pore} \left( \frac{T}{M_{H_2S}} \right)^{1/2} \quad (2.18)$$

where  $d_{pore}$  is the mean pore diameter.

### 2.3.5 Simultaneous hydrogen sulfide purification and wastewater treatment in a novel aerated alum sludge based constructed wetland

#### ➤ Experimental setup

The experiment (as illustrated in Figure 2.18) was composed of three parallel alum sludge-based aerated VFCWs (Al-VFCWs). The laboratory scale Al-VFCW system was constructed with a plexiglass column (diameter 15 cm), Gravel (15 cm depth) was filled into the bottom as the support medium, and 80 cm depth air-dried alum sludge cake (moisture content 63 %, particle size 2-5 cm) was filled as the main wetland medium layer, which gives a total volume of 16.8 L with initial porosity of 42 % (7 L liquid contained). Influent was introduced into the column from the top while effluent was drained from the bottom by peristaltic pumps. Aeration was supplied with a diffuser placed on the support layer (10 cm from the bottom) and controlled with an air flow meter. The system was seeded with activated sludge collected from a local municipal wastewater treatment plant for two weeks before it was formally operated. The experiment was run from Oct. 2018 to Apr. 2019 (Six months) under room temperature.





**Figure 2.18** The three parallel aerated alum sludge constructed wetland

The system was decided to operate in batch mode and aerated four hours (2 h + 2 h) per day at an airflow rate of 20 L/h (i.e. filling influent from 8:00 am, aerated from 8:30 to 10:30 and then from 16:30 to 18:30). Column 1 was intermittently aerated with waste gas, which is the 200 ppm  $\text{H}_2\text{S}$  based on air and stored in a steel cylinder; Column 2 was intermittently aerated with air, which is from the air pipe of lab, driven by a mechanical air compressor; while Column 3 was unaerated and served as a control. Synthetic wastewater (influent) was prepared from tap water, the composition of synthetic wastewater is as follows: NaAC 0.48 g/L,  $\text{NH}_4\text{Cl}$  0.12 g/L,  $\text{KH}_2\text{PO}_4$  0.04 g/L,  $\text{CaCl}_2$  0.015 g/L,  $\text{MgSO}_4$  0.012 g/L, with the COD, TN, TP approximately of 300, 30, 10 mg/l, respectively. The hydraulic retention time (HRT) is 3 days.

#### ➤ Analysis

Water samples were taken from the influent and effluent of the A1-VFCWs every 3 days and each time at 8:00 am, to analyze the transformation of organic matter (COD), phosphorus (P) nitrogen (N) and Sulfur (S). Merck Nova 60 spectrophotometer was employed to analyze COD according to its standard operating procedures; Shimadzu VCPH 5050A was positioned for TN analyzing;  $\text{NH}_4^+\text{-N}$  was analyzed by ionic chromatography (Dionex ICS 3000); TP and S were determined by Inductively Coupled Plasma-Atomic Emission Spectroscopy (ICP-AES) on HORIBA Jobin Yvon Ultima 2.

During the aeration period, a plexiglass cap (as shown in Figure 2.17) with rubber seal ring inside to prevent the  $\text{H}_2\text{S}$  leakage was tightly covered on the Column 1. The output  $\text{H}_2\text{S}$  concentration was monitored every two minutes using a gas analyzer from BW Technologies (Gas Alert QUATTRO). After the aeration, the cap was immediately removed to keep the surface water contact with atmosphere.

#### ➤ Data interpretation

Pollutant removal efficiency for the trials was calculated as a cumulative percent removal,



R, between the influent and the effluent Eq. (2.19), assuming that the system was in equilibrium at the time of sample collection:

$$RE = \frac{C_i - C_o}{C_i} * 100 \quad (2.19)$$

Where:

RE = pollutant removal efficiency (%)

C<sub>i</sub> = mean influent concentration across triplicate tests (mg/L)

C<sub>o</sub> = mean effluent concentration across triplicate tests (mg/L)

## 2.4 Summary

Different characterization was carried out on the two alum sludges in order to identify the potential for a beneficial reuse. It was confirmed once again that the properties of alum sludge were site-specific, due to the significant variabilities in the properties, which were mostly influenced by the source water quality and type of water treatment processes. The various elemental analysis indicated that alum sludge contains abundance of elements such as metals and carbon, which could be reused and even recovery [16]. The Carmaux sludge was alkaline, which suggested a high acidity-neutralizing potential; the presence of X-ray diffraction amorphous phases and calcites suggested that alum sludge could be safely applied as low-cost sustainable alternatives [17,18]. Analysis confirms that the alum sludge has higher specific surface area and microporous structure, reflecting that alum sludge has the potential as a low-cost sorbent for various pollutant removals [19-21]. The experimental methods related with this study were outlined, including five different experiments. The precise procedures and devices will be detailed in the corresponding Chapters, as well as the analytical methods used to treat and exploit the obtained results.

## Bibliography

1. KildareNow: 15.3 million Euro Ballymore Eustace Water Treatment Plant is complete. (2018). <https://www.kildarenow.com/news/e15-3-million-ballymore-eustace-water-treatment-plant-complete/257325> (Accessed in April 2019)
2. Ackah, L.A., Guru, R., Peiravi, M., Mohanty, M., Ma, X.M., Kumar, S., Liu, J.: Characterization of Southern Illinois Water Treatment Residues for Sustainable Applications. *Sustainability* **10**(5), 14 (2018). doi:10.3390/su10051374
3. Zhou, Z.M., Liu, Q.D., Li, S.W., Li, F., Zou, J., Liao, X.B., Yuan, B.L., Sun, W.J.: Characterizing the correlation between dephosphorization and solution pH in a calcined water treatment plant sludge. *Environ. Sci. Pollut. Res.* **25**(19), 18510-18518 (2018). doi:10.1007/s11356-018-2036-9
4. Ahmad, T., Ahmad, K., Alam, M.: Characterization and constructive utilization of sludge produced in clari-flocculation unit of water treatment plant. *Materials Research Express* **5**(3), 035511 (2018). doi:10.1088/2053-1591/aab23a
5. Coates, J.: Interpretation of infrared spectra, a practical approach. *Encyclopedia of analytical chemistry: applications, theory and instrumentation* (2006).
6. Ahmad, T., Ahmad, K., Alam, M.: Sustainable management of water treatment sludge through 3'R' concept. *J. Clean Prod.* **124**, 1-13 (2016). doi:10.1016/j.jclepro.2016.02.073
7. Hidalgo, A.M., Murcia, M.D., Gomez, M., Gomez, E., Garcia-Izquierdo, C., Solano, C.: Possible Uses for Sludge from Drinking Water Treatment Plants. *Journal of Environmental Engineering* **143**(3), 7 (2017). doi:10.1061/(asce)ee.1943-7870.0001176
8. Yadav, K.K., Gupta, N., Kumar, V., Khan, S.A., Kumar, A.: A review of emerging sorbents

- and current demand for defluoridation of water: Bright future in water sustainability. *Environment International* **111**, 80-108 (2018). doi:<https://doi.org/10.1016/j.envint.2017.11.014>
9. Thomas, H.C.: Heterogeneous Ion Exchange in a Flowing System. *Journal of the American Chemical Society* **66**(10), 1664-1666 (1944). doi:10.1021/ja01238a017
  10. Hutchins, R.: New methods simplifies design of activated carbon systems, Water Bed Depth Service Time analysis. *J Chem Eng Lond* **81**, 133-138 (1973).
  11. Yoon, Y.H., Nelson, J.H.: Application of Gas Adsorption Kinetics I. A Theoretical Model for Respirator Cartridge Service Life. *American Industrial Hygiene Association Journal* **45**(8), 509-516 (1984). doi:10.1080/15298668491400197
  12. Gutiérrez Ortiz, F.J., Aguilera, P.G., Ollero, P.: Modeling and simulation of the adsorption of biogas hydrogen sulfide on treated sewage-sludge. *Chemical Engineering Journal* **253**, 305-315 (2014). doi:<https://doi.org/10.1016/j.cej.2014.04.114>
  13. Klinkenberg, A.: Numerical Evaluation of Equations Describing Transient Heat and Mass Transfer in Packed Solids. *Industrial & Engineering Chemistry* **40**(10), 1992-1994 (1948). doi:10.1021/ie50466a034
  14. Ranz, W.E., Marshall, W.R.: Evaporation from droplets, parts I & II. *Chemical Engineering Progress* **48**(4), 173-180 (1952).
  15. Fuller, E.N., Schettler, P.D., Giddings, J.C.: NEW METHOD FOR PREDICTION OF BINARY GAS-PHASE DIFFUSION COEFFICIENTS. *Industrial & Engineering Chemistry* **58**(5), 18-27 (1966). doi:10.1021/ie50677a007
  16. Khattab, R.M., Badr, H.A., Abo-Almaged, H.H., Sadek, H.E.H.: Recycling of alum sludge for alpha Al<sub>2</sub>O<sub>3</sub> production using different chemical treatments. *Desalination and Water Treatment* **113**, 148-159 (2018). doi:10.5004/dwt.2018.22240
  17. Dube, S., Muchaonyerwa, P., Mapanda, F., Hughes, J.: Effects of sludge water from a water treatment works on soil properties and the yield and elemental uptake of *Brachiaria decumbens* and lucerne (*Medicago sativa*). *Agric. Water Manage.* **208**, 335-343 (2018). doi:10.1016/j.agwat.2018.06.015
  18. Andrade, J.J.D., Wenzel, M.C., da Rocha, G.H., da Silva, S.R.: Performance of rendering mortars containing sludge from water treatment plants as fine recycled aggregate. *J. Clean Prod.* **192**, 159-168 (2018). doi:10.1016/j.jclepro.2018.04.246
  19. Geng, Y.N., Zhang, J., Zhou, J.H., Lei, J.: Study on adsorption of methylene blue by a novel composite material of TiO<sub>2</sub> and alum sludge. *RSC Adv.* **8**(57), 32799-32807 (2018). doi:10.1039/c8ra05946b
  20. Hou, Q.J., Meng, P.P., Pei, H.Y., Hu, W.R., Chen, Y.: Phosphorus adsorption characteristics of alum sludge: Adsorption capacity and the forms of phosphorus retained in alum sludge. *Materials Letters* **229**, 31-35 (2018). doi:10.1016/j.matlet.2018.06.102
  21. Hua, T., Haynes, R.J., Zhou, Y.F.: Competitive adsorption and desorption of arsenate, vanadate, and molybdate onto the low-cost sorbent materials alum water treatment sludge and bauxite. *Environ. Sci. Pollut. Res.* **25**(34), 34053-34062 (2018). doi:10.1007/s11356-018-3301-7

## Chapter 3

### Alum sludge incorporated in clay brick manufacturing

This Chapter has been published in an international journal and the reference is: Yaqian Zhao, **Baiming Ren**, Andrew O'Brien & Simon O'Toole, *Using alum sludge for clay brick: an Irish investigation*. (2016) **International Journal of Environmental Studies** 73(5):719-730. <http://dx.doi.org/10.1080/00207233.2016.1160651>

#### Abstract

Throughout the world, alum sludge is dewatered and the resultant cakes are discarded in landfill. This paper reports a study to investigate the possible incorporation of alum sludge as a partial replacement for clay in clay brick manufacturing. It is the first study of this problem in Ireland. Alum sludge cakes and clay were separately dried, ground and sieved in preparation for making test specimens. Cylindrical clay bricks were made at different temperatures (800, 1000, 1100, 1200 °C), incorporating different percentages (0, 5, 10, 15, 20, 30, 40 % by dry weight) of alum sludge. The bricks were then subjected to compressive strength test and submersion. Loss on ignition, water absorption and weight reduction were calculated. It was found that bricks containing up to 20 % sludge, fired at 1200 °C, or containing 5 % sludge and fired at 1100 °C have met the European and Irish Standards as set out by Eurocode 6 – ‘Design of Masonry Structures’. The firing temperature and the increase in sludge content affected the final clay-sludge brick colour. By increasing the proportion of alum sludge, compressive strength decreased and the final weight of the brick was reduced. Firing temperatures that are too high may result in damage to the bricks during firing. This study has demonstrated the promising potential and prospects for Irish dewatered alum sludge cakes in clay-sludge brick making.

#### 3.1 Introduction

In 1976, alum sludge was firstly been cited as a recyclable by-product in the manufacturing of clay bricks in America [1]. Although it is not a new concept, to the best of our knowledge, there is no relevant study in Ireland. Moreover, clay has been used in Ireland to produce building brick and constant demand of clay for production of brick has made this material expensive and source of clay is depreciating with time [2]. Considering the “site-specific” properties of alum sludge, it is necessary to investigate the possible incorporation of alum sludge as a partial replacement for clay in Irish clay brick manufacturing.

To date, there have already been a number of studies into the feasibility of incorporating alum sludge as a substitute for clay in the clay brick manufacturing process worldwide [3]. The state of art has been reviewed and presented in Chapter 1 (Section 1.2.1). All these studies show that the quantity of sludge that should be added as a partial substitute for clay in brick manufacturing

depends on the underlying characteristics of the sludge being used [4]. Since the composition of the sludge depends on the quality of the raw water source, in every case the properties of the brick may be affected by the individual sludge, which may vary by location of the treatment plant and according to the raw water source.

To assess the practicalities and identify any possible disadvantages from using alum sludge as a partial replacement for clay in the manufacturing of clay bricks in Ireland, several trials were carried out, including compressive strength, loss on ignition (LoI, loss of weight through firing), water absorption, compressive strength after submersion in water for 24h, and general appearance and texture.

### 3.2 Materials and methods

#### 3.2.1 Alum sludge and clay

The alum sludge was collected from Dublin (Ireland) Ballymore Eustace WTP, and the relevant physicochemical properties were presented in Chapter 2. The clay used was obtained from a delivery of topsoil for use in the landscaping of a residential dwelling. The clay was high quality with minimum impurities such as plants and roots. After collection, the sludge and clay were dried separately in a specialist oven at 105 °C for 24 h. The particle size was then reduced using a grinding machine to obtain a consistent size, which ensured that the mixing of the materials would be thorough. They were then screened separately using an 850 µm sieve (Figure 3.1).



**Figure 3.1** The clay (lighter colour) and alum sludge after grinding and sieving

#### 3.2.2 Production of the sample bricks

The sample bricks were made with ratios ranging from 0 to 40 % sludge by weight, at increments of 10 %. The 0 % sludge (100 % clay) bricks were made for use as a comparison. Five pairs of bricks (total of ten bricks) were made in each batch. From each pair, one brick was

compression tested until failure, and the other was used for the water absorption tests. Four batches were produced. To obtain similar sized brick samples, ten identical moulds were used for the drying of each batch of bricks. The moulds were made of plastic with an internal diameter of 48 mm and a depth of 25 mm. Each mould was cut horizontally in one position to remove the bricks from the mould after drying (Figure 3.2). Water was slowly added to 100 g of the dried clay. It was found that 46ml of water formed a workable but not too moist mixture. This volume of water was not suitable for the mixtures with higher sludge content (they became too moist). This was judged by appearance and physical workability.

Each batch was allowed to dry in a constant temperature room at 20 °C for 24 h. Once the drying was complete, the plastic moulds were removed (Figure 3.2). Each brick was labelled, and the weights were recorded. Each batch of bricks was fired separately in a kiln at varying temperatures of 200-800 °C for Batch 1, 200-1000 °C for Batch 2, and 200-1200 °C for Batch 3 (Figure 3.3), while the temperatures were maintained for a period of 2 h.



**Figure 3.2** The moulds (left) and the bricks after drying

To ensure the removal of the maximum amount of water from the bricks, each batch was heated from room temperature to 100 °C. This temperature was maintained for 1 h before the temperature was increased to 200 °C for 1 h. After analyzing the compression strength results from Batches 1-3, the firing criteria for Batch 4 were decided: the temperature of the kiln was increased from 200 to 1100 °C and the temperature was again maintained for a period of 2 h. In all cases, after firing, the kiln door was kept shut until the kiln returned to room temperature, thus allowing the bricks to cool slowly and ensure the vitrification process was complete.





**Figure 3.3** The bricks from Batch 3 in the kiln after firing

### **3.3 Testing the sample bricks**

Half of the bricks were tested for compression strength, and the other half were tested for durability. All of the bricks were weighed between each stage and the data were used in calculating loss on ignition, water absorption, and weight reduction of each brick. These values were then compared to judge the effect of sludge on each of these properties. The main purpose of compression testing Batches 1-3 was to investigate the most suitable range for both sludge-percentage and firing temperature. These compressions results were used to decide the range of composition and firing temperature for Batch 4. Batch 4 also contained ten bricks, two of each composition. This batch consisted of a smaller range of compositions that were fired at the temperature that was found to be most suitable from the compression testing on Batches 1-3. Therefore, Batch 4 produced the most useful results and conclusions.

#### **3.3.1 Compression strength testing**

The strength testing was carried out using a compression machine (Figure 3.4). A brick from each pair was subjected to a compressive force until failure, and the force (kN) at failure was recorded. The results of the compression testing of Batches 1-3 provided the information needed to prepare Batch 4. Batch 4 was then prepared, dried, and fired as detailed above, with one brick from each of the five pairs being compression tested.





Figure 3.4 The compression strength testing

### 3.3.2 Loss on ignition testing

The weights before and after firing of each brick are manipulated to calculate the LoI. The weights that were recorded after firing are used for this comparison.

### 3.3.3 Water absorption testing

The other brick from each pair (from all 4 Batches) was submerged immediately in water for 24 h (Figure 3.5). The bricks each had their weight recorded before this test giving the ‘initial weights’. Each was then weighed after being submerged providing the ‘resultant weights’. The water absorption was then expressed as a percentage of the initial weight.

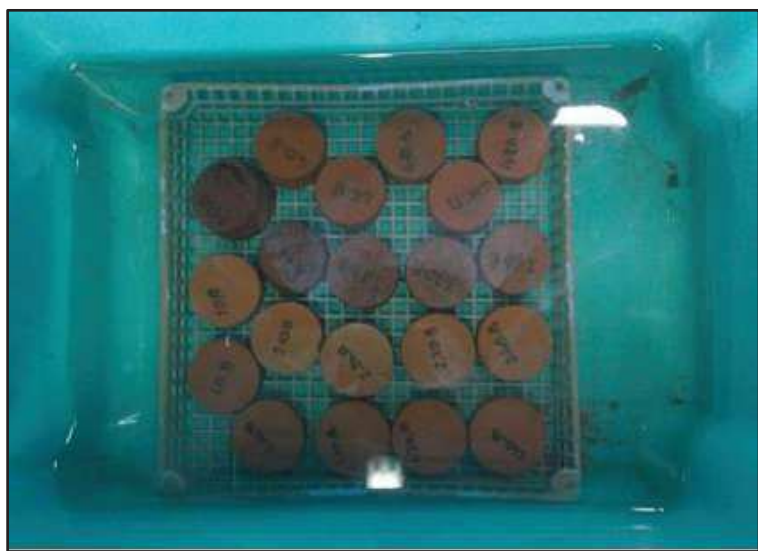


Figure 3.5 Water absorption testing

### 3.3.4 Compression testing after being submerged in water for 24 h

The purpose of this test is to analyse the difference in strength of the bricks before and after being submerged in water. The bricks were then subjected to the same compression test as described above, and the force at failure recorded.

### 3.3.5 General appearance & texture

As bricks are most commonly used as a visible element, such as a building facade or visible structural element, the colour and predictability of the final colour is important. After firing, the bricks are compared within each batch, and also against the entire range of firing temperatures. The firing temperature is known to have a clear effect on the final colour of bricks.

## 3.4 Results and discussion

### 3.4.1 Compressive strength results

Figure 3.6 shows the relationship between compressive strength (Percentage Weight Gain after Water Submersion) and percentage sludge addition. A clear decrease in compressive strength is observed as the sludge content of the brick increases. The 0 % sludge values for Batch 3 were ignored as the bricks became misshapen during firing. The results for Batches 1-3 (800, 1000, 1200 °C) were used in deciding the range and firing temperature for Batch 4. It was decided that a closer examination of alum sludge content in the range of 0-20 % sludge, at a firing temperature of 1100 °C would produce the most suitable data.

It appears that bricks containing up to approximately 15 % sludge, fired at 1100 °C, have greater compression-strength properties than 100 % clay bricks fired at 1000 °C. When the force at failure of this study is compared with that reported by Elangovan and Subramanian [5], the Irish alum sludge shows a better load-bearing. It is clear that addition of sludge has a negative effect on the compression strength of the bricks. But since bricks are more often used as a façade [6], this reduction in compression capacity may not have a major effect on their use. Indeed, alum bricks could be marketed with advice on the fitness for purpose and or limitations on suitability, and become commercial options.

There is a very notable difference in the compressive strength capacity between the 0 % sludge and 10 % sludge bricks fired at 1000 °C: a loss of 59.8 % strength from 20.9 N/mm<sup>2</sup> (0 % sludge) to 8.4 N/mm<sup>2</sup> (10 % sludge). The loss of compressive strength capacity between 0 % and 5 % is also large when fired at 1100 °C: a loss of 27.7 % from 54.9 N/mm<sup>2</sup> to 39.7 N/mm<sup>2</sup>. According to the Eurocode 6–Design of Masonry Structures [7], the ranges of compressive strengths available on the current market are from 12 to 70 N/mm<sup>2</sup>. This would imply that, for bricks fired at 1200 °C, sludge could be used as a partial replacement for clay up to 30 %; for bricks fired at 1100 °C, sludge could be used as a partial replacement for clay up to 20 %, and even higher. From the comparison of the bricks fired at 1000 and 1100 °C, the results suggest that sludge content up to 20 % will not affect the compressive strength if the firing temperature

is increased by 100 °C from 1000 to 1100 °C. This is important, as commercial clay bricks are typically fired at temperatures between 900 and 1100 °C [8].

By increasing the firing temperature, the compressive strength increases; but the raised temperature can also cause damage to the bricks, resulting in unusable specimens. It was found that a firing temperature of 1200 °C caused damage to the 0 % sludge bricks. This result is of significance as characteristics such as compressive strength and water absorption can be positively affected by an increase in firing temperature. This is owing to the completion of the crystallisation process known as vitrification as silicate particles fuse together to form a dense brick structure [8].

### 3.4.2 Loss on ignition

Figure 3.6 also shows that the LoI was found to increase with increased sludge content. For the bricks fired at 1100 °C (the typical maximum firing temperature for commercial clay bricks), the loss on ignition increased by 73 %, from 15.8 % for 100 % clay bricks to 27.5 % for 20 % sludge bricks. The relationship was approximately linear with the loss on ignition increasing to 19.3 % and 21.8 % for the 5 % and 10 % sludge bricks, respectively. A linear relationship between weight loss due to firing and percentage sludge content of the bricks was recorded. As the percentage of sludge used increases, the final weight of the brick reduces. This can be considered a positive result, as by decreasing the overall dead weight of the masonry, a lower strength brick may be required. An overall reduction in weight may also have positive effects on transport costs as these are often calculated by weight [9]. In addition, as the structure is lighter in weight, smaller foundations may be required leading to further overall cost reductions.

### 3.4.3 Water absorption testing

There are two major influences on water absorption from submersion for 24 h: firing temperature and sludge content [10,11]. Lower water absorption is desired. As the firing temperature increases, the water absorption values decrease, but as the sludge content increases so does the water absorption value. Figure 3.6 shows that the 30-40 % sludge bricks fired at 1200 °C exhibited similar water absorption values to the 0 % sludge bricks fired at 800 and 1000 °C (typical firing temperatures for commercial clay bricks). Therefore, by increasing the firing temperature by just 100-200 °C, bricks made with up to 40 % sludge will have similar water absorption values to standard clay bricks currently used in industry.

The values for water absorption from submersion in the 100 % clay bricks at 800 and 1000 °C (typical industry values) are 24.4 and 21.0 % respectively. These figures are higher than those collected from the 0, 10, and 20 % sludge bricks fired at 1200 °C, and the 0, 5, and 10 % bricks fired at 1100 °C. These results show that a small increase in firing temperature will counteract the negative side-effects of increased sludge content in regard to water absorption. When the water absorption of Batch 1 (800 °C) was compared with that reported by Elangovan

and Subramanian [5] different sludge composition in Batch 1 shows a little higher value. This may be caused by the different alum sludge characteristics [12]. For use on the commercial market, according to the European and Irish Standards (Eurocode 6–Design of masonry Structures) [7], the water absorption of the bricks must be below 19 %. The results from the 1200 °C batch suggest that sludge content up to approximately 20 % would meet this requirement. The results from the 1100 °C batch also meet this requirement up to approximately 5 %.

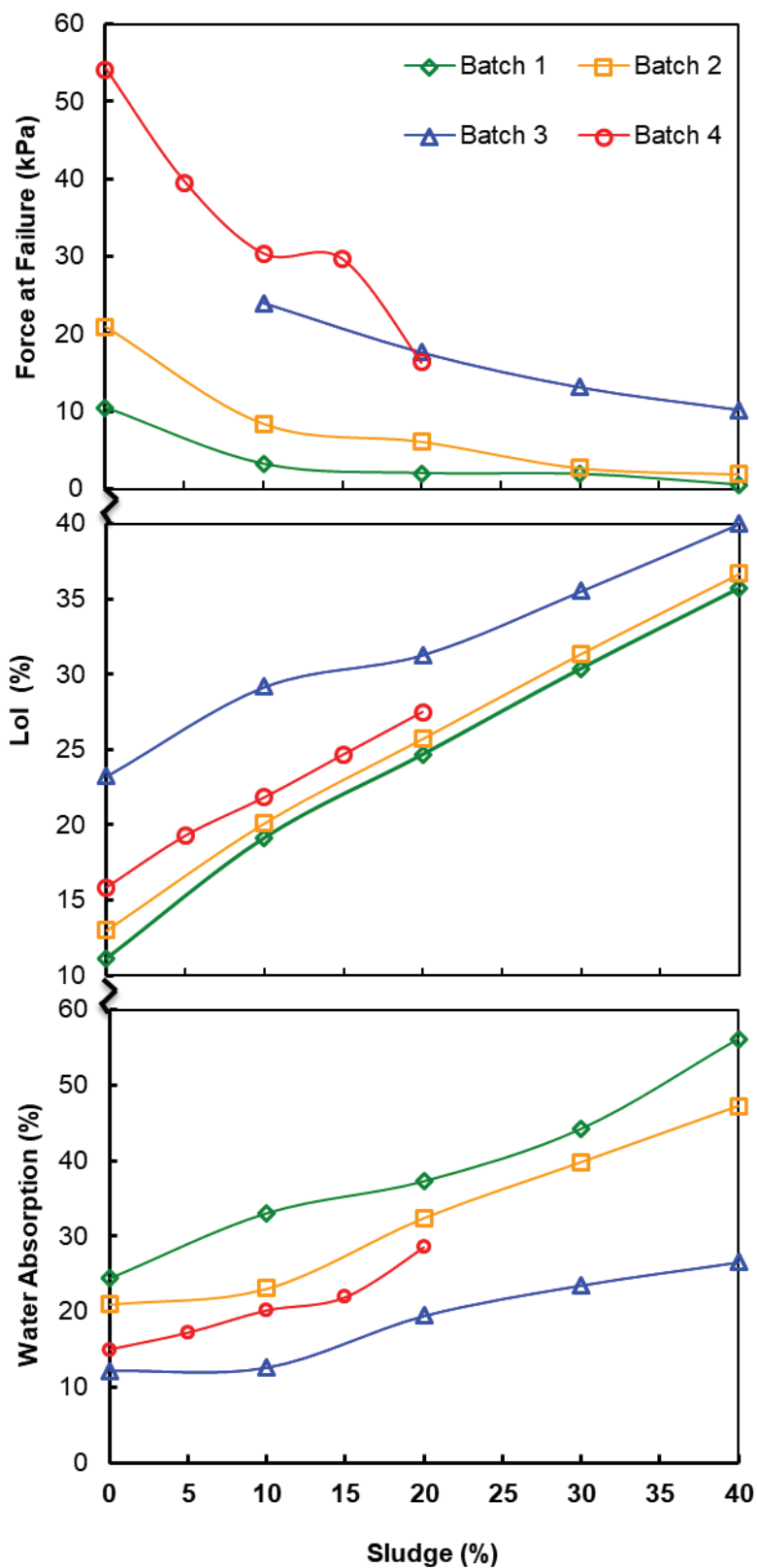


Figure 3.6 The relationship between compressive strength (LoI, Percentage Weight Gain after Water Submersion) and percentage sludge addition.

### 3.4.4 Compressive Strength after Submersion in Water for 24 h

The results show clear signs that water absorption had a very small negative effect on the compression strength of every sludge percentage (Table 3.1). There is also an indication that with increasing sludge content, there is a greater loss in strength from water [5], but this is still relatively small. Although it may not be a deciding factor in the use of sludge/clay bricks on the commercial market, the effect of water absorption on compressive strength must be considered. The durability of a brick depends on its water absorption value and if there is a marked decrease in compressive strength caused by high water absorption then the brick may not be fit for its purpose as a load bearing element.

**Table 3.1** Compressive strength after submersion (kPa)

Batch	Sludge (%)	Before	After
1	0	10.5	9.1
	10	3.2	3.0
	20	2.0	1.5
	30	1.9	0.5
	40	0.5	0.5
2	0	20.9	15.3
	10	8.4	7.6
	20	6.1	4.4
	30	2.7	3.0
	40	1.9	2.8
3	0	/	/
	10	24.0	15.7
	20	17.6	13.8
	30	13.1	12.3
	40	12.2	10.2
4	0	54.3	52.0
	5	39.7	37.5
	10	30.4	29.1
	15	29.7	23.9
	20	16.3	15.7

### 3.4.5 General appearance and texture

The sludge content of the bricks notably affected the colour of the finished bricks. As can be seen in the Figure 3.7(a), the higher sludge content appears to darken the final colour of the brick. For each batch, the 0 % sludge bricks are the lightest. It is believed that the added minerals and impurities present in sludge are the cause of this colour change. There is a notable difference in the colour of Batch 1 (fired at 800 °C) compared Batch 3 (fired at 1200 °C) This difference in the overall colour-range of each batch is attributable to the different firing temperatures. Vitrification of clay/sludge particles is more complete and further burning of clay particles takes place at higher temperatures, and therefore leads to a darker colour of the final bricks. As the bricks in Batch 1 were only fired at 800 °C (a relatively low temperature for brick production)



full vitrification/burning may not have been achieved. Thus, a lighter terracotta colour resulted; not the typical red/brown colour exhibited in commercial bricks. Batch 4 (fired at 1100 °C) exhibited more desirable colour (Figure 3.7(c)). The red/brown colour that resulted from firing at this temperature more closely resembled the typical brick colour as seen in the construction industry. Even with the inclusion of sludge up to 20 %, the firing temperature of 1100 °C appeared close to ideal to achieve a natural-looking colour and appearance. The ‘speckling’ of the bricks can also be attributed to the increase in minerals and impurities in the sludge [13]. No doubt, it will be very useful if detailed examination of the relations between minerals and impurities in the sludge and the colour of the resultant bricks can be conducted. This would be demanding research both because of the different characteristics related to the raw waters, and because of the need precisely to describe variations in the colour.

The texture of all the bricks in this batch was not totally satisfactory as they exhibited a layer of soft dust on the exterior that could be rubbed off by hand. This dust was more prevalent on the bricks with lower sludge content. Therefore, the addition of sludge improves this negative characteristic created by firing the bricks at lower temperatures. No signs of efflorescence are visibly apparent at this firing temperature. Batch 2 (Figure 3.7(b)) possessed a more satisfactory consistency and no ‘dust’ particles could be freely rubbed off by hand. These bricks had a very similar colour range, after firing, to the bricks fired at 800 °C, with the final colour being slightly darker as the sludge content decreased from 40 to 0 %. A small amount of efflorescence is apparent on the surface of the bricks, most notably on the bricks containing sludge.

The bricks fired at 1200 °C (Batch 3) exhibited distinct differences in texture and colour compared to the two previous batches (Figure 3.7(d)). The 0 % sludge brick exhibited a very dense nature with no visible impurities such as speckling. The bricks were smooth to touch, and no dust parted from the bricks when rubbed by hand. The 40 % sludge brick displayed a large amount of speckling which made the overall appearance of the brick much lighter in colour (Figure 3.7(e)). No efflorescence is apparent on the bricks fired at 1200 °C. Batch 4, fired at 1100 °C, exhibited the most consistent colour range and finish. The five bricks of Batch 4 had sludge contents between 0 and 20 % sludge at 5 % increments, unlike the other batches that were 0-40 % sludge at 10 % increments. The range in colour is as expected with a noticeable darkening as the sludge content decreases. The 0 % sludge brick was similar in appearance to normal industry clay bricks, the 20 % sludge brick having a lighter appearance and some speckling. The lighter patches on the surface of the bricks between 15 % sludge and 5 % sludge are caused by efflorescence. There were also signs of efflorescence on the 20 % sludge brick, but the lighter colour of the brick makes it difficult to notice.

It is clear that both the firing temperature and the increase in sludge content affect the final colour. The sludge also adds small light-coloured spots (speckles) to the bricks. This is one of the reasons why the bricks appear lighter in overall colour. These spots are less than 1 mm in size. Efflorescence is the appearance of lighter patches on the surface of the bricks. As bricks are fired, salts are often carried to the surface by escaping moisture and deposited on the brick

surface as the moisture evaporates. The effects of efflorescence could only be seen in bricks containing sludge in the firing range of 1000-1100 °C. This is because of the salts present in the alum sludge. No visible staining is visible on batches 1 or 3. In the case of Batch 3, the increased firing temperature will have removed the staining caused by salts. It is not clear why there is no evidence of efflorescence on the bricks fired at 800 °C, but it is supposed that it can be attributed to the lower firing temperature.

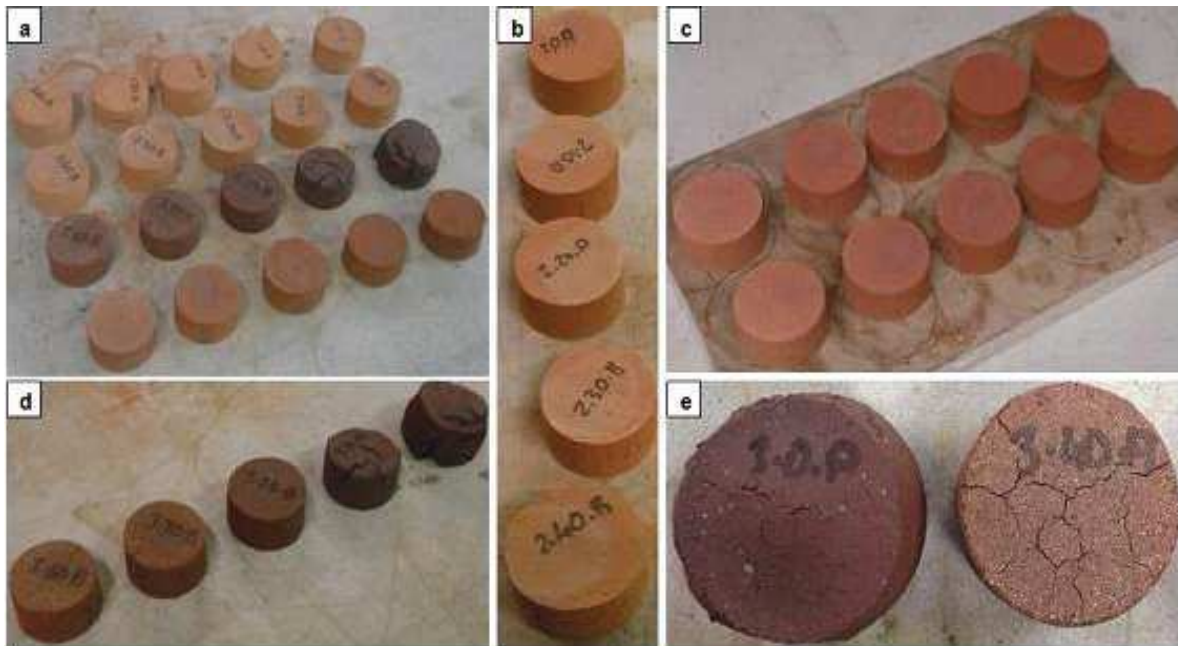


**Figure 3.7** General appearance: (a) Batch 1–4 from top to bottom in the picture; (b) Batch 2; (c) Batch 4; (d) Batch 3; (e) The 0 % sludge brick (left), and the 40 % sludge brick (right) fired at 1200 °C

### 3.5 Prospects

In Dublin Ballymore Eustace water treatment plant, where this study began, the production of alum sludge cakes is about 165 tons per day, costing over €10,000 on their disposal of landfill (at current rate of the cost of €65 per ton). The use of the sludge in the manufacturing of clay bricks would be an environment-friendly and economical way of disposing sludge in Ireland. This study suggests that if commercial bricks were to be fired at 1200 °C, a sludge incorporation of 10 and 20 % would also yield satisfactory strength and water absorption characteristics for bricks in commercial use. This proportion of sludge when fired at 1100 °C produced an appearance closest to standard commercial clay bricks. To date, no pilot project has been established to investigate the use of water treatment sludge in the manufacture of clay brick on an industrial scale in Ireland. It is recommended that there should be a pilot study. In addition, similarly, reuse of alum sludge-clay bricks for pavement and car park areas or general building construction materials in Ireland is also worth investigation, as a separate study.

### 3.6 Conclusions

Alum sludge content of up to approximately 20 % produces water absorption that meet the Irish and European Standards (Eurocode 6–Design of masonry Structures) when fired at 1200 °C. Similarly, bricks fired at 1100 °C can contain up to approximately 9 % sludge and still meet the required criteria concerning water absorption. The ideal firing temperature is 1100 °C, this ensures adequate compressive strength and durability is established within the brick. Firing at lower temperatures is unsuccessful; the water absorption values of these bricks would be unnecessarily high and compressive strength values too low. The ideal value of sludge incorporation to ensure adequate compressive strength before and after water absorption is 5 %. Even after water absorption has occurred, the brick still possesses a considerable compressive strength at 37.5 N/mm<sup>2</sup>. With an increase in sludge content, the colour became more pale – the appearance of very small white spots on the bricks. This effect could be used to enhance the final appearance of a building or structure. Novelty thus adds commercial value by the reuse of what otherwise is an expensive problem. The results of efflorescence were also visible on the surface of all of the bricks fired at 1100 °C that contained any sludge (5, 10, 15 and 20 %).

### Bibliography

1. Cone, J.R., Cochran, J.K.: USE OF ALUM SLUDGE FROM WATER TREATMENT AS A BRICK ADDITIVE. *Am. Ceram. Soc. Bull.* **55**(4), 455-456 (1976).
2. Pavía, S., Hanley, R.: Flexural bond strength of natural hydraulic lime mortar and clay brick. *Materials and Structures* **43**(7), 913-922 (2010). doi:10.1617/s11527-009-9555-2
3. Wang, L., Zou, F.L., Fang, X.L., Tsang, D.C.W., Poon, C.S., Leng, Z., Baek, K.: A novel type of controlled low strength material derived from alum sludge and green materials. *Construction and Building Materials* **165**, 792-800 (2018). doi:10.1016/j.conbuildmat.2018.01.078
4. Odimegwu, T.C., Zakaria, I., Abood, M.M., Nketsiah, C.B.K., Ahmad, M.: Review on Different Beneficial Ways of Applying Alum Sludge in a Sustainable Disposal Manner. *Civ. Eng. J.-Tehran* **4**(9), 2230-2241 (2018). doi:10.28991/cej-03091153
5. Elangovan, C., Subramanian, K.: Reuse of alum sludge in clay brick manufacturing. *Water Supply* **11**(3), 333-341 (2011). doi:10.2166/ws.2011.055
6. Zhang, L.: Production of bricks from waste materials – A review. *Construction and Building Materials* **47**, 643-655 (2013). doi:<https://doi.org/10.1016/j.conbuildmat.2013.05.043>
7. Eurocode 6:Design of Masonry Structures. <https://www.icevirtuallibrary.com/doi/book/10.1680/dms.31555> (Access on April 2019).
8. Karaman, S., Ersahin, S., Gunal, H.: Firing temperature and firing time influence on mechanical and physical properties of clay bricks. (2006).
9. Chen, Y., Zhang, Y., Chen, T., Zhao, Y., Bao, S.: Preparation of eco-friendly construction bricks from hematite tailings. *Construction and Building Materials* **25**(4), 2107-2111 (2011). doi:<https://doi.org/10.1016/j.conbuildmat.2010.11.025>
10. Raut, S.P., Ralegaonkar, R.V., Mandavgane, S.A.: Development of sustainable construction

- material using industrial and agricultural solid waste: A review of waste-create bricks. *Construction and Building Materials* **25**(10), 4037-4042 (2011). doi:<https://doi.org/10.1016/j.conbuildmat.2011.04.038>
11. Hegazy, B.E.-D., Hegazy, E., Fouad, H., Hassanain, A.: Brick Manufacturing From Water Treatment Sludge And Rice Husk Ash, vol. 6. (2012)
  12. Benlalla, A., Elmoussaouiti, M., Dahhou, M., Assafi, M.: Utilization of water treatment plant sludge in structural ceramics bricks. *Applied Clay Science* **118**, 171-177 (2015). doi:<https://doi.org/10.1016/j.clay.2015.09.012>
  13. da Silva, E., Morita, D., Lima, A., Teixeira, L.G.: Manufacturing ceramic bricks with polyaluminum chloride (PAC) sludge from a water treatment plant. *Water Science and Technology* **71**(11), 1638-1645 (2015).

## Chapter 4

### Alum Sludge and Irish Peat for Glyphosate Removal

This Chapter has been published in an international journal and the reference is: Yae Wang, **Baiming Ren**, Yaqian Zhao, Anthony English & Martin Cannon, *A comparison of alum sludge with peat for aqueous glyphosate removal for maximizing their value for practical use*. **Water Science & Technology** 2017(2):450-456. doi: 10.2166/wst.2018.165

#### Abstract

This study compares and contrasts the glyphosate removal efficiency of alum sludge (waterworks residue) and Irish peat in aqueous solution. Organic phosphonate of glyphosate aqueous solution was removed in pot tests separately filled with peat and alum sludge, while effluent samples were taken from each pot to analyse the concentration of phosphorus (P) and COD (chemical oxygen demand); physical and chemical analysis for both media before and after use was carried out subsequently. The results show that the P removal capacity of alum sludge was significant (>99 %), while the removal capacity of peat was considerably less than 10 % after 10 weeks. Both materials significantly reduced the levels of COD, but it was noted that peat had a marginally greater initial P removal capacity ( $68 \pm 22$  %) and did perform better than alum sludge ( $57 \pm 12$  %). Moreover, pretreatment is a crucial step to harness the full potential of peat. Overall, this study provides a scientific clue for sorbents selection when considering alum sludge and peat to maximize their value in practice.

#### 4.1 Introduction

Contaminant such as phosphorus (P) is among the most extensive pollutants that enter water system and is a direct cause of eutrophication. Conventionally, P in natural waters is found in three forms of phosphates: orthophosphate, polyphosphate and organic-phosphate. Glyphosate ( $C_3H_8NO_5P$ ) or (N-(phosphonomethyl)glycine) as an organic phosphonate and an active ingredient in pesticide is largely used worldwide especially in Ireland, since agriculture plays an integral role in Irish economy [1]. Therefore, there are increased concerns about its impacts on the environment, in which the glyphosate was entered via various routes during its manufacture, use and runoff after use etc.

Ireland has the third largest peat deposit in the world [2]. Historically, before the widespread use of commercial fossil fuels, peat played as the fuel source for those in rural areas [3]. Since 1940's, natural peat was applied for horticulture and afforestation, which caused the rapidly diminish the area of peatlands in Ireland. Nowadays, many conservation laws and practices, as well as some projects that aimed to reclaim the peatlands were carried out [4].

Natural peat has a high affinity for water, low mechanical strength, a tendency to shrink and/or swell and poor chemical stability. The formation of peat is initiated by the decomposition of trees and vegetation. The organic matter, which is preserved by moisture due to its waterlogged state, is slowly and continuously oxidized by microorganisms. This is metamorphosis in the biochemical stage, which usually occurs in the top few meters of surface matter, and peat is invariably found with high levels of moisture content between 2 and 5 m deep [4]. Indeed, Peat can be described in the preliminary production stages of coal, the major constituents are cellulose and lignin. The components lignin and humic acid are particularly noted because of their polar functional groups, such as ketones, alcohols, carboxylic acids, phenolic hydroxides and esters that may be present in chemical bonding [5].

To date, Peat has been a topic of research for almost four decades. Brooks [6] firstly proposed the use of peat for residential wastewater treatment. Since then peat had been tested for the adsorption of phosphate [7], thallium ions [8], arsenic [9], Malachite green [10], etc. from domestic and industrial effluents, it is noted that peat has a high absorption capacity for transition metals and polar organic molecules. Regarding P adsorption in aqueous, published data showed that the capacity for peat is in the range of 0.097 to 8.91 mg/g [7,11]. While alum sludge had been investigated for various adsorptions as well, which has been reviewed and summarized in Chapter 1 (Table 1.1).

Moreover, it has been noted that both the materials, peat and alum sludge, have been used in constructed wetlands as the main substrate for enhanced wastewater treatment [12,13]. With the recent development of constructed wetland technology, it has become a mainstream treatment technology for the mitigation of a variety of wastewater. In constructed wetlands, substrate and vegetation are two of the three main wetland components along with hydrology [14]. Studies have shown that the contribution to treatment of the overall system could be significantly enhanced by adopting alternative substrates including natural, manufactured and reclaimed materials. Peat is a natural material, while alum sludge is a water treatment by-product. Applications of both materials in constructed wetlands are generally preferable due to their low economic cost and geographical availability.

Nevertheless, it is noted that the individual studies were based on different experimental conditions and there is no report on the comparison purpose of using these two low-cost materials. Thus, knowledge of comparing the two cost-effective sorbents for pollutant immobilization is not only necessary for the materials choice, but is also useful for the beneficial reuse to maximize their value in practice. Therefore, the objective of the study was to compare and contrast of the two abundant and indigenous low-cost materials, i.e. Irish peat and alum sludge, addressing their Glyphosate removal capacity via pot tests.



## 4.2 Materials and methods

### 4.2.1 Materials

Dewatered alum sludge cake was collected from the Dublin Ballymore Eustace water treatment, the physicochemical properties were presented in Chapter 2. The peats used in this study were extracted from two ombrotrophic bogs in Co. Mayo, Ireland, one at Loughruseen, Castlebar and the other at Derrybeag, Kiltimagh (Figure 4.1). The initial 30-40 cm of the surface peatland layer was scrapped away from both sites and an appropriate mass of the peat beneath (below 30-40 cm from the surface) was extracted. Both peat samples were mixed evenly to achieve the advantages of both peat types for use in pot tests. Moisture content (MC) of peat is 80.2 %. Accordingly, the mass of peat used was 2.278 kg for each pot which equals to the mass of alum sludge of 1.498 kg. The P-containing contaminant used was Roundup™ Bioactive with glyphosate as its active ingredient and a target glyphosate concentration of 50 mg/l in artificial wastewater with the natural pH of 5.2–5.6 was decided. The diluted solution which resulted in 22.2 ml of the stock solution was used to make up the 1600 ml influent solution.

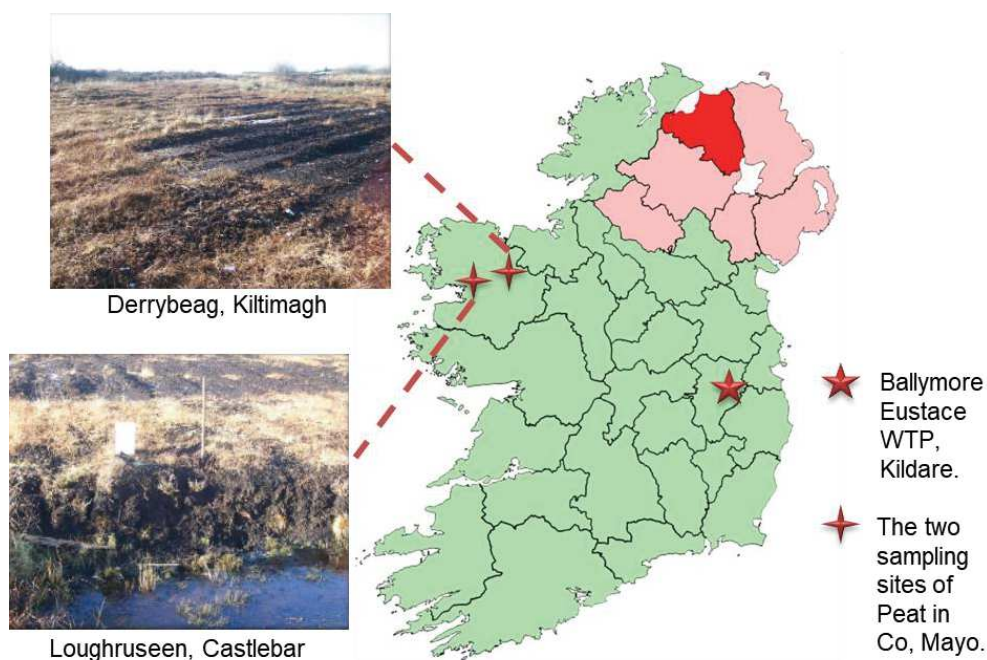


Figure 4.1 Map location of sampling sites in Ireland

### 4.2.2 Pot setup

Four identical plastic containers were sourced and hydraulic valves were attached to each pot at 35 mm from the base of the pot. The pot was 200 mm in diameter and 250 mm in height (Figure 4.2). The base of the pots was filled with washed gravel to an approximate height of 50 mm. After calculating the dry weight of both substrate types, the substrate with the large MC (peat) was filled into the first pot until there was only a free board of 50 mm at the top. The mass of the peat added was 2.278 kg. The allowable mass of alum sludge of 1.498 kg, which

was equivalent to the dry mass of the peat, was then placed in the corresponding pot to allow the mass of substrates being equal in both corresponding blank and active pots (Figure 4.3). The trimmed young reeds were then planted on the top of each pot.

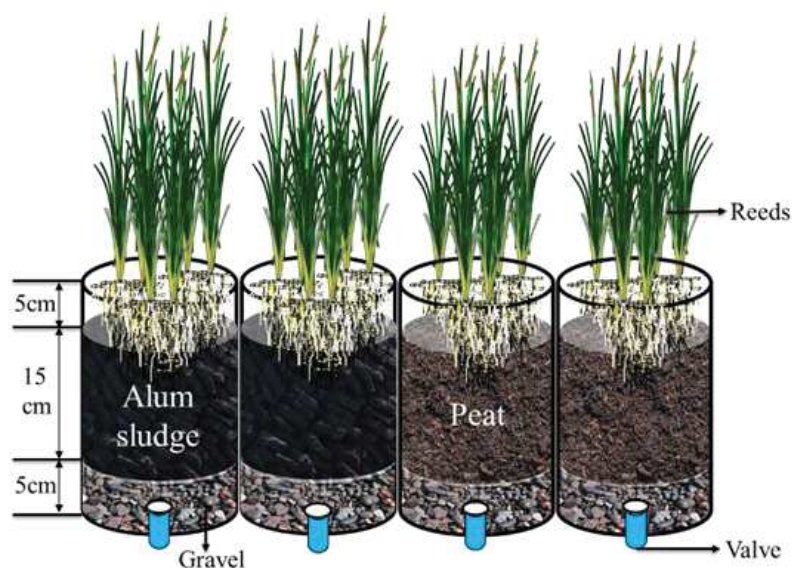


Figure 4.2 Schematic of pot apparatus



Figure 4.3 Pot setup (a) filled with gravel; (b) measuring the media mass; (c) filled with peat; (d) planting reeds

### 4.2.3 Dosing and sampling

As shown in Figure 4.4, the influent 1600 ml per pot was divided into two doses of 800 ml. One pot of each material was dosed with the selected herbicide solution at room temperature (22 °C), while the remaining two pots were filled with tap water and used as control blanks.

The pots were drained via the valve and refilled twice weekly for a 10-week period. Each pot was drained and then individually passed through a vacuum filter using a 0.45  $\mu\text{m}$  pore filter paper. The filtrate was then subjected to water quality monitoring.

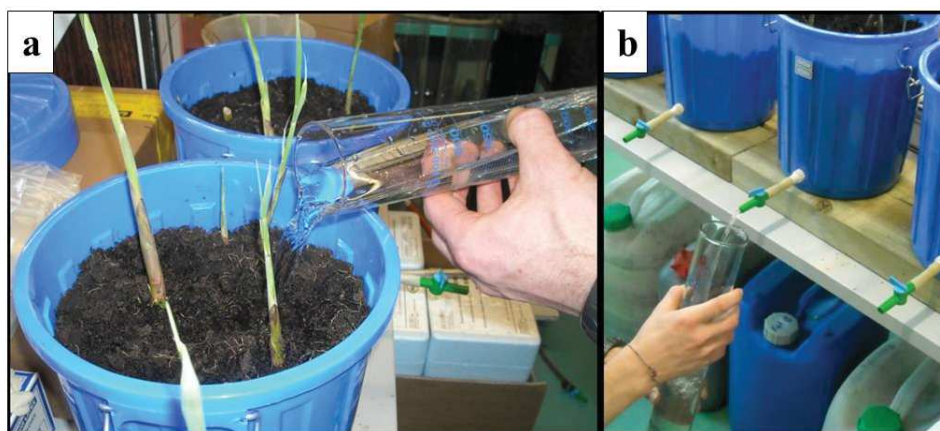


Figure 4.4 Dosing and sampling

#### 4.2.4 Analysis

Monitoring of P and chemical oxygen demand (COD) for filtrate from each pot (named as blank peat, peat, blank alum, alum) was conducted via a Unicam Helias- $\alpha$  spectrometer for P and a HACH DR-2400 spectrometer for COD with standard procedure. As the P source was an organic phosphonate the sample had to firstly undergo chemical and thermal treatment by autoclave method. In addition, samples of the alum sludge and peat before and after use in pot testing were naturally dried for physical and chemical properties examination. Their surfaces were observed under a scanning electron microscope (SEM) (LEO 1530 VP Germany) to visualize inner porosity, surface properties and changes to the surfaces of the four relevant particles from the four pots. The SEM was further combined with energy-dispersive X-ray (EDX) to determine the composition and relative distribution of elements particularly on the surface. The chemical components of four media were examined via Inductively Coupled Plasma Atomic Emission Spectrometry (ICP-AES, Profile DV, America Leeman Labs Inc.).

#### 4.3 Results and discussion

Figure 4.5 represents the comparison of glyphosate concentrations in both the effluents from peat and alum sludge pots, alongside the influent concentration. The glyphosate concentration in peat quickly rises towards the influent concentration. In contrast, the alum sludge remains practically at zero throughout, considering alum sludge has the high glyphosate adsorption capacity of 85.9 mg/g [15]. The smaller space between the influent line and peat line shows a steady decline of peat's adsorption capacity over time, and again the consistency of alum sludge can be clearly seen with virtually all traces of glyphosate removed. The percentage removal efficiency of both substrates being analyzed; Inthorn et al. [16] determines that removal efficiency less than 10 % is termed an exhaustion limit of the substrate. A similar exhaustion limit is shown in Figure 4.5. The peat substrate has been exhausted as the efficiency falls below



10 % on two occasions. Significantly, the degradation of peat's removal ability indicates an imminent intersection with the influent concentration line, thereby reaching theoretical saturation. It can be clearly seen from the results that at the end of the 10-week testing schedule the peat's removal capacity was practically exhausted. These findings conflict with results from other studies, such as those undertaken by Heavey [17], the P removal of peat to be up to 63 % although a significant decrease in capacity after a 6-month period was observed. There are a number of reasons that the peat may have underperformed. In a study of various filter materials, Kõiv et al. [18] found P removal was only initiated when the total P inflow was greater than 1.5 mg/l. The concentrations of the polluting materials must firstly reach a significant level in order to be removed from the influent. It was observed that P was not removed during the preliminary phase of operation when the total P inflow was too low. More significantly, Brown et al. [19] noted that peat adsorption is pH dependent, stating that in order for peat to offer significant adsorption capacity the pH must not exceed 8. Additionally, if the pH of the peat drops below 3, metal ions are exchanged by hydrogen ions resulting in leaching or stripping of metals from the peat. This phenomenon enables the regeneration and recovery of the peat being used for metal removal by washing with an acidic solution of pH less than 3. Kõiv et al. [18] also observed that P was not removed during the preliminary phase of operation which corresponded with the Figure 4.5 when the total P inflow was low. It was only due to a mechanical filter malfunction that the level of total P inflow was increased. With this increase, the filter showed a sizeable reduction of total P through the system. Pollutants and contaminants removed by peat occur through physical, chemical and biological processes. The removal of P by peat can occur through sedimentation, sorption or combination of complex compounds [20]. Some quantity of P may also be bound onto the biofilm of the peat. This study has proven that peat in its natural state performs unsatisfactorily in terms of P removal, but it is believed that peat may still be used as a low-cost sorbent for P if pre-treatment is essential. Peat used in the research of Sen Gupta et al. [21] was washed for 30 mins in HCl solution before use, as well as in the research of Hemmati et al. [10] that peat was washed several times using distilled water to remove the primary impurities, etc. It can be inferred that all the pre-treatment gave a uniformity and possible increased performance. In general, there is a wide range of pre-treatment processes which may be carried out. Some methods are simple as air drying which is aimed towards increasing hydraulic conductivity as well as improved removal performance. Thermal and chemical pre-treatments, surface thermolysis, EDTA (ethylenediaminetetraacetic acid) washing have also been implemented as methods used in an attempt to improve the removal efficiencies of peat.

However, the alum sludge results surpassed expectation based on previous literature, exhibiting an average glyphosate removal of 99.8 % over the 10-week test period. This result shows no trends indicating a significant change of its performance in the immediate future. To expand on the research completed in this study it would be wiser that the testing schedule must be increased to long term basis to determine the longevity of alum sludge. However, our previous study on the long-term use of alum sludge in constructed wetland have demonstrated and predicted its life span, while the current study is focusing on the comparison of the two materials. This result is also indicating that Yang et al. [22], who reported P removal via

adsorption, found alum sludge had greater capability to remove inorganic P compared to organic P.

The results of COD are displayed in Figure 4.5. Since the COD data was limited to 11 results, perhaps a more accurate description would be provided with increase in COD data over a longer period. The theoretical COD can be calculated from stoichiometry, 50 mg/l glyphosate = 23.5 mg/l COD (Theoretical). In contrast to the glyphosate removal, initially the peat's removal efficiency was very good and the alum sludge removal was quite poor. As the volume treated increased there was both a decrease and an increase in removal efficiency in the peat and alum sludge, respectively. The two substrates then appeared to reach removal equilibrium of approximately 70 %. Despite the poor removal of P, peat did perform better than alum sludge in terms of COD removal, demonstrating average removal of  $68 \pm 22$  %. The alum sludge had COD average removal of  $57 \pm 12$  % after an initial poor start. It should be noted that both the sorbents (peat and alum sludge) can release some organic material, thus increasing the COD level of the effluent. Detailed consideration of COD removal should consider the effect of COD release from both the sorbents via the extra trials.

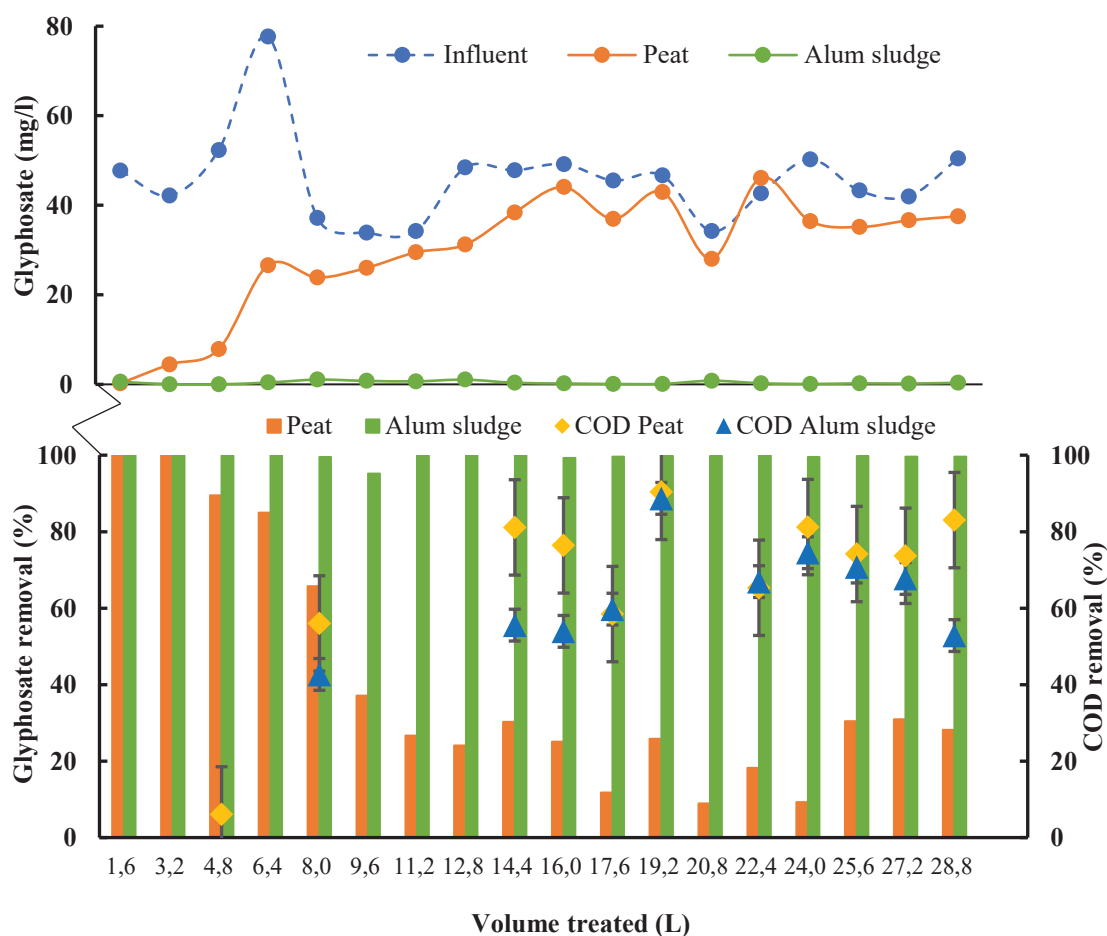
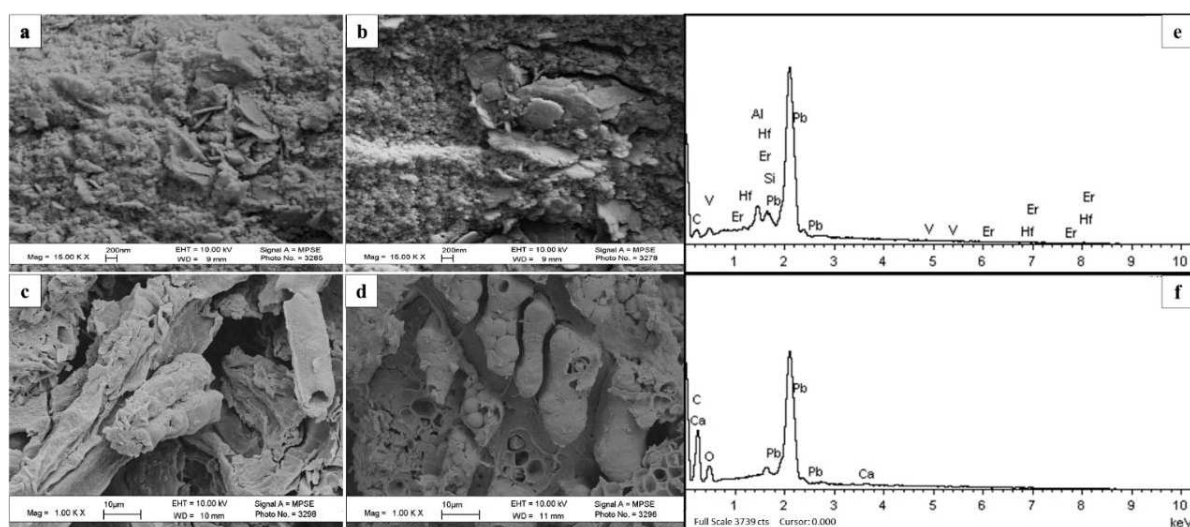


Figure 4.5 Glyphosate concentration/removal and COD removal rate

To provide an insight into the material's surface, either the raw media or after the P adsorption in the pot was observed by SEM, as shown in Figure 4.6 clearly shows the difference between the two alum sludges surfaces, before the adsorption (Figure 4.6a) the sludge particles have a porous structure, relating to the potential to adsorb P ions from the aquatic solution. However, following the adsorption for 10 weeks, the particle surface (Figure 4.6b) becomes much smoother than that of the original particles. The honeycomb hole in peat (Figure 4.6c) demonstrates the porous property. Qualitative assessment of the elemental distribution on the surface of the alum sludge and peat by the SEM-EDX (Figure 4.6e, f) showed the predominance of aluminum and this was expected to highly influence its P adsorption ability. Ippolito et al. (2003) found similar results using SEM-EDX. The elemental composition of the four media (alum sludge and peat before and after use) is given in Table 4.1. The aluminum sulphate coagulant used during the water treatment process is reflected in the composition of the alum sludge. The aluminum component in the alum sludge is about 130 times greater than peat, and only the cuprum levels in the alum sludge is comparatively low. In the last decades, aluminum is known to play a key role in P adsorption/precipitation by solid matrices via ligand exchange by phosphate ion reactions with aluminum oxides forming inner-sphere complexes [23]. Hence, substrates that are particularly rich in aluminum can effectively remove P by adsorption and/or precipitation of chemically stable phosphate phases. Table 4.1 further shows that the good retention of P in the pot. It can be inferred that Al oxides particles would provide an excellent material for construction of a P removal which corresponded to Arias et al. [24], who addressed the covering quartz particles with Al oxides provide a high capacity adsorption and immobilization of P, as well as Ronkanen et al. [25], who significantly addressed that the additional P was successfully retained in columns with accumulated metals. It is also noted in Table 4.1 that the cuprum levels in both the alum sludge and peat after use were considerably increased. The reason behind this was not clear and it deserves further investigation. However, it is noted from the Roundup formulation of the pesticide label that the CuO additive occurred as Cu source. This may possibly cause the observed Cu increase.



**Figure 4.6** SEM-EDX image: (a) raw alum sludge; (b) alum sludge after pot test; (c) raw peat; (d) peat after pot test; (e) alum sludge EDX; (f) peat EDX.



**Table 4.1** The major chemical composition of the four media

Element (mg/g)	Alum sludge	Alum sludge (blank)	Peat	Peat (blank)
Al	131	131	1.12	0.85
P	1165	744	372	235
Cu	73.4	31.1	116	2.8
Fe	15.3	16.7	2.8	2.7
Ca	9.3	3.0	5.3	3.5

#### 4.4 Conclusions

The results clearly show that the P removal capacity of the alum sludge cake was significant, while the removal capacity of peat was considerably less than expected. At the end of the 10-week pot testing schedule, the peat's removal capacity was practically below 10 % while alum sludge exhibiting an average glyphosate removal of 99.8 %. This result shows no trends indicating a significant change of its performance in the immediate future. It was found that both materials significantly reduced the levels of COD in the influent and it was noted that peat had a marginally greater initial removal capacity. Despite the poor removal of P, peat did perform better than alum sludge in terms of COD removal  $68 \pm 22$  % while alum sludge had an average of  $57 \pm 12$  % COD removal after an initial poor start. The different behaviour lies in the fact that peat in its natural state has poor P removal characteristics, in order to harness the full potential of peat, it must undergo pre-treatment prior to being used as a sorbent material.

#### Bibliography

1. Hu, Y., Zhao, Y., Zhao, X., Kumar, J.L.G.: High Rate Nitrogen Removal in an Alum Sludge-Based Intermittent Aeration Constructed Wetland. *Environmental Science & Technology* **46**(8), 4583-4590 (2012). doi:10.1021/es204105h
2. Rosca, C., Schoenberg, R., Tomlinson, E.L., Kamber, B.S.: Combined zinc-lead isotope and trace-metal assessment of recent atmospheric pollution sources recorded in Irish peatlands. *Science of the Total Environment* **658**, 234-249 (2019). doi:10.1016/j.scitotenv.2018.12.049
3. Holden, J., Chapman, P.J., Labadz, J.C.: Artificial drainage of peatlands: hydrological and hydrochemical process and wetland restoration. *Prog. Phys. Geogr.* **28**(1), 95-123 (2004). doi:10.1191/0309133304pp403ra
4. Council, I.P.C.: Irish Peatland Conservation Council. <http://www.ipcc.ie/> (Access on April 2019)
5. Renou-Wilson, F., Moser, G., Fallon, D., Farrell, C.A., Muller, C., Wilson, D.: Rewetting degraded peatlands for climate and biodiversity benefits: Results from two raised bogs. *Ecol. Eng.* **127**, 547-560 (2019). doi:10.1016/j.ecoleng.2018.02.014
6. Brooks, J.L.: A Field Study of the Efficiency of Sphagnum Peat as a Medium for the Treatment of Residential Wastewater. (1980).
7. Xiong, J.B., Mahmood, Q.: Adsorptive removal of phosphate from aqueous media by peat.

- Desalination **259**(1), 59-64 (2010). doi:<https://doi.org/10.1016/j.desal.2010.04.035>
8. Robalds, A., Klavins, M., Dreijalte, L.: Sorption of thallium(I) ions by peat. *Water Science and Technology* **68**(10), 2208-2213 (2013). doi:10.2166/wst.2013.479
  9. de Oliveira, L.K., Melo, C.A., Goveia, D., Lobo, F.A., Armienta Hernández, M.A., Fraceto, L.F., Rosa, A.H.: Adsorption/desorption of arsenic by tropical peat: influence of organic matter, iron and aluminium. *Environmental Technology* **36**(2), 149-159 (2015). doi:10.1080/09593330.2014.939999
  10. Hemmati, F., Norouzbeigi, R., Sarbisheh, F., Shayesteh, H.: Malachite green removal using modified sphagnum peat moss as a low-cost biosorbent: Kinetic, equilibrium and thermodynamic studies. *Journal of the Taiwan Institute of Chemical Engineers* **58**, 482-489 (2016). doi:<https://doi.org/10.1016/j.jtice.2015.07.004>
  11. Niedermeier, A., Robinson, J.S.: Hydrological controls on soil redox dynamics in a peat-based, restored wetland. *Geoderma* **137**(3), 318-326 (2007). doi:<https://doi.org/10.1016/j.geoderma.2006.08.027>
  12. Babatunde, A.O., Zhao, Y.Q., Zhao, X.H.: Alum sludge-based constructed wetland system for enhanced removal of P and OM from wastewater: Concept, design and performance analysis. *Bioresource Technology* **101**(16), 6576-6579 (2010). doi:<https://doi.org/10.1016/j.biortech.2010.03.066>
  13. Jin, M., Carlos, J., McConnell, R., Hall, G., Champagne, P.: Peat as substrate for small-scale constructed wetlands polishing secondary effluents from municipal wastewater treatment plant. *Water* **9**(12), 928 (2017).
  14. Vymazal, J.: Plants in constructed, restored and created wetlands. *Ecol. Eng.* **61**, 501-504 (2013). doi:<https://doi.org/10.1016/j.ecoleng.2013.10.035>
  15. Hu, Y.S., Zhao, Y.Q., Soroohan, B.: Removal of glyphosate from aqueous environment by adsorption using water industrial residual. *Desalination* **271**(1), 150-156 (2011). doi:<https://doi.org/10.1016/j.desal.2010.12.014>
  16. Inthorn, D., Tipprasertsin, K., Thiravetyan, P., Khan, E.: Color removal from textile wastewater by using treated flute reed in a fixed bed column. *Journal of Environmental Science and Health, Part A* **45**(5), 637-644 (2010). doi:10.1080/10934521003595803
  17. Heavey, M.: Low-cost treatment of landfill leachate using peat. *Waste Management* **23**(5), 447-454 (2003). doi:[https://doi.org/10.1016/S0956-053X\(03\)00064-3](https://doi.org/10.1016/S0956-053X(03)00064-3)
  18. Kõiv, M., Vohla, C., Mõtsep, R., Liira, M., Kirsimäe, K., Mander, Ü.: The performance of peat-filled subsurface flow filters treating landfill leachate and municipal wastewater. *Ecol. Eng.* **35**(2), 204-212 (2009). doi:<https://doi.org/10.1016/j.ecoleng.2008.04.006>
  19. Brown, P.A., Gill, S.A., Allen, S.J.: Metal removal from wastewater using peat. *Water Research* **34**(16), 3907-3916 (2000). doi:[https://doi.org/10.1016/S0043-1354\(00\)00152-4](https://doi.org/10.1016/S0043-1354(00)00152-4)
  20. Vohla, C., Kõiv, M., Bavor, H.J., Chazarenc, F., Mander, Ü.: Filter materials for phosphorus removal from wastewater in treatment wetlands—A review. *Ecol. Eng.* **37**(1), 70-89 (2011). doi:<https://doi.org/10.1016/j.ecoleng.2009.08.003>
  21. Sen Gupta, B., Curran, M., Hasan, S., Ghosh, T.K.: Adsorption characteristics of Cu and Ni on Irish peat moss. *J. Environ. Manage.* **90**(2), 954-960 (2009). doi:<https://doi.org/10.1016/j.jenvman.2008.02.012>

22. Yang, Y., Zhao, Y.Q., Kearney, P.: Influence of ageing on the structure and phosphate adsorption capacity of dewatered alum sludge. *Chemical Engineering Journal* **145**(2), 276-284 (2008). doi:<https://doi.org/10.1016/j.cej.2008.04.026>
23. Ippolito, J.A., Barbarick, K.A., Heil, D.M., Chandler, J.P., Redente, E.F.: Phosphorus Retention Mechanisms of a Water Treatment Residual. *Journal of Environmental Quality* **32**(5), 1857-1864 (2003). doi:10.2134/jeq2003.1857
24. Arias, M., Da Silva-Carballal, J., García-Río, L., Mejuto, J., Núñez, A.: Retention of phosphorus by iron and aluminum-oxides-coated quartz particles. *Journal of Colloid and Interface Science* **295**(1), 65-70 (2006). doi:<https://doi.org/10.1016/j.jcis.2005.08.001>
25. Ronkanen, A.-K., Marttila, H., Celebi, A., Kløve, B.: The role of aluminium and iron in phosphorus removal by treatment peatlands. *Ecol. Eng.* **86**, 190-201 (2016). doi:<https://doi.org/10.1016/j.ecoleng.2015.11.011>

## Chapter 5

# Co-conditioning of Waste-activated Sludge with Alum Sludge

This Chapter has been submitted to an international peer-reviewed journal as: **Baiming Ren**, Nathalie Lyczko, Yaqian Zhao, Ange Nzihou. *Co-conditioning of waste-activated sludge with alum sludge: A case study of a city in South France.*

### Abstract

This Chapter reports a case study based on Graulhet (France) water industry, as the unique geographical location of water and WWTP in Graulhet profited the environmental resources integration and sustainable development. Alum sludge was introduced to co-conditioning and dewatering with waste-activated sludge from the WWTP to examine the role of the alum sludge in improving the dewaterability of the mixed sludge. Experiments have demonstrated that the optimal mixing ratio for the two sludges is 1:1 (waste-activated sludge/alum sludge; v/v). The use of the alum sludge has been shown to beneficially enhance the dewaterability of the resultant mixed sludge, by decreasing both the specific resistance to filtration (SRF) and the capillary suction time (CST). Moreover, the optimal polymer (Sueprfloc-492HMW) dose for the mixed sludge (mix ratio 1:1) was 200 mg/l, highlighting a huge savings (14 times) in polymer addition. In addition, cost-effective analysis of process capabilities, sludge transport, increased cake disposal, additional administration of its potential full-scale application has demonstrated that the initial investment could be returned in 11 years. The co-conditioning and dewatering strategy can be viewed as a sustainable solution for Graulhet water industry development.

### 5.1 Introduction

Rapid expansion of urban areas and industrial development are often associated with substantial water demand that require intensive treatment of both water and wastewater. Large amount of sludges as inevitable by-product along with the water/wastewater purification process were generated worldwide, as shown in the Figure 0.1 (in the general introduction Chapter) [1]. Moreover, the wastewater sludge has the highly hydrophilic nature of extracellular polymeric substances (EPSs), which bind a large amount of water molecules to solid surfaces and trap the water within sludge flocs, forming a high compressibility of sludge matrix [2]. Thus, sludge dewatering as the vital step to reduce the sludge volume has been regarded as the most expensive and least understood process [3,4]. Accordingly, efficient sludge conditioning prior to mechanical dewatering is required. Various studies have been done to enhance sludge dewatering, such as: 1). the magnetic field pretreatment combined with cationic polyacrylamide

additive on waste-activated sludge dewatering [5]; 2). polyaluminum chloride (PACl) co-conditioning with two linear polyelectrolytes on the dewatering and drying performances of urban residual sludge [6]; 3). the combination of ultrasound-cationic polyacrylamide-rice husk on sludge conditioning [2]; and 4). the combined coagulation–flocculation process using PACl and a biopolymer harvested from anaerobically digested swine wastewater for sludge dewatering [7]. Wei et al. (2018) [8] has reviewed the updated process of coagulation/flocculation and their combinations with other pretreatments with massive information on this area. Nevertheless, practical operation indicates that the dewatering performance for waste activated sludge is still relatively poor [9]. In particular, the requirements of the extra energy as well as the highly complicated and multilevel structural features among these reported approaches seem to hinder their performance in sludge dewatering in wastewater treatment plants.

Alum sludge either in liquid phase or in solid phase (after dewatering), which can be easily obtained from the local waterworks [10]. As it has been discussed in Chapter 1, historically, it was discharged to a natural water body as a favorable and less cost manner. However, regulations implemented in many countries have now made these routes forbidden or less attractive due to the adverse environmental impacts [11]. Up to now, alum sludge is mechanically dewatered as cakes to significantly reduce its volume for final disposal in most of the places in the world. Landfilling has indeed been the most widely applied method in many countries [12]. Nowadays, converting the alum sludge as a useful material, rather than a waste for landfill has drawn international attention and beneficial reuse of the alum sludge becomes an overwhelming superiority in scientist and engineers especially in recent years [13, 14, 15]. Although the four major routes which include eleven possible ways of reusing alum sludge, such as the use in wastewater treatment process, use as building/construction materials, land-based application and recovery of the coagulant as illustrated in Figure 0.3 (in the general introduction Chapter) [15], had been developed and recognized, in fact, only few studies investigated alum sludge co-conditioning and dewatering with sewage sludge to improve the sewage sludge dewaterability. For example, Lai and Liu [16] indicated that alum sludge may act as a skeleton builder in the mixed sludge and thus has a beneficial effect in the dewatering process. Yang et al. [17,18] reported the studies of co-conditioning and dewatering of alum sludge with anaerobic digested activated sludge from a municipal WWTP in Ireland to examine the role of alum sludge in improving the wastewater sludge dewaterability. Their results had demonstrated that anaerobic digested sludge mixed with alum sludge in the optimal ratio of 2:1 on volume basis could improve the dewaterability of the resultant sludge, and more significantly it could cause about 99 % reduction in phosphorus loading in the reject water. In addition, the optimal polymer (Superfloc C2260) dosage required to for conditioning was also reduced to 15 mg/L (co-conditioning with alum sludge) from 120 mg/L (anaerobic digested sludge conditioning), thus providing a huge saving in polymer addition. However, considering the application of co-conditioning in practice, sludge transport of the haul distance (50 km away) between water treatment plant and WWTPs in Dublin, Ireland, made the benefits of co-conditioning and related economics became impossible and unrealistic.

In contrast, the WWTP of Graulhet, France, is uniquely located in 3 km away from the water treatment plant. Co-conditioning of the sludges generated from these two plants seems very realistic. The Graulhet WWTP employed the conventional biological treatment process with the capacity of 11000 m<sup>3</sup>/d, while the water treatment plant produced 2200 m<sup>3</sup> drinking water per day. More significantly, these two plants are operated by the same company (Régie Municipale de l'Eaux et de l'Assainissement de Graulhet). It gives the excellent opportunity of co-conditioning the sewerage sludge with alum sludge in order to achieve the sustainable development regarding sludge management of using “waste”, i.e. alum sludge, for sewage sludge treatment, i.e. used as “conditioner”. Therefore, a scientific investigation was needed to promote its application. This study was a technical study to examine the feasibility of co-conditioning sewerage sludge with liquid alum sludge in Graulhet, France. It is expected that this study forms the main technical issues of the co-conditioning and thus forms the basis of further investigation towards co-conditioning and dewatering of sewage sludge with alum sludge practice in Graulhet, France.

## 5.2 Materials and Methods

### 5.2.1 Materials

As illustrated in Figure 5.1. Liquid alum sludge with moisture content of 99.43 % was taken from the settlement tank of the treatment plant, located upstream of Graulhet right bank, where aluminum sulphate is used as coagulant for treating river water. The sewerage sludge (or excess/waste-activated sludge) with average water content of 96.46 % was taken from the bottom of secondary clarifier of Graulhet WWTP. Currently, the Graulhet WWTP used a cationic polymer Sueprfloc-492HMW (Kemira, Finland) for sludge condition before mechanical dewatering using belt press filter. Polymer Sueprfloc-492HMW was then collected from the sludge conditioning unit of the Graulhet WWTP.

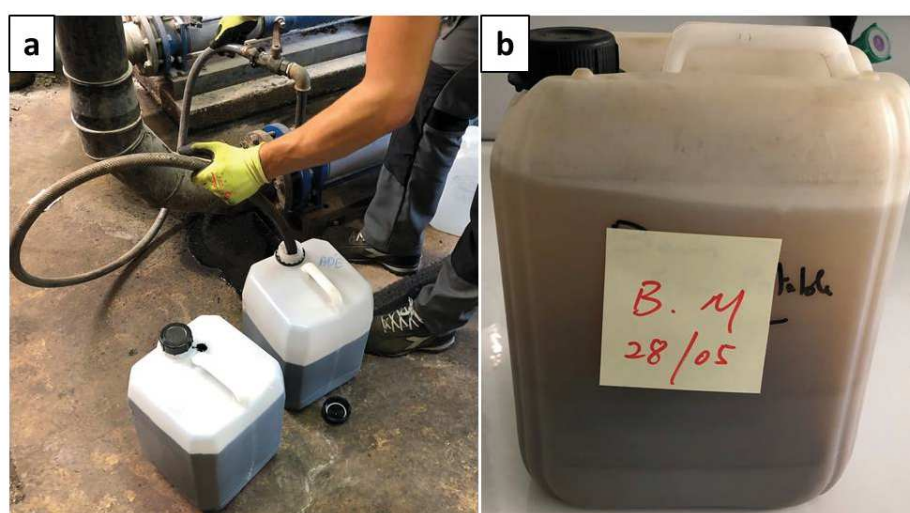


**Figure 5.1** Sludge sampling. (a) sewerage sludge taken from the bottom of secondary clarifier of Graulhet WWTP; (b) liquid alum sludge taken from the settlement tank of the treatment plant



### 5.2.2 Co-conditioning procedure

The conditioning tests were performed at room temperature using a four paddles standard jar-stirring apparatus as shown in Figure 5.2, where sludge samples of 600 mL in 1000 mL beakers were used in the experiments. Alum sludge and waste-activated sludge (the sludge which was taken from the bottom of secondary clarifier of WWTP) were mixed at different volume ratios of 2:1, 1:1, 1:2, 1:3, 1:4, respectively, for a series of jar tests to optimize the mixing ratio. The optimized mixing ratio (1:1, alum sludge:waste-activated sludge) was determined by the lowest phosphate concentration in the supernatant with the least amount of alum sludge addition.

Thereafter, the dosage range based on previous study [17, 18] (from 10-400mg/l, 10, 50 to 400 mg/l, at increments of 50 mg/l) of polymer Sueprfloc-492HMW was added as chemical conditioner to the optimized mixing ratio sludge to examine and achieve the optimal dosage of polymer. This procedure was also performed using the jar-stirring apparatus, where the sludge and various polymer doses were fast mixing at 200 rpm for 30 seconds, and then slowly mixing at 60 rpm for 300 seconds. In the end, the dewaterability of the resultant sludge was evaluated using capillary suction time (CST) and specific resistance to filtration (SRF).

CST (s) is a measure of the readiness with which a sludge sample “release” its water [17]. The sample is placed in a reservoir above a sheet of chromatography paper, and the time taken for the liquid to be drawn a certain radial distance by capillary action is measured. Much of the appeal of the method lies in its speed, simplicity, and need for only small volumes [16].

SRF (m/kg) is a kinetic parameter of a unit mass of sludge per unit area of filter, which could be obtained from the following Eqs. [17]:

$$\text{SRF} = \frac{\Delta P}{\phi_0 \rho_s \eta_L v} \frac{dt}{dv} \quad (5.1)$$

Where,  $\Delta P$  is the applied pressure,  $\phi_0$  is the bulk or initial porosity,  $\rho_s$  is the density of sludge,  $v$  is the specific filtrate volume (volume per unit superficial cross-sectional flow area) and  $\eta_L$  is the liquid viscosity.

Further, the adjustment to the SRF measurement with the intention of removing of filter-pore blocking, which occurs at high excess polymer doses [2, 3, 16]. The methods can be described as the following Eqs.:

$$\frac{dv}{dt} = \frac{\Delta P}{\eta_L (\alpha_m C v + r_m)} \quad (5.2)$$

Where,  $C$  is the mass of dry solids per volume of filtrate,  $r_m$  is a resistance due to the membrane (and drainage system),  $\alpha_m$  is the cake specific resistance, based upon mass of solids in cake (per unit area).



Figure 5.2 Jar-test apparatus

### 5.2.3 Characterization and analyses

To examine the elements in the solids phase and supernatant of the sludge, a laboratory-model centrifuge (Sigma 2K15, Germany) was operated at 8000 r/min to separate the sludge. The solids were then washed with distilled water three times. Thereafter, the solid was dried at 105 °C in an oven for 24 hours. The element content was tested by inductively coupled plasma-atomic emission spectroscopy (ICP-AES), and the elemental analyzer of CHNS (Thermoquest NA2100). Scanning electron microscopy (SEM) was associated with a Philips XL30 ESEM apparatus (FEI Company) which was coupled with an energy-dispersive X-ray spectroscopy (EDX analysis) was used to observe the sludge samples before and after dewatering.

The dewaterability of the sludge before and after co-conditioning was evaluated using the CST apparatus and SRF facility, as illustrated in Chapter 2 Figure 2.16. A Triton CST apparatus (Triton WPRL, Type 130) with a CST paper of size 7×9 cm was used for the CST measurement, while a Buchner funnel with a Whatman No. 1 qualitative filter paper (11 μm particle retention, 10 cm diameter) and equipped with a 70 mbar vacuum suction was used for the SRF test and measurement.

## 5.3 Results and discussion

### 5.3.1 Characterization of the two kinds of sludges

Table 5.1 presents the element composition of the solid and supernatant of two kinds of sludges. It shows that Al was the dominate element in solid phase of the alum sludge apart from silicon. Majority of elements were in the solid phase. However, Fe was the most abundant element observed in the solid phase of sewerage sludge. The majority of phosphate is distributed within the supernatant of sewerage sludge. This is because phosphorus can be released when bacteria containing stored phosphorus (i.e., phosphate-accumulating organisms, PAOs) were subjected to anaerobic conditions, which include thickening and/or anaerobic

digestion, leading to a phosphorus-enriched supernatant and filtrate obtained from mechanical dewatering of the sludge, this result was in agreement with [17].

**Table 5.1** The sludge element composition in the solid phase and the supernatant

Elements	Alum sludge	Sewerage sludge	Alum sludge	Sewerage sludge
	solid (mg/kg)	solid (mg/kg)	supernatant (mg/l)	supernatant (mg/l)
Al	7002	4915	/	/
Ca	1825	4818	11	70
Fe	1082	28853	/	58
K	1751	/	1	56
Mg	/	/	2	12
Mn	1977	/	/	/
Na	1541	/	4	349
P	/	2520	/	6
S	1194	6992	3	4
Si	134041	7108	/	4
<b>Total</b>	<b>150413</b>	<b>55206</b>	<b>21</b>	<b>548</b>

The element percentage of CHNS of the two kinds of sludges is shown in Table 5.2. Regarding the solid phase of the alum sludge, each of the carbon, nitrogen, sulphur and hydrogen only accounts less than 10 %. However, in the solid sewerage sludge, carbon is the overwhelming element compared with the other three elements, even there is very little percentage of sulphur in the sewerage sludge, which agreed with [19, 20]

**Table 5.2** CHNS of alum sludge and sewerage sludge (%)

Element (%)	C	H	N	S
Alum sludge	8	2	1	0
Sewerage sludge	40	8	7	0.5

From the SEM-EDX, as shown in Figure 5.3, the solid phase texture of the alum and sewerage as well as the complex composition of both sludges were presented. Regarding the result obtained from EDX analysis, Si was the most abundant element observed on point 1 and 2 of alum sludge, the point 1 of alum sludge contain more elements such as Fe, Mg and P compare with point 2. In Figure 5.3b, elements such as Na, Cl, Cr, etc. were identified in addition to the once reported in Table 5.1. This morphology indicated that alum sludge could be used as the physical conditioners or skeleton builders during the conditioning process with its unique structure [21,9].

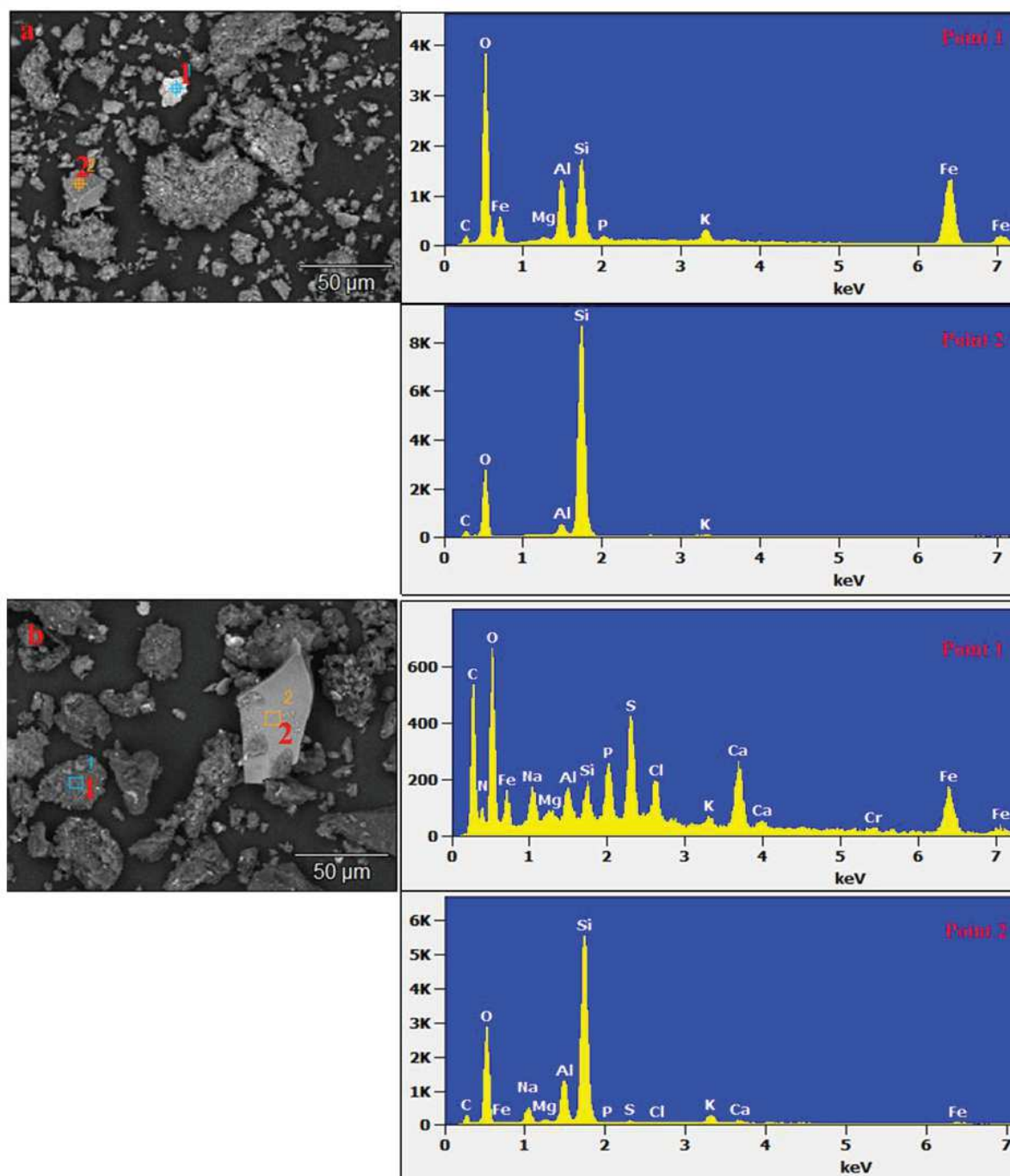
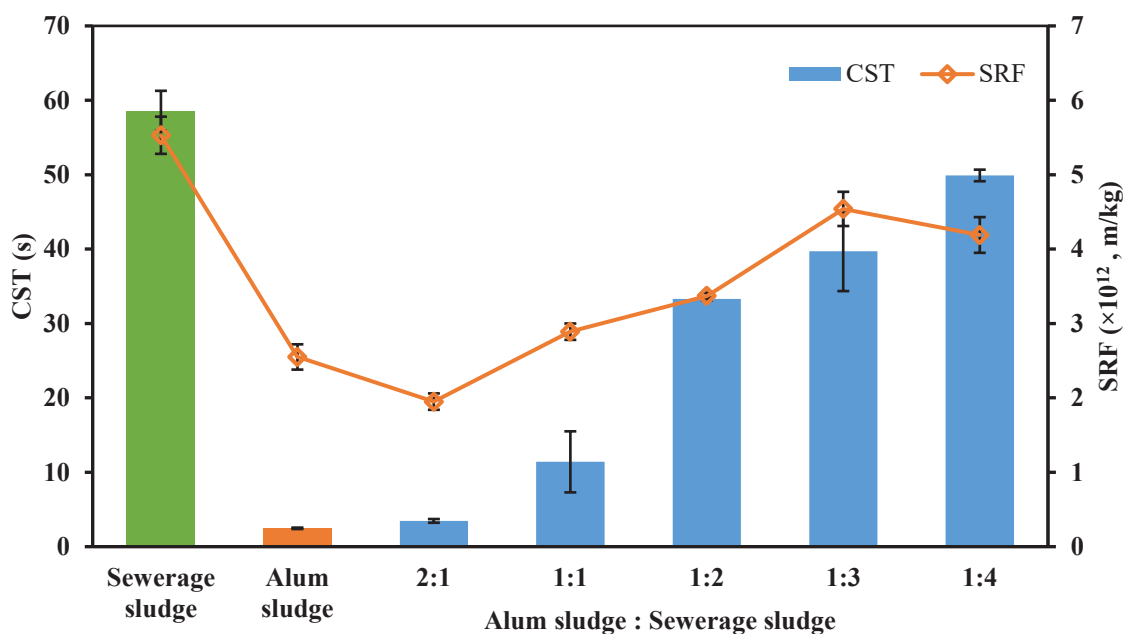


Figure 5.3 SEM-EDX of (a) alum sludge and (b) sewerage sludge

### 5.3.2 Optimal mixing ratio of the sludges

As illustrated in Figure 5.4, the CST and SRF of the sewerage sludge is 59 seconds and  $5.5 \times 10^{12}$  m/kg, respectively, the dewaterability of the sewerage sludge can be characterized as poor (compare with alum sludge). In contrast, the alum sludge presents the good dewaterability with 3 seconds of CST and  $2.5 \times 10^{12}$  m/kg of SRF, respectively. To examine the effect of the amount of alum sludge addition on both the sewerage sludge dewaterability and the phosphorus level in the supernatant, different ratios (alum sludge/sewerage sludge, v/v) of the two sludges were mixed, and the resultant sludge dewatering characteristics and the supernatant phosphorus

concentration of the mixed sludge were measured. The results are shown in Figure 5.4 and Table 5.3.



**Figure 5.4** CST & SRF of two kinds of raw sludges and the mixed sludges

It can be seen from Figure 5.4 that the addition of the alum sludge can improve the dewaterability of the sewerage sludge. Improved dewaterability can be obtained with an increasing amount of alum sludge addition. The SRF of the sewerage sludge was decreased from  $5.5 \times 10^{12}$  to  $1.9 \times 10^{12}$  m/kg, and the corresponding CST was reduced from 58.6 to 3.5 seconds, while the mix ratio was changed from 0:1 (sewerage sludge only) to 1:4. This was attributed to a large portion of insoluble aluminum hydroxides in the alum sludge acting as a coagulant in chemical coagulation/flocculation by particle-particle bridging and surface charge neutralization mechanisms [22, 23]. Many researchers reported the similar results about using alum sludge as a chemical coagulant. For example, Nair et al. [24] examined the alum sludge as a coagulant for the post-treatment of up-flow anaerobic sludge blanket (UASB) reactor treating urban wastewater. Foroughi et al. [25] reported turbidity removal in drinking water treatment using alum sludge as a coagulant agent. Mazari et al. [11] investigated the potential reuse of alum sludge as primary coagulant in terms of membrane fouling reduction. Significantly, alum sludge can not only be used as the chemical coagulant but also act as a skeleton builder or filter aids [26], which are effective to reduce the sludge compressibility, and help the sludge cake to form a permeable and rigid structure while maintain the sludge cake porous, even under a high compression pressure, as its physical morphology is rigid could be act as a skeleton.

Table 5.3 shows the different elements concentration, in supernatant of the mixed sludge at different mix ratios. Overall, by increasing the sewerage sludge ratio could result in the relevant elements rising in mixed sludge, such as Al, Fe, Na, etc. However, it can be clearly

seen that the addition of the alum sludge can lead to a significant reduction of phosphorus in the aqueous phase of the mixed sludge since Al owns strong affinity with P [18], and ligand exchange is the dominating adsorption mechanism, which has been discussed in Chapter 1 (see Eqs. 1.1). The initial P concentration in the supernatant of the sewerage sludge is 6 mg/l (see Table 5.1). However, the range of P concentration in the supernatant was 0, 0.4, 1.7, 2.4, 1.8 mg/l at mix ratios of 2:1, 1:1, 1:2, 1:3 and 1:4, respectively (see Table 5.3). By considering the fact that the addition of alum sludge can potentially increase the overall volume of the mixed sludge, which will increase the hydraulic load on the dewatering unit in the WWTP, the optimal mix ratio was chosen as 1:1 for the ensuing sludge conditioning tests using organic polymer as a conditioner.

**Table 5.3** The elements in supernatant under different mix ratio (alum sludge:sewerage sludge)

Elements (mg/l)	2:1	1:1	1:2	1:3	1:4	Variation (2:1 to 1:4)
Al	/	3.7	19.3	15.7	13.9	13.9
Ca	43.7	20.2	35.2	44.0	46.9	3.2
Cr	/	/	0.3	0.3	0.4	0.4
Fe	1.5	1.7	6.5	13.1	14.3	12.8
K	22.5	45.7	95.1	103.0	93.4	70.9
Mg	7.4	4.5	7.4	9.4	9.7	2.3
Mn	3.0	0.3	0.4	0.5	0.4	-2.6
Na	176.5	370.2	614.4	654.0	569.0	392.5
P	/	0.4	1.7	2.4	1.8	1.8
S	3.7	4.2	10.8	10.9	13.8	10.1
Si	2.1	2.0	4.3	4.7	5.0	2.9

### 5.3.3 Polymer conditioning of the mixed sludge

The 1:1 mix ratio was determined as the optimal mixing ratio that ensures the lowest phosphate concentration in the supernatant with the least amount of alum sludge addition. However, as a chemical conditioner, organic polymer has been widely used in sludge treatment practice for significantly improve the sludge dewaterability. It is believed that the addition of polymer in optimal mixed sludge could further improve the sludge dewaterability but with an obviously reduced dosage (compared with the sewerage sludge conditioning). Figure 5.5 shows the dewatering behavior of the mixed sludge (at ratio of 1:1) conditioned by a cationic polyacrylamide Superfloc-492HMW. The results show that the polymer conditioning results in a significant improvement of the mixed sludge dewaterability, as evaluated by the SRF and CST. The values of SRF and CST decreased from  $2.9 \times 10^{12}$  to  $1.4 \times 10^{12}$  m/kg and from 5 to 2 seconds, respectively, with the polymer dosage increased from 10 to 200 mg/L. The optimal polymer dosage for the mixed sludge was determined to be 200 mg/L because a further increase of polymer dosage beyond 200 mg/L did not bring about any further decrease of SRF or CST, as shown in Figure 5.5.



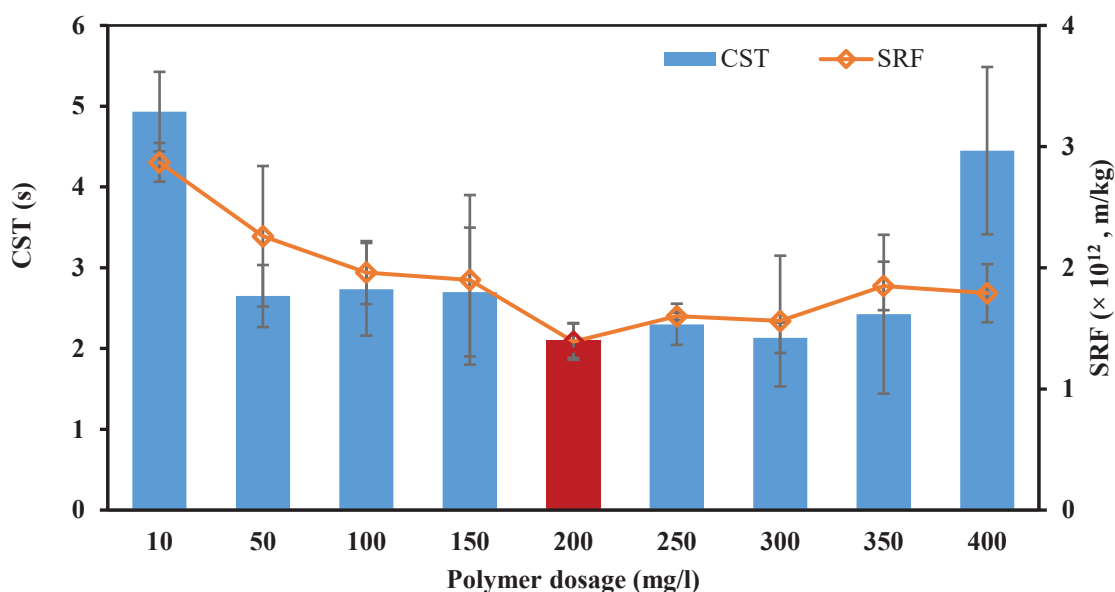


**Figure 5.5** The optimum polymer dosage of at mix ratio 1:1

Thus, it becomes clear that a significant reduction of polymer dosage can be achieved when alum sludge is involved in the sewerage sludge co-conditioning. The optimal polymer (Superfloc-492HMW) dosage was reduced from 2.8 g/L (when the sewerage sludge was conditioned alone) to 200 mg/L (when the sewerage sludge was co-conditioned with alum sludge at mix ratio of 1:1). This results agreed with [16], who claimed a corresponding decrease in the required dosage of a cationic polyelectrolyte when alum sludge was co-conditioned with an activated sludge. They postulated that the alum sludge acted as a skeleton builder, making the mixed sludge more incompressible and rendering the dewatering process more effective.

### 5.3.4 Case analysis

The process illustrated in Figure 5.6 details the proposed integration of the alum sludge in co-conditioning and dewatering with the waste-activated sludge from the Graulhet WWTP. Since the waterworks of Graulhet is just located 3 Km away from the Graulhet WWTP and they are operated by the same company, it is practical to build a drain pipe from the waterworks to the Graulhet WWTP. Considering the sludge production balance in these two sources, the maximum liquid alum sludge generation rate of the water treatment plant is 66 m<sup>3</sup>/d (3 % of the treatment water volume), while the design compacity of sewerage sludge thickening tank in Graulhet WWTP is 400 m<sup>3</sup>. Thus, a steel tank of is needed to store the alum sludge. Table 5.4 summaries the main pipe materials and estimated costs with the pipe manufacturing, tank construction, and electricity needed. The unit prices are based on [27]. The flow velocity of liquid alum sludge in the cement-mortar-lined ductile iron pipe was estimated at 1.0 m/s, thus the diameter of 100 mm pipe could fulfill the requirement. The prices of commercially-available steel tank was based on a France steel supplier. The horizontal multistage centrifugal pump was estimated with 70 m pump head, while the price is from “2016 price list of Salmson Warehouse,

Laval, France”. It can be seen that 418,577 Euro should be invested for the co-conditioning strategy.

**Table 5.4** the main materials and costs of initial investment

Materials	Unit Prices (€)	Specification	Costs (€)	Reference
Cement-mortar-lined ductile iron pipe	50	3000 (m)	150,000	[27]
Commercially-available steel tank	/	450 (m <sup>3</sup> )	265,000	A France steel supplier
Horizontal multistage centrifugal pump	3577	MULTI-H1600	3,577	“2016 price list of Salmson Warehouse, Laval, France”
<b>In Total</b>	-	-	<b>418,577</b>	-

Regarding the co-conditioning process, currently Graulhet WWTP could consume 25 kg polymer per day. However, if the strategy of co-conditioning with liquid alum sludge was applied, the annual polymer saving could be 8473 kg. Currently, the price of polymer (from a local supplier in France) is 5.24 Euro/kg (including tax). It means that the polymer saving equals to 44,399 Euro per year, which accounts for the 93 % of current polymer annual costs. On the other hand, the potential increases of sludge cakes will be from 25,000 kg/d to 25,321 kg/d when liquid alum sludge is introduced. Accordingly, the relevant sludge disposal cost will be arising approximately 7,100 Euro per year. (considering the average sludge disposal fee of 65 Euro/ton [28]).

Although it needs extra capital investment and construction cost of approximately 418,577 Euro in the initial period as well as the extra sludge disposal fee of approximately 7,100 Euro/year, the continuously benefits of the polymer savings of 44,399 Euro/year can be achieved, which means the initial investment and operational expenses could be returned by polymer saving in 11 years. It seems a long time, but compared with the long-term effect for the local “circular economy”, it is a relatively short period. Significantly, the sustainable sludge management route should have priority since the legislation is not allowed the liquid alum sludge from the water treatment plant drainage to the river anymore. In addition, in spite of the increased quantity of the reject water from dewatering unit, the significant reduction of P in reject water could benefit the wastewater treatment process regarding P loading. Overall, from technical point-of-view, the co-conditioning and dewatering strategy is practicable, and the cost-effective analysis also demonstrated that the initial investment fee could be returned.

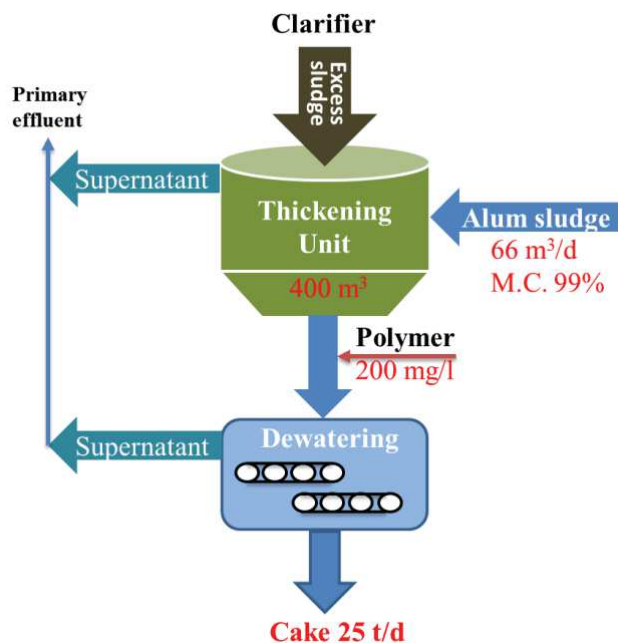


**Figure 5.6** Schematic of a proposed strategy of alum sludge co-conditioning with the waste-activated sludge of Graulhet WWTP

## 5.4 Conclusion

Alum sludge can be successfully used to co-condition with the sewerage sludge. When alum sludge was introduced to co-conditioning and dewatering with waste-activated sludge, the optimal mixing ratio gauged by both the phosphate concentration in the supernatant and the improvement of dewaterability of the resultant sludge is 1:1 (sewerage sludge:alum sludge, v/v). The addition of alum sludge to the waste-activated sludge improved its dewaterability. The optimal polymer (Superfloc-492HMW) dosage for the mixed sludge was 200 mg/l, while the current dosage for the waste-activated sludge in Graulhet WWTP is 2.8 g/l. An integrated cost-effective evaluation of process capabilities, sludge transport, increased cake disposal, additional administration, etc. has proved that the co-conditioning and dewatering strategy is practicable, the initial investment could be returned in 11 years.

## Bibliography

1. Zhao, Y., Liu, R., Awe, O.W., Yang, Y., Shen, C.: Acceptability of land application of alum-based water treatment residuals – An explicit and comprehensive review. *Chemical Engineering Journal* **353**, 717-726 (2018). doi:<https://doi.org/10.1016/j.cej.2018.07.143>
2. Zhu, C., Zhang, P., Wang, H., Ye, J.: Conditioning of sewage sludge via combined ultrasonication-flocculation-skeleton building to improve sludge dewaterability. *Ultrasonics Sonochemistry* **40**, 353-360 (2018). doi:<https://doi.org/10.1016/j.ultsonch.2017.07.028>
3. Chang, G.R., Liu, J.C., Lee, D.J.: Co-conditioning and dewatering of chemical sludge and waste activated sludge. *Water Research* **35**(3), 786-794 (2001). doi:10.1016/s0043-

1354(00)00326-2

4. Xiong, Q., Zhou, M., Yang, H., Liu, M., Wang, T., Dong, Y., Hou, H.: Improving the Dewaterability of Sewage Sludge Using Rice Husk and Fe<sup>2+</sup>-Sodium Persulfate Oxidation. *ACS Sustainable Chemistry & Engineering* **6**(1), 872-881 (2018). doi:10.1021/acssuschemeng.7b03227
5. Bi, D.S., Guo, X.P., Cai, Z.H., Yu, Z., Wang, D.M., Wang, Y.Q.: Enhanced dewaterability of waste-activated sludge by combined cationic polyacrylamide and magnetic field pretreatment. *Environmental Technology* **36**(4), 455-462 (2015). doi:10.1080/09593330.2014.952341
6. Pambou, Y.B., Fraikin, L., Salmon, T., Crine, M., Leonard, A.: Enhanced sludge dewatering and drying comparison of two linear polyelectrolytes co-conditioning with polyaluminum chloride. *Desalination and Water Treatment* **57**(58), 27989-28006 (2016). doi:10.1080/19443994.2016.1178602
7. Guo, J., Chen, C., Jiang, S., Zhou, Y.: Feasibility and Mechanism of Combined Conditioning with Coagulant and Flocculant To Enhance Sludge Dewatering. *ACS Sustainable Chemistry & Engineering* **6**(8), 10758-10765 (2018). doi:10.1021/acssuschemeng.8b02086
8. Wei, H., Gao, B., Ren, J., Li, A., Yang, H.: Coagulation/flocculation in dewatering of sludge: A review. *Water Research* **143**, 608-631 (2018). doi:<https://doi.org/10.1016/j.watres.2018.07.029>
9. Qi, Y., Thapa, K.B., Hoadley, A.F.A.: Application of filtration aids for improving sludge dewatering properties – A review. *Chemical Engineering Journal* **171**(2), 373-384 (2011). doi:<https://doi.org/10.1016/j.cej.2011.04.060>
10. Wang, Y., Ren, B.M., Zhao, Y.Q., English, A., Cannon, M.: A comparison of alum sludge with peat for aqueous glyphosate removal for maximizing their value for practical use. *Water Science and Technology*, 450-456 (2018). doi:10.2166/wst.2018.165
11. Mazari, L., Abdessemed, D., Szymczyk, A.: Evaluating Reuse of Alum Sludge as Coagulant for Tertiary Wastewater Treatment. *Journal of Environmental Engineering* **144**(12) (2018). doi:10.1061/(asce)ee.1943-7870.0001462
12. Yang, Y., Zhao, Y.Q., Liu, R.B., Morgan, D.: Global development of various emerged substrates utilized in constructed wetlands. *Bioresource Technology* **261**, 441-452 (2018). doi:10.1016/j.biortech.2018.03.085
13. Ren, B., Zhao, Y., Lyczko, N., Nzihou, A.: Current Status and Outlook of Odor Removal Technologies in Wastewater Treatment Plant. *Waste and Biomass Valorization* (2018). doi:10.1007/s12649-018-0384-9
14. Odimegwu, T.C., Zakaria, I., Abood, M.M., Nketsiah, C.B.K., Ahmad, M.: Review on Different Beneficial Ways of Applying Alum Sludge in a Sustainable Disposal Manner. *Civ. Eng, J.-Tehran* **4**(9), 2230-2241 (2018). doi:10.28991/cej-03091153
15. Ahmad, T., Ahmad, K., Alam, M.: Sustainable management of water treatment sludge through 3'R' concept. *J. Clean Prod.* **124**(Supplement C), 1-13 (2016). doi:<https://doi.org/10.1016/j.jclepro.2016.02.073>
16. Lai, J.Y., Liu, J.C.: Co-conditioning and dewatering of alum sludge and waste activated sludge. *Water Science and Technology* **50**(9), 41-48 (2004).

17. Yang, Y., Zhao, Y.Q., Babatunde, A.O., Kearney, P.: Co-conditioning of the anaerobic digested sludge of a municipal wastewater treatment plant with alum sludge: Benefit of phosphorus reduction in reject water. *Water Environment Research* **79**(13), 2468-2476 (2007). doi:10.2175/106143007x184753
18. Yang, Y., Zhao, Y.Q., Babatunde, A.O., Kearney, P.: Two strategies for phosphorus removal from reject water of municipal wastewater treatment plant using alum sludge. *Water Science and Technology* **60**(12), 3181-3188 (2009). doi:10.2166/wst.2009.609
19. Gutiérrez Ortiz, F.J., Aguilera, P.G., Ollero, P.: Biogas desulfurization by adsorption on thermally treated sewage-sludge. *Separation and Purification Technology* **123**, 200-213 (2014). doi:<https://doi.org/10.1016/j.seppur.2013.12.025>
20. Gutiérrez Ortiz, F.J., Aguilera, P.G., Ollero, P.: Modeling and simulation of the adsorption of biogas hydrogen sulfide on treated sewage–sludge. *Chemical Engineering Journal* **253**, 305-315 (2014). doi:<https://doi.org/10.1016/j.cej.2014.04.114>
21. Qi, Y., Thapa, K.B., Hoadley, A.F.A.: Benefit of lignite as a filter aid for dewatering of digested sewage sludge demonstrated in pilot scale trials. *Chemical Engineering Journal* **166**(2), 504-510 (2011). doi:<https://doi.org/10.1016/j.cej.2010.11.003>
22. Chu, W.: Dye Removal from Textile Dye Wastewater Using Recycled Alum Sludge. *Water Research* **35**(13), 3147-3152 (2001). doi:[https://doi.org/10.1016/S0043-1354\(01\)00015-X](https://doi.org/10.1016/S0043-1354(01)00015-X)
23. Basibuyuk, M., Kalat, D.G.: The use of waterworks sludge for the treatment of vegetable oil refinery industry wastewater. *Environmental Technology* **25**(3), 373-380 (2004). doi:10.1080/09593330409355471
24. Nair, A.T., Ahammed, M.M.: The reuse of water treatment sludge as a coagulant for post-treatment of UASB reactor treating urban wastewater. *J. Clean Prod.* **96**, 272-281 (2015). doi:<https://doi.org/10.1016/j.jclepro.2013.12.037>
25. Foroughi, M., Chavoshi, S., Bagheri, M., Yetilmesoy, K., Samadi, M.T.: Alum-based sludge (AbS) recycling for turbidity removal in drinking water treatment: an insight into statistical, technical, and health-related standpoints. *Journal of Material Cycles and Waste Management* **20**(4), 1999-2017 (2018). doi:10.1007/s10163-018-0746-1
26. Li, J., Liu, L., Liu, J., Ma, T., Yan, A., Ni, Y.: Effect of adding alum sludge from water treatment plant on sewage sludge dewatering. *Journal of Environmental Chemical Engineering* **4**(1), 746-752 (2016). doi:10.1016/j.jece.2015.07.021
27. Herstein, L.M., Filion, Y.R.: Life-cycle assessment of common water main materials in water distribution networks. *J. Hydroinform.* **13**(3), 346-357 (2011). doi:10.2166/hydro.2010.127
28. Zhao, Y., Ren, B., O'Brien, A., O'Toole, S.: Using alum sludge for clay brick: an Irish investigation. *International Journal of Environmental Studies* **73**(5), 719-730 (2016). doi:10.1080/00207233.2016.1160651

## Chapter 6

# Alum Sludge as An Efficient Sorbent for Hydrogen Sulfide Removal

This Chapter has been submitted an international peer-reviewed journal as: **Baiming Ren**, Nathalie Lyczko, Yaqian Zhao, Ange Nzihou. *Alum sludge as an efficient sorbent for hydrogen sulfide removal: experimental, mechanisms & modeling studies*.

### Abstract

This Chapter presented a systematic study of using alum sludge for H<sub>2</sub>S adsorption. Various trials were performed at ambient temperature in a fixed bed column to study the effect of the flow rate, bed depth on the adsorption efficiency. The dynamics of the breakthrough curve was simulated by three adsorption models namely, Thomas, Bed Depth Service Time and Yoon-Nelson model. The mechanisms of H<sub>2</sub>S adsorption onto alum sludge was examined by different physiochemical characterizations of exhausted and raw alum sludge. Moreover, several (external, overall, etc.) mass transfer coefficients were determined from mathematical description of breakthrough curves. It can be concluded that the adsorption capacity of alum sludge is 374.2 mg of H<sub>2</sub>S/g of alum sludge, it slightly decreased with the increasing flow rate and significant increased with the increasing bed depth. All the three models were successfully predicted breakthrough curves which could be used for scaling up purpose. The microporous structure, alkaline pH, the inherent metal species of alum sludge promoted the formation of metal sulfide and metal sulfate species, etc. At last, the overall mass transfer coefficients were obtained. This study demonstrated that alum sludge could be used as cost-effective, largely available, and efficient sorbent for desulfurization.

### 6.1 Introduction

There is generally increasing public concern and intolerance of odors and other air contaminants from wastewater facilities. Management of air/odor emissions has become a significant activity in wastewater treatment plants (WWTP). Furthermore, national and local regulations in U.S., Europe and China require a number of air pollutants be controlled [1]. Hydrogen sulfide (H<sub>2</sub>S), a wide concern in the last decades, is one of several odorous gases from industrial effluents such as WWTP, landfill sites, petrochemical industries etc. [2]. It is a poisonous, flammable, colorless gas with a characteristic odor of rotten eggs. The average odor threshold of H<sub>2</sub>S is reported to be 7 to 9 part per billion (ppb) [3].

It has been comprehensively reviewed in Chapter 1, treatment technologies of H<sub>2</sub>S in wastewater treatment plant include physical/chemical (such as adsorption, chemical scrubbing)



and biological methods (biofiltration, biotrickling, activated sludge diffusion etc.) [4]. Adsorption in particular, a process based on the transfer of odorants from the gas to a solid phase, has been broadly implemented. It is one of the most suitable methods for the removal of H<sub>2</sub>S from a gas stream, as it allows a deep purification (down to H<sub>2</sub>S concentration less than 1 ppmv) and a cost-effective approach [5]. For instance, in recent studies, Singh et al. [6] use zinc oxide-decorated multi-wall carbon nanotubes (ZnO-MWCNTs), which was synthesis by the carbon nanotube and zinc oxide, for a high values (98 %) of H<sub>2</sub>S removal in a bench-scale fixed bed reactor at the ambient temperature and atmospheric; Sánchez-González et al. [7] investigated Mg- based metal–organic frameworks (MOFs) as a highly reversible sorbent showed by the sequestration performance upon multiple cycles of adsorption and desorption for H<sub>2</sub>S removal. The dynamic adsorption experiments were performed at 303 K using a tubular quartz adsorber filled with Mg-MOF, results show that the H<sub>2</sub>S adsorption capacity of Mg-MOF was 3.1 mmol H<sub>2</sub>S/g, under the 15 vol % H<sub>2</sub>S feed concentration. Hervy et al. [8] reported the H<sub>2</sub>S removal by chars obtained from pyrolysis of wastes under ambient temperature in various dry gas matrices (N<sub>2</sub>, Air, Syngas). It concluded that the most efficient material was the steam activated char from food waste and coagulation-flocculation sludge, with a removal capacity of 65 mg H<sub>2</sub>S/g under dry syngas.

Earlier, several materials have been reported as sorbents for H<sub>2</sub>S removal which include fly ash, activated carbon, polymers, carbon-coated polymers, ceramics, and synthetic zeolites etc. The H<sub>2</sub>S removal efficiency of those materials was range from 8.63 to 210 mg H<sub>2</sub>S/g [9-11]. Most of the studies dealing with gas desulfurization at room temperature using activated carbon were focused on H<sub>2</sub>S removal from moist air, the removal efficiency is over 90 %. In the presence of oxygen and humidity, the interactions between H<sub>2</sub>S and the complex surface properties of the materials (O-containing groups, mineral species, pH) lead to several retention mechanisms including dissociative adsorption and oxidation [8]. However, the removal capacity of H<sub>2</sub>S by adsorptive materials depends on physicochemical properties (such as elemental composition, pore structure, surface O-containing groups, mineral species, pH, etc.) of the materials and varies with experimental conditions (temperature, water and/or oxygen, etc.) [2]. Indeed, adsorption has the common shortcoming including material cost and the complexity of the sorbents' preparation. Therefore, direct utilization of low-cost raw materials from industrial by-product for H<sub>2</sub>S removal has attracted intensive research interests.

As presented in Chapter 2, alum sludge is an inescapable by-product during drinking water processing in waterworks where aluminum salt was used as the coagulant for purifying raw water [12]. It is a locally, easily and largely available material in towns, cities and metropolis and free of charge for the moment. Unfortunately, it is treated as a “waste” for landfilling in most of the places in the world. Therefore, identifying novel sustainable reusing methods of alum sludge can provide significant social and environmental benefits. Actually, alum sludge has been intensively studied as a low-cost sorbent for phosphorous and other pollutants immobilization [13-15] and has been advocated to be a valuable recyclable product, offering promising potential for a number of pollutants immobilization with unique feature of using “waste” for waste treatment [16,17]. However, to the best of our knowledge, none of the studies

ever chose alum sludge in gas purification of H<sub>2</sub>S even it has been intensively studied and demonstrated to be a good material for impurities adsorption in wastewater treatment, i.e. pollutants in aquatic phase [18-20].

Furthermore, a continuous fixed-bed column does not run under equilibrium conditions, so the flow conditions and mass-transfer aspects throughout the column affect the performance [21,22]. The dynamic behavior of a fixed bed column is described in terms of the effluent concentration-time profile (the breakthrough curve), which is essential in the evaluation of the efficacy of a material. The shape of the breakthrough curve, which is also affected by both inter- and intra-particle transfer phenomena in the column and sorbent [23]. Therefore, accurate measurement of the breakthrough curves and mass transfer phenomena are fundamental.

Accordingly, this Chapter systematically reported the experimental, adsorption behavior modeling and mechanisms of using alum sludge for H<sub>2</sub>S adsorption in a fixed-bed column at room temperature. The effects of reaction/adsorption conditions were trialed while three modeling approaches (Thomas, Bed Depth Services Time, Yoon-Nelson model) were examined and compared. Moreover, the mass transfer coefficient was determined, which could be used to design and evaluate the alum sludge column on a larger scale. This work intends to pave a novel reusing route of alum sludge as H<sub>2</sub>S abatement media.

## 6.2 Materials and Methods

### 6.2.1 Sorbent and Characterization

Dewatered raw alum sludge cakes taken from a sludge dewatering unit of Carmaux drinking water treatment plant located in Tarn, France, were used as sorbent in this study. The plant produces and supplies 3014 m<sup>3</sup>/day of drinking water by treating the water using aluminum sulfate as coagulant. After collection, the sludge was dried, mechanically ground by a blender and sieved with 250 μm mesh as sorbent and characterized. Moisture content of alum sludge cake was carried out by drying the raw alum sludge cake in the oven at 105 °C for 24h and measuring the mass differences before and after drying.

Different physicochemical techniques were used for analyzing sorbents before and after the test of H<sub>2</sub>S removal. The pH of the alum sludge before and after the H<sub>2</sub>S removal tests was measured by adding 0.5 g of alum sludge to 20 ml of distilled water. The suspension was stirred at least 24 h before measuring the pH of the suspension. Particle size distribution was determined by a laser particle sizer MALVERN Laser Mastersizer Hydro 2000 at size interval of 0.01-1000μm by wet analysis. Inductively coupled plasma atomic emission spectroscopy (ICP-AES) was performed identify and quantify the elemental composition of the sorbent using a HORIBA Jobin–Yvon Ultima 2. Before the analysis by ICP, mineralization was carried out by the dissolution of alum sludge particles by adding a mixture of hydrogen fluoride (HF), hydrogen peroxide (H<sub>2</sub>O<sub>2</sub>) and nitric acid (HNO<sub>3</sub>) (aqua regia) with a volume ratio of 1:1:1 (2.5ml of each). The dissolution of particles was done on SCP DigiPREP Jr mineralization

device by heating samples on heating block (coated graphite Teflon<sup>®</sup>) at temperature of 220°C for 48 hours. Scanning electron microscopy (SEM-EDX) was carried out to observe the morphology of the sorbents as well as to identify the various elements on the sorbent surface, by applying Philips XL30 ESEM apparatus (FEI Company) which was coupled with an energy-dispersive X-ray spectroscopy (EDX analysis). The transmission electron microscopy (TEM) was carried out on the JEOL JEM-ARM200F and the elemental mapping of chemical specials in the sample was performed by using an EDX module in the same microscope. Specific surface area and pore structure were determined by BET method using a Micromeritics Gemini Vacprep 061. A sample mass of about 300 mg was introduced into a tube and degassing is carried out for 6 hours at 105°C under vacuum. The sample is subjected to five different pressures of nitrogen at the temperature of liquid nitrogen. The adsorption isotherm is identified by the nitrogen pressure, which allows deducing the volume of adsorbed gas from the gas pressure  $P$  and its saturated vapor pressure  $P_0$  and so deducing the specific surface  $m^2/g$ . The pore structure of alum sludge was determined by nitrogen adsorption at 77K using a Micromeritics 3Flex high-resolution analyzer.

Thermogravimetric analysis device (ATG STA409PC, Netzsch) coupled with a mass spectrometer (OMNISTAR, Pfeiffer) were used to study the decomposition temperature of the different sulfur compounds, with the following settings: heating rate of 20 °C/min up to 800 °C with a nitrogen flow rate of 3 L/h. For each measurement, a sample of 200-300 mg of alum sludge was analyzed. The derivative thermogravimetric (DTG) curves were used for data analysis. The temperatures at which the mass losses were observed, and the composition of the gas produced provided information on the nature of the sulfur compounds.

### 6.2.2 Sorption Test

The tests of H<sub>2</sub>S removal were carried out at room temperature ( $\pm 20$  °C) and atmospheric pressure using a glass fixed-bed column. Fixed bed column fits well with adsorption test as it can be easily scaled up from a laboratory to an industrial application [24]. Figure 6.1 shows the photo from the experimental setup and the scheme of the system used. The column (length 60 mm, internal diameter  $D=11$  mm) was equipped with a porous glass disc at the bottom which could hold the sorbent and allow H<sub>2</sub>S gas passing through. The height of sorbent layer varied from about 5 to 11 mm, corresponding to the apparent density and the amount of sorbent used for each experiment (0.5 to 1.0 g). A synthetic gas containing 200 ppmv of H<sub>2</sub>S (based on dry air) passed through the sorbent layer with different flow rates of 3, 4, 5 L/h, respectively, was controlled by a flow meter. The output H<sub>2</sub>S concentration was monitored every two minutes using a gas analyzer from BW Technologies (Gas Alert QUATTRO). The effluent gas was treated by CaO solution before it was released to the atmosphere. Sorption experiments were stopped when the H<sub>2</sub>S sorption rate significantly decreased. In this paper, the following terms are used in order to compare the different experimental conditions:

- H<sub>2</sub>S<sub>input</sub> (mg): the total accumulated quantity of H<sub>2</sub>S introduced to the bed at a given reaction time.

- Accumulated<sub>sorbent</sub> (mg): the total accumulated quantity of H<sub>2</sub>S on the sorbent at a given reaction time.

The amount of H<sub>2</sub>S<sub>input</sub> and Accumulated<sub>sorbent</sub> was calculated with the Eqs. (6.1) and (6.2), respectively:

$$H_2S_{input} = \frac{PQM}{10^6 RT} C_0 t \quad (6.1)$$

$$Accumulated_{sorbent} = \frac{PQM}{10^6 RT} [C_0 t - \int_0^t C_t dt] \quad (6.2)$$

Where, P is the pressure of gas (1 atm), Q is the inlet flow rate (L min<sup>-1</sup>), M is the molecular weight of H<sub>2</sub>S (34.06 g mol<sup>-1</sup>), W is the mass of sorbent used (g), C<sub>0</sub> is the inlet concentration of H<sub>2</sub>S (200 ppmv), C<sub>t</sub> is the outlet concentration of H<sub>2</sub>S (ppmv), t is the reaction time (min), R is the ideal gas constant (8.31 J/mol·K), T is the temperature (K).

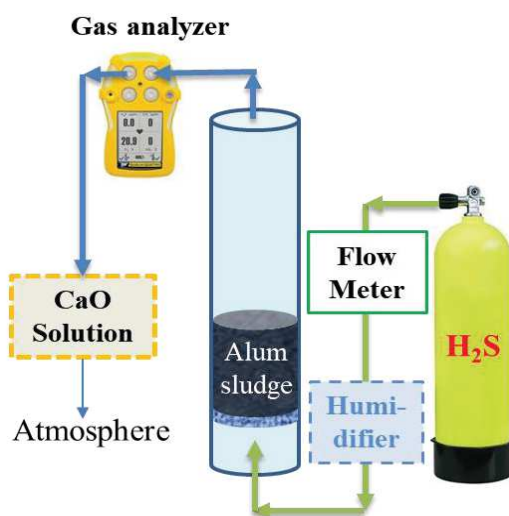


Figure 6.1 Photo and scheme of the fixed-bed adsorption column.

### 6.2.3 Modeling

Mathematical models are useful to describe and predict the behavior of fixed-bed reactors and help to optimize as well as to design the system. The most commonly used three models to describe the experiment data in breakthrough curves were the Thomas, Bed Depth Service Time, and Yoon-Nelson model, which were applied in this study [22,24,25].

#### ➤ The Thomas model

The Thomas model [26] is one of the most general and widely used models. It is applied to evaluate adsorption capacity of sorbent in fixed bed column, which is very important in designing adsorption column in practical application. The model was based on the hypothesis that: (i) the process follows Langmuir isotherms and second-order kinetics of sorption–desorption with no axial dispersion; (ii) the adsorption is not limited by the chemical reaction, but controlled by the mass transfer at the interface. The linearized form of the model is given as:

$$\ln\left(\frac{C_0}{C_t} - 1\right) = \frac{K_{Th}q_0m}{F} - K_{Th}C_0t \quad (6.3)$$

Where,  $K_{Th}$  is the Thomas rate constant ( $L\ mg^{-1}\ min^{-1}$ ),  $q_0$  is the maximum adsorption capacity ( $mg\ g^{-1}$ ),  $m$  is the mass of sorbent in the column ( $g$ ).  $F$  is the Volumetric flow rate ( $L\ min^{-1}$ ). The kinetic coefficient  $K_{Th}$  and the adsorption capacity of the sorbent  $q_0$  can be determined from a plot of  $\ln[(C_0/C_t)-1]$  against  $t$  at a given flow rate.

#### ➤ The Bed Depth Service Time (BDST) model

The BDST model [27], describes a relation between the service time and the packed-bed depth of the column. It mainly focuses on predicting the time taken by the sorbent to remove a specific amount of adsorbate from bulk phase (service time) before exhaustion. This model was derived based on the assumption that the diffusion steps (external and internal) are very fast, and the surface reaction step is rate-controlling. The model has the following form:

$$t = \frac{N_0h}{uC_0} - \frac{1}{Kc_0} \ln\left(\frac{C_0}{C_t} - 1\right) \quad (6.4)$$

Where,  $K$  is the adsorption rate constant ( $L\ mg^{-1}\ min^{-1}$ ),  $N_0$  is the adsorption capacity ( $mg\ L^{-1}$ ),  $h$  is the bed depth ( $cm$ ),  $u$  is the linear flow rate ( $cm\ min^{-1}$ ) and  $t$  is the service time to breakthrough ( $min$ ). Experimental data obtained are used to plot BDST curves and estimate the characteristic parameters  $K$  and  $N_0$  from the slope and intercept of the plots.

#### ➤ The Yoon–Nelson mode

The Yoon-Nelson model [28] is to evaluate a fixed bed adsorption kinetic, which is based on the assumption that the rate of decrease in the probability of adsorption for each adsorbate molecule is proportional to the probability of adsorbate adsorption and the probability of



adsorbate breakthrough on the sorbent. The model provides information about the breakthrough rate in a fixed-bed column and the time entailed to achieve 50 % breakthrough. The linearized model for a single component system is expressed as:

$$\ln \frac{C_t}{C_0 - C_t} = K_{YN}t - \tau K_{YN} \quad (6.5)$$

Where,  $K_{YN}$  is the rate constant ( $\text{min}^{-1}$ ) and  $\tau$  is the time required for 50 % adsorbate breakthrough (min). The calculation of theoretical breakthrough curves for a single-component system requires the determination of the parameters  $K_{YN}$  and  $\tau$  for the adsorbate from the plot of  $\ln[C_t / (C_0 - C_t)]$  versus sampling time (t).

### 6.2.4 Determination of mass transfer coefficient

A lumped overall resistance describes mass transfer, and where the sorbent particle is treated as a homogeneous phase in which diffusion takes place with a constant effective diffusivity; the reaction kinetics is assumed to be much faster than the mass transport [21]. Thus, the mass transfer rate is represented as proportional to the deviation from equilibrium:

$$\frac{\partial q}{\partial t} = K_a(q_e - q) \quad (6.6)$$

where  $K_a$  is the overall effective mass transfer coefficient,  $q_e$  is the value of  $q$  in equilibrium with  $C$ ,  $q$  is the concentration of  $\text{H}_2\text{S}$  (or load) in solid phase.

If the equilibrium isotherm is linear ( $q_e = K_e C$ ), an analytic expression can be derived, such as Klinkenberg did [29] using dimensionless equations as follows:

Mass balance in the bed:

$$\frac{\partial \phi}{\partial \xi} + \frac{\partial \varphi}{\partial \tau} = 0 \quad (6.7)$$

Adsorption velocity:

$$\frac{\partial \varphi}{\partial \tau} = \phi - \varphi \quad (6.8)$$

Where:

$$\phi = \frac{C}{C_0}; \quad \varphi = \frac{q}{q_s}; \quad \xi = \frac{K_e K_a Z}{u} \left( \frac{1-\varepsilon}{\varepsilon} \right); \quad \tau = K_a \left( t - \frac{Z}{u} \right)$$

$q_s$  is the exhausted value of  $q$ ,  $K_e$  is the equilibrium constant of a linear adsorption isotherm,  $z$  is the distance from the bed entrance,  $u$  is the gas interstitial velocity,  $\varepsilon$  is the bed void fraction,  $t$  is the time.

Thus, using the above mentioned initial and boundary conditions, the analytical solution is:

$$\frac{C}{C_0} \approx \frac{1}{2} \left[ 1 + \text{erf} \left( \sqrt{\tau} - \sqrt{\xi} + \frac{1}{8\sqrt{\tau}} + \frac{1}{8\sqrt{\xi}} \right) \right] \quad (6.9)$$

where  $\text{erf}(x)$  is the error function of Gauss, defined by Eq. (6.10).



$$\operatorname{erf}(x) = \frac{2}{\sqrt{\pi}} \int_0^x e^{-t^2} dt \quad (6.10)$$

The coefficient of overall mass transfer (which includes both the external and internal mass transfer) was determined as follows:

$$\frac{1}{K_e K_a} = \frac{d_p}{6K_{ext}} + \frac{d_p^2}{60D_e} \quad (6.11)$$

$d_p$  is the mean particle diameter,  $D_e$  is the effective diffusivity.

The external mass transfer coefficient ( $K_{ext}$ ) was calculated by the Ranz–Marshall correlation [30]:

$$Sh = 2 + 1.58 Re^{0.4} Sc^{1/3}; 10^{-3} \leq Re \leq 5.8 \quad (6.12)$$

Where:

$$Sh = \frac{K_{ext} d_p}{D_m}; Re = \frac{u \varepsilon d_p \rho}{\mu}; Sc = \frac{\mu}{\rho D_m}$$

$D_m$ ,  $d_p$ ,  $q$  and  $\mu$  are the molecular diffusivity, particle diameter, gas density and gas viscosity, respectively.  $D_m$  was calculated by the Fuller-Schettler-Gridding correlation [31]:

$$D_m = \frac{10^{-3} T^{1.75} \left( \frac{1}{M_{gas}} + \frac{1}{M_{H_2S}} \right)^{0.5}}{P (V_{gas}^{1/3} + V_{H_2S}^{1/3})^2} \quad (6.13)$$

with  $D_m$  in  $\text{cm}^2/\text{s}$ ,  $T$  in K,  $P$  in atm,  $M$  is molecular weight, and  $V$  is the diffusion volume.  $D_e$  is effective diffusivity, which could be calculated by the Bosanquet equation [21]:

$$D_e = \frac{\varepsilon_p}{f_{tor}} \left[ \frac{1}{D_m} + \frac{1}{D_K} \right]^{-1} \quad (6.14)$$

$\varepsilon_p$  is the particle porosity and  $f_{tor}$  is the tortuosity factor. Finally,  $D_K$  is the Knudsen diffusivity, which is calculated by Eq (6.15).

$$D_K = 4850 d_{pore} \left( \frac{T}{M_{H_2S}} \right)^{1/2} \quad (6.15)$$

Where  $d_{pore}$  is the mean pore diameter. The Knudsen diffusivity occurs in microporous systems. The two sludges investigated for instance have shown the pore size of microporous.

## 6.3 Results and Discussion

### 6.3.1 Sorbent characterization

Table 6.1 shows the moisture content, mean particle diameter, elements composition, pH, total carbon,  $S_p$  of the initial alum sludge. The moisture content of alum sludge cake was 63 %, while the mean particle diameter ( $d_{50}$ ) of the alum sludge was 16.5  $\mu\text{m}$ . It shows that aluminum and calcium were the most abundant elements. Other elements were also present, including various metals, silicon and phosphorus. The pH of the alum sludge is 10, indicating the basicity.

The total carbon is 30.6 wt % which is composed of 3.6 wt % inorganic carbon and 27.0 wt % organic carbon. Significantly, alum sludge shows a high specific surface area with BET value of 257.1 m<sup>2</sup>/g, higher than normal sorbent such as used wood pellets chars of 78.8 m<sup>2</sup>/g [8]; municipal solid waste incineration (MSWI) fly ash of 17.7 m<sup>2</sup>/g [3]; rice husk activated carbon of 168 m<sup>2</sup>/g [32]. This high specific surface area is due to the addition of activated carbon before the raw water purification processes in Carmaux WTP, in order to remove the odor and tastes of raw water.

**Table 6.1** Characterization of the alum sludge sorbent

Characteristics	Alum Sludge
Moisture content (%)	63
Mean diameter, d <sub>50</sub> (μm)	16.5
Al (mg/kg)	17581
Ca (mg/kg)	21156
Ba (mg/kg)	119
Cr (mg/kg)	4
Mg (mg/kg)	1331
Mn (mg/kg)	416
Sn (mg/kg)	34
Zn (mg/kg)	5
K (mg/kg)	4526
Fe (mg/kg)	4892
Mo (mg/kg)	33
Li (mg/kg)	1
Na (mg/kg)	144
As (mg/kg)	122
V (mg/kg)	33
Zr (mg/kg)	6
Si (mg/kg)	2391
P (mg/kg)	625
pH	10.0
TC (%)	30.6 (3.6 IC+27.0 TOC)

$S_p$ (m <sup>2</sup> /g)	257.1
$d_{\text{pore}}$ (nm)	2.4-3.2-5.0

Figure 6.2 presents the microstructures of the alum sludge obtained by SEM and a representative EDX analysis, showing the chemical composition of its surface. Analysis result by EDX indicated large amount of C on the alum sludge. From the physical texture, the alum sludge presents a porous and rigid structure with many irregular particles being observed on the plate. In particular, as shown in the EDX analysis, there are various metal elements on the surface of alum sludge, such as Al, Fe, Mg, Ca, and it have been demonstrated that adsorption of H<sub>2</sub>S largely depends on the metal species contained in the materials and reacted with H<sub>2</sub>S to produce metal sulfides [8].

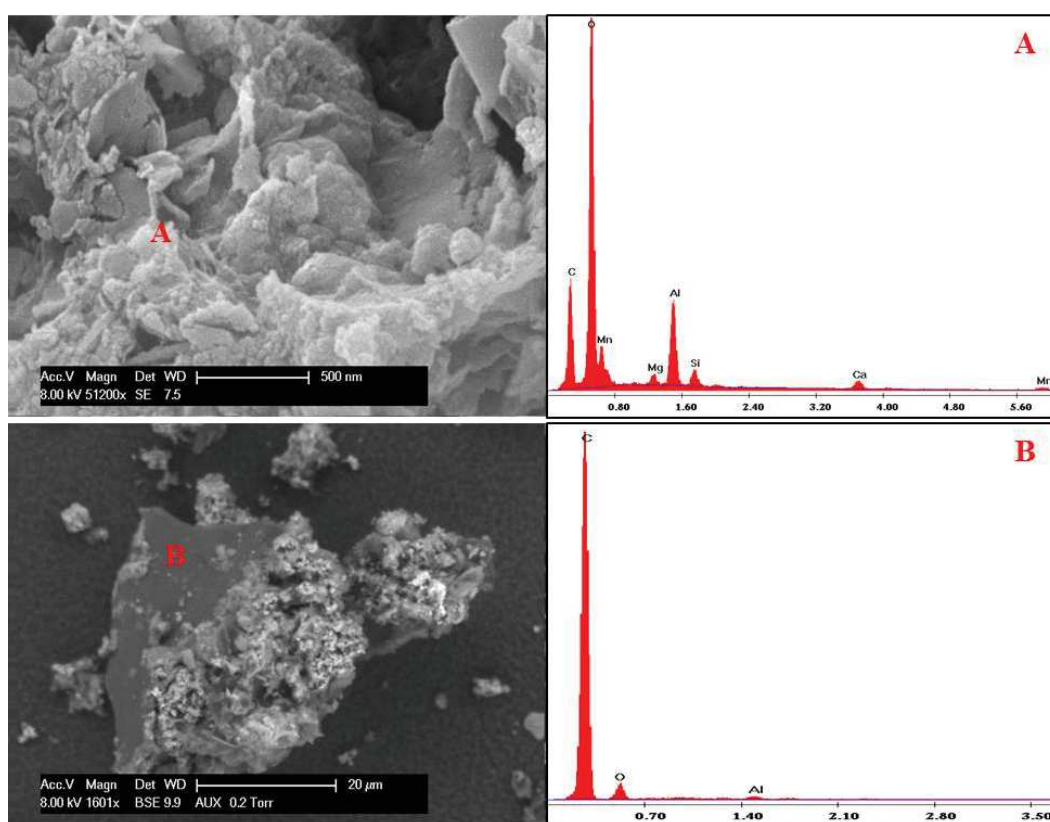
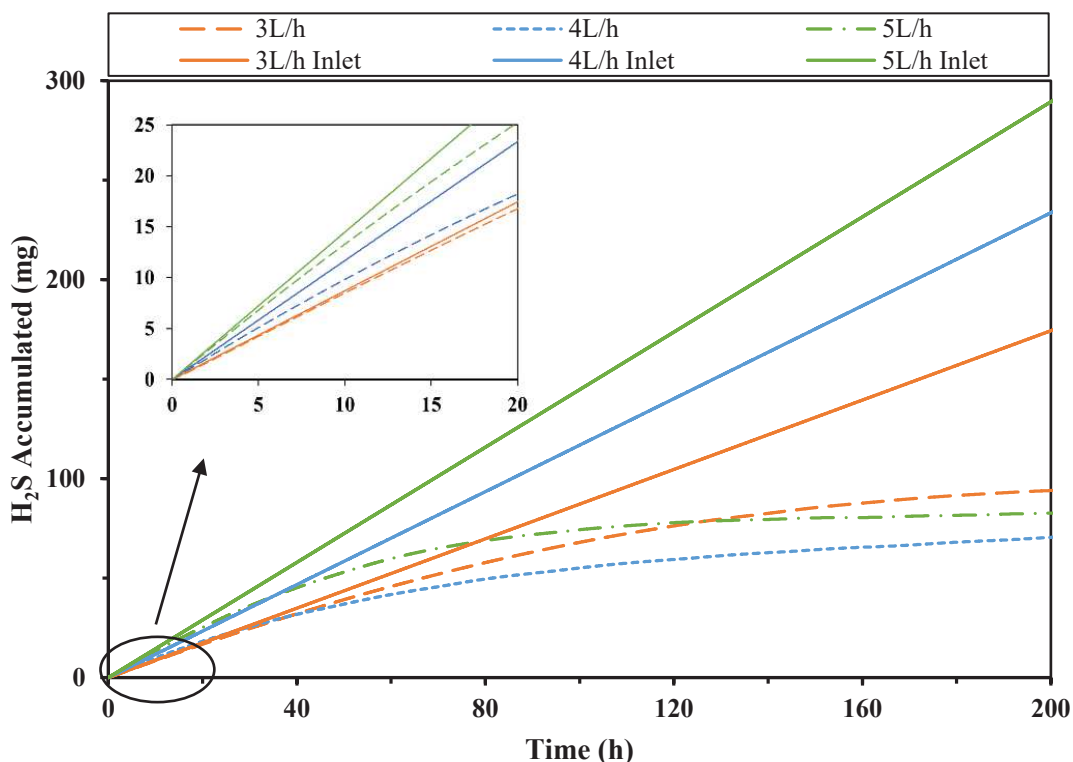


Figure 6.2 SEM-EDX of the alum sludge sorbent

### 6.3.2 Sorption trials

Figure 6.3 shows the sorption results obtained with 0.5 g alum sludge under different flow rate of 3, 4, 5 L/h, respectively. The inlet curve represents the accumulated quantity of H<sub>2</sub>S introduced into the reactor. Other curves represent the quantity of H<sub>2</sub>S accumulated in the alum sludge. In general, sorption performance showed that in the initial period of the test, sorption occurred rapidly, and then became slowly to gradually reach flat stage with time under all three flow rates. The minimum flow rate (3 L/h) obtained the largest fixed quantity of 95.9 mg for 0.5 g of alum sludge, which is 191.8 mg H<sub>2</sub>S/g alum sludge at 200 h. In particular, the flow rate

of 3 L/h shows the best performance from the beginning of sorption. However, after about 133.3 h, the sorbent under flow rate of 5 L/h was the adsorption rate decreases quickly than under the flow rate of 3 L/h. Indeed, the adsorption capacity revealed no significant dependence on the flow rate, for example, at 200 h, the accumulated  $H_2S$  on 0.5 g alum sludge under 3, 4, 5 L/h was 95.7, 72.2, 82.9 mg, respectively. In addition, for the 0.5 g alum sludge trials under 5 L/h, it has been repeated three time to check repeatability. This is an expected outcome because the adsorption capacity does not depend on the operational parameters since it is an intrinsic characteristic of the sorbent.



**Figure 6.3** Quantity of the  $H_2S$  fed into the reactor (Inlet curve) and fixed on 0.5 g alum sludge under different flow rate

To test the effect of the sorbent quantity on the sorption performance, the amount of alum sludge was doubled while the gas flow rate remained unchanged. Figure 6.4 shows the results obtained with 0.5 g and 1.0 g alum sludge, which corresponding to the 0.5 and 1.1 cm bed height under 5 L/h flow rate. It was observed that the accumulated  $H_2S$  on 0.5 g and 1.0 g alum sludge at 215 h are 82.9 mg (165.8 mg  $H_2S$ /g alum sludge) and 235.4 mg  $H_2S$ /g alum sludge, respectively. The increase of the sorbent quantity strongly improved the performance of  $H_2S$  removal; thus, the contact time was found to be a crucial parameter for the purification of  $H_2S$ . More significantly, at about 666.7 h, the accumulated  $H_2S$  was 374.2 mg  $H_2S$ /g of alum sludge, the capacity of the alum sludge-based sorbent is much higher than the majority sorbents, such as pyrolysis char of 57.6 mg  $H_2S$ /g [8],  $Fe_2O_3$ -based sorbent of 17.1 mg  $H_2S$ /g [22], sewerage sludge-based sorbents of 8.63 mg  $H_2S$ /g [21], etc., the reason is possibly derived from the specific surface area and pore structural difference. It can be seen from Table 1, the Carmaux alum sludge presents microporous pore structure moreover it has been demonstrated by [33]

that most of the adsorption takes place in pores with a smaller diameter, perhaps from 2 nm and below. On the other hand, the various metals such as Al, Ca, Mg, Fe contained inherently in the alum sludge (as illustrated in Table 6.1 and Figure 6.2) could facilitated the H<sub>2</sub>S adsorption as well [8].

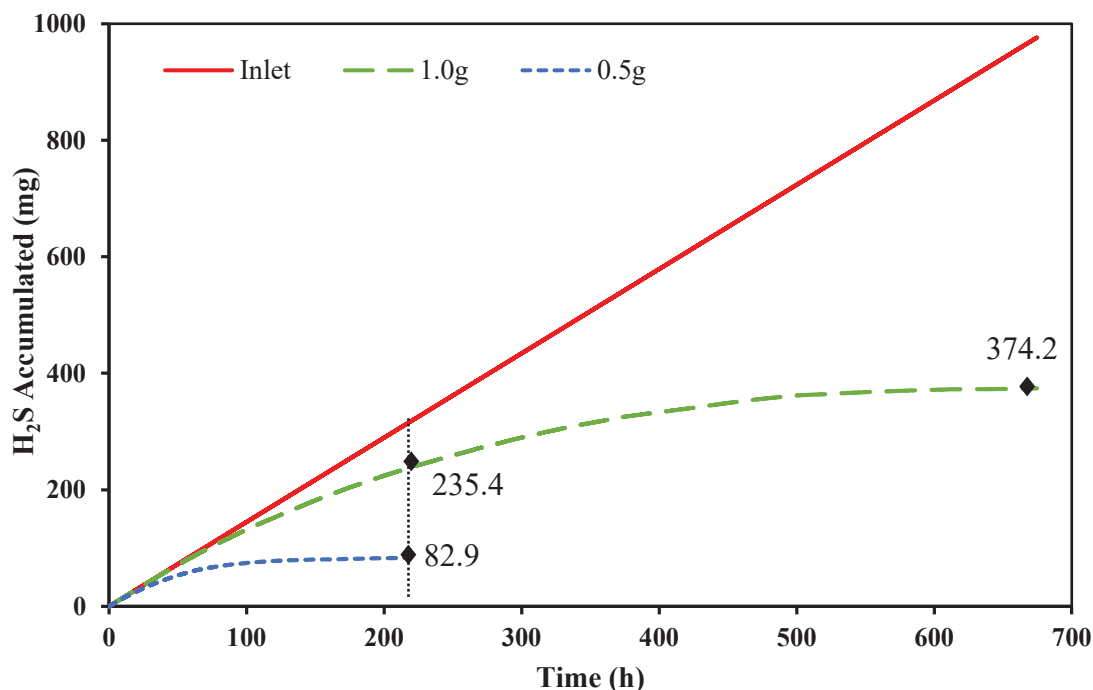


**Figure 6.4** Quantity of the H<sub>2</sub>S fed into the reactor (Inlet curve) and fixed on different mass of alum sludge under 5L/h flow rate

### 6.3.3 Breakthrough through curves modeling

#### ➤ Model parameters

The shape of the breakthrough curve and the time for the breakthrough appearance are the predominant factors for determining the operation and the dynamic response of an adsorption column [34]. In order to explain the dynamic adsorption behavior and to scale it up for industrial application, Thomas, BDST, Yoon-Nelson model were used to analysis the experiment data in breakthrough curves.

The determined relative constants and correlation coefficients were obtained through linear regression analysis of three dynamic adsorption models and are shown in Table 6.2. It is observed that, all the model constant  $K_{Th}$ ,  $K$ ,  $K_{YN}$  increased with the decreasing of bed height, which might be due to the increase in mass transfer resistance with increasing bed depth in columns [21,25]. As the flow rate increased, the value of  $K_{Th}$  increased and  $q_0$  decreased, which may be attributed to the lower empty bed contact time (EBCT) resulting in insufficient contact between the adsorbate with the available active sites on the surface of the sorbent.

The correlation coefficients  $R^2$  of Thomas BDST and Y-N model were 0.90, 0.93, 0.91

respectively, under 1 g alum sludge and 5 L/h flow rate. While Thomas model has the highest  $R^2$  of 0.93 under the 0.5 g alum sludge and 5 L/h. However, the  $R^2$  the three models were not satisfied under the 0.5 g alum sludge 4 L/h condition, this is due to the experiment data turbulence and could not fit well with the models. As can be seen from the Figure 6.5b, the experimental points deviate from a model straight line passing through the origin, indicating the complex nature of  $H_2S$  adsorption process by alum sludge, which might include more than one rate limiting step [25]. Additionally, the Thomas, BDST, Y-N models'  $R^2$  under the 0.5 g alum sludge and 3 L/h condition were 0.9, 0.93, 0.92, respectively, it indicated that all the three models could well predicated the breakthrough time in this regard.



**Table 6.2** Model parameters calculation

$C_0$ (mg/kg)	$m$ (kg)	$Q$ (L/min)	$K_{Th}$ (m <sup>3</sup> /kg-min)	$q_0$ (kg/L)	$R^2$	$K$ (L/kg-min)	$N_0$ (kg/L)	$R^2$	$K_{YN}$ (min <sup>-1</sup> )	$\tau$ (min)	$R^2$
200	0.001	0.083	0.4612	0.235	0.90	0.5	0.222	0.93	0.0001	14477.9412	0.91
200	0.0005	0.083	1.9765	0.107	0.93	2.3	0.108	0.89	0.0006	3301.3600	0.85
200	0.0005	0.067	1.3835	0.083	0.78	1.1	0.090	0.75	0.0004	3537.1429	0.70
200	0.0005	0.050	1.4165	0.124	0.90	1.4	0.118	0.93	0.0004	5930.2326	0.92

The comparison of simulated breakthrough curves and the experimental data was jointly presented in Figure 6.5. The general position of the breakthrough curve along the time axis depends on the capacity of the sorbent with respect to bed height and flow rate. Apart from the breakthrough part of Figure 6.5 (a) and initial part of (d), and compared with correlation coefficients, both Thomas, BDST and Y-N model can better describe the adsorption behavior. As shown in Table 6.3, the 50 % ( $C_t/C_0 = 0.5$ ) experimental breakthrough time and their corresponding simulated time by the three models were calculated and presented. The Thomas, BDST and Y-N model could well predicate the breakthrough time of 0.5 g alum sludge under 3 L/h with the same 2.0 % deviation. However, the deviation was 28.3, 33.3, 34.5 % when applied those models to 0.5 g alum sludge under 4 L/h condition, this is due to the turbulence of experimental time data around 50 % breakthrough capacity, as shown in Figure 6.5b the turbulence of the data make the three simulation curves behind of the experimental time. Regarding the 0.5 g alum sludge under 5 L/h flow rate, the prediction of Thomas model was the best with the deviation of 1.9 %, compare with the BDST model (3.6 %), Y-N model (5.4 %). In addition, among the three models, the BDST model could well predicate the 1.0 g alum sludge under 5 L/h, with the lowest deviation of 3.1 %.

Table 6.3 Experimental and simulated breakthrough time

Models	$C_t/C_0=0.5$		Deviation (%)
	Experimental (h) (mass, flow rate)	Simulated (h)	
Thomas Model	0.5g, 3L/h	102	2.0
	0.5g, 4L/h	38	28.3
	0.5g, 5L/h	53	1.9
	1.0g, 5L/h	220	5.6
BDST Model	0.5g, 3L/h	102	2.0
	0.5g, 4L/h	38	33.3
	0.5g, 5L/h	53	3.6
	1.0g, 5L/h	220	3.1
Y-N Model	0.5g, 3L/h	102	2.0
	0.5g, 4L/h	38	34.5
	0.5g, 5L/h	53	5.4
	1.0g, 5L/h	220	8.3

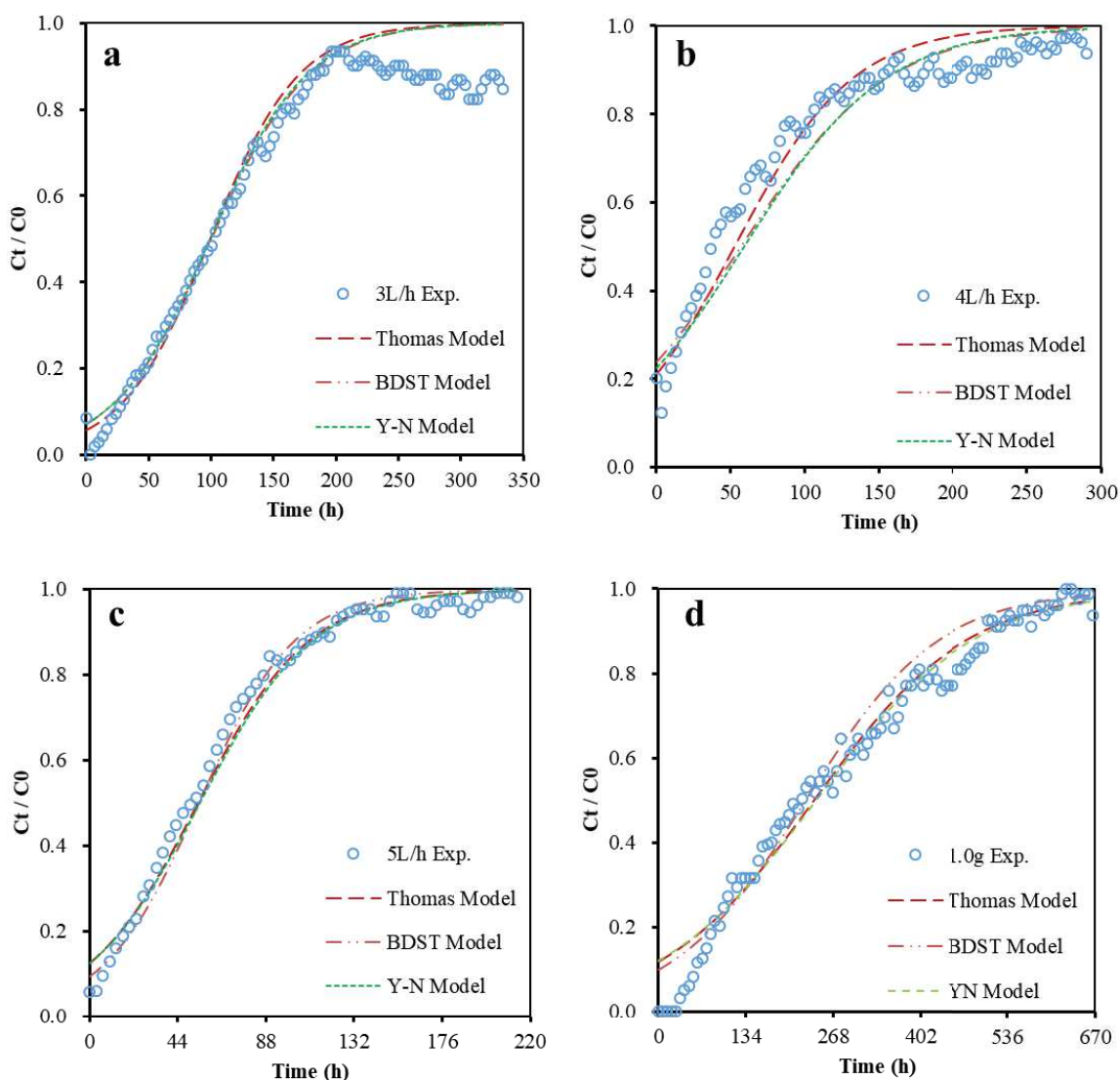


**Figure 6.5** The simulative curves and experiment data under three different model, (a), (b), (c) 0.5 g alum sludge under the flow rate of 3, 4, 5 L/h, (d) 1g alum sludge under the flow rate of 5 L/h.

### ➤ Effect of flow rate

Figure 6.5 (a), (b), (c) show the effects of flow rate on the sorption. It was studied by keeping constant inlet  $\text{H}_2\text{S}$  concentration (200 ppmv) and the mass (0.5 g) of alum sludge under the variable flow rate of 3, 4, 5 L/h, respectively. It was observed that the flow rate represents the major influence in the shape of the breakthrough curve. By increasing the flow rate from 3 to 5 L/h, resulted in a decrease in both breakthrough and exhaustion times from 350 to 220 h. The lower flow rate presented a longer breakthrough time, and it reflects a wider mass transfer zone. Moreover, the results in Table 6.3 also indicated that by increasing the flow rate at a constant bed height (mass), the breakthrough time tend to become lower, for example, for  $m=0.5$  g,  $\text{H}_2\text{S}$  adsorption saturation time varied from 200 to 151.7 h with the flow rate increasing from 3 to 5 L/h. Higher flow rate triggered lower residence time, and it has given rise to weaker adsorbate-sorbent interaction and disturbed the intraparticle mass transfer between the  $\text{H}_2\text{S}$  and the alum sludge. Moreover, this is a consequence of the fact that higher flow rate decreases the contact time between the  $\text{H}_2\text{S}$  and the alum sludge, resulting in lower mass transfer efficiency of  $\text{H}_2\text{S}$  to the sorbent [35]. As the adsorption rate is mainly controlled

by intra-particulate diffusion, the capacity tends to increase as the flow rate decreases because the residence time is longer. Thus, the intra-particulate diffusion becomes more effective [36,37]. On the other hand, at lower flow rate, more contact time ensued more adsorbate-sorbent interaction and higher diffusion of adsorbate onto the sorbents making use of the maximal percentage of the sorbent bed, thus more durability in column bed performance. Similar trend was reported by earlier researchers using other materials [22,25]. Additionally, in Figure 6.5a, the differences of experimental data and three dynamic adsorption model curves observed near the breakthrough point can be attributed to lower concentration gradient between adsorbate in the sorbent surface and in the bulk phase, similar phenomenon was reported by [24], the lower flow rate showed flatter breakthrough profiles, with a more extended breakthrough zone.

#### ➤ Effect of bed height

Figure 6.5 (c), (d) present the effects of bed height on the sorption. It was carried out by keeping constant inlet H<sub>2</sub>S concentration (200 ppmv) and the flow rate (5 L/h), using different mass of alum sludge (0.5 & 1.0 g) for H<sub>2</sub>S adsorption, which corresponding to the different bed height of 0.5cm and 1.1 cm. It can be observed that increasing the bed depth from 0.5 to 1.1 cm resulted in an increase in both breakthrough and exhaustion times from 220 to 670h. Similarly, breakthrough volume and exhaustion volume exhibited increasing trend with increased bed depths. However, contrarily to the effect of the flow rate, as the bed depth increases, the breakthrough and the saturation time also raise, a longer EBCT, resulting in a higher operating time to take the column to the exhaustion point. Furthermore, with increasing bed depths, the slope of the breakthrough curves became flatter, leading to the formation of an expanded mass transfer zone (MTZ). This is due to the fact that as much quantity of sorbent was introduced in the column, more binding sites are available for sorption [38]. For the smaller bed depths, the axial dispersion phenomena predominate in the mass transfer process, leading to a reduction of the diffusivity of the H<sub>2</sub>S. Consequently, the H<sub>2</sub>S does not have enough time to diffuse into the alum sludge, allowing H<sub>2</sub>S leaving the column earlier. On the other hand, the contact time between the H<sub>2</sub>S and the alum sludge is higher when the bed depth increases [25]. Similar types of results have already been reported in earlier researches, such as [22,24,37]

### 6.3.4 Adsorption Mechanisms of H<sub>2</sub>S onto alum sludge

#### ➤ Sorbent characteristics before and after the adsorption trials

As illustrated in Table 6.4, the abundant element S was significantly increased from 0 to 34981 mg/kg after the adsorption, it confirms that large amount of H<sub>2</sub>S was adsorbed onto alum sludge. During the H<sub>2</sub>S removal trials, the pH of the alum sludge decreased from 10 to 7.5. The change of pH from basic to neutral values accounts for the dissolution of H<sub>2</sub>S in the water film and the formation of sulfuric acids in the alum sludge, and also suggested that the presence of O<sub>2</sub> in the gas composition promoted the formation of acidic species leading to the acidification of the alum sludge surface [8]. Nevertheless, the pH decrease was low compared to literature. For example, Bandosz [39] reports that the pH of activated char from coconut shell used for H<sub>2</sub>S removal from moist air decreased from 9.7 to 2.8. It can be concluded that the formation of sulfur oxide species is relatively low in our study.

Moreover, it has been pointed out by Yan et al. [33], the local pH in the pore system has a significant effect on the efficiency of hydrogen sulfide dissociation and its oxidation to various sulfur species. A pH in the basic range promotes the dissociation of H<sub>2</sub>S. This results in a high concentration of HS<sup>-</sup> ions, which are then oxidized to sulfur polymers [39]. On the contrary, a

moderately low average pH of the sorbent surface is expected to suppress the dissociation of H<sub>2</sub>S and the creation of hydrogen sulfide ions. These ions, when present in low concentration in small pores, are oxidized to sulfur oxides from which sulfuric acid is formed. A threshold value (pH=4.5) was previously suggested [33]: when the pH is lower than 4.5, only physical adsorption can occur, and the concentration of dissociated hydrogen sulfide ions is negligible.

As such, the adsorption process of alum sludge was dominated by the chemisorption as the pH value of alum sludge is 10. The pK<sub>a</sub> constants of hydrogen sulfide are 7.2 and 14 for the first and second dissociation, respectively. Therefore, HS<sup>-</sup> ions will be at high concentration, capable of creating polysulfides. As the extent of the reaction progressed, pH reduced and transformed from caustic to neutral.

**Table 6.4** Elemental analysis and pH of the sorbent

Characteristics	Alum sludge	Exhausted alum sludge
pH	10.0	7.5
S (mg/kg)	0	34981
C (%)	30.7	20.0
N (%)	0.5	0.5

It can be seen from Table 6.5 that alum sludge has high micropore volume and BET surface area. The pore structural properties of alum sludge were significantly modified during the H<sub>2</sub>S removal trials. The adsorption of H<sub>2</sub>S severely reduces the micropore volume and the surface area S<sub>p</sub> of alum sludge which decreases from 238 to 65 m<sup>2</sup>/g. The microporous volume of alum sludge was zero after the adsorption trials, which can be explained by the higher amount of H<sub>2</sub>S adsorbed by alum sludge in these pores.

In addition, the adsorption process of H<sub>2</sub>S increases the average pore diameter values of the alum sludge. The exhausted alum sludge has a value of 5.3 nm compared with the raw alum sludge value of 2.4 nm. This could be an indication that most of the adsorption takes place in pores with a smaller diameter. When this happens, the number of smaller pores present becomes less, while the number of pores with a diameter larger than 2 nm is less affected, the average value of the overall pore diameter is pushed up when the nitrogen adsorption test was carried out on the exhausted alum sludge. Similar observations were made by [8,40,41]. Yan et al. [33] also states that a good physical environment for H<sub>2</sub>S adsorption and subsequent oxidation requires pores that are large enough to contain important functional groups and yet also small enough for a water film to be created even at low humidity, and this seem to lie between the 0.5-1 nm region. In addition, by heating the exhausted alum sludge to 200 °C, the relevant S<sub>p</sub> and the microporous volume was increase, it suggested that the H<sub>2</sub>S is desorbed. The exhausted alum sludge could be used again by thermal regeneration and could be another interesting study for the regeneration of exhausted alum sludge sorbent.

**Table 6.5** Structural properties of alum sludge

Samples	S <sub>p</sub> (BET) (m <sup>2</sup> /g)	S <sub>mic</sub> (m <sup>2</sup> /g)	V <sub>mic</sub> (cm <sup>3</sup> /g)	V<2 nm (cm <sup>3</sup> /g)	V < 25 nm (cm <sup>3</sup> /g)	d <sub>pore</sub> nm
Alum sludge	238 (105°C)	119.56	0.05	0.082	0.237	2.4-3.2-5.0
Exhausted alum sludge	65 (105 °C)	1.74	0.00	0.015	0.136	3.3-5.3
	111	29.13	0.01	0.033	0.154	2.4-3.2-5.0

(150 °C)						
198	93.45	0.04	0.069	0.195	2.4-3.2-5.0	
(200 °C)						

The SEM-EDX image in Figure 6.6 was obtained from the exhausted alum sludge. It can be seen from the EDX peaks, the adsorbed sulfur was significant identified from the other element EDS peaks, which confirms again the good performance of H<sub>2</sub>S adsorption onto alum sludge [42]. Regarding the other element analysis, it was in accordance with the ICP results (Table 6.2), as well as the TEM-EDX image which is presented in Figure 6.7.

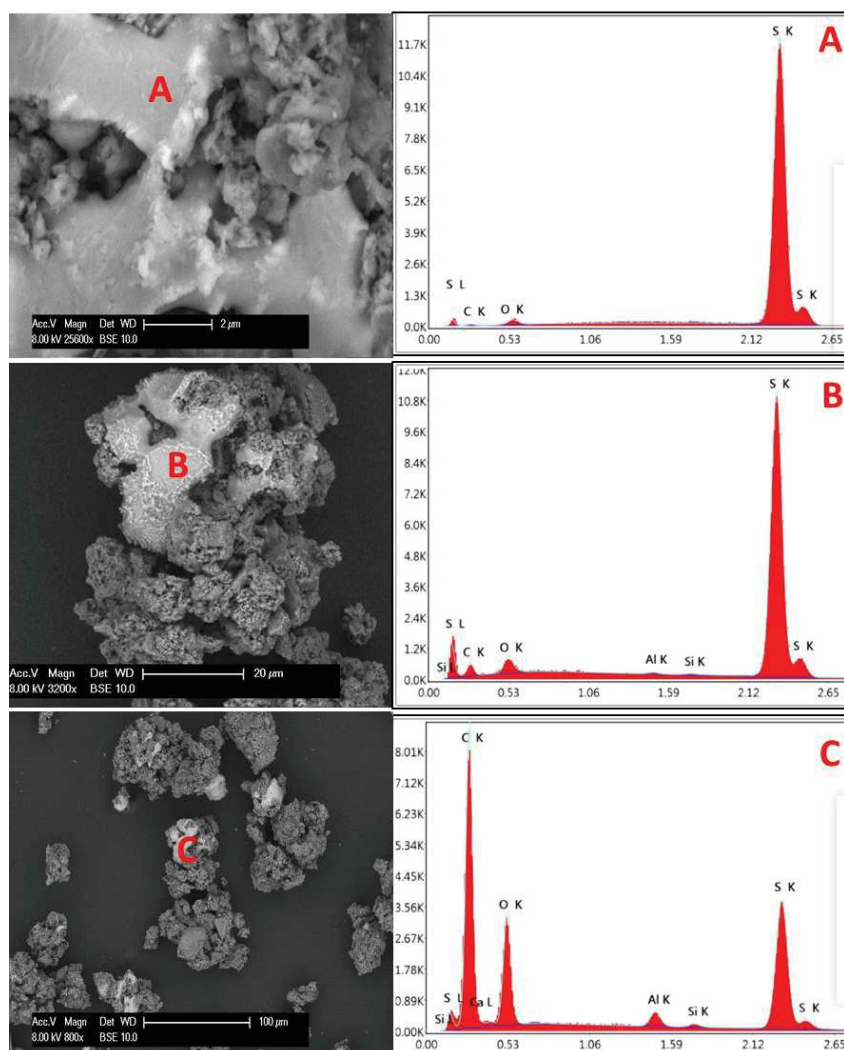


Figure 6.6 SEM-EDX of the exhausted alum sludge sorbent

It can be seen from Figure 6.7, the main element of the exhausted alum sludge are various metals such as Al, Ca, Fe, Mg, K, in addition C, Si and O was also found on the surface of exhausted alum sludge, which was correspond with the abovementioned ICP and SEM-EDX result. Apart from that, S was observed and it was homogeneously distributed throughout the alum sludge surface. Noteworthy, the S distribution (yellow dots) presents a highly similarity with various metals distribution, such as Fe (light green dots), Ca (pink dots), Mg (orange dots), as well as the O distribution (blue dots), it indicated that the H<sub>2</sub>S adsorption process was mostly preferred on the metal oxide species inherently contained in the alum sludge, the reaction between various metal oxide species with H<sub>2</sub>S could produce metal sulfides [41]. Additionally,



the O-containing groups also triggered the H<sub>2</sub>S oxidation reaction and increased the H<sub>2</sub>S removal capacity [8].

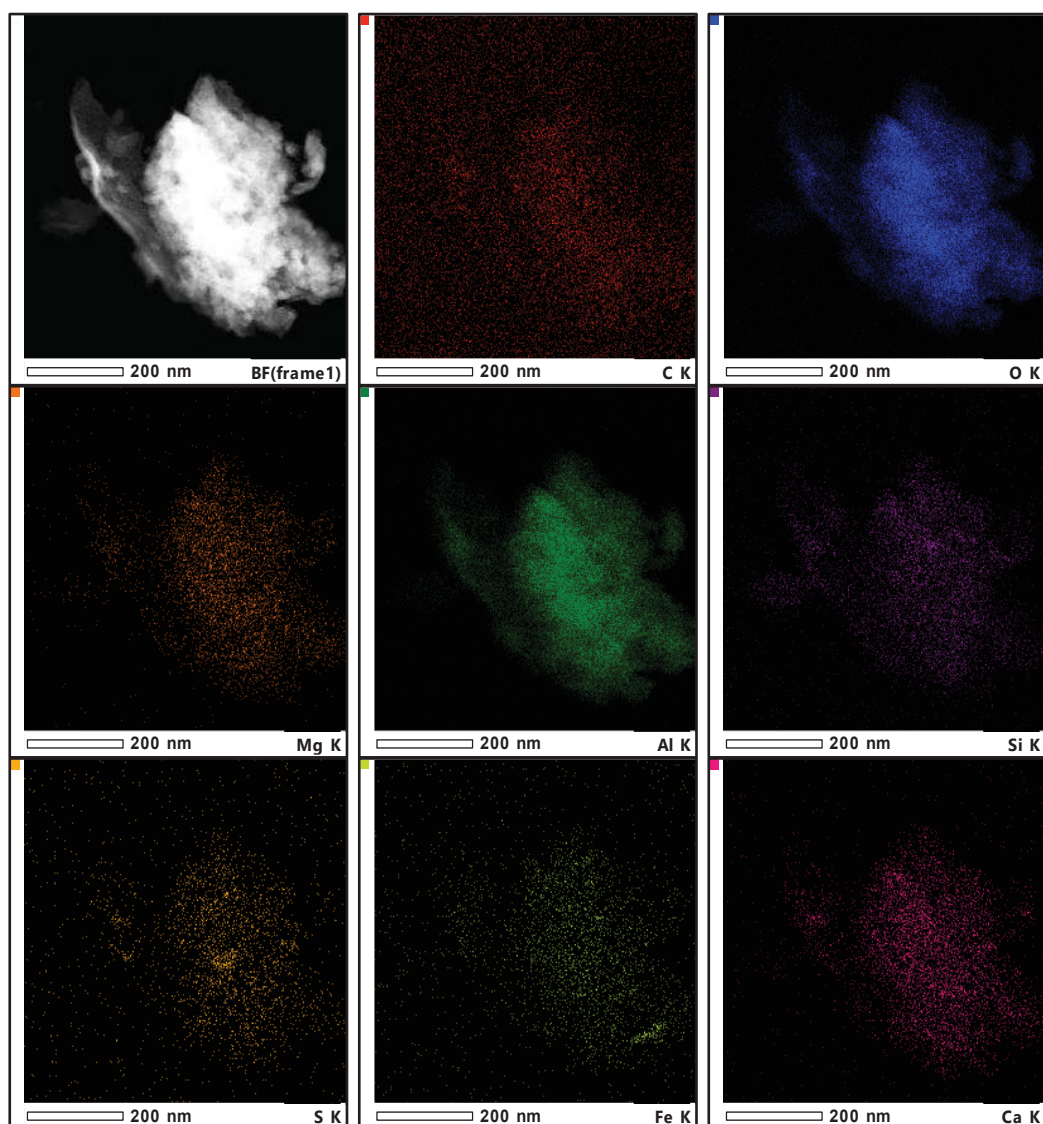


Figure 6.7 TEM-EDX images of the exhausted alum sludge sorbent

### ➤ Identification of sulfur products

To go further in the identification of the gas removed during the thermal treatment sulfur species were coupled with MS analyses were performed with raw and used alum sludge. Figure 6.8 shows the derivative thermogravimetric (DTG) curves and the corresponding composition of the effluent gas as a function of the temperature. Each DTG peak corresponds to a weight loss due to desorption of species from the alum sludge at the specific temperature. The taller the peak or the larger the area means more weight loss. Based on the literature [8,32,33,43], the sulfur compounds desorption can occur in two temperature ranges, and the corresponding effluent gas composition provides information on the nature of these compounds:

- 1) In the first zone (plotted in green in Figure 5) between 200 and 350°C, a SO<sub>2</sub> release indicates the desorption of physisorbed SO<sub>2</sub> or other sulfur oxides, while a H<sub>2</sub>S release reveals the decomposition of metallic sulphides.

- 2) In the second zone (plotted in orange in Figure 5) between 350 and 600°C: a release of SO<sub>2</sub> reflects the decomposition of sulfur radicals and/or elemental sulfur, while a release of H<sub>2</sub>S indicates the decomposition of polysulfides.

As shown in Figure 6.8, the DTG curves of raw and exhausted alum sludge both present two prominent peaks at around 110 °C and 300 °C. Regarding the peak around 110 °C, it corresponds to the dehydration processes as well as the desorption of weakly adsorbed H<sub>2</sub>S [43]. The weight loss of exhausted and raw alum sludge in this stage are 20.8 and 6.7 %, respectively. However, the second DTG peaks (around 300 °C) of exhausted alum sludge is wider than the DTG peak curve of raw alum sludge, the weight loss of exhausted and raw alum sludge in this stage are 21.7 and 3.1 %, respectively, and in agreement with the ICP results. Moreover, the mass lost between raw and exhausted sorbent from was 31.7 %, and from the ICP analysis, the increased S in exhausted sorbent was 33.5 %. It represents the removal of SO<sub>2</sub> from the decomposition of oxysulfur acids or H<sub>2</sub>S from decomposition of alkali metal sulfides, while the peak at 350-600 °C is probably the result of the desorption of elemental sulfur and decomposition of the surface reaction products [44].

The Mass Spectrometry analyses coupled with the thermal analyzes allowed to identify the gas associated with a thermal transformation of the solid. For exhausted alum sludge, the first mass loss occurred at 310°C and was related to a simultaneous release of H<sub>2</sub>S (red curve) and SO<sub>2</sub> (orange curve), while the second appeared at 510 °C related to a release of H<sub>2</sub>S, SO<sub>2</sub> and CO<sub>2</sub>, it indicated the production of sulfur radicals, elemental sulfur, and/or metal sulfides during the H<sub>2</sub>S removal tests [8,39,45]. Therefore, based on the literature data, this behavior (mass loss at 310°C and a simultaneous release of H<sub>2</sub>S and SO<sub>2</sub>) indicated that the main sulfur products formed on alum sludge were sulfur oxide species and alkali metal sulfides (310-350 °C), as well as the sulfur radicals and/or elemental sulfur (SO<sub>2</sub> release from 350-500 °C) and polysulfides and/or metal sulfides (H<sub>2</sub>S release from 350-500°C). Previous work published by other authors also have the similar observation [43,44,40], which established that the first peak in the range of 200 to 600 °C is due to the desorption of oxidized sulfur species, while the second comes from elemental sulfur components.

The exact locations of the two peaks of DTG vary in temperature from paper to paper, such as in the study carried out by Yan et al. [45], the DTG peaks of the exhausted sorbent was at around 290 °C and 530 °C respectively, while in the study of Hervy et al. [8] the two DTG peaks was at 285 and 370 °C; but it is in agreement that the peak relative to sulfur oxides comes before the elemental sulfur peak. The different temperatures where the peaks of DTG occur happen because of the different physical and chemical characteristics of the sorbent. Yan et al. [33] pointed out that the sulfur oxides are supposed to be more soluble than the elemental sulfur, some washing could be performed on the selected exhausted carbon samples to check for differences in their thermal desorption pattern, and this could be forming another interesting study regarding the H<sub>2</sub>S adsorption onto alum sludge.

The presence of various forms of sulfur compounds in addition to the oxides of sulfur on the surface of alum sludge after H<sub>2</sub>S adsorption indicates that the chemical reactions are involved in H<sub>2</sub>S retention. The alkaline and chemical promoter present on the surface and water facilitate dissociation, dimerization and oxidation reactions.

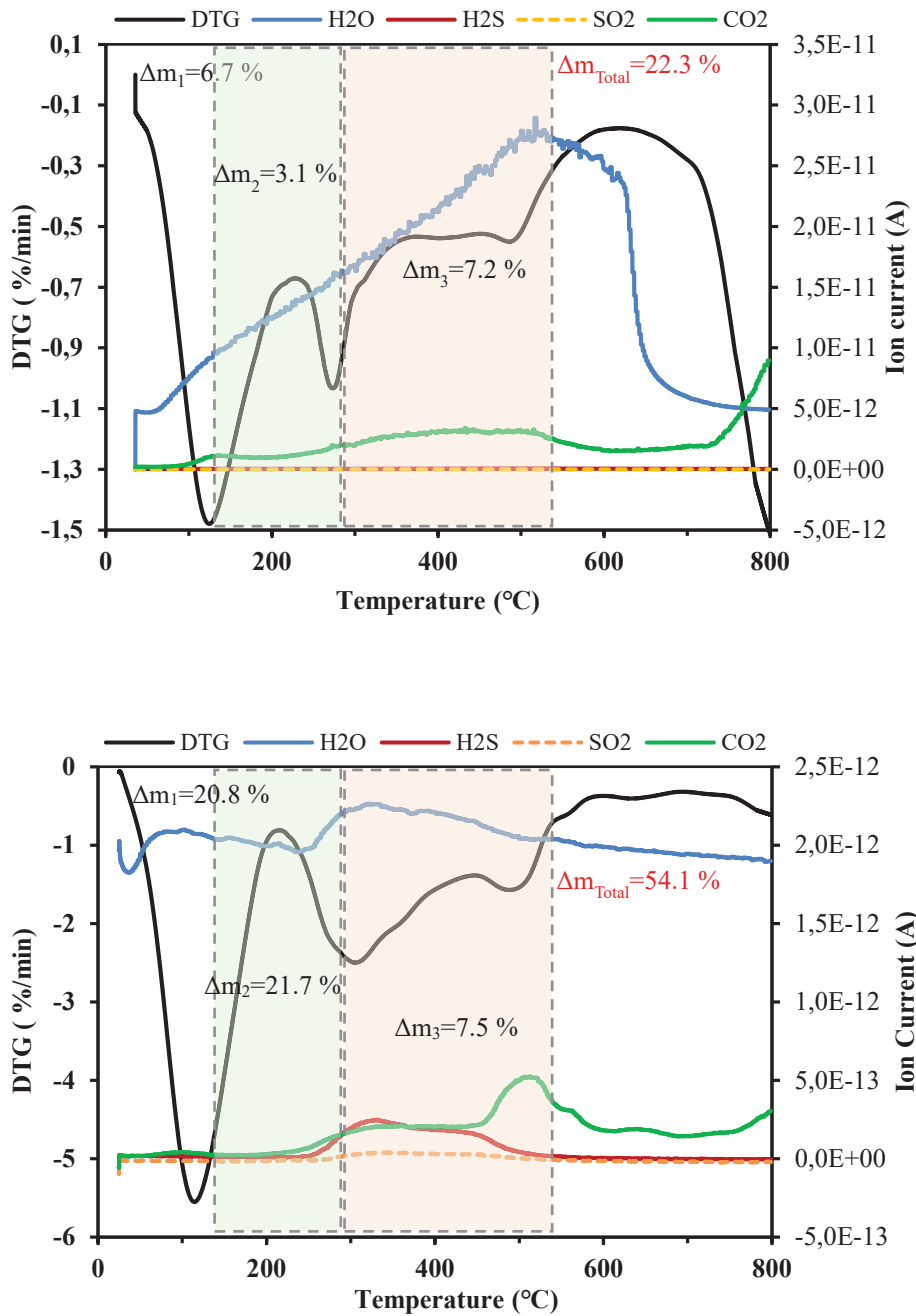


Figure 6.8 TGA-MS analysis of raw alum sludge before (up) and after (down) the adsorption trials

➤ **Proposed mechanisms of H<sub>2</sub>S removal by alum sludge**

The sulfur compounds adsorbed evidenced that the retention process of H<sub>2</sub>S on the alum sludge surface consists of a complex reaction mechanism involving the physicochemical properties of the alum sludge. This is due to the presence of various types of active sites, such as the carbon and the metal oxides or carbonates [2,8]. Based on these results, the following reactions (Figure 6.9) proposed are expected to occur in the H<sub>2</sub>S retention mechanism [46,47].

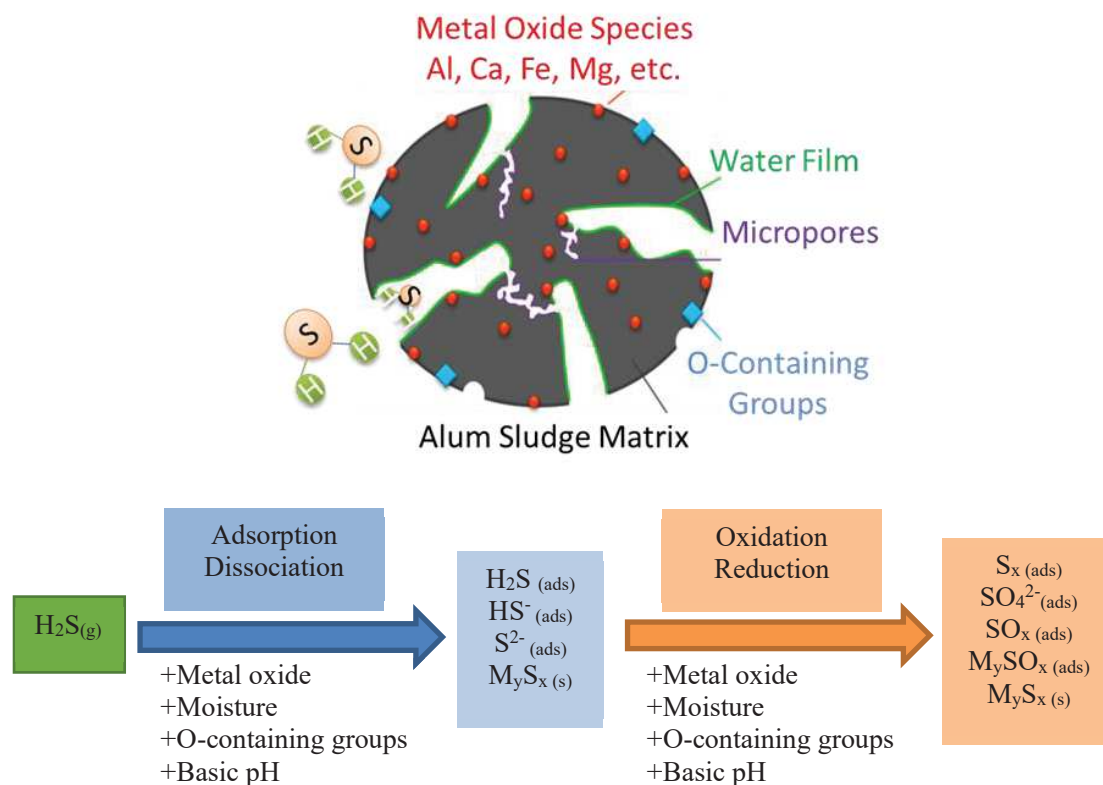
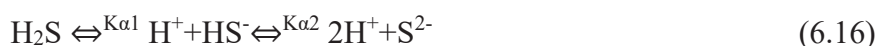


Figure 6.9 Mechanisms of H<sub>2</sub>S adsorption onto alum sludge

When the adsorption process begins, firstly, H<sub>2</sub>S molecules were located on active sites at the alum sludge surface, the humidity/moisture of the alum sludge can dissociate the H<sub>2</sub>S [8]:



With  $K_{\alpha 1} = 10^{-7}$  and  $K_{\alpha 2} = 10^{-13}$ : the H<sub>2</sub>S acidity constants for the first and second dissociation. When the pH is basic, the concentration of HS<sup>-</sup> is much higher, which forces the created sulfur atoms to be close to each other, capable of creating polysulfides.

Secondly, H<sub>2</sub>S reacted with the metal oxide species (MO<sub>x</sub>) inherently contained in the alum sludge to produce metal sulfides (MS<sub>x</sub>) [3,8]. Further oxidation of the metal sulfur with oxygenated organic and inorganic species led to the formation of metal sulphate [39]. The reaction is as following:



In the last, the O-containing groups also increased the H<sub>2</sub>S removal capacity, by the H<sub>2</sub>S oxidation reaction [45]. In the presence of air, the important acidification of the surface can be explained by the oxidation of H<sub>2</sub>S to H<sub>2</sub>SO<sub>4</sub> [39].



### 6.3.5 Determination of the mass transfer coefficient

The adsorption mechanism is governed by different types of mass transfer: external and internal diffusion. Thus, correctly estimated the various mass transfer coefficients is a vital step. To predict the dynamics of the hydrogen sulfide adsorption, the mathematical model must include the adsorption isotherm, the mass-energy balance inside the sorbent particle and the mass-energy balance of the gaseous phase in the bed, as well as mass transfer phenomena (an equation for the mass flux) [24]. In the fixed-bed columns, the concentrations in gas phase change through the time and space. As the process is unsteady, the development of a model that describes the concentration profile in the bed with the time is quite complex. Comprehensive fixed-bed models that take into account the nonlinear equilibrium behavior as well as axial dispersion, resistance to mass transfer, and sorption kinetics are described in terms of partial differential equations, which generally involve a very difficult numerical solution [36]. Consequently, simplified or shortcut methods for correlating the breakthrough curves of sorbents columns are extensively used for the initial design and analysis of fixed-bed columns, and frequently, they provide a straightforward and helpful approach.

Indeed, the modeling and simulation of empirical models such as Thomas, Bed Depth Service Time and Yoon-Nelson model for H<sub>2</sub>S adsorption was already investigated in our previous studies. However, these models are based on the assumption that the rate of adsorption is controlled by the surface reaction. Thus, this study mainly focuses on the overall mass transfer coefficients determination from mathematical description of breakthrough curves and their dependency on experimental conditions, which means the external and internal diffusion limitations are not absent in the overall process. Moreover, adsorption may not be limited by kinetics of chemical reaction, but controlled by external and/or internal mass transfer. Thus, an alternative approach is to consider both inter- and intra-particle mass transfer to control the adsorption process.

Table 6.6 includes the parameters used, the value of tortuosity factor is based on [21], the equilibrium constants ( $K_e$ ) were computed by fitting the experimental results of adsorption isotherm to the linear isotherm. Known overall mass transfer coefficients are used for the estimation of H<sub>2</sub>S surface diffusivity over interior surface of alum sludge.

**Table 6.6** Parameters used in the determination of mass transfer coefficient

Parameters	Value	Unit
Mean pore diameter ( $d_{\text{pore}}$ )	3.50E-09	m
Molecular weight of H <sub>2</sub> S ( $M_{\text{H}_2\text{S}}$ )	34.1	g/mol
Temperature (T)	293.15	k
Pressure (P)	1	atm
Molecular weight of air ( $M_{\text{air}}$ )	28.79	g/mol
Diffusion volume of gas ( $V_{\text{gas}}$ )	20.1	/
Diffusion volume of H <sub>2</sub> S ( $V_{\text{H}_2\text{S}}$ )	20.96	/
Particle porosity ( $\epsilon_p$ )	0.6	/
Tortuosity factor ( $f_{\text{tor}}$ )	3	/
Particle diameter ( $d_p$ )	1.65E-05	m
Gas density ( $\rho_{\text{gas}}$ )	1.225	kg/m <sup>3</sup>

---

H <sub>2</sub> S gas density ( $\rho_{\text{H}_2\text{S}}$ )	1.434	kg/m <sup>3</sup>
Gas viscosity ( $\mu_{\text{air}}$ )	1.82E-05	kg/m s

---

Regarding the adsorption process, H<sub>2</sub>S molecules are located on the surface of alum sludge. The diffusion mechanisms govern the transport of H<sub>2</sub>S molecules into the pores of alum sludge. In porous materials, diffusion mechanisms are of four types: molecular diffusion caused by collisions between molecules, Knudsen diffusion caused by collisions of the molecules with the walls of the pore, surface diffusion caused by the electrostatic forces exerted by the walls on the molecules. Since the alum sludge has microporous structure, from the pore diameter in Table 6.5. It can be concluded that Knudsen diffusion was the main diffusion mechanisms.

Results from the different estimates of the mass transfer coefficient from experimental breakthrough fronts at several conditions are shown in Table 6.7. External and overall mass transfer coefficients are slightly decrease along with the flow rate decreasing. It should be noted that the external and overall mass transfer coefficients should be the same by using the same sorbent, however an error of 35 % under the flow rate of 3 L/h could be caused by the slow flow rate, leading to a very long saturation time (667 h). The Knudsen diffusion contribute to internal diffusion [38], however, this contribution is very small compared to the contribution of external diffusion.

In addition, the Knudsen, Molecular, Effective and Pore diffusivity were remaining the same under different flow rate and mass of sorbent. It indicated that the adsorption mechanisms were the same regardless of the experimental conditions.



**Table 6.7** Determination of the various mass transfer coefficient

Flow rate (L/h)	Mass (g)	Knudsen diffusivity $D_k$ (m <sup>2</sup> /s)	Molecular diffusivity $D_m$ (m <sup>2</sup> /s)	Effective diffusivity $D_e$ (m <sup>2</sup> /s)	Pore diffusion $D_p$ (m <sup>2</sup> /s)	Re	Sc	Sh	External mass transfer coefficient $K_{ext}$ (m/s)	Overall mass transfer coefficient $K_a$ (s <sup>-1</sup> )
5	1.0	4.98E-05	1.753E-05	2.5895E-06	1.2948E-05	1.00E-02	0.8490	2.2373	2.37	0.0017
5	0.5	4.98E-05	1.753E-05	2.5895E-06	1.2948E-05	1.00E-02	0.8490	2.2373	2.37	0.0017
4	0.5	4.98E-05	1.753E-05	2.5895E-06	1.2948E-05	0.0080	0.8490	2.2171	2.35	0.0017
3	0.5	4.98E-05	1.753E-05	2.5895E-06	1.2948E-05	0.0060	0.8490	2.1935	2.33	0.0011

## 6.4 Perspectives

Alum sludge as an easily, largely available by-product of water purification processes was firstly reused for H<sub>2</sub>S abatement. From this study, the H<sub>2</sub>S adsorption capacity of the alum sludge tested is quite good compared with majority of sorbents in the literature. Significantly, alum sludge could be directly reused as the “ready to use media” without any extra treatment. The results from this study have demonstrated that the use of alum sludge for H<sub>2</sub>S control could be an emerged promising approach. In particular, alum sludge could be a good material/sorbent for adsorption system, it will open a new way for desulfurization even odor abatement as well as the sludge management. Indeed, a large amount of cost in adsorption technologies is the media replacement, i.e. the replacement of media/substrate in adsorption column. No doubt, the choice of eco-friendly, sustainable, and low-cost alum sludge is in line with the need to develop a “circular economy”. However, this is the first time and small-scale trials and more studies, large-scale investigations are highly desirable to confirm with this result. Various alum sludge from different sites should be tested in the future, in addition, the regeneration of exhausted sorbent and final disposal route which also needs further investigation.

## 6.5 Conclusions

The dynamic adsorption of H<sub>2</sub>S by alum sludge was firstly examined. The breakthrough curves were measured at different bed depths and flow rates. Three kinetic models which are Thomas, BDST, YN model were applied to the experimental data to determine the kinetic parameters and predict the breakthrough time of the pilot column.

The alum sludge can be used for H<sub>2</sub>S adsorption at room temperature with adsorption capacity of about 374.2 mg/g depending on the adsorption conditions. The H<sub>2</sub>S adsorption capacity of the alum sludge was higher than that of several sorbent reported in literature in the dynamic condition test. Application of Thomas, BDST and YN model for the reactor revealed that the models can simulated well the breakthrough curves. The breakthrough and exhaustion of the bed were found to be regulated by the bed depth and flow rate. It was observed that an increase in bed depth or a decrease in flow rate resulted in an increase in the adsorption capacity of the bed. Under varying experimental conditions all the three models, e.g., Thomas, BDST and Y-N models with R<sup>2</sup> values range from 0.7 to 0.93, and successfully predicted breakthrough curves, and hence, be used for scaling up.

The important alum sludge properties for H<sub>2</sub>S removal are: high specific surface area and microporous volume, alkaline pH surface, presence of metal species (especially Ca, Al, Fe), O-containing groups. The mechanisms results highlighted the large variety of sulfur compounds produced during the H<sub>2</sub>S removal trials, resulting from a complex reaction mechanism involving the physicochemical properties of the alum sludge.

The overall mass transfer coefficients considering film resistance and pore resistance obtained by numerical modelling allowed to evaluate surface diffusivity of H<sub>2</sub>S over the interior surface of alum sludge. Since the alum sludge has microporous structure, it can be concluded that Knudsen diffusion was the main diffusion mechanisms, moreover, the Knudsen, Molecular, Effective and Pore diffusivity were remaining the same under different flow rate and mass of sorbent. It indicated that the adsorption mechanisms were the same regardless of the

experimental conditions.

With the easily, largely locally available and relatively high capacity nature, the alum sludge sorbent can be suitable for practical applications, therefore it opens a novel reusing perspective of alum sludge as well as a cost-effective solution for waste gas purification.

## Bibliography

1. de Oliveira, J.A.P.: Why an air pollution achiever lags on climate policy? The case of local policy implementation in Mie, Japan. *Environment and Planning A* **43**(8), 1894-1909 (2011).
2. Bamdad, H., Hawboldt, K., MacQuarrie, S.: A review on common sorbents for acid gases removal: Focus on biochar. *Renewable and Sustainable Energy Reviews* **81**, 1705-1720 (2018). doi:<https://doi.org/10.1016/j.rser.2017.05.261>
3. Wu, H., Zhu, Y., Bian, S., Ko, J.H., Li, S.F.Y., Xu, Q.: H<sub>2</sub>S adsorption by municipal solid waste incineration (MSWI) fly ash with heavy metals immobilization. *Chemosphere* **195**, 40-47 (2018). doi:<https://doi.org/10.1016/j.chemosphere.2017.12.068>
4. Ren, B., Zhao, Y., Lyczko, N., Nzihou, A.: Current Status and Outlook of Odor Removal Technologies in Wastewater Treatment Plant. *Waste and Biomass Valorization* (2018). doi:10.1007/s12649-018-0384-9
5. Patel, H.: Fixed-bed column adsorption study: a comprehensive review. *Applied Water Science* **9**(3), 45 (2019). doi:10.1007/s13201-019-0927-7
6. Singh, A., Pandey, V., Bagai, R., Kumar, M., Christopher, J., Kapur, G.S.: ZnO-decorated MWCNTs as solvent free nano-scrubber for efficient H<sub>2</sub>S removal. *Materials Letters* **234**, 172-174 (2019). doi:<https://doi.org/10.1016/j.matlet.2018.09.091>
7. Sánchez-González, E., Mileo, P.G.M., Sagastuy-Breña, M., Álvarez, J.R., Reynolds, J.E., Villarreal, A., Gutiérrez-Alejandre, A., Ramírez, J., Balmaseda, J., González-Zamora, E., Maurin, G., Humphrey, S.M., Ibarra, I.A.: Highly reversible sorption of H<sub>2</sub>S and CO<sub>2</sub> by an environmentally friendly Mg-based MOF. *Journal of Materials Chemistry A* **6**(35), 16900-16909 (2018). doi:10.1039/C8TA05400B
8. Hervy, M., Pham Minh, D., Gérente, C., Weiss-Hortala, E., Nzihou, A., Villot, A., Le Coq, L.: H<sub>2</sub>S removal from syngas using wastes pyrolysis chars. *Chemical Engineering Journal* **334**, 2179-2189 (2018). doi:<https://doi.org/10.1016/j.cej.2017.11.162>
9. Wang, J., Wang, L., Fan, H., Wang, H., Hu, Y., Wang, Z.: Highly porous copper oxide sorbent for H<sub>2</sub>S capture at ambient temperature. *Fuel* **209**, 329-338 (2017). doi:<https://doi.org/10.1016/j.fuel.2017.08.003>
10. Sitthikhankaew, R., Chadwick, D., Assabumrungrat, S., Laosiripojana, N.: Effects of humidity, O<sub>2</sub>, and CO<sub>2</sub> on H<sub>2</sub>S adsorption onto upgraded and KOH impregnated activated carbons. *Fuel Processing Technology* **124**, 249-257 (2014). doi:<https://doi.org/10.1016/j.fuproc.2014.03.010>
11. Sharma, S., Verma, A.S.: A theoretical study of H<sub>2</sub>S adsorption on graphene doped with B, Al and Ga. *Physica B: Condensed Matter* **427**, 12-16 (2013). doi:<https://doi.org/10.1016/j.physb.2013.05.019>
12. Zhao, X.H., Hu, Y.S., Zhao, Y.Q., Kumar, L.: Achieving an extraordinary high organic and hydraulic loadings with good performance via an alternative operation strategy in a multi-stage constructed wetland system. *Environ. Sci. Pollut. Res.* **25**(12), 11841-11853 (2018). doi:10.1007/s11356-018-1464-x
13. Liu, R.B., Zhao, Y.Q., Yang, Y., Awe, O.W.: Diagnosis and evaluation of an early-stage green bio-sorption reactor by life cycle assessment. *J. Clean Prod.* **200**, 100-109 (2018).

- doi:10.1016/j.jclepro.2018.07.208
14. Wang, Y., Ren, B.M., Zhao, Y.Q., English, A., Cannon, M.: A comparison of alum sludge with peat for aqueous glyphosate removal for maximizing their value for practical use. *Water Science and Technology*, 450-456 (2018). doi:10.2166/wst.2018.165
  15. Zhao, Y., Liu, R., Awe, O.W., Yang, Y., Shen, C.: Acceptability of land application of alum-based water treatment residuals – An explicit and comprehensive review. *Chemical Engineering Journal* **353**, 717-726 (2018). doi:<https://doi.org/10.1016/j.cej.2018.07.143>
  16. Yang, Y., Zhao, Y.Q., Liu, R.B., Morgan, D.: Global development of various emerged substrates utilized in constructed wetlands. *Bioresource Technology* **261**, 441-452 (2018). doi:10.1016/j.biortech.2018.03.085
  17. Zhao, Y., Ren, B., O'Brien, A., O'Toole, S.: Using alum sludge for clay brick: an Irish investigation. *International Journal of Environmental Studies* **73**(5), 719-730 (2016). doi:10.1080/00207233.2016.1160651
  18. Odimegwu, T.C., Zakaria, I., Abood, M.M., Nketsiah, C.B.K., Ahmad, M.: Review on Different Beneficial Ways of Applying Alum Sludge in a Sustainable Disposal Manner. *Civ. Eng. J.-Tehran* **4**(9), 2230-2241 (2018). doi:10.28991/cej-03091153
  19. Hidalgo, A.M., Murcia, M.D., Gomez, M., Gomez, E., Garcia-Izquierdo, C., Solano, C.: Possible Uses for Sludge from Drinking Water Treatment Plants. *Journal of Environmental Engineering* **143**(3), 7 (2017). doi:10.1061/(asce)ee.1943-7870.0001176
  20. Ahmad, T., Ahmad, K., Alam, M.: Sustainable management of water treatment sludge through 3'R' concept. *J. Clean Prod.* **124**, 1-13 (2016). doi:10.1016/j.jclepro.2016.02.073
  21. Gutiérrez Ortiz, F.J., Aguilera, P.G., Ollero, P.: Modeling and simulation of the adsorption of biogas hydrogen sulfide on treated sewage–sludge. *Chemical Engineering Journal* **253**, 305-315 (2014). doi:<https://doi.org/10.1016/j.cej.2014.04.114>
  22. Long, N.Q., Loc, T.X.: Experimental and modeling study on room-temperature removal of hydrogen sulfide using a low-cost extruded Fe<sub>2</sub>O<sub>3</sub>-based sorbent. *Adsorption* **22**(3), 397-408 (2016). doi:10.1007/s10450-016-9790-0
  23. Kubonova, L., Obalova, L., Vlach, O., Troppova, I., Kalousek, J.: MODELLING OF NO ADSORPTION IN FIXED BED ON ACTIVATED CARBON. *Chem. Process Eng.* **32**(4), 367-377 (2011). doi:10.2478/v10176-011-0029-z
  24. de Franco, M.A.E., de Carvalho, C.B., Bonetto, M.M., de Pelegrini Soares, R., Féris, L.A.: Diclofenac removal from water by adsorption using activated carbon in batch mode and fixed-bed column: Isotherms, thermodynamic study and breakthrough curves modeling. *J. Clean Prod.* **181**, 145-154 (2018). doi:<https://doi.org/10.1016/j.jclepro.2018.01.138>
  25. Rout, P.R., Bhunia, P., Dash, R.R.: Evaluation of kinetic and statistical models for predicting breakthrough curves of phosphate removal using dolochar-packed columns. *Journal of Water Process Engineering* **17**, 168-180 (2017). doi:<https://doi.org/10.1016/j.jwpe.2017.04.003>
  26. Thomas, H.C.: Heterogeneous Ion Exchange in a Flowing System. *Journal of the American Chemical Society* **66**(10), 1664-1666 (1944). doi:10.1021/ja01238a017
  27. Hutchins, R.: New methods simplifies design of activated carbon systems, Water Bed Depth Service Time analysis. *J Chem Eng Lond* **81**, 133-138 (1973).
  28. Yoon, Y.H., Nelson, J.H.: Application of Gas Adsorption Kinetics I. A Theoretical Model for Respirator Cartridge Service Life. *American Industrial Hygiene Association Journal* **45**(8), 509-516 (1984). doi:10.1080/15298668491400197
  29. Klinkenberg, A.: Numerical Evaluation of Equations Describing Transient Heat and Mass Transfer in Packed Solids. *Industrial & Engineering Chemistry* **40**(10), 1992-1994

- (1948). doi:10.1021/ie50466a034
30. Ranz, W.E., Marshall, W.R.: Evaporation from droplets, parts I & II. *Chemical Engineering Progress* **48**(4), 173-180 (1952).
  31. Fuller, E.N., Schettler, P.D., Giddings, J.C.: NEW METHOD FOR PREDICTION OF BINARY GAS-PHASE DIFFUSION COEFFICIENTS. *Industrial & Engineering Chemistry* **58**(5), 18-27 (1966). doi:10.1021/ie50677a007
  32. Nam, H., Wang, S., Jeong, H.-R.: TMA and H<sub>2</sub>S gas removals using metal loaded on rice husk activated carbon for indoor air purification. *Fuel* **213**, 186-194 (2018). doi:<https://doi.org/10.1016/j.fuel.2017.10.089>
  33. Yan, R., Chin, T., Ng, Y., Duan, H., Tee Liang, D., Tay, J.-H.: Influence of Surface Properties on the Mechanism of H<sub>2</sub>S Removal by Alkaline Activated Carbons, vol. 38. (2004)
  34. Dong, Z., Zhao, L.: Covalently bonded ionic liquid onto cellulose for fast adsorption and efficient separation of Cr(VI): Batch, column and mechanism investigation. *Carbohydrate Polymers* **189**, 190-197 (2018). doi:<https://doi.org/10.1016/j.carbpol.2018.02.038>
  35. Zheng, M., Hu, H., Zhang, G., Ye, Z., Chen, X.: Combination of adsorption-diffusion model with CFD for study of desulfurization in fixed bed. *Journal of Environmental Chemical Engineering* **5**(4), 4141-4150 (2017). doi:<https://doi.org/10.1016/j.jece.2017.08.002>
  36. Arim, A.L., Neves, K., Quina, M.J., Gando-Ferreira, L.M.: Experimental and mathematical modelling of Cr(III) sorption in fixed-bed column using modified pine bark. *J. Clean Prod.* **183**, 272-281 (2018). doi:<https://doi.org/10.1016/j.jclepro.2018.02.094>
  37. Aguilera, P.G., Gutiérrez Ortiz, F.J.: Prediction of fixed-bed breakthrough curves for H<sub>2</sub>S adsorption from biogas: Importance of axial dispersion for design. *Chemical Engineering Journal* **289**, 93-98 (2016). doi:<https://doi.org/10.1016/j.cej.2015.12.075>
  38. Ahmed, M.J., Hameed, B.H.: Removal of emerging pharmaceutical contaminants by adsorption in a fixed-bed column: A review. *Ecotoxicology and Environmental Safety* **149**, 257-266 (2018). doi:<https://doi.org/10.1016/j.ecoenv.2017.12.012>
  39. Bandosz, T.J.: On the adsorption/oxidation of hydrogen sulfide on activated carbons at ambient temperatures. *Journal of Colloid and Interface Science* **246**(1), 1-20 (2002). doi:10.1006/jcis.2001.7952
  40. Sigot, L., Ducom, G., Germain, P.: Adsorption of hydrogen sulfide (H<sub>2</sub>S) on zeolite (Z): Retention mechanism. *Chemical Engineering Journal* **287**, 47-53 (2016). doi:<https://doi.org/10.1016/j.cej.2015.11.010>
  41. de Falco, G., Montagnaro, F., Balsamo, M., Erto, A., Deorsola, F.A., Lisi, L., Cimino, S.: Synergic effect of Zn and Cu oxides dispersed on activated carbon during reactive adsorption of H<sub>2</sub>S at room temperature. *Microporous and Mesoporous Materials* **257**, 135-146 (2018). doi:10.1016/j.micromeso.2017.08.025
  42. Nam, H., Wang, S., Jeong, H.R.: TMA and H<sub>2</sub>S gas removals using metal loaded on rice husk activated carbon for indoor air purification. *Fuel* **213**, 186-194 (2018). doi:10.1016/j.fuel.2017.10.089
  43. Zeng, F., Liao, X.F., Hu, H., Liao, L.: Effect of potassium hydroxide activation in the desulfurization process of activated carbon prepared by sewage sludge and corn straw. *Journal of the Air & Waste Management Association* **68**(3), 255-264 (2018). doi:10.1080/10962247.2017.1407378
  44. Siriwardane, I.W., Udangawa, R., de Silva, R.M., Kumarasinghe, A.R., Acres, R.G., Hettiarachchi, A., Amaratunga, G.A.J., de Silva, K.M.N.: Synthesis and characterization of nano magnesium oxide impregnated granular activated carbon composite for H<sub>2</sub>S removal applications. *Materials & Design* **136**, 127-136 (2017).

- doi:10.1016/j.matdes.2017.09.034
45. Yan, R., Liang, D.T., Tsen, L., Tay, J.H.: Kinetics and Mechanisms of H<sub>2</sub>S Adsorption by Alkaline Activated Carbon. *Environmental Science & Technology* **36**(20), 4460-4466 (2002). doi:10.1021/es0205840
  46. Zulkefli, N., Masdar, M., Jahim, J., Harianto, E.: Overview of H<sub>2</sub>S removal technologies from biogas production. *International Journal of Applied Engineering Research* **11**(20), 10060-10066 (2016).
  47. Galera Martínez, M., Pham Minh, D., Nzihou, A., Sharrock, P.: Valorization of calcium carbonate-based solid wastes for the treatment of hydrogen sulfide in a semi-continuous reactor. *Chemical Engineering Journal* **360**, 1167-1176 (2019). doi:10.1016/j.cej.2018.10.169



## Chapter 7

# Simultaneous Hydrogen Sulfide Purification and Wastewater Treatment in a Novel Aerated Alum Sludge-Based Constructed Wetland

This Chapter to be submitted to an international peer-reviewed journal as: **Baiming Ren**, Nathalie Lyczko, Yaqian Zhao, Ange Nzihou. *Simultaneous hydrogen sulfide purification and wastewater treatment in a novel aerated alum sludge based constructed wetland.*

### Abstract

This Chapter deals with an experimental study of alum sludge cakes reused as the substrates of an aerated vertical flow constructed wetlands (Al-VFCWs). It was aimed to enhance the pollutants removal in wastewater and simultaneously eliminating the waste gas (H<sub>2</sub>S). During the six-month trials, three lab-scale parallel columns were operated in batch model and intermittent aerated with 200 ppm H<sub>2</sub>S (column 1), air (column 2) and unaerated (column 3 as blank), respectively. The COD, TN, NH<sub>4</sub>-N, TP and the effluent H<sub>2</sub>S concentration of column 1 were monitored regularly. Results show that all the three columns presented a high removal efficiency (> 98 %) of TP, and a completed removal of H<sub>2</sub>S (100 %) in column 1. The waste gas and air could significantly enhance the removal efficiency of COD of 94.3 ± 3.0, 94.8 ± 1.9 %, and TN of 86.2 ± 14.2, 91.6 ± 5.4 %. In particular, there was no significant difference regarding the COD, TN removal performances between the “waste gas driven” Al-VFCW (column 1) and the aerated Al-VFCW (column 2). It demonstrated that the intermittent waste gas (H<sub>2</sub>S) aerated Al-VFCW would be a promising “wise choice” to simultaneous wastewater purification and waste gas (H<sub>2</sub>S) abatement in the same unit.

### 7.1 Introduction

Traditionally, the primary goal of wastewater treatment is to remove the various pollutants (i.e. organic and nutrients) from wastewater and reduce the environmental impact on receiving waters. It is common that the wastewater treatment processes also release unpleasant odors and pose a threat to public health, as most of the wastewater treatment plants lack odor abatement units [1]. Furthermore, odors emanating from wastewater treatment processes are composed of a mixture of various chemical compounds, including ammonia (NH<sub>3</sub>), hydrogen sulfide (H<sub>2</sub>S) and VOCs. Seventy eight kinds of main odor-producing compounds relating to wastewater collection and treatment facilities have been reported [2]. In particular, hydrogen sulfide (H<sub>2</sub>S) is considered as the most important cause for both odor emission and even corrosion in wastewater collection and treatment facilities [3].

In literature [4-6], various technologies including physical/chemical and biological methods have been applied for wastewater odor abatement to avoid the annoyance and to meet the strict regulations. Generally, the physical/chemical treatment options have technical-economical drawbacks such as high operating and processing costs to change the sorbents regularly, the generation of hazardous byproducts in the leaching of chemical scrubbing, as well as its high pressure/temperature requirements, etc. [7,8]. Therefore, they are relatively impractical for abatement of odor both in economic and environmental terms. Moreover, recent research on odor control has centered on development of novel and environmentally benign treatment methods that can handle odor via simple, efficient, and effective processes [5,9,10]. Biofiltration (BF) which is indisputably the most commonly employed biotechnology for odor treatment was intensively studied in the last decades [5]. In BF, the humified odorant is forced through a packed bed on which the microorganisms are attached as a biofilm. The pollutants are sorbed by the filter material and degraded by the biofilm [3]. It aims maximizing odor removal efficiency by utilizing coherent, efficient, and robust microorganisms and optimized design parameters with ameliorated processing costs and energy requirements. However, there is one concern that BF presented the large land requirements which still need further improvement [9].

On the other hand, CWs which are defined as man-made systems, have been widely used in the last decades as an efficient, cost-effective and sustainable wastewater treatment technology from vast scattered rural and residential areas etc. [11]. In particular, vertical flow constructed wetlands (VFCWs) was developed in which the beds are pulse loaded with a large amount of water to temporarily flood the surface of the bed [12,13]. Moreover, VFCWs seems to be a better choice due to the low footprint and high efficiency for pollutant removal, compare with the other type of CWs, it only requires 1-3 m<sup>2</sup>/PE [11,14]. Nevertheless, the nitrogen removal efficiency remained around 50 % in most operated VFCWs under a nitrogen loading rate of 0.6-2.0 g m<sup>-2</sup> d<sup>-1</sup> (Hu et al. 2012), which is still far from satisfactory and failed to meet the increasingly stringent nitrogen discharge standards [14,15]. Thus, improving the internal dissolved oxygen (DO) concentration is very important for regulating the nitrification process and enhancing the efficiency of N biological removal, to improve the overall removal efficiency in VFCWs.

Hitherto, the arise from worldwide research directions over the last decade was to focus on how to improve nitrogen removal performance via intensified strategies [16], such as recirculation, artificial aeration, tidal flow, flow direction reciprocation, etc. [12,17]. In especially, artificial aeration has been proved to be a good solution to create aerobic condition favorable of nitrification. Earlier, continuous artificial aeration strategies were adopted in most studies [18,19]. However, it inhibits denitrification because of lacking anoxic zone and which could decrease the removal of total nitrogen (TN). On the other hand, intermittent aeration has been proved to be an efficient method to promote nitrification efficiency, as the alternative aerobic and anaerobic environments were created, which is benefit to both of nitrification and denitrification and enhance the removal efficiency of TN [20,21]. Unfortunately, the operation costs of aeration remain questionable [17]. Since the decision to aerated leads to the additional

costs for operation and maintenance of the facility. Aeration is only justified when its lifecycle cost is sufficiently offset by the reduction in the capital cost by the net savings of reduced wetland area size [12].

Therefore, it is of great interest to integrated BF with intermittent aerated VFCWs, i.e. using waste gas for VFCWs' aeration, in order to achieve the simultaneous waste gas purification and waste water treatment purposes. Significantly, to develop the novel "waste gas" driven VFCWs could not only partial remedy the high operation costs of the aeration in VFCWs, but also reduce the extra land requirement for the waste gas (odor) treatment. It also could propose a "win-win" strategy for the upgrade of the existing WWTPs, by adding a series of novel aerated VFCWs at the end of existing plants to achieve the enhanced wastewater performance and odor abatement at the same units. Thus, this study developed three parallel novel aerated alum sludge based unplanted VFCWs, which were aerated with air, 200 ppm H<sub>2</sub>S and unaerated (as blank), respectively, to investigate the wastewater treatment performance of the novel alum sludge based VFCWs as well as the H<sub>2</sub>S removal efficiency.

## **7.2 Material and methods**

### **7.2.1 Alum sludge based VFCW configuration**

Alum sludge cakes were taken from the Carmaux water treatment plant which located in Tarn, France, the plant produces and supplies 3014 m<sup>3</sup>/day drinking water by treating the reservoir water using aluminum chloride hydroxide sulfate (HYDREX 3531 Veolia, France) as coagulant and the treated water serving for 7,000 consumers. The characterization of alum sludge cakes can be found in Chapter 2.

As illustrated in Figure 7.1, the three columns were made by plexiglass with the diameter of 15 cm, height of 100 cm. The aeration diffusers were erecting joint with the bottom of two of the columns, the height of the aeration diffusers was 10 cm from the bottom, see Figure 7.1a. The outlet valves were installed at 5 cm from the bottom of each columns, see Figure 7.1b.

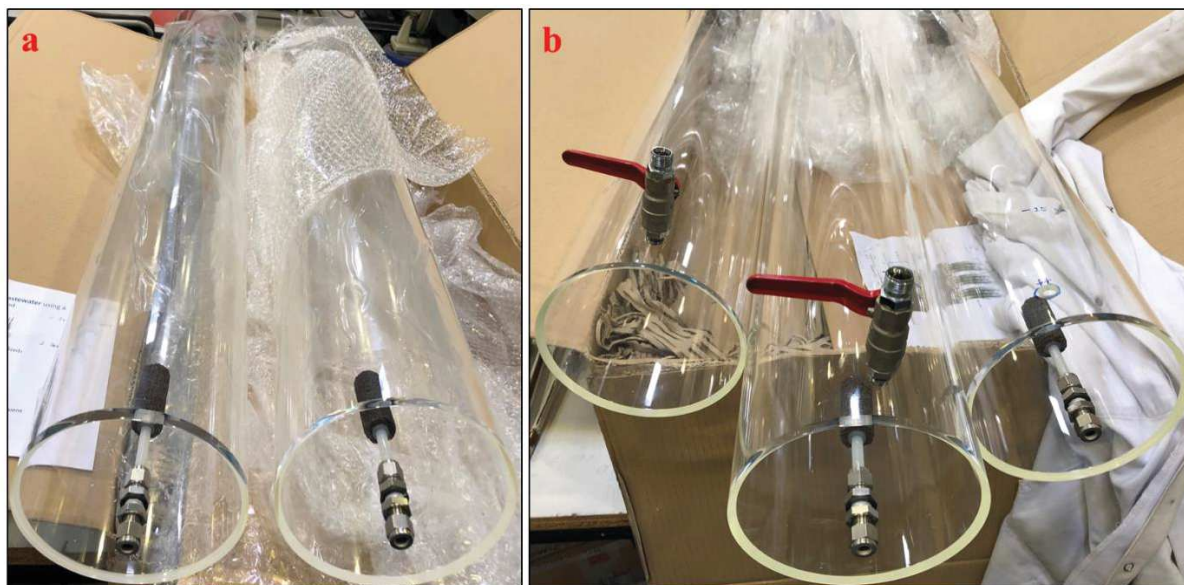


**Figure 7.1** The columns setup; (a) the aeration diffuser of the column, (b) the outlet valves of the columns

After the aeration diffusers and outlet valves installation (as illustrated in Figure 7.2a), the three columns were filling into substrates, as shown in Figure 7.2 b and c. Firstly, the prewashed gravel with the particle diameter of 2-4 cm was filled into the bottom as the support layer with a height about 15 cm, as shown in Figure 7.2b. Afterwards, the same quantity of alum sludge cakes with the particle diameter of 3-5 cm were filled in the three columns as the main wetland medium layer, with the height of 80 cm, see Figure 7.2c.

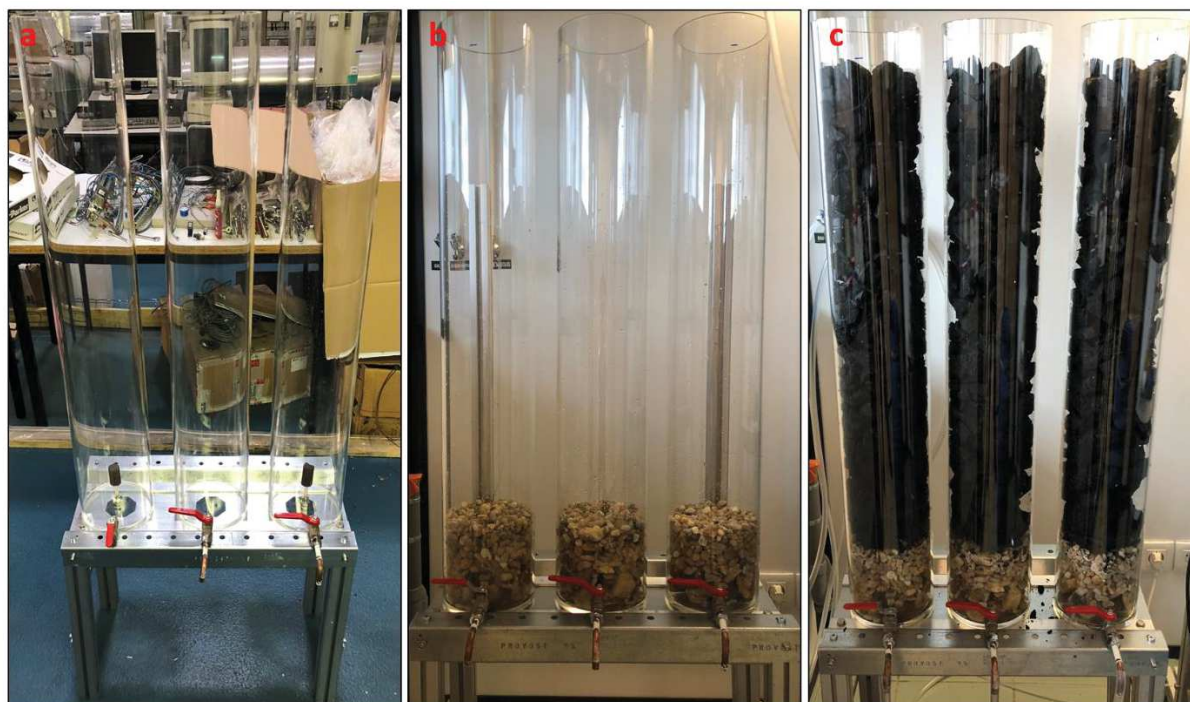


**Figure 7.2** Filling of the columns, (a) the empty columns; (b) the gravel layer in the columns; (c) the substrates (gravel + alum sludge cake) of the columns



After the three columns were filled with substrates, the system was seeded with activated sludge which was collected from the Graulhet (France) municipal wastewater treatment plant (the details of this WWTP can be found in Chapter 5) for two weeks before it was formally operated. The seeding process was shown in Figure 7.3a, it can be observed that the activated sludge flocs was settled on the surface of alum sludge cakes as well as the gravel. Before the experiment was formally operated, the three alum sludge-based aerated VFCWs (Al-VFCWs) were covered with black plastics film (as illustrated in Figure 7.3b), in order to prevent the algae etc. growth on the walls of the columns which could easily cause the constructed wetlands clogging and influence the outlet sampling.



**Figure 7.3** The experimental process (a) the activated sludge seeding process; (b) the experimental formal running process

The laboratory scale Al-VFCW with a total volume of 16.8 L and initial porosity of 42 % (7 L liquid contained). The scheme of experiment operation was shown in Figure 7.4. Influent was introduced into the column from the top while effluent was drained from the bottom by peristaltic pumps. Aeration was supplied with a diffuser placed on the support layer and controlled with an air flow meter. The experiment was run from October 2018 to April 2019 (Six months) under room temperature.

Before this experiment, determination of the optimal aeration strategies was carried out, by applying minimum aeration times and aeration rates in Al-VFCW, in order to achieve the highest TN removal efficiency. The results indicated that the best TN removal efficiency (85 %)

was reached at the aeration time and rate of 4 h/d and 20 L/h, respectively. Thus, the system was then decided to operate in batch mode and aerated four hours (2 h + 2 h) per day at an airflow rate of 20 L/h (i.e. filling influent from 8:00 am, aerated from 8:30 to 10:30 and next aeration period was from 16:30 to 18:30). Column 1 was intermittently aerated with waste gas, which is 200 ppm H<sub>2</sub>S based on air and stored in a steel cylinder; column 2 was intermittently aerated with air, the air is from the air pipe of lab, which is driven by a mechanical air compressor; while column 3 was unaerated and served as a control. Synthetic wastewater (as influent) was prepared from tap water, the composition of synthetic wastewater is as follows: NaAC 0.48 g/L, NH<sub>4</sub>Cl 0.12 g/L, KH<sub>2</sub>PO<sub>4</sub> 0.04 g/L, CaCl<sub>2</sub> 0.015 g/L, MgSO<sub>4</sub> 0.012 g/L, with the COD, TN, TP approximately of 300, 30, 10 mg/l, respectively.

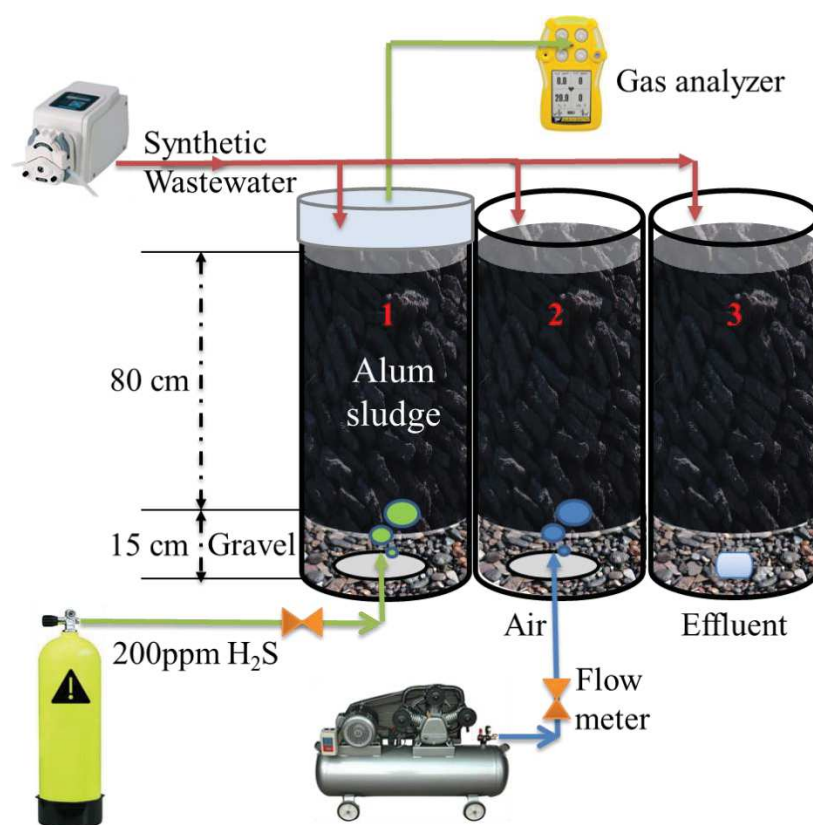


Figure 7.4 Three parallel Al-VFCWs configuration

### 7.2.2 Analysis

Water samples were taken from the influent and effluent of the Al-VFCWs every 3 days and each time at 8:00 am, to analyze the transformation of organic matter (as COD), total phosphorus (TP), total nitrogen (TN) and ammonia-nitrogen (NH<sub>4</sub>-N). Merck Nova 60 spectrophotometer were employed to analyze the COD according to its standard operating procedures; Shimadzu VCPH 5050A was positioned for TN analyzing; NH<sub>4</sub><sup>+</sup>-N was analyzed by ionic chromatography (Dionex ICS 3000); TP were determined by Inductively Coupled Plasma-Atomic Emission Spectroscopy (ICP-AES) on HORIBA Jobin Yvon Ultima 2.



Online H<sub>2</sub>S effluent concentration was analyzed during the “2h + 2h” aeration period each day. A plexiglass cap (as shown in Figure 1) with rubber seal ring inside to prevent the H<sub>2</sub>S leakage was tightly covered on the Column 1. The output H<sub>2</sub>S concentration was monitored and record every two minutes using a gas analyzer from BW Technologies (Gas Alert QUATTRO). After the aeration, the cap was immediately removed to keep the surface water contact with atmosphere.

### 7.2.3 Data interpretation

Pollutant removal efficiency for the trials was calculated as a cumulative percent removal, RE, between the influent and the effluent Eq. (7.1), assuming that the system was in equilibrium at the time of sample collection:

$$RE = \frac{C_i - C_o}{C_i} * 100 \quad (7.1)$$

where:

RE = pollutant removal efficiency (%)

C<sub>i</sub> = mean influent concentration across triplicate tests (mg/L)

C<sub>o</sub> = mean effluent concentration across triplicate tests (mg/L)

## 7.3. Results and discussion

### 7.3.1 Pollutants removal performance of the three columns

The COD removal performance of the three columns was shown in Figure 7.5. After one month's acclimatization, three parallel AI-VFCWs showed stable COD removal performance. The average effluent COD concentrations of column 1, 2, 3 were  $17.27 \pm 8.51$ ,  $15.99 \pm 5.19$ ,  $217.47 \pm 31.66$  mg/L, respectively, which are corresponding to the columns aerated with H<sub>2</sub>S, air and the blank column. It can be observed that the COD removal performance in the traditional VFCWs (column 3 without aeration) was not satisfied during the six-month's trials. Indeed, different studies clearly revealed that in non-aerated VFCWs the level of DO was very low (0.12-1.3 mg/L) [12], thus the organic matter cannot be well oxidized and removed in unaerated AI-VFCWs (column 3). On the other hand, it can be observed that intermittent aeration (column 1 and 2) significantly enhanced the COD treatment performance by 92.1 and 92.6 %, respectively, compare with the unaerated AI-VFCW (column 3). This is due to the intermittent oxygen supply in column 1 and 2 created an aerobic-anaerobic environment, as organic compounds are degraded by bacteria under this (aerobic and anaerobic) conditions [11]. It worth to noted that the COD removal performance of column 1 (aerated with H<sub>2</sub>S) presents almost the same level with column 2 (aerated with air), it indicated that H<sub>2</sub>S aeration have very limited influence on the COD effluent concentration, as it can be observed that the six-months' average effluent COD concentration of column 1 (aerated with H<sub>2</sub>S ) was just 7 % higher than the column 2 (aerated with air).

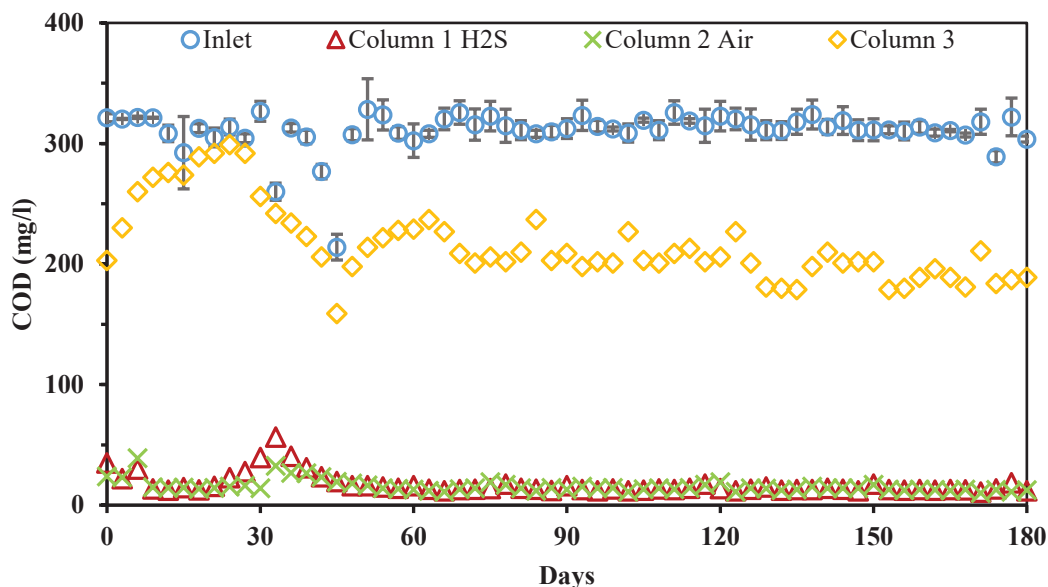
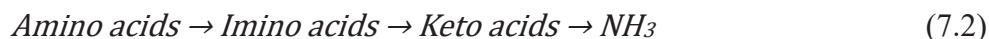


Figure 7.5 COD removal performance in the three columns

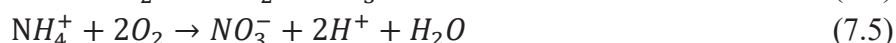
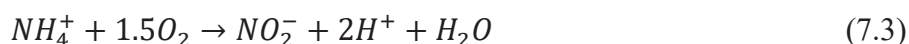
The TN removal performance of the three parallel columns was shown in Figure 7.6. The average effluent TN concentration of Column 1, 2, 3 were  $3.79 \pm 2.44$ ,  $2.75 \pm 1.55$ ,  $30.46 \pm 0.84$  mg/L respectively. It has been demonstrated by Vymazal [15], the nitrogen transformation in CWs mainly includes volatilization, ammonification, nitrification, denitrification, plant uptake and matrix adsorption.

In fact, not all the processes occur in all types of CWs and the magnitude of individual processes varies among types of CWs, For example, volatilization may be a significant route for nitrogen removal in CWs only with open water surface where algal assemblages can create high pH values during the day through their photosynthetic activity. Thus, it is near zero in VFCWs due to the small open water surface. Ammonification (mineralization) is the process where organic N is biologically converted into ammonia. The oxidative deamination can be written as:



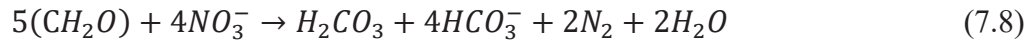
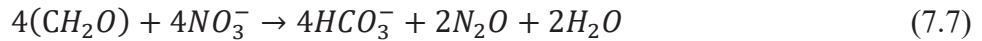
Kinetically, ammonification proceeds more rapidly than nitrification.

Nitrification is defined as the biological oxidation of ammonium to nitrate with nitrite as an intermediate in the reaction sequence, which has been typically associated with the chemoautotrophic bacteria. It can be described as the following Eqs. [11,12]

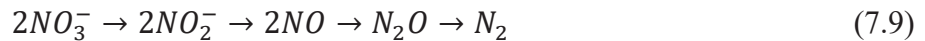


Denitrification is defined as the process in which nitrate is converted into dinitrogen via

intermediates nitrite, nitric oxide and nitrous oxide. It is illustrated by the following Eqs.[15]:



This reaction is irreversible, and occurs in the presence of available organic substrate only under anaerobic or anoxic conditions, where nitrogen is used as an electron acceptor in place of oxygen. Additionally, it is generally agreed that the actual sequence of biochemical changes from nitrate to elemental gaseous nitrogen is:



Moreover, the vital stage of TN removal is during the nitrification-denitrification processes, the conversion of NH<sub>4</sub>-N to NO<sub>3</sub>-N and NO<sub>2</sub>-N via nitrification, and the denitrification must transform the NO<sub>3</sub>-N and NO<sub>2</sub>-N into N<sub>2</sub> to finish N removal completely. However, in the unaerated Al-VFCW (column 3), the DO level was always low, causing an anaerobic environment and thus, may have resulted in negligible nitrification process, as a result, the TN removal performance is limited. On the other hand, compare with the column 3, the intermitted aeration in column 1 and 2 significantly increasing the TN removal performance of 87.6, 91.0 %, respectively. Moreover, the TN removal performance of column 1 and 2 were almost in the same level and no significant influence was observed. In addition, nitrification-denitrification can be limited by various factors such as excess inorganic N (including nitrate and nitrite) in effluent, excess oxygen and an insufficient organic carbon source [22], these reasons were hypothesized for the turbulence between day 27 and 45.

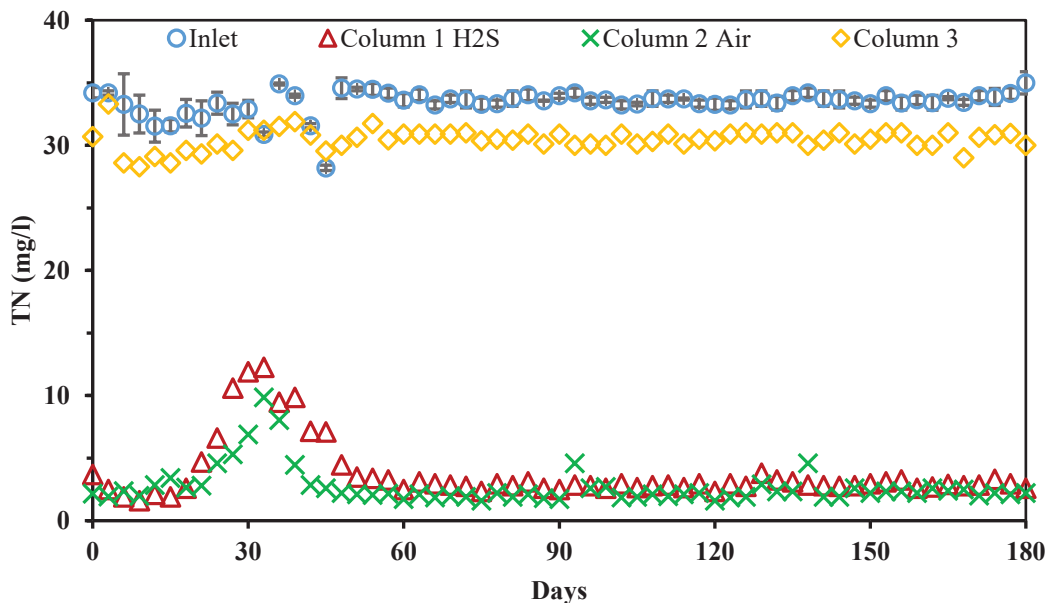


Figure 7.6 TN removal performance in the three columns

The NH<sub>4</sub>-N removal performance of the three columns was presented in Figure 7.7. The average NH<sub>4</sub>-N effluent concentration of column 1, 2, 3 were  $1.45 \pm 2.98$ ,  $0.60 \pm 1.66$ ,  $27.34 \pm 1.58$  mg/L, respectively. Aforementioned, nitrification is indispensable and the primary step when NH<sub>4</sub>-N was transformed into NO<sub>3</sub>-N for the TN elimination. An efficient nitrification often requires high DO concentration, thus the NH<sub>4</sub>-N removal performance in column 1 and 2 are 94.7, 97.8 % higher than the column 3. It also reveals that the aeration strategy is successful, and the nitrification process was sufficient to convert NH<sub>4</sub>-N to NO<sub>3</sub>-N and NO<sub>2</sub>-N.

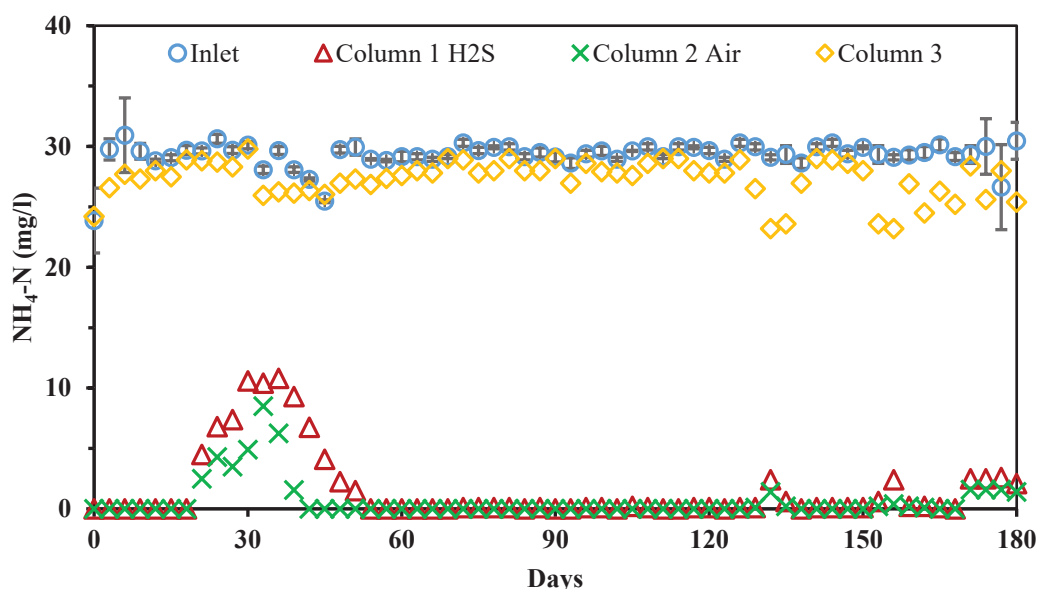


Figure 7.7 NH<sub>4</sub>-N removal performance in three columns

The TP removal performance of the three columns was illustrated in Figure 7.8. The average TP effluent concentration in column 1, 2, 3 were  $0.18 \pm 0.20$ ,  $0.15 \pm 0.14$ ,  $0.13 \pm 0.16$  mg/L, respectively. The major processes responsible for phosphorus removal in CWs are adsorption on the substrate media, chemical precipitation, and assimilation into microbial and plant biomass [23]. Furthermore, precipitation can refer to the reaction of phosphate ions with metallic cations such as Fe, Al, Ca or Mg, forming amorphous or poorly crystalline solids. These reactions typically occur at high concentrations of either phosphate or the metalloid cations. A variety of cations can precipitate phosphate under certain conditions. Some important mineral precipitates in the wetland environment are: Apatite  $\text{Ca}_5(\text{Cl,F})(\text{PO}_4)_3$ , Hydroxyl apatite  $\text{Ca}_5(\text{OH})(\text{PO}_4)_3$ , Variscite  $\text{Al}(\text{PO}_4) \cdot 2\text{H}_2\text{O}$ , Strengite  $\text{Fe}(\text{PO}_4) \cdot 2\text{H}_2\text{O}$ , Vivianite  $\text{Fe}_3(\text{PO}_4)_2 \cdot 8\text{H}_2\text{O}$  and Wavellite  $\text{Al}_3(\text{OH})_3(\text{PO}_4)_2 \cdot 5\text{H}_2\text{O}$ . In addition to direct chemical reaction, phosphorus can co-precipitate with other minerals, such as ferric oxyhydroxide and the carbonate minerals, such as calcite (calcium carbonate),  $\text{CaCO}_3$ .

It can be observed that a distinctive superior performance regarding P removal in all the three columns, and this is attributed to the P removing ability of the alum sludge used as substrate in the system, and the adsorption and precipitation reactions of P with aluminum ( $\text{Al}^{3+}$ )

in the alum sludge. However, in most of the CWs, it is often a challenge to achieve concurrent high removal efficiencies for P and organic matters, the efficiency of P removal is usually low compared to other parameters such as COD [24].

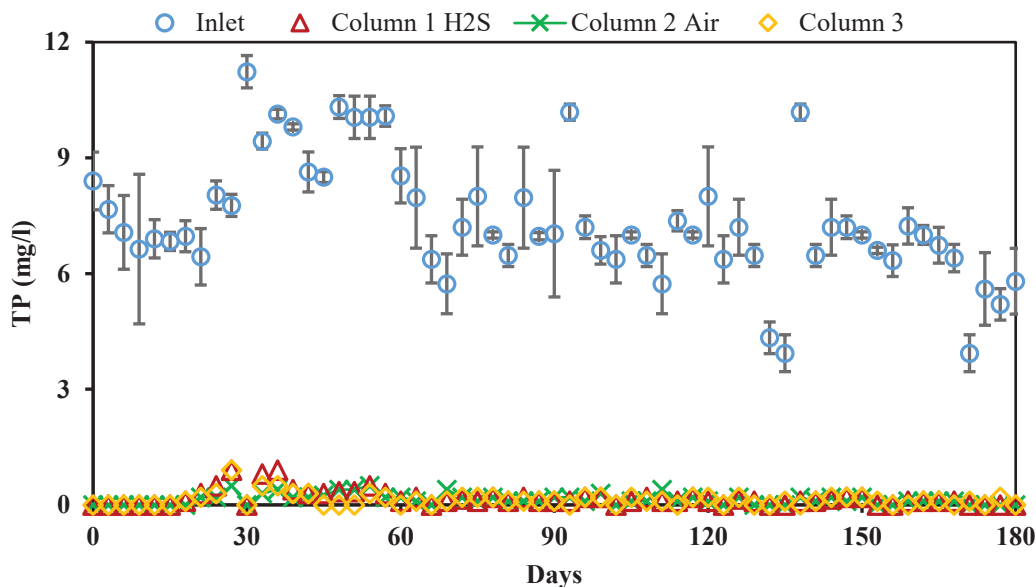


Figure 7.8 TP removal performance in three columns

### 7.3.2 The overall removal efficiency of pollutants in three columns

The six-month's average RE of COD, TN, NH<sub>4</sub>-N, TP of the three columns were shown in Figure 7.9. The RE of COD in column 1, 2, 3 were  $94.3 \pm 3.0$ ,  $94.8 \pm 1.9$ ,  $30.2 \pm 11.0$  %, respectively. Compared with the unaerated AI-VFCW (column 3), the introduction of waste gas and air into the AI-VFCWs greatly improved COD removal efficiency. Generally, the non-aerated VFCWs could achieve of 61-80 % COD removal [12,25,26], however in this study the column 3 (unaerated) presented a relatively low RE of COD, this is possibly due to this unaerated AI-VFCW (column) was single stage, the wastewater cannot have sufficient time contact with the biofilm which are on the surface of alum sludge, and resulted in a low RE of COD. On the other hand, the intermittent aeration with H<sub>2</sub>S and air could achieve 64.1 and 64.6 % additional RE of COD. In particular, no significant difference in COD removal was observed between column 1 and 2. It demonstrated that the H<sub>2</sub>S aeration have no influence on the COD removal, it could achieve almost the same RE as aerated AI-VFCW. Moreover, the average RE of COD of intensified CWs in literature were estimated at  $84 \pm 12$  % [12], it indicated that the H<sub>2</sub>S aerated AI-VFCWs was even more efficient than the average level of intensified CWs such as effluent recirculation and tidal flow CWs.

The TN RE of column 1, 2, 3 were  $86.2 \pm 14.2$ ,  $91.6 \pm 5.4$ ,  $8.8 \pm 3.8$  %, respectively. This result indicating that the introduction of waste gas and air could effectively develop alternate

aerobic and anaerobic conditions in the Al-VFCWs to improve TN removal. In literature, various studies clearly demonstrated a large variation in nitrogen removal of non-aerated VFCWs, the RE was ranging from 26 to 65 % [12]. In this study, the column 3 (unaerated) only presented an average RE of  $8.8 \pm 3.8$  % during the six-months' trials. The reason has been discussed in above section, as the DO level in column 3 was always low, causing an anaerobic environment and thus, may have resulted in negligible nitrification process, as a result, the TN removal performance is limited. However, in column 1 and 2, the additional TN RE was 77.4, 82.8 %, respectively, and compare with the study reported by [26], it was higher than the additional removal of 64 % of TN in an traditional intermittent aeration VFCW. Moreover, [25] also reported that a 63 % additional removal of TN was achieved in a VFCW with intermittent aeration fed with domestic wastewater. Thus, it indicated that the H<sub>2</sub>S aeration in Al-VFCW could achieved a high TN RE, even higher than the traditional intermittent aeration VFCWs. However, the six months' average RE of TN in column 1 was 5.4 % lower than the column 2, this is due to the long term H<sub>2</sub>S feeding, in the presents of microorganisms which could oxidize sulfides such as Thiobacillus bacteria, the reaction products (e.g., sulfates) will then be converted into sulfuric acid in the wastewater, and sulfuric acid may inhibit microbial activity and decrease the mass transfer rate, resulted in a reducing removal efficiency of TN [7]. Significantly, this result was contrary with [27], it pointed out that the best TN RE ( $51.88 \pm 3.42$  %) was observed in the waste gas aerated VFCW, and the worst TN removal performance ( $23.14 \pm 2.12$  %) was in the VFCW intermittently aerated with air. The reason is from the different aeration strategies, in this study intermittently aerated at an airflow rate of 20 L/h for two cycles in a day, and each cycle was 120 mins could successfully create the nitrification-denitrification environment and facilitating the TN removal.

The NH<sub>4</sub>-N RE of the three columns were  $92.1 \pm 18.2$ ,  $97.8 \pm 6.5$ ,  $6.6 \pm 5.9$  % respectively. It is worth noted that in aeration Al-VFCWs (column 1, 2), the RE of NH<sub>4</sub>-N was over 90 %, it indicated that the nitrification process was successful. However, in the unaerated Al-VFCW (column 3), the DO level was always low, causing an anaerobic environment and, thus, may have resulted in negligible nitrification. Moreover, the six-months' average RE of NH<sub>4</sub>-N in column 1 (aerated with H<sub>2</sub>S) was slightly lower (5.7 %) than the average RE of NH<sub>4</sub>-N in column 2 (aerated with air), since the long term biological H<sub>2</sub>S degrade processes could generated sulfuric acid, which may inhibit microbial activity and resulted in a lower RE of NH<sub>4</sub>-N in column 1. This is contrary with the study of Zhang et al. [27], which demonstrated that the waste gas aerated system has better nitrification performance. This is possibly due to the waste gas composition and concentration, the waste gas from the sequencing batch reactor (SBR) with low concentration of H<sub>2</sub>S ( $0.0045 \pm 0.0006$  mg/m<sup>3</sup>) was applied to their VFCW, and this low concentration waste could be used by microbial community to reproduction and led to an optimized nitrogen transformation processes.

Regarding TP removal, the average RE of the three columns were  $98.1 \pm 1.7$ ,  $98.1 \pm 1.7$ ,  $98.3 \pm 1.9$  %, respectively. No significant differences were found among the three columns, indicating that artificial aeration had a slight effect on TP removal. Likewise, [23] found that artificial aeration did not have significant influence on P removal. The previous studies suggest



that in all types of CWs, the removal of TP varied between 40 and 60 % with removed load ranging between 45 and 75 g P m<sup>2</sup>/year depending on CW types and flow loading [15]. The superior performance of TP removal was attributed to the alum sludge, which has been intensively investigated as a media for various CWs in the literature [28].

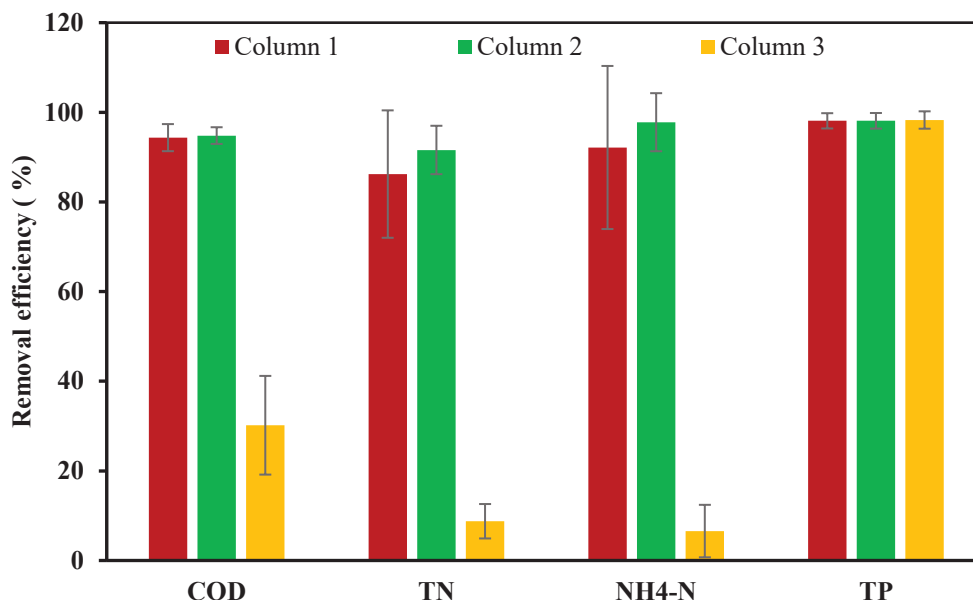


Figure 7.9 Overall removal efficiency of COD, TN, NH<sub>4</sub>-N and TP in three columns

### 7.3.3 H<sub>2</sub>S removal efficiency

In previous studies, it was found that acclimatization could shorten or even eliminate the biofilter start-up phase [29]. Thus, before the H<sub>2</sub>S was introduced to the Column 1, air was supplied at a flow rate of 20 L/h and 4 hours per day for two weeks to acclimatize and develop the bio-film in column 1 and 2. During this period, the column 1 and 2 were running as the same aerated VFCWs.

After the two weeks' acclimatization, 200 ppm H<sub>2</sub>S based on air was introduced into column 1 at the same flow rate of 20 L/h, the H<sub>2</sub>S concentrations in the outlet was continuously recorded during the 4 hours aeration period every day. As illustrated in Figure 7.10, the H<sub>2</sub>S was completely removed during the "2h+2h" aeration periods each day. In particular, this complete H<sub>2</sub>S removal efficiency was keep stable on each day and all through the six-month's trials. To double confirm with this completed H<sub>2</sub>S removal efficiency, at each aeration cycle, the gas analyzer was replaced with gas sampling bags for 15 mins, by collecting the effluent gas and for  $\mu$ -GC analysis (My GC, Agilent), the results also shown that a completed removal of H<sub>2</sub>S in each cycle.

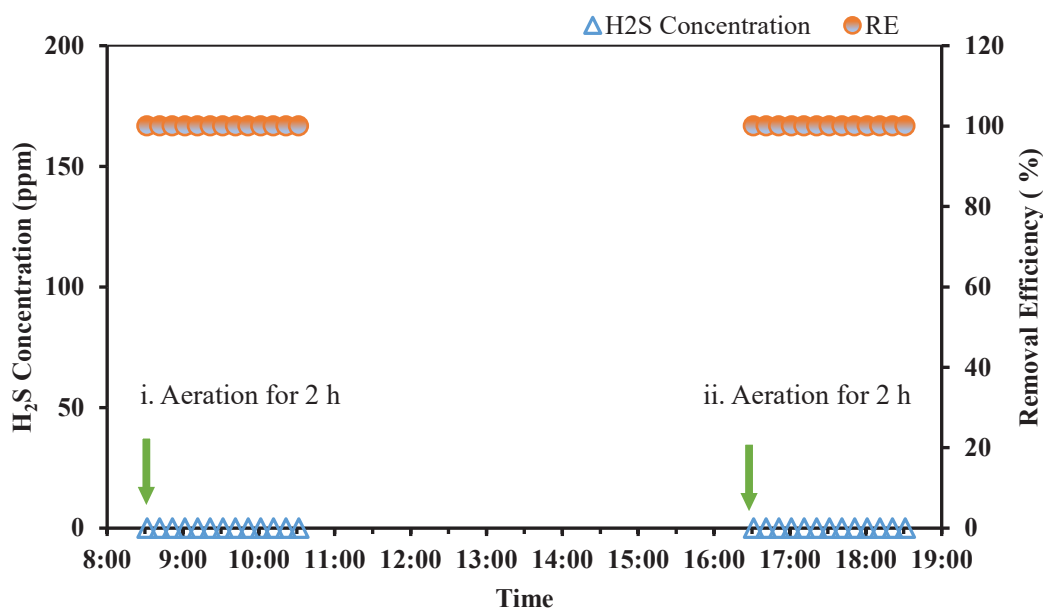


Figure 7.10 H<sub>2</sub>S effluent online analysis and removal efficiency

In this study, the Al-VFCW (column 1) acted as a biofilter to purify H<sub>2</sub>S. When the H<sub>2</sub>S researches the wastewater, the sulfide was adsorbed on the media surface with subsequent microbial degradation. Various bacteria have been used in bioprocesses to decompose H<sub>2</sub>S to elemental sulfur based on their functions as biocatalysts, such as Phototrophic bacteria, also known as green sulfur bacteria (GSB), chemotrophs and Xanthomonas, etc [29].

Moreover, from the literature [7,30], bioconversion of H<sub>2</sub>S in presence of oxygen as a main electron acceptor can be described by Eqs. (7.10)-(7.12):



The intermediate biodegradation products of H<sub>2</sub>S (such as HS<sup>-</sup> and S<sup>2-</sup>) are utilized by microorganisms as energy sources, contributing to environmentally benign and self-reliant operation [7]. Sulfate (SO<sub>4</sub><sup>2-</sup>) is the main sulfur species that is formed during the bioconversion of H<sub>2</sub>S [31]. It also has been reported by [7] that the accumulation of sulfate may inhibit microbial activity and decrease the mass transfer rate of H<sub>2</sub>S into the biofilm (due to reduced pH), reducing removal efficiency significantly. However, the effluent from the Al-VFCW (column 1) can mitigate SO<sub>4</sub><sup>2-</sup> accumulation problems and also be effective to avoid the inhibitory effect caused by SO<sub>4</sub><sup>2-</sup>, since the SO<sub>4</sub><sup>2-</sup> is washed out by the effluent. Moreover, the end products of H<sub>2</sub>S biodegraded processes (sulfur or sulfate) are non-hazardous, and sulfate can be discharged directly into the sea or brackish receiving waters [8].

### **7.3.4 Alum sludge as a media for H<sub>2</sub>S abatement**

Although alum sludge cakes have been used as a substrate in CWs for a decade and it has been proved to be an efficient media for pollutant removal from wastewater, to the best of our knowledge, it is the first time that alum sludge cakes were used as a media for H<sub>2</sub>S abatement and wastewater treatment, simultaneously. Indeed, it has been widely acknowledged that biofilter media should have a high surface area, a low-pressure drop, excellent moisture retention, and high durability, the support medium is also expected to provide nutrients and an environment for an active biolayer including a diverse community of microbes [7]. It is worth to note that alum sludge has a higher specific surface area, range from 40-300 m<sup>2</sup>/g, depends on the raw water quality and treatment processes; the porous structure and contains carbon as well as various metal elements like Al, Ca, Fe, etc., which has been discussed in Chapter 2. Thus, it is reasonable to believe that alum sludge could be a good material for the novel VFCWs media, due to the inherent characteristics of alum sludge, and this study have demonstrated that alum sludge could be used as a novel VFCWs media for H<sub>2</sub>S abatement.

In particular, the high removal efficiency of TN achieved in column 1 and 2 during the six-months trials, which due to the nitrification and denitrification processes. It indicated that there would have been large numbers of nitrifying bacteria in the columns and which means the alum sludge cakes could provide a good biolayer and nutrition to microbial communities. On the other hand, the microbial activity of the columns could therefore have been reflected by the conversion of NH<sub>4</sub>-N to NO<sub>x</sub>-N and then to N<sub>2</sub>. Moreover, a biofilter media should also have a large buffer capacity to avoid pH variations. Additionally, they should be able to homogeneously distribute water and air in the bed to create a suitable microenvironment for microbial growth [32]. In this study, the alum sludge cakes used in three columns were at basic pH, and no acidification was found to occur. As higher H<sub>2</sub>S removal efficiencies have been found using basic media than acidic media [3]. In fact, organic materials (e.g., compost, wood chip, pine bark, and peat) have been used successfully as packing media for H<sub>2</sub>S biofiltration given the availability of indigenous nutrients and microbes [5]. Nevertheless, these organic packing media might suffer compaction, causing pressure drops and non-uniform distributions of air and water. Thereafter, inorganic materials (such as pozzolan, lava, and expanded schist) are developed as packing media due to their mechanistic advantages [7]. However, alum sludge cakes would be a promising biofiltration media, as it presents both the merits of organic and inorganic packing media, and significantly it is a “ready to use” material in towns, cities and metropolis.

### **7.4 Conclusions**

This study developed a novel alum sludge based aerated VFCW, aims to provide an effective method to enhance overall Al-VFCWs performance and eliminate waste gas pollution, such as H<sub>2</sub>S. Through the six-month trials, the high removal efficiency of TP (> 98 %) was achieved in all the three columns, it was contribution to the alum sludge media. In addition, the H<sub>2</sub>S was completely removed (100 %) through each day's operation. Moreover, the introduction of waste

gas and air could significantly enhance the removal efficiency of COD and TN, compare with the unaerated AI-VFCW (column 3). In particular, there was no significant difference regarding the COD, TN removal performances between the “waste gas driven” AI-VFCW (column 1) and the aerated AI-VFCW (column 2). It showed that intermittent aerated AI-VFCW using waste gas would be a potential “wise choice” to intensify pollutant removal performance for the wastewater. However, the application of this novel aerated AI-VFCW in full-scale and long-term system needs to be further research. Overall, this study firstly demonstrated that alum sludge cakes could be a promising low-cost media in novel aerated VFCWs for H<sub>2</sub>S removal and wastewater treatment, simultaneously.

## Bibliography

1. Ren, B., Zhao, Y., Lyczko, N., Nzihou, A.: Current Status and Outlook of Odor Removal Technologies in Wastewater Treatment Plant. *Waste and Biomass Valorization* (2018). doi:[10.1007/s12649-018-0384-9](https://doi.org/10.1007/s12649-018-0384-9)
2. Talaiekhozani, A., Bagheri, M., Goli, A., Talaei Khoozani, M.R.: An overview of principles of odor production, emission, and control methods in wastewater collection and treatment systems. *J. Environ. Manage.* **170**, 186-206 (2016). doi:<https://doi.org/10.1016/j.jenvman.2016.01.021>
3. Omri, I., Aouidi, F., Bouallagui, H., Godon, J.-J., Hamdi, M.: Performance study of biofilter developed to treat H<sub>2</sub>S from wastewater odour. *Saudi Journal of Biological Sciences* **20**(2), 169-176 (2013). doi:<https://doi.org/10.1016/j.sjbs.2013.01.005>
4. Burgess, J.E., Parsons, S.A., Stuetz, R.M.: Developments in odour control and waste gas treatment biotechnology: a review. *Biotechnology Advances* **19**(1), 35-63 (2001). doi:[https://doi.org/10.1016/S0734-9750\(00\)00058-6](https://doi.org/10.1016/S0734-9750(00)00058-6)
5. Barbusinski, K., Kalemba, K., Kasperczyk, D., Urbaniec, K., Kozik, V.: Biological methods for odor treatment – A review. *J. Clean Prod.* **152**, 223-241 (2017). doi:<https://doi.org/10.1016/j.jclepro.2017.03.093>
6. Lebrero, R., Bouchy, L., Stuetz, R., Muñoz, R.: Odor Assessment and Management in Wastewater Treatment Plants: A Review. *Critical Reviews in Environmental Science and Technology* **41**(10), 915-950 (2011). doi:[10.1080/10643380903300000](https://doi.org/10.1080/10643380903300000)
7. Vikrant, K., Kailasa, S.K., Tsang, D.C.W., Lee, S.S., Kumar, P., Giri, B.S., Singh, R.S., Kim, K.-H.: Biofiltration of hydrogen sulfide: Trends and challenges. *J. Clean Prod.* **187**, 131-147 (2018). doi:<https://doi.org/10.1016/j.jclepro.2018.03.188>
8. Lin, S., Mackey, H.R., Hao, T., Guo, G., van Loosdrecht, M.C.M., Chen, G.: Biological sulfur oxidation in wastewater treatment: A review of emerging opportunities. *Water Research* **143**, 399-415 (2018). doi:<https://doi.org/10.1016/j.watres.2018.06.051>
9. Alfonsín, C., Lebrero, R., Estrada, J.M., Muñoz, R., Kraakman, N.J.R., Feijoo, G., Moreira, M.T.: Selection of odour removal technologies in wastewater treatment plants: A guideline based on Life Cycle Assessment. *J. Environ. Manage.* **149**, 77-84 (2015). doi:<https://doi.org/10.1016/j.jenvman.2014.10.011>
10. Shareefdeen, Z., Herner, B., Singh, A.: Biotechnology for Air Pollution Control — an Overview. In: Shareefdeen, Z., Singh, A. (eds.) *Biotechnology for Odor and Air*

- Pollution Control. pp. 3-15. Springer Berlin Heidelberg, Berlin, Heidelberg (2005)
11. Vymazal, J.: Constructed wetlands for wastewater treatment: five decades of experience. *Environmental science & technology* **45**(1), 61-69 (2010).
  12. Ilyas, H., Masih, I.: The performance of the intensified constructed wetlands for organic matter and nitrogen removal: A review. *J. Environ. Manage.* **198**, 372-383 (2017). doi:<https://doi.org/10.1016/j.jenvman.2017.04.098>
  13. Freeman, A.I., Surridge, B.W.J., Matthews, M., Stewart, M., Haygarth, P.M.: New approaches to enhance pollutant removal in artificially aerated wastewater treatment systems. *Science of The Total Environment* **627**, 1182-1194 (2018). doi:<https://doi.org/10.1016/j.scitotenv.2018.01.261>
  14. Liu, F.-f., Fan, J., Du, J., Shi, X., Zhang, J., Shen, Y.: Intensified nitrogen transformation in intermittently aerated constructed wetlands: Removal pathways and microbial response mechanism. *Science of The Total Environment* **650**, 2880-2887 (2019). doi:<https://doi.org/10.1016/j.scitotenv.2018.10.037>
  15. Vymazal, J.: Removal of nutrients in various types of constructed wetlands. *Science of the total environment* **380**(1-3), 48-65 (2007).
  16. Hou, J., Wang, X., Wang, J., Xia, L., Zhang, Y., Li, D., Ma, X.: Pathway governing nitrogen removal in artificially aerated constructed wetlands: Impact of aeration mode and influent chemical oxygen demand to nitrogen ratios. *Bioresource Technology* **257**, 137-146 (2018). doi:<https://doi.org/10.1016/j.biortech.2018.02.042>
  17. Wu, S., Kuschik, P., Brix, H., Vymazal, J., Dong, R.: Development of constructed wetlands in performance intensifications for wastewater treatment: a nitrogen and organic matter targeted review. *Water research* **57**, 40-55 (2014).
  18. Maltais-Landry, G., Maranger, R., Brisson, J., Chazarenc, F.: Nitrogen transformations and retention in planted and artificially aerated constructed wetlands. *Water Research* **43**(2), 535-545 (2009). doi:10.1016/j.watres.2008.10.040
  19. Ouellet-Plamondon, C., Chazarenc, F., Comeau, Y., Brisson, J.: Artificial aeration to increase pollutant removal efficiency of constructed wetlands in cold climate. *Ecol. Eng.* **27**(3), 258-264 (2006). doi:10.1016/j.ecoleng.2006.03.006
  20. Stefanakis, A.I., Bardiau, M., Trajano, D., Couceiro, F., Williams, J.B., Taylor, H.: Presence of bacteria and bacteriophages in full-scale trickling filters and an aerated constructed wetland. *Science of The Total Environment* **659**, 1135-1145 (2019). doi:<https://doi.org/10.1016/j.scitotenv.2018.12.415>
  21. Zhou, X., Wang, R.G., Liu, H., Wu, S.B., Wu, H.M.: Nitrogen removal responses to biochar addition in intermittent-aerated subsurface flow constructed wetland microcosms: Enhancing role and mechanism. *Ecol. Eng.* **128**, 57-65 (2019). doi:10.1016/j.ecoleng.2018.12.028
  22. Martínez, N.B., Tejada, A., Del Toro, A., Sánchez, M.P., Zurita, F.: Nitrogen removal in pilot-scale partially saturated vertical wetlands with and without an internal source of carbon. *Science of The Total Environment* **645**, 524-532 (2018). doi:<https://doi.org/10.1016/j.scitotenv.2018.07.147>
  23. Ilyas, H., Masih, I.: The effects of different aeration strategies on the performance of constructed wetlands for phosphorus removal. *Environ. Sci. Pollut. Res.* **25**(6), 5318-

- 5335 (2018).
24. Zhao, Y.Q., Babatunde, A.O., Hu, Y.S., Kumar, J.L.G., Zhao, X.H.: Pilot field-scale demonstration of a novel alum sludge-based constructed wetland system for enhanced wastewater treatment. *Process Biochemistry* **46**(1), 278-283 (2011). doi:<https://doi.org/10.1016/j.procbio.2010.08.023>
  25. Wu, H., Fan, J., Zhang, J., Ngo, H.H., Guo, W., Hu, Z., Liang, S.: Decentralized domestic wastewater treatment using intermittently aerated vertical flow constructed wetlands: Impact of influent strengths. *Bioresource Technology* **176**, 163-168 (2015). doi:<https://doi.org/10.1016/j.biortech.2014.11.041>
  26. Fan, J., Wang, W., Zhang, B., Guo, Y., Ngo, H.H., Guo, W., Zhang, J., Wu, H.: Nitrogen removal in intermittently aerated vertical flow constructed wetlands: Impact of influent COD/N ratios. *Bioresource Technology* **143**, 461-466 (2013). doi:<https://doi.org/10.1016/j.biortech.2013.06.038>
  27. Zhang, X., Hu, Z., Ngo, H.H., Zhang, J., Guo, W., Liang, S., Xie, H.: Simultaneous improvement of waste gas purification and nitrogen removal using a novel aerated vertical flow constructed wetland. *Water research* **130**, 79-87 (2018).
  28. Yang, Y., Zhao, Y., Liu, R., Morgan, D.: Global development of various emerged substrates utilized in constructed wetlands. *Bioresource Technology* **261**, 441-452 (2018). doi:<https://doi.org/10.1016/j.biortech.2018.03.085>
  29. Yuan, J., Du, L.L., Li, S.Y., Yang, F., Zhang, Z.Y., Li, G.X., Wang, G.Y.: Use of mature compost as filter media and the effect of packing depth on hydrogen sulfide removal from composting exhaust gases by biofiltration. *Environ. Sci. Pollut. Res.* **26**(4), 3762-3770 (2019). doi:10.1007/s11356-018-3795-z
  30. Elias, A., Barona, A., Arreguy, A., Rios, J., Aranguiz, I., Peñas, J.: Evaluation of a packing material for the biodegradation of H<sub>2</sub>S and product analysis. *Process Biochemistry* **37**(8), 813-820 (2002). doi:[https://doi.org/10.1016/S0032-9592\(01\)00287-4](https://doi.org/10.1016/S0032-9592(01)00287-4)
  31. Das, J., Rene, E.R., Dupont, C., Dufourny, A., Blin, J., van Hullebusch, E.D.: Performance of a compost and biochar packed biofilter for gas-phase hydrogen sulfide removal. *Bioresource Technology* **273**, 581-591 (2019). doi:<https://doi.org/10.1016/j.biortech.2018.11.052>
  32. Allievi, M.J., Silveira, D.D., Cantão, M.E., Filho, P.B.: Bacterial community diversity in a full scale biofilter treating wastewater odor. *Water Science and Technology* **77**(8), 2014-2022 (2018). doi:10.2166/wst.2018.11



## Conclusions and Prospects

### Conclusions

Drinking water is a vital resource, and the safe water treatment plant residues (WTRs) disposal has emerged as a significant element of water resource planning and environmental management issues. However, currently practiced WTRs disposal method, such as landfilling and directly discharge to water body, poses danger to the environment and public health. In the literature, the utilization of WTRs has been proven feasible in a wide variety of environmental applications, from small-scale laboratory to field-scale settings (e.g. alum sludge reused as the substrates for constructed wetlands for wastewater treatment). Therefore, developing the novel beneficial reuse options became paramount for sustainable WTRs management. Furthermore, such reuse of the WTRs should have a multi-dimensional approach, offering both economic and environmental sustainability. Overall, this work has investigated and demonstrated five alum sludge reuse options, which would positively contribute in developing suitable WTRs management strategies and sustainable development under stringent environmental norms.

- **This work confirmed that the properties of the alum sludge were “site-specific”** (they vary over the period and place). For instances, regarding the two sources alum sludge considered in this work, the Carmaux alum sludge presented alkaline nature (pH = 10), smaller particle size ( $d_{50} = 16.5 \mu\text{m}$ ), microporous pore structure, more crystalline phase and a high amount of total element composition (53419 mg/kg) for instance. This is owing to the significant variabilities in the properties, which were mostly influenced by the source water quality, nature of the chemicals used, and type of raw water purification processes involved. Results of the various characterizations have also indicated that these properties are important while selecting potential reuse options. Hence, prior knowledge of physical as well as chemical properties of the alum sludge is necessary to reuse and recycle it into safe and sustainable disposal alternatives. In addition, it is also important to review treatment plant process to enhance the alum sludge reuse potential as the alum sludge generated at different processing steps involved in the purification of raw water are varied.
- **This work firstly demonstrated that incorporated alum sludge with clay bricks manufacturing has met the European and Irish Standards** as set out by Eurocode 6 – “Design of Masonry Structures”. Results also indicating that the firing temperature and the increase in sludge content affected the final clay-sludge brick color. By increasing the proportion of alum sludge, compressive strength decreased and the final weight of the brick was reduced. Firing temperatures that are too high may result in damage to the bricks during firing. With an increase in sludge content, the color became more pale – the appearance of very small white spots on the bricks. This effect could be used to enhance

the final appearance of a building or structure. Novelty thus adds commercial value by the reuse of what otherwise is an expensive problem. The results of efflorescence were also visible on the surface of all of the bricks fired at 1100 °C that contained any sludge (5, 10, 15 and 20 %).

- **This work provides a scientific clue for sorbents selection when considering alum sludge and Irish peat for glyphosate wastewater treatment to maximize their value in practice.** It reveals that alum sludge has the priority as the glyphosate removal capacity of alum sludge was significant (>99 %), while the removal capacity of Irish peat was considerably less than 10 %. It was also found that both materials significantly reduced the levels of COD in the influent, and it was noted that peat had a marginally greater initial removal capacity. Despite the poor removal of P, peat did perform better than alum sludge in terms of COD removal at  $68 \pm 22$  % while alum sludge had an average of  $57 \pm 12$  % COD removal after an initial poor start. The different behavior lies in the fact that peat in its natural state has poor P removal characteristics; in order to harness the full potential of peat, it must undergo pre-treatment prior to being used as an sorbent material.
  
- **Another approach allowed to show that alum sludge can be successfully used to co-condition with the sewerage sludge based on a case study in France, particularly provided a sustainable sludge management technical route for the local water industry.** When alum sludge was introduced to co-conditioning and dewatering with waste-activated sludge, the optimal mixing ratio gauged by both the phosphate concentration in the supernatant and the improvement of dewaterability of the resultant sludge is 1:1 (sewerage sludge:alum sludge, v/v). The addition of alum sludge to the waste-activated sludge improved its dewaterability. The optimal polymer dosage for the mixed sludge was 200 mg/l, while the current dosage for the waste-activated sludge in WWTP is 2.8 g/l. An integrated cost-effective evaluation of process capabilities, sludge transport, increased cake disposal, additional administration, etc. has proved that the co-conditioning and dewatering strategy is practicable, the initial investment could be returned in 11 years.
  
- **The use of alum sludge as a sorbent for H<sub>2</sub>S removal was firstly validated, and revealed the adsorption phenomenon from various aspects including kinetics, mechanisms, mass transfer coefficients, etc.** The H<sub>2</sub>S adsorption capacity of the alum sludge (374.2 mg/g) was higher than that of several sorbent reported in literature in the dynamic condition test. Application of Thomas, BDST and YN model for the reactor revealed that the models can simulated well the breakthrough curves. The breakthrough and exhaustion of the bed were found to be regulated by the bed depth and flow rate. Under varying experimental conditions all the three models, e.g., Thomas, BDST and Y-N models with R<sup>2</sup> values range from 0.7 to 0.93, and successfully predicted breakthrough curves, and hence, be used for scaling up. The important alum sludge properties for H<sub>2</sub>S removal are: high specific surface area and microporous volume, alkaline pH surface, presence of metal species (especially Ca, Al, Fe), O-containing groups. The mechanisms results highlighted the large variety of sulfur compounds produced during the H<sub>2</sub>S removal trials, resulting

from a complex reaction mechanism involving the physicochemical properties of the alum sludge. The overall mass transfer coefficients considering film resistance and pore resistance obtained by numerical modelling allowed to evaluate surface diffusivity of H<sub>2</sub>S over the interior surface of alum sludge. Since the alum sludge has microporous structure, Knudsen diffusion was the main diffusion mechanisms, moreover, the Knudsen, Molecular, Effective and Pore diffusivity were remaining the same under different flow rate and mass of sorbent. It indicated that the adsorption mechanisms were the same regardless of the experimental conditions. It opens a novel reusing perspective of alum sludge as well as a cost-effective solution for waste gas purification.

- **The last approach was to develop a novel aerated alum sludge based vertical flow constructed wetland (Al-VFCW) to enhance the pollutants removal in wastewater and eliminating the waste gas (H<sub>2</sub>S), simultaneously.** Through the six-month trials, the high removal efficiency of TP (> 98 %) was achieved in all the three columns, it was contribution to the alum sludge media. In addition, the H<sub>2</sub>S was completely removed (100 %) through each day's operation. Moreover, the introduction of waste gas and air could significantly enhance the removal efficiency of COD and TN, compare with the unaerated Al-VFCW. In particular, there was no significant difference regarding the COD, TN removal performances between the "waste gas driven" Al-VFCW and the aerated Al-VFCW. It showed that intermittent aerated Al-VFCW using waste gas would be a potential "wise choice" to intensify pollutant removal performance for the wastewater. It firstly demonstrated that alum sludge cakes could be a promising low-cost media in novel aerated VFCWs for H<sub>2</sub>S removal and wastewater treatment, simultaneously.

### WTRs adopting a "Circular Economy"

A Circular Economy (i.e. circularity) is an economic system aimed at minimizing waste and making the most of resources. This regenerative approach is in contrast to the traditional linear economy, which has a 'take, make, dispose' model of production.

Both China and Europe have taken the lead in pushing a circular economy. On December 2012, the European Commission published a document entitled "Manifesto for a Resource Efficient Europe". This manifesto clearly stated that "In a world with growing pressures on resources and the environment, the EU has no choice but to go for the transition to a resource-efficient and ultimately regenerative circular economy." Furthermore, the document highlighted the importance of "a systemic change in the use and recovery of resources in the economy" in ensuring future jobs and competitiveness, and outlined potential pathways to a circular economy, in innovation and investment, regulation, tackling harmful subsidies, increasing opportunities for new business models, and setting clear targets.

However, the conventional WTRs management route is the linear "take, make, dispose" industrial processes, which end up in landfills or in incinerators. The circular approach, by

contrast, takes insights from the reuse of WTRs. It considers the "closed loop" or "regenerative" terms. The generic circular economy label can be applied to or claimed by several different aspects of thought, but all of them gravitate around the same basic principles.

In particular, a circular economy within the WTRs industry refers to the practice of WTRs continually being recycled, to re-enter the economy as much as possible rather than ending up as waste, as illustrated in Figure C.1. The alum sludge as a by-product was generated from the WTP has proved that it can be reused in Clay brick manufacturing (Chapter 3), Glyphosate removal (Chapter 4), Sewerage sludge co-conditioning (Chapter 5), H<sub>2</sub>S purification (Chapter 6), as well as the novel aerated CWs (Chapter 7). It is in response to the current linear model of the waste disposal industry, in which raw surface water are treated into commercial portable water and then the raw water purification by product were eventually discarded by waste. The take-make-dispose model not only leads to an economic value loss, but also has numerous negative environmental and societal impacts as discussed in Chapter 1. Such environmental effects include million tons of WTRs ending up in landfills, while the societal effects put human health at risk.

Although the WTRs industry has a long way to go to reach a sustainable future, a circular economy could be the answer to the social and environmental issues that the current linear model has created.

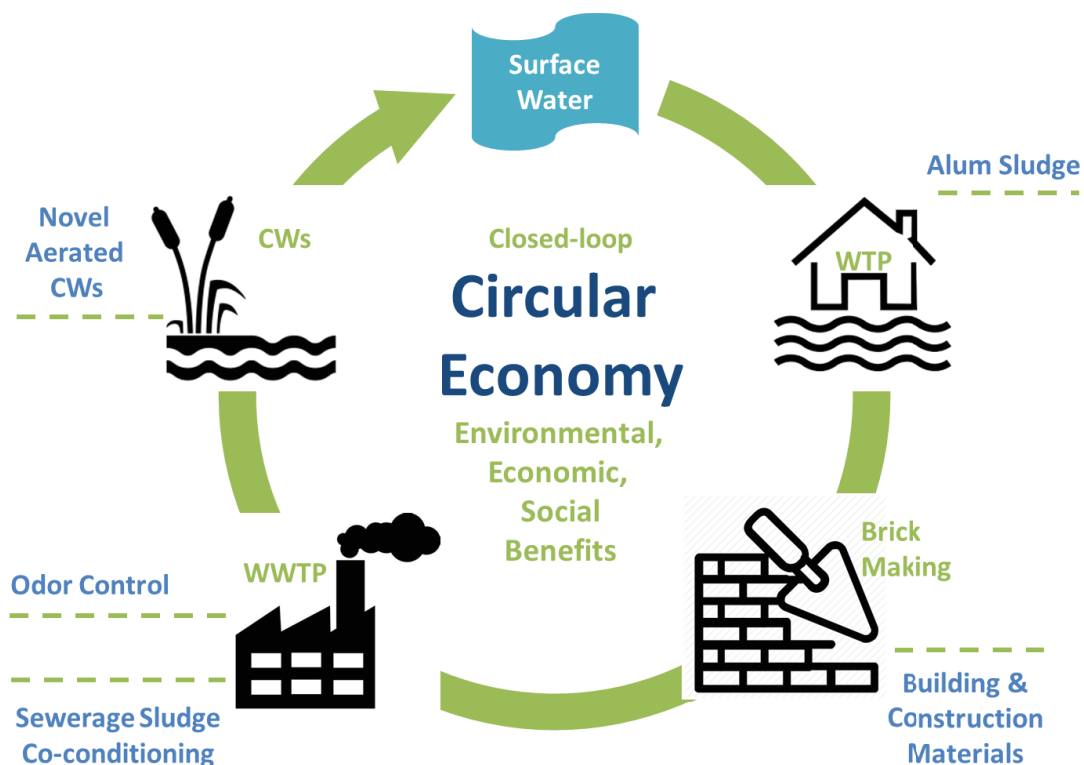


Figure C.1 The WTRs industries adopting a circular economy

## **Prospects**

Drinking water treatment sludge disposal is an issue of increasing concern, and reliable data on the beneficial reuse of WTRs is correspondingly valuable. Further work to help fill some of the remaining knowledge gaps would unquestionably be beneficial.

- ✧ The present has only characterized two origins alum sludge, it has not and could not properly consider every permutation. Future research needs to be conducted in order to expand on the number of WTRs in the region and beyond, in order to ascertain their appropriateness for beneficial uses. The physiochemical nature of the alum sludge produced during different processing operation is different and the estimation as well as characterization of such residue is essential for more opportunistic recycling. Further extensive investigations are required to find a steady and reliable source of the WTRs, with minimal compositional variability for fearless and optimum utilization. For instance, to make a cartography of characteristics of the alum sludge as a function of their location, and to identify the possible reuse routes.
- ✧ The use of the sludge in the manufacturing of clay bricks would be an environment-friendly and economical way of reusing sludge in Ireland. Our study suggests that if commercial bricks were to be fired at 1200 °C, a sludge incorporation of 10 and 20 % would also yield satisfactory strength and water absorption characteristics for bricks in commercial use. This proportion of sludge when fired at 1100 °C produced an appearance closest to standard commercial clay bricks. To date, no pilot project has been established to investigate the use of water treatment sludge in the manufacture of clay brick on an industrial scale in Ireland and France. It is recommended that there should be a pilot study. In addition, similarly, reuse of alum sludge-clay bricks for pavement and car park areas or general building construction materials in Ireland and France is also worth investigation, as a separate study.
- ✧ The significant glyphosate removal efficiency of alum sludge surpassed expectation based on previous literature over the 10-week test period, the result shows no trends indicating a significant change to its performance in the immediate future. Further research could be carried out with a longer period and increasing the scale, to gain a further insight into the ability of alum sludge as a low cost sorbent, the schedule must be increased to several years to determine the longevity of alum sludge cakes as we have proved that alum sludge is extremely effective at phosphorus removal in the short term at least. It would be also recommended that the effect of pH and initial dosage concentration of glyphosate could be taken into place to give a better analysis of the removal capacity. In addition, the future studies of peat must include a comprehensive review of pre-treatment methods for peat and the effects on the pollutant removal performance.
- ✧ The co-conditioning and dewatering strategy were identified as a “win–win” situation from the technical standpoint. On the other hand, for various onsite full-scale applications of

alum sludge in the co-conditioning process, integrated the local “site-specific” cost-effective analysis of process efficiencies, sludge transport, additional administration, and other process parameters should be considered in the final analysis.

- ✧ From the H<sub>2</sub>S removal experiments, the adsorption capacity of the alum sludge tested showed good compared with majority of sorbents used classically. Significantly, alum sludge could be directly reused as the “ready to use media” without any extra treatment. This study has demonstrated that the use of alum sludge for H<sub>2</sub>S control could be a good material/sorbent for adsorption system, it will open a new way for desulfurization even odor abatement as well as the sludge management. This work needs to be completed by more experiments for the repeatability, different time at lab scale trials to identify the kinetic mechanism and the saturation time of the solid. Large-scale investigations are highly desirable to confirm results obtained at lab scale. Alum sludge with different characteristics from different sites should be tested in the future to understand what are the most important properties that control the adsorption of H<sub>2</sub>S by alum sludge. In addition, the regeneration of exhausted sorbent and final disposal route which also H<sub>2</sub>S needs further investigation.
- ✧ The alum sludge has been first proved to be an efficient sorbent/media for H<sub>2</sub>S removal in columns as well as the novel aerated constructed wetlands. However, the various odorants such as ammonia (NH<sub>3</sub>), VOCs and the mixed pollutants must be considered in the future studies, and it is the same situation in novel Al-VFCWs. In order to develop a systematic profile of alum sludge odor removal. Moreover, the sorbent regeneration, exhausted sorbent and media (in Al-VFCWs) final disposal issues should be discussed in detail in the future. In addition, it is necessary to mention again that the alum sludge characterization is vital step to select the sorbent, before the adsorption trials. For instance, the Dublin alum sludge and Carmaux alum sludge present significant difference regarding the H<sub>2</sub>S adsorption removal efficiency.

The last but not the least, the author also claims that creating awareness among the water treatment plant operators, municipalities, government officials, and general public, regarding benefits of the WTRs reuse could also promote sustainable management and recycling.



---

## Appendix I

### List of Figures

<b>Figure 0.1</b> Annual WTRs generation of different countries (Before 2015).....	1
<b>Figure 0.2</b> Diagram of waste hierarchy as regulated European Directive.....	2
<b>Figure 0.3</b> The beneficial reusing ways of alum sludge .....	3
<b>Figure 0.4</b> Structure of the thesis.....	4
<b>Figure 1.1</b> Conventional water treatment processes.....	8
<b>Figure 1.2</b> Dublin (Ireland) Ballymore Eustace Water Treatment Plant. (a). the 1600mm intake pipes (green) and the coagulant dosing system (purple pipework); (b). desludging pipes & drain of clarifier; (c). Clarifier .....	9
<b>Figure 1.3</b> Physical/chemical abatement technologies: adsorption system (left), chemical scrubber (right).....	21
<b>Figure 1.4</b> Concentration profiles in the case of rate-limiting film diffusion.....	23
<b>Figure 1.5</b> Concentration profiles in the case of pore diffusion .....	23
<b>Figure 1.6</b> Concentration profiles in the case of surface diffusion.....	24
<b>Figure 1.7</b> Traveling of the mass transfer zone (MTZ) through the column and development of the breakthrough curve (BTC) .....	25
<b>Figure 1.8</b> Biotechnological treatment: (a) open biofilter; (b) biotrickling filter; (c) bioscrubber; (d) activated sludge diffusion. ....	27
<b>Figure 2.1</b> Alum sludge being collected for disposal in Dublin Ballymore Eustace WTP .....	52
<b>Figure 2.2</b> Filter press in Carmaux WTP.....	52
<b>Figure 2.3</b> Alum sludge; (a) raw alum sludge cake (b) Dublin alum sludge; (d) Carmaux alum sludge .....	53
<b>Figure 2.4</b> Particle size distribution of alum sludge .....	56
<b>Figure 2.5</b> X-ray diffraction pattern of two sources alum sludge.....	57
<b>Figure 2.6</b> FT-IR spectrum of the two sources alum sludge.....	58
<b>Figure 2.7</b> SEM-EDX images of two sources of alum sludge, (a, c, e) Dublin sludge; (b, d, f) Carmaux sludge .....	60
<b>Figure 2.8</b> TEM-EDX images of Dublin alum sludge .....	61
<b>Figure 2.9</b> TEM-EDX images of Carmaux alum sludge.....	62
<b>Figure 2.10</b> N <sub>2</sub> adsorption isotherms for the two sludges .....	64
<b>Figure 2.11</b> TGA of Dublin alum sludge .....	65
<b>Figure 2.12</b> TGA of Carmaux alum sludge .....	65
<b>Figure 2.13</b> (a) the bricks after the drying stage; (b) the kiln; (c) the compression machine .....	67

---

<b>Figure 2.14</b> Schematic of pot trials.....	68
<b>Figure 2.15</b> Jar-test apparatus of co-conditioning trials .....	69
<b>Figure 2.16</b> The experiment apparatus of (a) specific resistance to filtration (SRF), (b) capillary suction time (CST). .....	70
<b>Figure 2.17</b> The lab-scale experimental apparatus .....	71
<b>Figure 2.18</b> The three parallel aerated alum sludge constructed wetland .....	75
<b>Figure 3.1</b> The clay (lighter colour) and alum sludge after grinding and sieving .....	79
<b>Figure 3.2</b> The moulds (left) and the bricks after drying .....	80
<b>Figure 3.3</b> The bricks from Batch 3 in the kiln after firing .....	81
<b>Figure 3.4</b> The compression strength testing.....	82
<b>Figure 3.5</b> Water absorption testing.....	82
<b>Figure 3.6</b> The relationship between compressive strength (LoI, Percentage Weight Gain after Water Submersion) and percentage sludge addition. ....	86
<b>Figure 3.7</b> General appearance: (a) Batch 1–4 from top to bottom in the picture; (b) Batch 2; (c) Batch 4; (d) Batch 3; (e) The 0 % sludge brick (left), and the 40 % sludge brick (right) fired at 1200 °C .....	89
<b>Figure 4.1</b> Map location of sampling sites in Ireland.....	94
<b>Figure 4.2</b> Schematic of pot apparatus .....	95
<b>Figure 4.3</b> Pot setup (a) filled with gravel; (b) measuring the media mass; (c) filled with peat; (d) planting reeds.....	95
<b>Figure 4.4</b> Dosing and sampling.....	96
<b>Figure 4.5</b> Glyphosate concentration/removal and COD removal rate .....	98
<b>Figure 4.6</b> SEM-EDX image: (a) raw alum sludge; (b) alum sludge after pot test; (c) raw peat; (d) peat after pot test; (e) alum sludge EDX; (f) peat EDX.....	99
<b>Figure 5.1</b> Sludge sampling. (a) sewerage sludge taken from the bottom of secondary clarifier of Graulhet WWTP; (b) liquid alum sludge taken from the settlement tank of the treatment plant.....	105
<b>Figure 5.2</b> Jar-test apparatus.....	107
<b>Figure 6.1</b> Photo and scheme of the fixed-bed adsorption column. ....	121
<b>Figure 6.2</b> SEM-EDX of the alum sludge sorbent .....	126
<b>Figure 6.3</b> Quantity of the H <sub>2</sub> S fed into the reactor (Inlet curve) and fixed on 0.5 g alum sludge under different flow rate .....	127
<b>Figure 6.4</b> Quantity of the H <sub>2</sub> S fed into the reactor (Inlet curve) and fixed on different mass of alum sludge under 5L/h flow rate .....	128
<b>Figure 6.5</b> The simulative curves and experiment data under three different model, (a), (b), (c) 0.5g alum sludge under the flow rate of 3, 4, 5L/h, (d) 1g alum sludge under the flow rate of 5L/h.....	132
<b>Figure 6.6</b> SEM-EDX of the exhausted alum sludge sorbent .....	135
<b>Figure 6.7</b> TEM-EDX images of the exhausted alum sludge sorbent.....	136
<b>Figure 6.8</b> TGA-MS analysis of raw alum sludge before (up) and after (down) the adsorption trials .....	138
<b>Figure 6.9</b> Mechanisms of H <sub>2</sub> S adsorption onto alum sludge .....	139
<b>Figure 7.1</b> The columns setup; (a) the aeration diffuser of the column, (b) the outlet valves	

---

of the columns .....	151
<b>Figure 7.2</b> Filling of the columns, (a) the empty columns; (b) the gravel layer in the columns; (c) the substrates (gravel + alum sludge cake) of the columns.....	151
<b>Figure 7.3</b> The experimental process (a) the activated sludge seeding process; (b) the experimental formal running process .....	152
<b>Figure 7.4</b> Three parallel AI-VFCWs configuration.....	153
<b>Figure 7.5</b> COD removal performance in the three columns .....	155
<b>Figure 7.6</b> TN removal performance in the three columns .....	156
<b>Figure 7.7</b> NH <sub>4</sub> -N removal performance in three columns .....	157
<b>Figure 7.8</b> TP removal performance in three columns .....	158
<b>Figure 7.9</b> Overall removal efficiency of COD, TN, NH <sub>4</sub> -N and TP in three columns	160
<b>Figure 7.10</b> H <sub>2</sub> S effluent online analysis and removal efficiency .....	161
<b>Figure C.1</b> The WTRs industries adopting a circular economy .....	169

## Appendix II

### List of Tables

<b>Table 1.1</b> Various pollutants and heavy metals adsorbed by alum sludge.....	14
<b>Table 1.2</b> Performance of BF in lab and on-site systems .....	30
<b>Table 1.3</b> Performance of BTF in lab and on-site systems.....	34
<b>Table 1.4</b> Summary of different odor control technologies in WWTPs .....	38
<b>Table 2.1</b> Physical characteristics of alum sludge .....	56
<b>Table 2.2</b> Element composition of two sources alum sludge .....	63
<b>Table 2.3</b> Pore structure of two sources alum sludge .....	64
<b>Table 3.1</b> Compressive strength after submersion (kPa) .....	87
<b>Table 4.1</b> The major chemical composition of the four media .....	100
<b>Table 5.1</b> The sludge element composition in the solid phase and the supernatant .....	108
<b>Table 5.2</b> CHNS of alum sludge and sewerage sludge ( %).....	108
<b>Table 5.3</b> The elements in supernatant under different mix ratio (alum sludge:sewerage sludge).....	111
<b>Table 5.4</b> the main materials and costs of initial investment.....	113
<b>Table 6.1</b> Characterization of the alum sludge sorbent .....	125
<b>Table 6.2</b> Model parameters calculation.....	130
<b>Table 6.3</b> Experimental and simulated breakthrough time .....	131
<b>Table 6.4</b> Elemental analysis and pH of the sorbent.....	134
<b>Table 6.5</b> Structural properties of alum sludge.....	134
<b>Table 6.6</b> Parameters used in the determination of mass transfer coefficient .....	140
<b>Table 6.7</b> Determination of the various mass transfer coefficient .....	142

---

## Appendix III

### Scientific Contributions

#### a) Peer-Reviewed International Journal Publications

1. **Baiming Ren**, Nathalie Lyczko, Yaqian Zhao, Ange Nzihou, Simultaneous hydrogen sulfide purification and wastewater treatment in a novel aerated alum sludge based constructed wetland. (Under preparation)
2. **Baiming Ren**, Nathalie Lyczko, Yaqian Zhao, Ange Nzihou, Alum sludge as an efficient sorbent for hydrogen sulfide removal: Experimental, mechanisms & modeling studies. (2019) *Chemical Engineering Journal*. (Under review)
3. **Baiming Ren**, Nathalie Lyczko, Yaqian Zhao, Ange Nzihou, Co-conditioning of waste-activated sludge with alum sludge: A case study of a city in South France. (2019) *Environmental Science and Pollution Research*. (Under review)
4. **Baiming Ren**, Yaqian Zhao, Nathalie Lyczko, Ange Nzihou, Current Status and Outlook of Odor Removal Technologies in Wastewater Treatment Plant. (2019) *Waste and Biomass Valorization*. 10(6): 1443-1458. doi:10.1007/s12649-018-0384-9.
5. Yae Wang, **Baiming Ren**, Yaqian Zhao, Anthony English & Martin Cannon, A comparison of alum sludge with peat for aqueous glyphosate removal for maximizing their value for practical use. (2017) *Water Science & Technology* 2017(2): 450-456.
6. Yaqian Zhao, **Baiming Ren**, Andrew O'Brien & Simon O'Toole, Using alum sludge for clay brick: an Irish investigation. (2016) *International Journal of Environmental Studies* 73(5): 719-730.
7. Ranbin Liu, Yaqian Zhao, Caroline Sibille, **Baiming Ren**, Evaluation of natural organic matter release from alum sludge reuse in wastewater treatment and its role in P adsorption. (2016) *Chemical Engineering Journal* 302: 120-127.
8. Yae Wang, Yaqian Zhao, Lei Xu, Wenke Wang, Liam Doherty, Cheng Tang, **Baiming Ren** & Jinhui Zhao, Constructed wetland integrated microbial fuel cell system: looking back, moving forward. (2017) *Water Science & Technology* 76(2):471-477.

#### b) International Conferences Attendances and Publications

1. **Baiming Ren**, Yaqian Zhao, Nathalie Lyczko, Ange Nzihou. Simultaneous waste gas purification & wastewater treatment in a novel alum sludge based CWs. 8th International Symposium on Wetland Pollutant Dynamics and Control (2019), Aarhus University, Denmark. (**Oral presentation & Full-length paper**)
2. **Baiming Ren**, Yaqian Zhao, Nathalie Lyczko, Ange Nzihou. Towards sustainable water-

---

wise cities: reusing waterworks residues for wastewater treatment plant odour control, IWA World Water Congress & Exhibition 2018, Tokyo, Japan. (Poster)

3. **Baiming Ren**, Yaqian Zhao, Nathalie Lyczko, Ange Nzihou, Valorisation and effectiveness of using two water works residues for gas purification. 7th International Conference on Engineering for Waste and Biobmass Valorisation (WasteEng 18) Prague, Czech Republic. **(Oral presentation)**
4. **Baiming Ren**, Yaqian Zhao, Nathalie Lyczko, Ange Nzihou, Waterworks sludge management in a sustainable world: novel value-added alum sludge products for harmful gas purification. 5th International Conference on Sustainable Solid Waste Management, Athens, Greece. E-proceedings Session IV. (2017) **(Oral presentation)**
5. **Baiming Ren**, Yaqian Zhao, Transforming alum sludge into clay brick manufacturing: Irish investigation and prospects. The 26th Irish Environmental Researchers' Colloquium, ENVIRON 2016. Limerick, Ireland. (Poster)
6. Yaqian Zhao, **Baiming Ren**. Innovation in the management of waterwoks sludge. 6th International Conference on Engineering for Waste and Biomass Valorisation (WasteEng 2016), Albi, France. **(Oral presentation)**
7. Liam Doherty, Yaqian Zhao, **Baiming Ren**, Development of constructed wetland-microbial fuel cell utilizing a ceramic separator. IWA Specialist Conference on Wetland Systems for Water Pollution Control (ICWS 2016), Gdansk, Poland. Vol.1, 208-226. **(Oral presentation & Full-length paper)**



## **Transforming alum sludge into value-added products for various reuse**

The production of drinking water always accompanied by the generation of water treatment residues (WTRs). Alum sludge is one of the WTRs, it is an easily, locally and largely available by-product worldwide. This work focuses on the identification of different ways to valorize the alum sludge for environmentally friendly reuse. Two alum sludges collected from France and Ireland have been reused in various fields as a function of their characteristics.

Firstly, alum sludge was used as a partial replacement for clay in brick making, by incorporating different percentages of alum sludge and calcined at different temperatures (range from 800 to 1200 °C). The resultant bricks were tested for compression, Loss on Ignition, water absorption, appearance, etc. Results show that alum sludge-clay bricks have met the “European and Irish Standards” and demonstrated the huge industrial application potential for alum sludge in Irish clay brick manufacturing. Glyphosate is an active ingredient in pesticide which is massive employed in agriculture. Alum sludge and Irish peat were compared for glyphosate removal in pot tests, results show that alum sludge present significant glyphosate removal capacity (>99 %) and could reduce the level of Chemical Oxygen Demand (COD). It provided a scientific clue for sorbents selection when considering the agricultural wastewater treatment in Ireland and to maximize their value in practice. The co-conditioning and dewatering of sewerage sludge with liquid alum sludge was also investigated in Jar-test based on the case analysis of a water industry in France. Results show that the optimal sludge mix ratio is 1:1, the use of the alum sludge has been shown to beneficially enhance the dewaterability of the resultant mixed sludge, and highlighting a huge polymer saving (14 times less than the current technologies) and provided a sustainable and technical sludge disposal route for the local water industry. The use of alum sludge as a sorbent for gas purification was studied by H<sub>2</sub>S adsorption experiments in a fixed-bed reactor with various operating parameters. The experimental breakthrough data were modeled with empirical models based on adsorption kinetics. Results show that alum sludge is an efficient sorbent for H<sub>2</sub>S removal (capacity of 374.2 mg/g) and the mechanisms including dissociative adsorption and oxidation were proposed. Moreover, the overall mass transfer coefficients were calculated which could be used for the process scaling up. Finally, alum sludge cakes were reused in the novel aerated alum sludge constructed wetland (CW), which were designed for simultaneous H<sub>2</sub>S purification and wastewater treatment. Results show that H<sub>2</sub>S was completely removed in the six months’ trials, while the high removal efficiencies of COD, total nitrogen (TN), total phosphates (TP) were achieved. Thus, a novel eco-friendly CW for simultaneous H<sub>2</sub>S purification and wastewater treatment was developed. In the different approaches and process considered, in particular it was put in investigating and describing the mechanisms involved. Overall, this work demonstrated alum sludge could be a promising by-product for various novel beneficial reuse rather than landfilling and provided a “Circular Economy” approach for WTRs management.

**Keywords:** Wastewater treatment, Alum sludge, Gas purification, Process adsorption mechanisms, Brick manufacturing, Valorization, Circular economy